Mutagenesis and functional characterisation of toxin HicA from the HicBA TA system in *Burkholderia pseudomallei.*

Submitted by Harriet Leah Bare to the University of Exeter
as a thesis for the degree of
Doctor of Philosophy in Biological Science in October 2016

This thesis is available for Library use on the understanding that it is copyright material and that no quotation from the thesis may be published without proper acknowledgement.

I certify that all material in this thesis which is not my own work has been identified and that no material has previously been submitted and approved for the award of a degree by this or any other University.

Signature: ……..

Abstract

Four type II toxin-antitoxin (TA) systems were previously identified in *Burkholderia pseudomallei* K96243. Type II TA toxins are able to induce cell growth arrest or death by interfering with key processes within the organism. *BPSS0390-0391* is one of the TA systems previously identified and has homology to *hicBA* system in *Acinetobacter baumannii. B. pseudomallei* HicA is able to cause a reduction in the number of culturable cells after expression in *E. coli*. This study aimed to characterise *B. pseudomallei* HicA in three ways: by inducing expression of HicA in bacterial species other than *E. coli*, by identifying amino acids in HicA involved in toxicity and neutralisation by the antitoxin HicB and by examining the interaction of HicA with other TA antitoxins identified within *B. pseudomallei* genome.

A broad host range plasmid encoding *BPSS0390* was transformed into a range of Gram negative bacteria including *Yersinia pseudotuberculosis* IP32953, *Vibrio vulnificus* E64MW, *Salmonella enterica* serovar Typhimurium SL1344 and *Burkholderia thailandensis* E264. Expression of *BPSS0390* was toxic in all bacterial species tested, despite the presence of antitoxin BPSS0391 homologues in some species. Unregulated expression in *E. coli* resulted in the appearance of escape mutants encoding non-toxic variants of HicA.

An alanine scanning mutagenesis study of HicA identified 20 mutants where toxicity was abolished despite high levels of expression, but identified no mutants that affected TA complex formation.

Finally an existing co-expression assay was modified to examine interactions between HicA and other type II TA antitoxins in *B. pseudomallei*. The assay revealed no interaction between HicA and non-cognate antitoxins and clarified the role of IPTG as an inhibitor of P_{BAD} promoter on the arabinose operon.

Table of Contents

List of figures

List of Tables

Posters

Host specificity of TA toxins identified in *Burkholderia pseudomallei.*

Harriet L. Bare, Claudia M. Hemsley, Aaron Butt, Timothy P. Atkins and Richard W. Titball

Society for General Microbiology Spring Conference 2013- Manchester, UK. March 2013. Poster.

Further characterisation of TA system *BPSS0390-0391* identified in *Burkholderia pseudomallei*

Harriet L. Bare, Claudia M. Hemsley, Aaron Butt, Timothy P. Atkins and Richard W. Titball

World Melioidosis Congress- Bangkok, Thailand. September 2013. Poster.

Further characterisation of TA system *BPSS0390-0391* identified in *Burkholderia pseudomallei*

Harriet L. Bare, Claudia M. Hemsley, Aaron Butt, Timothy P. Atkins and Richard W. Titball

Infection and immunity meeting- Hua Hin, Thailand. September 2013. Poster.

Declaration

Unless otherwise stated, the results and data presented in this thesis were solely the work of Harriet Bare.

Scanning Electron Microscopy was performed by Peter Splatt.

Acknowledgements

Firstly, I would like to thank my supervisors Prof. Rick Titball and Dr. Claudia Hemsley for their continued support and patience throughout the PhD project. I would also like to thank Dr. Helen Atkins and Dr. Tim Atkins at DSTL.

I also wish to thank all members of the 4th floor, past and present, from whom I have learnt so much. I'd especially like to thank Dr. Monika Bokori-Brown for all her support over the last 4 years.

To Dr. Vanessa Francis and Dr. Michael Steele; I will miss our chats, carrots and coffee.

To Odette Wills and Georgia Collins, thank you for the running, swimming and cake, but mostly the cake.

My heartfelt thanks to Julian French and Sue Wiggins for your calm understanding and understated support throughout this work.

To my parents, Lorraine and Martin Bare, thank you for your continued support in this and all my other endeavours. Thank you for your guidance and belief in me.

I am wholly indebted to Cameron Bell. Thank you for your seemingly unending patience and good humour. I don't know where I'd be without you. If I have you, then I have everything.

Abbreviations

%	Percent
Δ	Delta
3D	Three dimensional
^{o}C	Degrees centigrade
α	Alpha
AI2	Auto-inducer 2
ANOVA	Analysis of variance
ATP	Adenosine triphosphate
β	Beta
BLAST	Basic local alignment search tool
bp	Base pair
ccd	Coupling cell division
CFU	Colony forming unit
DCL1	Dicer-like 1 protein
ds	Double stranded
DMSO	Dimethyl sulphoxide
DNA	Deoxyribonucleic acid
dNTPs	Deoxynucleotides
dsRBD	Double stranded RNA binding domain
dsRNA	Double stranded RNA
ε	Epsilon
EDF	Extracellular death factor
EDTA	Ethylenediaminetera acetic acid
Ef-Tu	Elongation factor thermo unstable
g	grams
GI	Genomic Island
GTP	Guanosine triphosphase
γ	gamma
hip	high persistence
HTH	Helix turn helix
HYP1	Hyponastic leaves 1 protein
ICE	Integrative and conjugative element
IPTG	Isopropyl β-D-1 thiogalactopyranoside
L	Litre
LB	Luria broth
Mb	Mega base
µ	Micro
m	Milli or metres
M	Molar
MBC	Minimum bactericidal concentration
MGE	Mobile genetic element
min(s)	minute(s)
mRNA	messenger ribonucleic acid
MW	Molecular weight
n	Nano
NaOH	Sodium hydroxide

NaCl	Sodium chloride
NCBI	National Centre for Biotechnology Information
NMR	Nuclear magnetic resonance
ω	Omega
OD	Optical density
ORFs	Open reading frames
P	pico or probability
PAGE	Polyacrylamide gel electrophoresis
PBS	Phosphate buffered saline
PBST	Phosphate buffered saline Tween
PCD	Programmed cell death
PCR	Polymerase chain reaction
pH	Potential of hydrogen-measure of hydrogen ions associated with acidity
PolyP	polyphophate
(p)ppGpp	guanosine (penta) or tetraphosphate
PPX	exopolyphosphatase
PSK	postsegregational killing
qPCR	qualitative real time polymerase chain reaction
RBD	RNA binding domain
RHH	Ribbon helix helix
RNA	Ribonucleic acid
RPM	Revs per minute
rRNA	Ribosomal ribonucleic acid
s	Subunit
σ	Sigma
secs	Seconds
SD	Shine Dalgarno
SDM	Site directed mutagenesis
SDS	Sodium dodecyl sulphate
SEM	Standard error of the mean or scanning electron microscopy
SI	Superintegron
TA	Toxin-antitoxin
TAE	Tris-acetate-EDTA
TBS	Tris buffered saline
TBST	Tris buffered saline Tween
TCBS	Thiosulfate-citrate-bile salts-sucrose agar
TIR	Translation initiation region
tRNA	Transfer ribonucleic acid
UV	Ultraviolet
UNAG	Uridine diphosphate-N-acetylglucosamine
UTI	Urinary tract infection
v	Volume
V	Volts
VBNC	Viable but non culturable
WT	Wildtype
W/V	Weight to volume
x g	Centrifugal force
Xlrbpa	*Xenopus leavis* RNA binding protein A
ζ	Zeta

Chapter 1: Introduction

1.0 Toxin-antitoxin (TA) systems: classification, biological functions and applications

TA systems typically consist of a gene pair, where one gene encodes a protein toxin and the other a cognate antitoxin. The unstable antitoxin molecule is able to counteract or neutralise the more stable toxin or its action. However, if production of the antitoxin is stopped, the rapid degradation of the remaining antitoxin molecules allows toxin activation. Free toxins are then able to induce cell growth arrest or death by targeting key cellular processes (Unterholzner et al. 2013).

Initially identified on plasmids, TA modules prevent plasmid loss at cell division though post-segregational killing (PSK) (Ogura & Hiraga 1983). Daughter cells that lack the plasmid bearing the TA module experience a rapid decrease in antitoxin levels and the activated toxin kills the plasmid-free cell (Brantl 2012; Unterholzner et al. 2013). Since then, many chromosomally encoded TA systems have been identified and characterised, although their biological functions are less clear.

1.0.1 Classification of TA systems

It is possible to classify TA systems into six different types, based on the antitoxin and its interaction with its cognate toxin (Figure 1.1). All antitoxins regulate toxin activity (Brantl & Jahn 2015; Gerdes & Maisonneuve 2012).

1.0.1.1 Type I TA systems

In type I systems, the antitoxin is a small antisense RNA molecule that binds to toxin-encoding mRNA through base pairing (Yamaguchi *et al*., 2011). The type I gene pair may be either; overlapping and convergently transcribed (cis-encoded antisense RNA antitoxin) or located apart and divergently transcribed (trans-encoded small RNA) (Brantl 2012; Brantl & Jahn 2015).

Originally identified on plasmids, chromosomal loci have since been discovered and may be present in multiple copies in both Gram-positive and Gram-negative bacteria. There is some evidence to suggest that the number of copies may be linked to the ecological niche of the host (Gerdes et al. 1985; Fozo et al. 2010; Fozo 2012). Antitoxins regulate toxin activity by either inhibiting translation of the toxin mRNA or promoting toxin mRNA degradation. Inhibition of translation may be direct, where the antitoxin binds at a region that overlaps the ribosome binding site (RBS) (*Escherichia coli symE*/SymR)(Kawano et al. 2007), or indirect where the antitoxin binds to the Shine-Dalgarno (SD) sequence of leader peptides required for translation of the toxin (*E. coli hok*/Sok, *ldrD*/RdlD)(Gerdes & Wagner 2007). In *E. coli tisB*/IstR1 translation of the toxin is also indirectly inhibited, as the IstR antitoxin binds upstream of the translation initiation region (TIR) at an unstructured ribosome standby site and thus prevents ribosomes from binding and sliding into the TIR (Darfeuille et al. 2007). Meanwhile, in a different system in *Enterococcus faecalis*, antitoxin RNAII and *fst* mRNA interact at different regions located apart and binding results in a partial RNA duplex, which improves stability of the mRNA and prevents translation (Weaver 2015).

In all *Bacillus subtilis* type I systems investigated to date, the antitoxin binds at the 3' end of the toxin mRNA to encourage degradation by endoribonuclease III (*txpA*/RatA, *bsrE*/SR5)(Durand et al. 2012; Meißner et al. 2016). Interestingly, one system, *bsrG*/SR4, promotes degradation of toxin mRNA and also induces a conformational change to block ribosome binding at *bsrE* RBS. This antitoxin has been described as bifunctional (Jahn & Brantl 2013; Brantl & Jahn 2015).

Several other regulatory principles are used to ensure tight regulation of toxin expression. Ribosome binding at the toxin SD site is prevented by molecular

base pairing (*tisB*, *shoB*, *bsrG*, *txpA*) and translation initiation may be reduced by the use of unusual start codons. Additionally, *txpA* and *yonT* mRNAs have “perfect SD sequences” that are thought to effectively recruit but slowly release ribosomes. Often, some degree of mRNA processing is required to produce translationally competent molecules (*hok*, *tisB*, *shoB*) and toxin genes may only be transcribed under certain condition (*tisB* and *symE*). Stability of toxin transcripts has been observed to be temperature dependent and toxin SymE is prone to digestion by Lon protease (Durand et al. 2012; Gerdes & Wagner 2007; Kawano 2012).

Toxins are typically small, hydrophobic proteins with transmembrane domains capable of inducing membrane pores, impairing ATP synthesis and consequently affecting transcription, translation and replication, leading to cell death. TisB toxin from *E. coli* was shown to produce groups of narrow anion-selective pores in the lipid bilayer, whilst Ldr toxin was able to cause nucleoid condensation, affecting purin metabolism and decreasing cAMP levels(Gurnev et al. 2012; Kawano 2012). Some toxins are enzymes; RalR cleaves methylated and unmethylated DNA, whilst SymE degrades RNA (Guo et al. 2014; Gerdes & Wagner 2007)

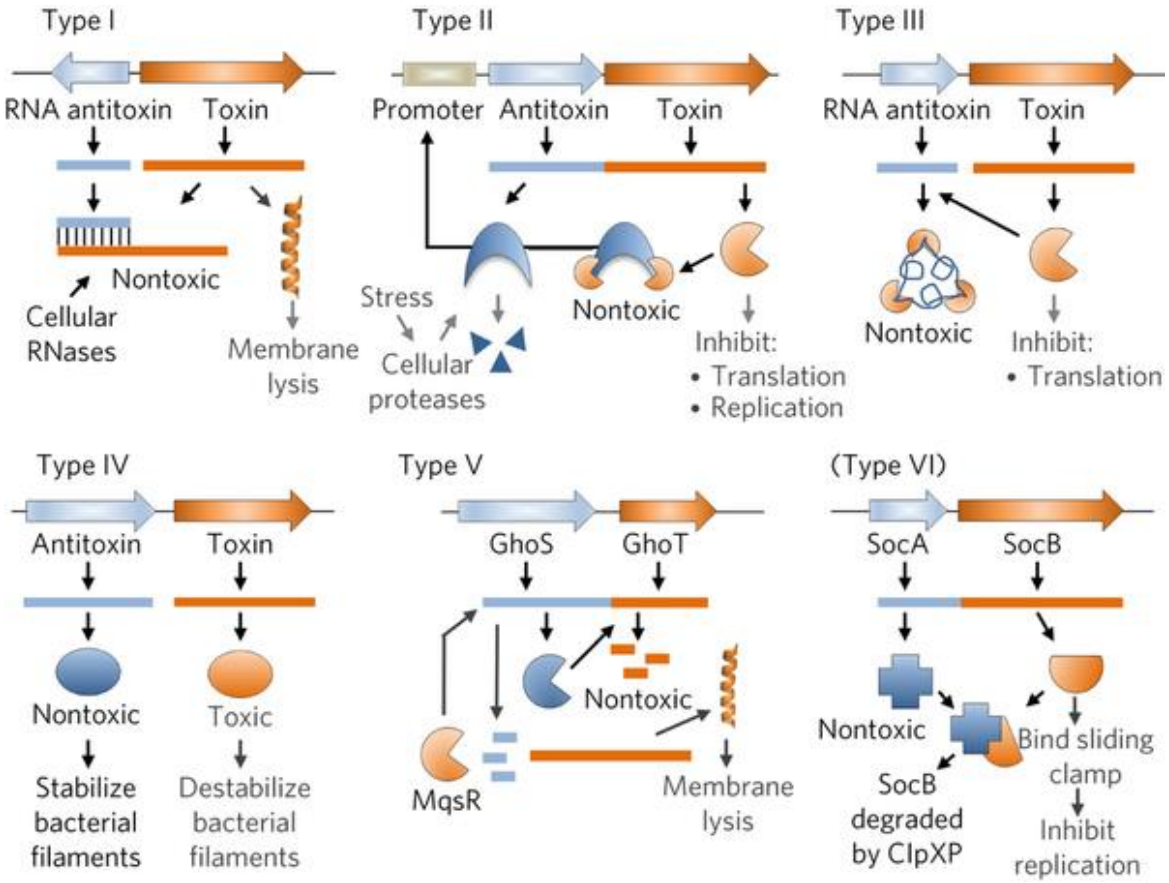

Figure 1.1: Classification of toxin-antitoxin systems. Toxins are coloured orange and antitoxins blue; non-toxic activities labelled in black font, and toxic activities labelled in grey. TA systems are classified into 6 different types: type I: the RNA antitoxin base pairs with toxin mRNA to inhibit translation; type II: both toxin and antitoxin are proteins. Under stressful conditions, cellular proteases cleave antitoxins; type III: RNase toxin preferentially cleaves antitoxin, generating an RNA pseudoknot-toxin complex; type IV: Antitoxin stabilises bacterial filaments, antagonising toxin; type V: the antitoxin GhoS is an RNase specific for the toxin ghoT mRNA; type VI: the SocA antitoxin is an adaptor protein that binds the SocB toxin to promote its degradation by ClpXP. Reprinted by permission from Macmillan Publishers Ltd: Nature Chemical Biology, (Page & Peti 2016), Copyright 2016.

.

1.0.1.2 Type II TA systems

Both the toxin and antitoxin are small proteins. Typically, both genes are grouped onto a self-regulated operon with the antitoxin encoding gene upstream of the toxin encoding gene, although there are some exceptions, for example, the *higBA* and *hicBA* modules (Tian et al. 2001; Makarova et al. 2006). Some three component systems have also been discovered, where the third component is either involved in regulating the activity of the promoter, such as the ω-ε-ζ system, identified on *Streptococcus pyogenes* pSM19035 plasmid, where ω is the regulatory component (Zielenkiewicz & Cegłowski 2005), or enhancing TA complex formation, for example, the *pasA/pasB/pasC* module from plasmid pTF-FC2 from *Thiobacillus ferrooxidans*, where PasC enhances complex formation (Smith & Rawlings 1997).

The antitoxin binds to the protein to form a protein-protein complex that remains inactive in the bacterial cytoplasm whilst conditions are not stressful. Autoregulation of transcription of the antitoxin or TA complex controls cellular levels of the complex; this process is sometimes augmented by conditional co-operativity (Gerdes & Maisonneuve 2012; Garcia-Pino et al. 2010). Antitoxins are labile and prone to degradation by Lon or Clp family proteases, whilst the toxic protein is stabile (Diago-Navarro et al. 2010; Van Melderen et al. 1996). Toxins have diverse structures and cellular targets. Type II TA systems will be discussed in more detail later.

1.0.1.3 Type III TA systems

Similar to type I systems, the antitoxin is a small RNA molecule, which acts by binding the toxic protein directly. Two type III systems have been well characterised: toxN/ToxI and abiQ/AntiQ. toxN/ToxI system was identified on a

plasmid from *Pectobacterium atrosepticum* subspecies *atroseptica* (Fineran et al. 2009). Both genes were co-transcribed, with the antitoxin encoding gene upstream of the toxin encoding gene and both genes separated by a Rho-independent transcriptional terminator. Occasional read through of this terminator results in an excess of antitoxin. ToxI antitoxin monomers are encoded by short tandem repeats that form a pseudoknot after sequence specific processing by ToxN, an RNase. Three ToxN proteins are bound by three ToxI monomers to form a complex that inhibits toxin function (Fineran et al. 2009; Tim R Blower et al. 2011).

Despite having only 31% sequence similarity to toxN/ToxI, abiQ/AntiQ has a similar gene organisation and the AntiQ is comprised of short tandem repeats that form pseudoknots. AbiQ is also an RNAse that cleaves repeats from its antitoxin (Samson et al. 2013; Brantl & Jahn 2015). Recent structure based homology searches and protein sequence comparisons identified three independent type III families, suggesting that this type of TA system is more diverse than previously thought (Blower, Short, et al. 2012).

1.0.1.4 Type IV TA systems

In this system, the antitoxin is a protein that acts as an antagonist of the toxin and does not interact with it directly. In the *E. coli yeeU-yeeV* (or *ctbA-ctbB)* system, the toxin inhibits polymerisation of cytoskeletal proteins MreB and FtsZ, preventing cytoskeletal assembly and altering cell morphology. Antitoxin YeeU counteracts YeeV by stabilising MreB and FtsZ polymers (Masuda et al. 2012). A second system, *cptA-cptB* (or *ygfX-ygfY)* had been described and has similar mechanisms and interactions (Masuda et al. 2012).

1.0.1.5 Type V systems

Only one type V system has been characterised to date; *ghoST* from *E. coli*. The toxin (GhoT) is a small, membrane lytic peptide that causes a ghost cell phenotype (cells with damaged membranes), while GhoS is a protein antitoxin with sequence specific endoribonuclease activity, which degrades toxin mRNA. This prevents translation of the toxin and is the first example of protein antitoxin inhibiting toxin expression by mRNA cleavage (Wang et al. 2012). *ghoST* is also the first TA system to be regulated by another TA system. During stress, antitoxin GhoS mRNA is degraded by type II toxin MqsR, allowing translation of toxin genes, increasing ghost cell formation and persistence (Wang et al. 2014).

1.0.1.6 Type VI TA system

A sixth type of TA system has been recently proposed. The SocAB system, where both toxin and antitoxin are proteins, was recently identified in *Caulobacter crescentus.* However, the SocA antitoxin promotes degradation of the toxin by acting as a ClpXP protease adaptor for the SocB toxin. SocB toxin inhibits DNA replication elongation through a direct interaction with a β sliding clamp (Aakre et al. 2013; Markovski & Wickner 2013).

1.0.2 Putative biological roles of TA systems

Whilst the function of TA systems identified on plasmids is well understood, the role of chromosomal TA systems is more enigmatic (Frampton et al. 2012). Chromosomal TA systems are thought to be involved in maintaining the integrity of DNA, coping with stress and may also be linked to pathogenicity. Alternatively, chromosomally encoded TA systems may have no physiological function. The antitoxin gene is indispensable for cells carrying the cognate toxin gene, demonstrating strong interdependence and suggesting that TA loci act as selfish gene elements. Any physiological functions caused by TA systems may

simply be a bi-product of TA maintenance (Van Melderen & De Bast 2009). A description of putative roles of plasmid-borne and chromosomal TA systems is given below.

1.0.2.1 Post-segregational killing (PSK)

TA systems determine plasmid maintenance using PSK. In bacterial cells containing a plasmid with TA module, both the toxin and antitoxin will be expressed. If this plasmid is not transmitted to daughter cells, depletion of antitoxin levels through degradation will activate the more stable toxin. The toxin will then inhibit the growth of, or kill, plasmid- free cells, increasing the number of plasmid-containing cells within the growing population (Figure 1.2) (Unterholzner et al. 2013; Hernández-arriaga et al. 2014).

The first TA plasmid maintenance system described was the coupling cell division (ccd) type II system, which stabilised plasmid F 10-fold; when cells with only a single copy of the plasmid divided, daughter cells containing the plasmid were able to continue dividing, while in plasmid-free daughter cells, division was arrested after only a few divisions (Ogura & Hiraga 1983; Jaffe et al. 1985) . A similar mechanism was also observed when the first type I TA system, *hok-sok*, was identified and found to increase the stability of plasmid R1 by two orders of magnitude with no change in copy number (Gerdes et al. 1986). Together, these observations established the PSK concept (Hernández-arriaga et al. 2014). More recently, PSK has been indirectly linked to virulence, for example, a pEMB1 plasmid recovered from *E. coli* isolated from soil, was found to contain a β-lactamase gene and a *parDE* TA system. The TA system enhanced plasmid stability in the absence of ampicillin (Lee et al. 2015).

PSK eliminates plasmid free cells from the population and increases the percentage of plasmid containing cells by vertical transfer (Hernández-arriaga et al. 2014).

An alternative hypothesis suggests that PSK systems have evolved through benefitting host plasmids in environments where plasmids have to compete during horizontal transfer. A plasmid-encoded *parDE* PSK system mediated the exclusion of an isogenic Δ*parDE* plasmid, supporting this “competition” hypothesis, where the success of PSK systems results from plasmid-plasmid competition rather than plasmid-host relationship(Cooper & Heinemann 2000; Cooper et al. 2010) (Figure 1.2).

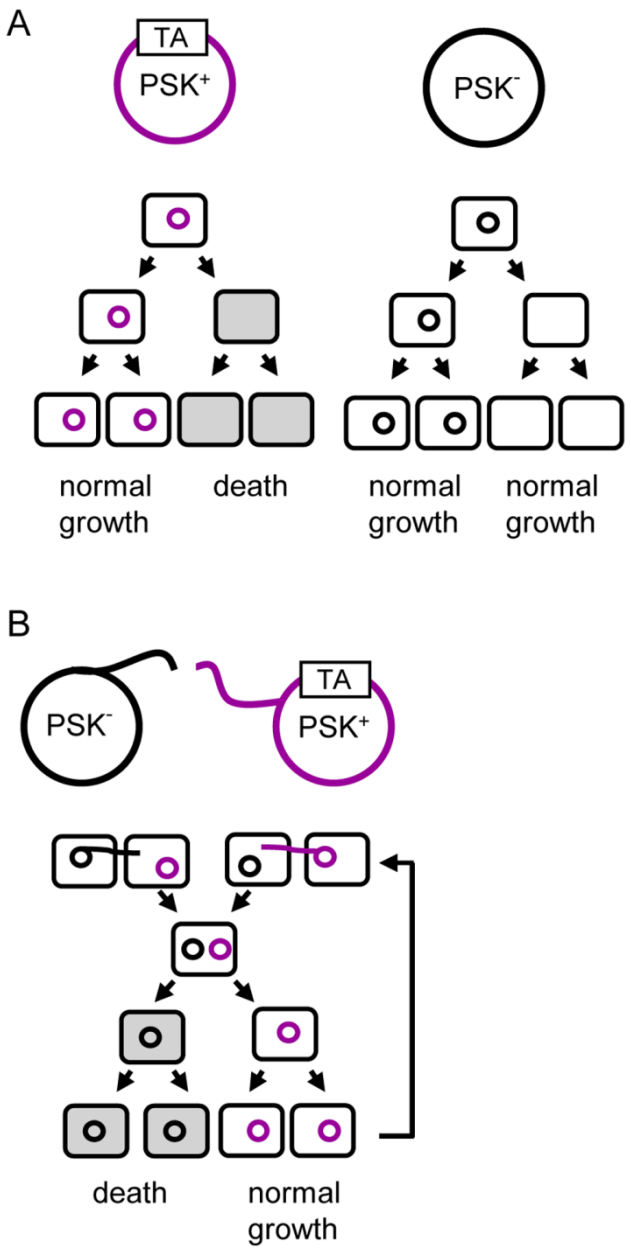

Figure 1.2: Advantage conferred by plasmid encoded TA systems. a) Vertical transmission increasing plasmid prevalence within a population by PSK. PSK+ (with TA system) plasmid is purple. When daughter cells do not inherit a plasmid copy, degradation of labile antitoxins by host proteases will free the toxin and lead to selective killing of plasmid-free bacteria. b) Horizontal transmission, PSK^+ (with TA system) plasmid (in purple) and the PSK^- (without TA system) plasmid (in black) belong to the same incompatibility group and are conjugative. Conjugants containing both plasmids are generated but only bacteria that maintain PSK+ plasmid will avoid toxin activation. Figure reproduced with permission from (Van Melderen & De Bast 2009).

1.0.2.2 Stabilisation of mobile genetic elements (MGEs)

Chromosomally encoded TA modules located with genomic islands could stabilise MGEs, using a similar mechanism to TA systems located on plasmids (Pandey & Gerdes 2005; Makarova et al. 2011). A 100kb integrative and conjugative element (ICE) identified in clinical isolates of *Vibrio chlorae* and termed SXT, was found to contain a type II TA system, *mosAT*. Expression from the *mosAT* locus was increased when SXT was excised from the chromosome before conjugation but MosA reduced expression from *mosAT* loci when integrated into the chromosome (Wozniak & Waldor 2009). A similar mechanism has also been observed in *Acidithiobacillus ferrooxidans,* where four TA systems were found to be exclusive to strains with the active mobile element ICEAfe1 and proposed to play a role in ICE maintenance (Bustamante et al. 2014).

Superintergrons (SIs) are large, stable, chromosomal, genetic elements containing many gene cassettes, which are integrated by site specific recombination. Bioinformatic analysis has revealed that TA loci were found on large SIs but not small ones (Van Melderen 2010; Rowe-Magnus et al. 2003). Introduction of two TA systems from a *Vibrio vulnificus* SI into the *E. coli* chromosome was shown to prevent deletion of flanking DNA (Szekeres et al. 2007), suggesting that TA systems located on MGEs could limit extensive gene loss. However, some chromosomally encoded TA systems, for example, *dinJ-yafQ* of *E. coli* K12 and ccd_{o157} of *E. coli* O157: H7, could not prevent deletion of flanking DNA when inserted into the chromosome, indicating that perhaps different systems could have different functions, dependent on their location (Szekeres et al. 2007; Wilbaux et al. 2007; Hernández-arriaga et al. 2014). This notion is further supported by the observation that 2 *higBA* systems from *V.*

chlorae are very efficient at stabilising an unstable replicon (Christensen-Dalsgaard & Gerdes 2006).

Interestingly, three *parDE* systems identified in *V. chlorae* chromosome II were found within a SI and showed that chromosomal TA systems might exhibit PSK. The three ParE homologues were revealed to degrade chromosome I in *V. chlorae* cells that had lost chromosome II, suggesting that chromosome mis-segregation encourages ParE mediated killing of aneuploid daughter cells (Yuan et al. 2011; Hernández-arriaga et al. 2014). Chromosome II qualifies as a "*bona fide"* chromosome but replicates like the plasmid/phage P1 and so may have evolved from an MGE (Egan et al. 2005; Srivastava & Chattoraj 2007).

1.0.2.3 Defence against bacteriophages

The evolutionary arms race between bacteria and bacteriophages has led to considerable diversity in defensive strategies and chromosomal TA modules have been linked to this. The *hok-sok* (type I) system from *E. coli* plasmid R1 was shown to exclude T4 phages and the *mazEF* (type II) system provoked abortive infection after attack by P1 bacteriophage (Pecota & Wood 1996; Hazan & Engelberg-Kulka 2004; Unterholzner et al. 2013).

The type III toxN/ToxI system was initially identified as it was able to confer resistance against bacteriophages (Hernández-arriaga et al. 2014). The ToxN toxin acts as a sequence specific endoribonuclease, processing the *toxI* RNA to generate pseudoknots that bind ToxN. After bacteriophage infection, *toxI* RNA was degraded by an unknown mechanism, releasing ToxN, resulting in growth arrest of the infected cell, and subsequently preventing replication, and propagation of the phage within the bacterial population (Fineran et al. 2009).Unsurprisingly, some phages have evolved sequences that can

neutralise ToxN by mimicking the *toxI* antitoxin sequence and allowing evasion of host defence systems (Blower et al. 2014; Blower, Evans, et al. 2012).

1.0.2.4 Gene regulation

There are several examples of TA toxins differentially shaping gene expression in bacteria by altering the transcriptome, or creating a specialised ribosome (Bertram & Schuster 2014).

Overexpression of a VapC homologue identified in *Mycobacterium smegmatis* resulted in differential expression of 3% of the genome. Carbohydrate metabolism genes showed dramatic downregulation after overexpression of VapC, demonstrating how TA systems are able to influence bacterial metabolism (McKenzie et al. 2012).

The endoribonuclease MazF from *E. coli* cleaves specifically at ACA sequences and so when induced, cleaves the bulk of all cellular mRNAs. Subsequently, up to 90% of encoded proteins are no longer produced, leading to growth impediment (Zhang et al. 2003; Yamaguchi & Inouye 2009). Unexpectedly, 16S rRNA was also processed by MazF, removing the anti-SD sequence to yield “stress ribosomes”. “Stress ribosomes” were able to translate a set of leaderless mRNAs with SD sequences that had also been clipped by MazF, producing approximately 50 proteins (Vesper et al. 2011).

YafQ toxin (structurally similar to RelE) associates with the 50S ribosomal subunit to cleave selected mRNAs at AAA [AG] consensus sequences. The AAA codon is overrepresented at codon +2 in secretory proteins, suggesting that expression of YafQ might specifically arrest their translation (Zalucki et al. 2007). The ribonucleic activity of RelE has also been linked to significant changes in the proteome (Korch et al. 2015).

Finally, the MqsRA type II TA system has been shown to regulate expression of *ghoST* type V TA system. MqsR toxin enriches *ghoT* mRNA *in vivo* and *in vitro* as the *ghoT* transcript lacks the primary recognition site of MqsR toxin (Wang et al. 2013).

1.0.2.5 Programmed cell death (PCD)

PCD is not restricted to multicellular organisms; bacterial communities can induce death in part of the population after exposure to various stress conditions. Typically, PCD is induced by TA mechanisms in response to oxidative stress, exposure to radiation, nutrient deprivation or phage infection (Allocati et al. 2015).

PCD in *E. coli* is facilitated by the *mazEF* type II TA system and dependent on a quorum-sensing linear pentapeptide named extracellular death factor (EDF). The EDF specifically acts on toxin MazF, magnifying its enzymatic activity. However, not all groups report this as a universal phenomenon (Christensen et al. 2001; Tsilibaris et al. 2007). Similar results in *E. coli* have also been observed with *chpBIK* type II system (Hazan & Engelberg-Kulka 2004; Belitsky et al. 2011).

Intriguingly, EDFs have been identified from Gram positive *B. subtilis* and Gram negative *Pseudomonas aeruginosa,* which were able to trigger *mazEF* in *E. coli*. This suggests that induction of PCD by EDFs may be used by one bacterial species undergoing stressing conditions, to kill a different species in a mixed population (Kumar et al. 2013).

1.0.2.6 Persister cell formation

Persistence was first described in the 1940s, when a small population of persister cells survived treatment with penicillin through dormancy, a different

mechanism to traditional antibiotic resistance (Hobby et al. 1942; Bigger 1944). The characteristics used to define the persister phenotype are frequently updated but persister cells comprise a subpopulation of genetically identical, metabolically slow-growing cells, which are tolerant of antibiotics and other environmental stresses (Page & Peti 2016).

The first gene directly associated with persistence was *E. coli hipA* encoding high persister protein (Hip) A, a kinase that inactivates glutamyl-tRNA synthesase (Germain et al. 2013; Kaspy et al. 2013). A *hipA* variant, *hipA7*, increased persistence ~100 – 1,000- fold as it destabilised the oligomers that formed when the HipBA complexes bound to the *hipBA* operator, rendering the toxin more active (Moyed & Bertrand 1983; Schumacher et al. 2015). HipA toxin activity was revealed to lead to the ppGpp-mediated activation of type II RNase toxins and consequently persistence (Germain et al. 2015).

While it may not always be possible to elucidate the role of individual TA loci, the importance of type II RNase toxins in persistence has been demonstrated extensively. Microarray experiments on *E. coli* persisters revealed that multiple type II toxins, especially RNase toxins, were highly upregulated in persisters compared to non-persister cells (Keren et al. 2004; Shah et al. 2006). A direct role for TA systems was also evidenced by ectopic expression of RNase toxins (increases persistence) and the deletion of TA loci (deletion of ten TA systems from *E. coli* resulted in 100-fold reduction in persistence) (Harrison et al. 2009; Keren et al. 2004; Kim & Wood 2010; Maisonneuve et al. 2011). Examples of the importance of type II TA systems in persistence are not limited to *E. coli*. Recent studies have demonstrated that systematic deletion of individual type II TA modules from *Salmonella* reduced macrophage-induced persisters and

highlighted 14 different type II TA systems that were activated once cells were phagocytosed (Helaine & Kugelberg 2014).

Type I toxins have also been linked to persistence. Obg, a GTPase that is universally conserved, induced persistence through activation of transcription of *hokB*. Toxin HokB acts to depolarise the bacterial cell membrane, leading to persistence. Interestingly, whilst the exact molecular mechanism for *hokB* activation by Obg is unknown, it was found to rely on ppGpp (Verstraeten et al. 2015).

Cells entrance into and exit from the persister state is closely linked to TA expression. Persister cells are formed when toxin concentration exceeds a threshold set by that of its antitoxin concentration (Page & Peti 2016). Levels of free toxin within the cell are controlled by toxin sequestration in complexes of differing stoichiometry, rather than by gene regulation. If the toxin translation rate exceeds twice the antitoxin translation rate, toxins accumulate within cells (Figure 1.3) (Gelens et al. 2013).

Some cells within a population may enter persistence when they experience micro-starvation conditions due to local accessibility of nutrients within the population. Nutrient deprivation increases the level of alarmone (p)ppGpp, activating Lon protease and subsequently resulting in antitoxin degradation. The overall result switches the TA ratio from low to high, allowing the newly freed toxin to exert its effects (Germain et al. 2015; Maisonneuve & Gerdes 2014; Maisonneuve et al. 2013).

How bacterial cells exit persistence using TA systems is less well characterised. One potential mechanism used by type II TA systems is conditional cooperativity (Afif et al. 2001; Garcia-Pino et al. 2010). Typically, type II TA loci

are transcriptionally autoregulated (Guglielmini & Van Melderen, 2011) and antitoxins are able to bind both DNA and their cognate antitoxin. Antitoxins bind to one or more operators within the promoter of their TA loci, thus repressing transcription. DNA binding is often enhanced when cognate toxins are bound to the antitoxin, resulting in a more potent repression of transcription than would be observed with the antitoxin alone (Page & Peti 2016; Gotfredsen & Gerdes 1998; Afif et al. 2001; Garcia-Pino et al. 2010; Overgaard et al. 2009). In the Doc/PhD TA system, it was observed that large excesses of toxin de-repressed rather than repressed transcription (Magnuson & Yarmolinsky 1998). The switch from a repression to a de-repression complex was accompanied by changes in oligomerisation states. Similar studies on *ccdAB* revealed that maximal DNA binding (and so repression) was observed when the ratio of CcdB (toxin): CcdA (antitoxin) was 1:1. Ratios above 1 abolished DNA binding and enhanced transcription (Afif et al. 2001). From these observations, it was suggested that under conditions of excess toxin, transcription and translation of both toxin and antitoxin would increase, generating a ratio of CcdB:CcdA that would permit cells to exit persistence and grow normally (Page & Peti 2016). Several other TA systems have been shown to be regulated by conditional cooperativity: *relBE*, *parDE*, *kid/kis, vapBC* and *phd/doc* (Overgaard et al. 2009; Johnson et al. 1996; Monti et al. 2007; Wang et al. 2013; Magnuson & Yarmolinsky 1998).

The molecular basis of conditional cooperativity has been observed for *relBE* TA system (Figure 1.4). Antitoxin RelB has a weak affinity for its operator, whilst the RelB2-RelE complex binds extremely tightly to inhibit transcription from the locus. Any further increases in toxin RelE concentration destabilised DNA

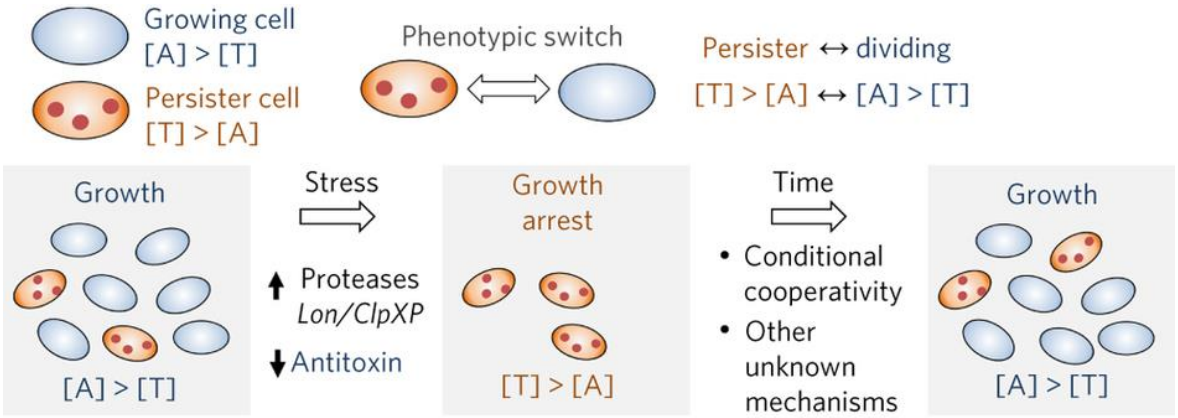

Figure 1.3: TA systems and persistence. Growing cells are coloured blue and the concentration of antitoxin [A] exceeds that of the toxin [T]. The reverse is true of persister cells, coloured orange, where the concentration of toxin [T] exceeds the antitoxin [A] concentration. To switch phenotypic states, the ratio of [T]: [A] has to change. Within a growing population, a small number of cells will be in the persister state; exposure to stress, for example, antibiotics or nutrient deprivation, activates bacterial proteases, which cleave antitoxins, leaving behind an excess of toxin. How cells exit persistence is less well characterised. Reprinted by permission from Macmillan Publishers Ltd: Nature chemical biology, (Page & Peti 2016), copyright 2016.

binding, resulting in an affinity similar to RelB alone (Overgaard et al. 2009; Page & Peti 2016). The 3D structure of a $RelB_2E_2$ complex reveals why DNA binding is not possible (Boggild et al. 2012). Two $RelB_2E$ complexes may bind the operator with no problems. However, increased concentrations of RelE led to formation of $RelB_2E_2$ complexes, which cannot bind the operator as the additional RelE molecules clash with neighbouring proteins. Failure of the complexes to bind both operators at the same time resulted in de-repression of the operon and an increase in transcription (Page & Peti 2016).

The conditional cooperativity hypothesis in TA systems, combined with the growth inhibition activity of free toxin molecules explains how TA systems can provide the bi-stability necessary to support one actively growing population and one dormant population within a single culture (Cataudella et al. 2013; Gelens et al. 2013).

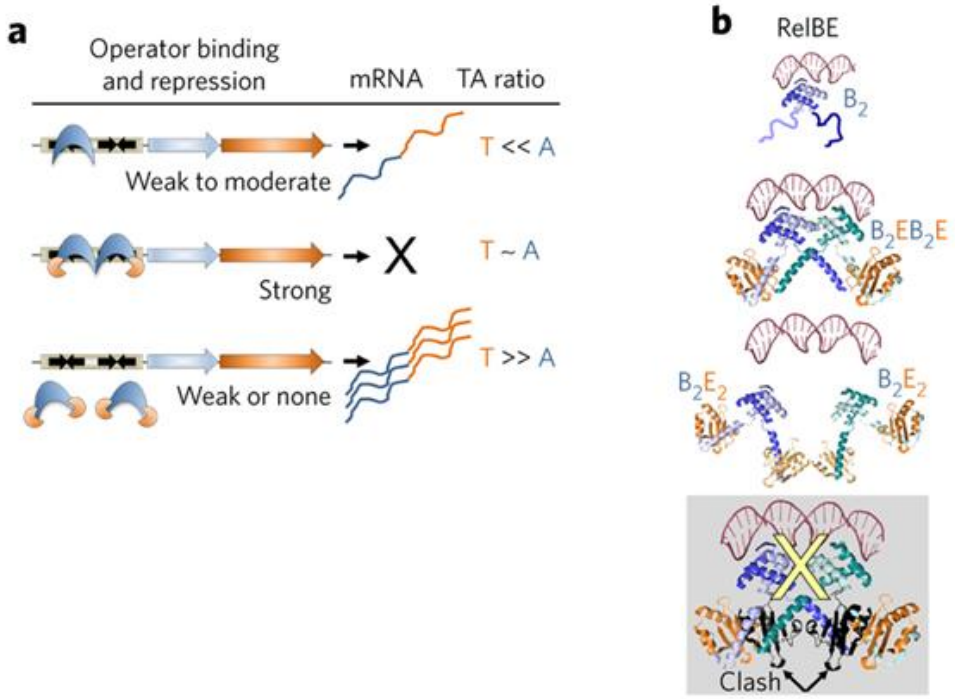

Figure 1.4: Molecular basis of conditional cooperativity. a) Picture illustrating oligomerisation states of TA complexes, their abilities to bind their promoters and resulting transcription levels. Gene loci are represented as arrows, toxins in orange, antitoxins in blue and promoters in beige. b) In the absence of RelE (orange), antitoxin RelB (blue) binds its promoter, which has two adjacent operators, with weak affinity. At a 2:1 RelB: RelE ratio, both operators are bound by the RelB dimers but only one RelB within the dimer is bound to RelE toxin. Increases in concentrations of RelE lead to a 1:1 ratio and a RelB-RelE complex that is incompatible with DNA binding as newly bound RelE would clash with the adjacent B2E2 dimer. Figure adapted from (Page & Peti 2016).

1.0.2.7 Biofilms

A biofilm could be described as a population of microbial cells embedded within an extracellular matrix that adheres to both biotic and abiotic surfaces. The extracellular matrix is mostly composed of polysaccharides, glycoproteins and DNA, which enables adhesion and protects the bacterial cells from the surrounding environment. Within a biofilm, the population displays multicellular-like behaviour (Stewart & Franklin 2008; Sauer et al. 2007; Martínez & Vadyvaloo 2014).

Biofilms are heavily involved in the majority of human bacterial chronic inflammatory and infectious diseases, and pose a serious therapeutic challenge (Hall-Stoodley et al. 2004; Barbara & Hayes 2016). Biofilms are also multidrug tolerant and are one of the main strategies used by pathogenic bacteria to survive against host immune defence (Rybtke et al. 2011). Biofilms are involved in recalcitrance of infections due mostly to the presence of persister cells within the matrix; upon treatment with antibiotic, the majority of the cells are killed, except the persisters. The immune system cannot reach the biofilm-embedded cells and so the persisters may then repopulate the biofilm (Lewis 2007; Lewis 2010).

Development and formation of biofilms is well-controlled and the transition between planktonic and biofilm phases requires precise and well-coordinated gene expression (Ren et al. 2004; Wen et al. 2014). In *E. coli*, biofilm production has been shown to be influenced by multiple TA systems (Barbara & Hayes 2016). The role of the MqsR-MqsA type II pair was the first identified in biofilm formation and is the best documented. Antitoxin MqsA directly inhibits expression of RpoS, the master regulator of stress that controls expression of up to 10% of genes involved in the response to various different stresses (Wang

et al. 2011). MqsA has also been shown to decrease production of CsgD, a master regulator that activates expression of several important components of the extracellular matrix (Soo & Wood 2013; Brombacher et al. 2006). Finally, MqsA has been linked to increased motility though activation of *flhD,* a regulator of flagella biosynthesis (Barbara & Hayes 2016). Under stressful conditions, MqsA is degraded by Lon protease, leading to de-repression of *rpoS* and *csgD*, and inhibition of *flhD*, resulting in decreased motility and increased biofilm formation (X. Wang et al. 2011).

Toxin MqsR has also been linked to the regulation of biofilm production. Expression of *mqsR* is stimulated by autoinducer 2 (AI-2), which controls flagellar synthesis, chemotaxis and motility in *E. coli* (Ren et al. 2004; Wood 2009; González Barrios et al. 2006; Barbara & Hayes 2016). MqsR also indirectly inhibits synthesis of McbA, preventing production of colonic acid, an exopolysaccharide important for formation of the biofilm architecture (González Barrios et al. 2006; Zhang et al. 2008; Prigent-Combaret et al. 2000). Additionally, MqsR post-transcriptionally regulates GhoST, a type V system that has been linked to early biofilm formation and motility (Wang et al. 2012).

The HipBA system has also been shown to influence biofilm formation through the production of extracellular DNA (eDNA) required for the biofilm matrix. Activation of HipA toxin affects the integrity of *E. coli* cells and may induce lysis of a subpopulation to increase the eDNA concentration (Zhao et al. 2013).

TA systems have also been implicated in the formation of biofilms in species other than *E. coli*. In *Burkholderia cenocepacia,* expression of TA modules was found to be higher in in untreated sessile cells than in untreated planktonic cells and RelE and VapC toxin homologues were found to contribute to biofilm

formation (Van Acker et al. 2014). In *B. subtilis,* TxpA and YqcG toxins were found to eliminate defective cells from biofilms to ensure symmetry is maintained. Toxin TxpA was also able to act to dissolve and lyse established biofilms (Bloom-Ackermann et al. 2016).

Several TA systems were upregulated in biofilm cells in *Treponema denticola*, a spirochete associated with chronic periodontitis (Mitchell et al. 2010), whilst MqsRA from *Xylella fastidiosa* was found to positively regulate biofilm formation and negatively regulate cell movement (Merfa et al. 2016).

1.0.2.8 Virulence

TA systems are indirectly involved in virulence through maintenance of MGEs, PSK, PCD and persister cell formation. However, TA systems have also been described as having a direct impact on the pathogenicity of bacteria, and the identification of a correlation between the number of TA modules in the genome and the virulence capacity of bacteria, would support this description (Wen et al. 2014; Georgiades & Raoult 2011).

The existence of a subpopulation of persister cells is certainly an important aspect of the protracted infection caused by *Mycobacterium tuberculosis.* Reawakened persisters from the latent infection trigger recurrent relapses, characteristic of the disease (Getahun et al. 2015). However, TA systems have also been linked to mycobacterial pathogenesis in other ways. Three TA systems, two *relBE* cassettes and one *yefM-yoeB* locus are upregulated in response to nitrogen starvation and oxidative stress, and down regulated in response to hypoxia, all conditions relevant to those prevailing during *M. tuberculosis* infection (Sala et al. 2014; Barbara & Hayes 2016; Korch et al. 2009; Ramage et al. 2009). Hypoxia also increases expression of one of the

many *vapBC* homologues and a *higBA* locus (Ramage et al. 2009). Nevertheless, deletion of any of these homologues did not affect survival or persistence in mice (Singh et al. 2010). Interestingly, although expression of the two *relBE* cassettes and one *yefM-yoeB* locus could not be detected during the early or middle stages of infection, expression of both *relE* genes, one of the *relB* genes and *yoeB* gene was apparent in late stage infection (Korch et al. 2009). Macrophages from the immune system phagocytose infecting microbes so expression of TA genes, specifically at the late infection stage, suggests that the genes may be involved in bacterial survival in this specific hostile environment (Barbara & Hayes 2016).

In uropathogenic *E. coli* (UPEC), individual deletions of seven type II TA loci revealed that mutants lacking *pasTI,* were outcompeted by the wild type strain in the kidneys, but not the bladder, of a mouse model urinary tract infection (UTI) system. Deletion of *pasTI* also reduced kidney colonisation but not gastrointestinal tract colonisation. How the *pasTI* locus facilitates kidney colonisation is not known (Norton & Mulvey 2012).

Expression of *chpBK* and *mazEF* genes was elevated in *Leptospirosis interrogans* within human macrophages compared to bacterial cells in culture medium. Mutants lacking either TA module were able to induce late stage apoptosis less efficiently than wild type, suggesting that the *chpBK* and *mazEF* TA loci have roles in cellular necrosis by *L. interrogans* (Komi et al. 2015). Similarly, a VapC toxin homologue in *Rickettsia* species has been linked to host cell apoptosis. *Rickettsia* species with multiple type II TA systems promote higher levels of host cell apoptosis than species with fewer TA genes (Audoly et al. 2011; Socolovschi et al. 2013; Botelho-Nevers et al. 2012).

Type I TA loci have also been shown to contribute to pathogenicity. The *hok/sok* locus from *E. coli* prolonged the lag phase of host cell cultures, allowing cells time to adapt before increasing the growth rate at exponential phase. As well as increasing propagation of resistance genes and tolerance to β-lactam antibiotics, this locus enhanced survival of cells grown at high temperature and at a low starting cell density. Finally, the *hok/sok* locus might complement an existing or defective SOS mechanism. All of these effects would enhance the ability of pathogenic bacteria to establish infections and so might contribute to virulence (Chukwudi & Good 2015).

1.0.3 Biotechnological and therapeutic applications of TA systems

Infectious diseases are one of the leading causes of human mortality worldwide and increasing antimicrobial resistance threatens effective treatment of bacterial diseases (Lee & Lee 2016). TA systems are attractive antibacterial targets as they are widely distributed in bacteria but not in eukaryotes. Several strategies have been suggested on how TA systems could be exploited for the development of novel antibiotic drugs.

One proposed strategy is to artificially activate the toxin by disrupting TA complex formation (Ghafourian et al. 2014; Ghafourian & Raftari 2012; Williams & Hergenrother 2008). In type II systems, this would involve using structural and biochemical information available on TA complexes to design peptides that inhibit interactions at the TA interface. The crystal structure of VapBC30 from *M. tuberculosis* was used to design peptides to mimic the TA interface. Three peptides of varying lengths mimicking part of the toxin were tested and two were found to increase the ribonuclease activity of VapC (I.-G. Lee et al. 2015). Meanwhile, an octapeptide predicted to form an α helix was found to occupy the TA binding interface between PemK and PemI from *B. anthracis,* inhibiting TA

complex formation but also decreasing the ribonuclease activity of toxin PemK (Chopra et al. 2011). The limited information available on TA protein-protein interactions and the size of the TA protein interface present difficulties when trying to identify suitable peptides. Care must also be taken to target toxins that are effective at mediating cell death, rather than inducing persister cell formation and contributing to chronic infection (Lee & Lee 2016).

In other types of TA systems it is possible to disrupt complex formation using antisense RNA that binds to antitoxin encoding mRNA without affecting translation of the toxin. One example of this method is the sequestration of type I antitoxin Sok-RNA by anti -Sok peptide nucleic acid (PNA) oligomers. The oligomers competitively inhibited *hok* mRNA:: Sok-RNA interactions. In *E. coli* cells harbouring *hok/sok,* the anti-Sok PNAs were more bactericidal than the antibiotic rifampicin and expression resulted in ghost cell formation (Faridani et al. 2006).

A second proposed strategy involves increasing the rate of degradation of bound antitoxin by Lon or Clp proteases, resulting in premature release of toxins and cell death. Over-expression of Lon protease activates YoeB from its complex with YefM and leads to inhibition of global translation and cell death (Christensen et al. 2004). Several other antibiotic molecules that bind to activate ClpP in other systems have already been identified (Leung et al. 2011; Famulla et al. 2016). Biomolecules that are able to bind to the DNA promoter and subsequently prevent further transcription would also be of interest.

Finally, toxin molecules themselves can be treated as potential antimicrobial drug candidates. However, the poor oral availability and high costs of bioprocessing make this proposal unlikely to be realised (Lee & Lee 2016).

Toxins may also be poor choices as potential antimicrobials as several are capable of lysing bacterial and eukaryotic cells. The PepA1 type I toxin from *Staphylococcus aureus* was found to lyse bacteria and human erythrocytes, though chemical optimisation was able to enhance its antibacterial activity and decrease the haemolytic side effects (Sayed et al. 2012; Solecki et al. 2015). Toxins may also be difficult to deliver to the site of infection, although bacteriophages would be able to deliver toxin genes into specific pathogens (Huys et al. 2013).

PepA1 is not the only toxin capable of targeting eukaryotes. When RelE toxin was expressed in a human osteosarcoma cell line, it was able to retard growth and cause cell death through apoptosis (Yamamoto et al. 2002). Toxin MazF has also been suggested as a suitable candidate for gene therapy as when expressed in human embryonic kidney cells that had formed a tumour in mice, it was able to make the tumours regress (Shimazu et al. 2014). Zymogenised MazF was also able to cleave cells infected with hepatitis C, a prominent cause of chronic liver disease (Shapira et al. 2012). Finally, the Kid toxin from *E. coli* has also been repurposed to demonstrate selective killing of oncogenically stressed human cells (Preston et al. 2016).

TA systems have been used in several expression systems as they provide plasmid maintenance without the need for antibiotics. The GATEWAY system cloning vectors include the *kid* gene to facilitate cloning. Cloning sites within the vectors are designed to disrupt toxin expression when DNA has successfully inserted, and cells harbouring plasmids without an insert do not grow (Walhout et al. 2000).

The Gene Guard system is a plasmid system designed for safety to reduce unintentional plasmid propagation in *E. coli* and *B. subtilis* and uses toxins ζ or Kid in an auxiliary manner to make the vector disadvantageous for strains lacking the cognate antitoxin (Wright et al. 2015) . A similar “containment” system was developed using the *relBE* system for *Saccharomyces cerevisiae*, where RelE toxin expression was controlled under lab conditions using a glucose-repressible promoter and basal RelB expression (Kristoffersen et al. 2000).

Lastly, TA systems have been used to improve yields in microbial production. Inducible cell lysis systems, such as PCD, facilitate the release of products from cells on an industrial scale, whilst keeping production costs down (Gao et al. 2013). A novel food grade expression system for *B. subtilis* was stabilised by TA systems, generating a greater biomass and increasing the amount of product when compared to expression systems where antibiotics are used (Yang et al. 2016).

1.1 Type II TA systems

In type II systems the antitoxin is a labile protein (Leplae, Geeraerts, Hallez, *et al.*, 2011) capable of neutralising the toxin by sequestering it in a protein-protein complex and rendering it post-transcriptionally inactive (Galvani et al. 2001; Lee & Lee 2016). However, under stressful environmental conditions (Yamaguchi et al. 2011; Kolodkin-Gal & Engelberg-Kulka 2008) the antitoxin is rapidly degraded by ATP-dependent proteases, such as those from Clp and Lon families (Christensen et al. 2001; Christensen et al. 2004; Lehnherr & Yarmolinsky 1995; Diago-Navarro et al. 2013), releasing the toxin and resulting in cell growth arrest or death (Yamaguchi et al. 2011; Unterholzner et al. 2013).

In response to amino acid starvation, bacteria downregulate synthesis of rRNAs and tRNAs by increasing the concentration of the alarmones, tetraphosphate (ppGpp) and penta-phosphate (pppGpp). Both ppGpp and pppGpp are synthesised by RelA, which is activated by uncharged tRNAs present at the ribosomal A-site. Both alarmones also accumulate in response to carbon starvation and due instead to the inhibition of SpoT. The increased concentration of alarmones directs RNA polymerase towards the synthesis of biosynthetic operon mRNAs (rather than stable RNAs) and are bound to RNA polymerase and subsequently decrease the half-life of promoter open complexes. ppGpp and pppGpp also inhibit exopolyphosphatase (PPX), which results in accumulation of polyphosphate (PolyP) , a signalling molecules that binds to Lon protease, directing it to degrade available ribosomal proteins to generate amino acids for protein synthesis (Gerdes, Christensen & Løbner-Olesen 2005).

Levels of transcription of the TA system are governed by the differing binding stoichiometry of antitoxins and TA complexes and their ability to repress transcription; this mechanism is called conditional cooperativity (Lee & Lee 2016; Page & Peti 2016).

Antitoxins typically form dimeric proteins and within each monomer, the N-terminus is usually required for dimerization and the C-terminus for binding the toxin. Generally, antitoxins block the catalytic site of the toxin molecule, however, as antitoxins are intrinsically disordered and fold upon binding to the toxin, this can make it difficult to determine the structure (Lee & Lee 2016).

Differing toxic modes of action, sequence homology and structural features have allowed type II TA systems to be further classified into families (and sub-families) (Gerdes, Christensen & Lobner-Olesen 2005; S. J. Park et al. 2013).

1.1.1 Identification of type II TA systems and confirmation of their activity

Candidate TA systems are often identified initially by bioinformatics, using programmes such as RASTA or BLAST (Butt et al. 2013; Jurenaite et al. 2013). However, it is still necessary to confirm functionality experimentally, typically by over-expression of TA toxins in their native host or *E. coli* and monitoring cultures for growth arrest or cell death (Zheng et al. 2015; Iqbal, Guérout, et al. 2015). Recently, type II TA systems were identified through shotgun cloning, as a functional toxin may only be cloned with its cognate antitoxin. During shotgun Sanger sequencing the whole genome is randomly fragmented, ligated into a vector and transformed into *E. coli.* If a toxin is detached from its antitoxin, the clone will no longer grow and will not be recovered (Sberro et al. 2013).

1.1.2 Distribution of type II TA systems

Type II TA systems are widely distributed and the number of systems present varies greatly, not only between species but also between isolates from the same species(Raphaël Leplae et al. 2011) . On average, bacterial chromosomes and plasmids encode 3.8 and 0.4 type II TA systems respectively (Goeders & Melderen 2014). Toxin-antitoxin systems are present in nearly all free-living prokaryotes (Pandey & Gerdes , 2005) and there is some evidence to suggest that the number of TA loci present in an loci present in a genome is dependent on the lifestyle of the organism.

Bioinformatic analysis of 126 complete prokaryote genomes revealed that species that appeared to lack TA loci were mostly obligate, host associated

parasites or came into close contact with other organisms. Almost all free-living bacteria living in changing environments have multiple TA loci, whereas bacteria living in constant environments have few (Pandey & Gerdes 2005).

This same analysis also determined that the number of TA modules within the genome is not directly correlated to its size but rather to the growth rate of free living prokaryotes. Both *Nitrosomas europea*, an obligate chemolithotrophic soil organism with 43 TA loci and *M. tuberculosis,* with over 30 TA loci (Park et al. 2013), have many TA systems and are both associated with low growth rates. In contrast, only two TA loci were identified in *M. smegmatis* the fast growing relative of *M. tuberculosis* (Pandey & Gerdes 2005).

1.1.3 Classification of type II TA systems into families

Type II TA systems were classified into 14 families based on structural features, amino acid sequence similarity of toxins and the assumption that each toxin was specifically associated with one antitoxin family (Guglielmini & Van Melderen, 2011). Eleven of these families are two component systems and three are three component systems (Table 1.1). However, the identification of functional 'hybrid' systems within genomes, where the toxin is from one family, for example, RelE, and the antitoxin from a different family, for example, VapB, has led to suggestions that type II TA components should be classified separately into superfamilies (Leplae, Geeraerts, Hallez, *et al.*, 2011; Anantharaman & Aravind, 2003). Seventeen toxin super-families, their representative sequences and activities have been experimentally validated, including, RelE/ParE, CcdB/MazF, Zeta, Doc, VapC, HipA, YafO, VapD, RnlA, HicA, GinA, GinC, GinD, GinE, GinF, GinG and GinH, but this nomenclature is not widely used in the literature at the present (Leplae, *et al.*, 2011).

Table 1.1: The fourteen type II TA families in prokaryotes

TA family name	Toxin	Antitoxin	Target	Cellular process
Ccd	CcdB	CcdA	DNA gyrase	Replication
HicBA	HicA	HicB	RNA cleavage	Translation
HipBA	HipA	HipB	Phosphorylate EF-Tu	Translation
MazEF (ChpA)	MazF (ChpAK)	MazE (ChpAI)	mRNA cleavage	Translation
ParD (PemKI)	Kid (PemK)	Kis (PemI)	mRNA cleavage	Translation
ParDE	ParE	ParD	DNA gyrase	Replication
Phd-Doc	Doc	PhD	Ribosome	Translation
RelBE [1]	RelE	RelB	Ribosome	Translation
VapBC (Vag)[2]	VapC	VapB	Endoribonuclease	Unknown
MosAT	MosT	MosA	Unknown	Unknown
YeeUV	YeeV	YeeU	Unknown	Unknown
ω-ε-ζ	ζ	ε	Phosphotransferase	Unknown
PasABC	PasB	PasC	Unknown	Unknown
PaaR-PaaA-ParE	ParE	PaaA	DNA gyrase	Replication

[1] Five subfamilies: RelBE, HigBA, YefM-YoeB, YgiTU(MqsAR) and PrlF-YhaV

[2] Two subfamilies: YapBC and Bat-Bto.

Adapted from (S. J. Park et al. 2013).

1.1.4 Interactions between type II toxins and their targets

Type II toxins target key cellular processes, including but not limited to replication, translation and peptidoglycan synthesis (Yamaguchi et al. 2011; Unterholzner et al. 2013). A brief description is given below.

1.1.4.1 DNA replication

CcdB and ParE toxins both target DNA gyrase (Miki et al. 1992). DNA gyrase is a class II topoisomerase, an enzyme that introduces negative supercoils into the DNA using ATP. The enzyme also has double-strand break and re-joining activity. CcdB toxin does not generate double stranded breaks by itself but inhibits the re-ligation step of DNA gyrase, through binding to the A subunit of the molecule and stabilising the resulting complex (Gerdes, Christensen & Løbner-Olesen 2005). This generates double stranded breaks (Bernard et al. 1993) ParE also targets DNA gyrase, although through a different mechanism requiring ATP (S. J. Park et al. 2013).

1.1.4.2 Ribosome dependent mRNA interferases

The RelE toxin cleaves ribosomally bound RNA by at the A-site of the ribosome and is perhaps the best studied ribosome dependent mRNA interferase (Christensen & Gerdes 2003). Cleavage occurs between the second and third bases of A-site codons. Cleavage efficiency is also dependent on the codon present at the ribosomal site. UAG and UAA codons are cleaved 800- and 100-fold, respectively, more efficiently than stop codons (Gerdes, Christensen & Lobner-Olesen 2005).

YoeB, a homologue of RelE, also requires the ribosome for cleavage of mRNA. In contrast to RelE, YoeB associates with the 50S ribosomal subunit and

cleaves immediately downstream of the initiation codon (Yamaguchi & Park 2011).

The HigB toxin binds to the 50S region of the 70S subunit and cleaves A-rich sequences in mRNA. Ribonuclease activity is only displayed when HigB is associated with the ribosome, but the toxin is able to cut in frame and out of frame AAA sequences all of the time (Hurley & Woychik 2009)**.**

1.1.4.3 Ribosome independent mRNA interferases

MazF is by far the best studied RNAse and cleaves mRNA at ACA sequences, although characterisation of MazF homologues from have revealed recognition sites of 3, 5 or 7 base pairs long (Christensen & Gerdes 2003; Zhang et al. 2003; Jørgensen et al. 2009; Winther & Gerdes 2011). Unusually, MazF is also capable of degrading its own mRNA, suggesting that expression could be negatively regulated (Hazan et al. 2004). E. coli ChpBK, a toxin homologous to MazF, is a sequence-specific endoribonuclease cleaving single-stranded mRNAs at ACA, ACG, and ACU sequences (Belitsky et al. 2011).

Other ribosome independent mRNAases include HicA and VapC. HicA cleaves mRNA and tmRNA at an unknown recognition sequence (Jørgensen et al. 2009). VapC toxins belong to the PIN-domain family and inhibit translation by either cleaving tRNAfMet in the anticodon stem loop, or cleaving mRNA at -AUA(U/A)-hairpin-G- sequences or by sequence-specific RNA binding (Cook et al. 2013).

1.1.4.4 Ribosomes

Doc toxin, from PhD-Doc system, inhibits translation elongation by associating with the 30S ribosomal subunit, in the same 16S rRNA region in the ribosome as hygromycin B (Liu et al. 2008).

1.1.4.5 Cell wall formation

ζ toxin inhibits cell wall formation by phosphorylation of the peptidoglycan precursor uridine diphosphate-N-acetylglucosamine (UDP-GlcNAc), inhibiting MarA protein, which catalyses the first step in peptidoglycan synthesis (Mutschler et al. 2011).

1.1.4.6 Elongation factor TU (EF-Tu)

HipA can autophosphorylate itself, subsequently phosphorylating elongation factor EF-Tu. EF-Tu is essential for translation as it catalyses aminoacyl-transfer RNA binding to the ribosome. As GTP is hydrolysed to GDP, EF-Tu undergoes a conformational change and so can no longer bind to ribosomes (Germain et al. 2013).

1.1.5 Interaction between toxins and antitoxins

Determination of many TA complexes by X-ray crystallography or NMR has revealed many of the protein-protein interactions responsible for complex formation. Comparison of these structures has revealed that TA systems, with very little sequence homology, share 3D structural homology (S. J. Park et al. 2013). The structures of antitoxins and TA complexes from *E. coli* (and one from *Y. pestis)* are depicted in Figure 1.5.

It is possible to classify type II and type III toxins into 6 different sub-groups based on structural similarity. The first sub-group consists of members

of the Kid family (Kid, MazF, CcdB and YdcE) and act primarily as mRNA interferases (except CcdB). These proteins are composed of compact globular folds with anti-parallel beta-sheet cores surrounded by α-helices. The second sub-group contains RelE, MqsR and YoeB, which have a four β –strand core, surrounded by 4 α helices. The other four groups include VapC family, which contains a PIN domain consisting of a 3-layer α/βα sandwich around a central 5- stranded β-sheet, the HipA toxin family which is similar structurally to Ser/Thr kinase, the phosphyltransferase ζ toxin and the α-helical Doc toxin (Blower et al. 2011)

Generally, type II antitoxins have two domains; one for binding its cognate toxin and one for binding DNA within its operon (Yamaguchi & Park 2011). The DNA binding domain may be either a helix-turn-helix (HTH) or a ribbon-helix-helix (RHH) and binds to a palindromic sequence within the promoter region (Seok et al. 2007; Brown et al. 2004; Fasani & Savageau 2015).

Antitoxins bind their cognate toxins though hydrophobic and electrostatic interactions, and may interact directly with the active site of the toxin, or indirectly by binding elsewhere and causing a conformational change to prevent substrate binding. The HipB antitoxin dimer cross contact with the N and C terminal domains of toxin HipA to cause HipA to undergo an active and inactive conformation (Schumacher et al. 2009)

Recently, it has been suggested that non-cognate *M. tuberculosis* TA can interact physically and functionally. A spectrum of pair-wise combinations of cognate and non-cognate *M. tuberculosis* toxin-antitoxins using *in vivo* toxicity and rescue experiments, alongside *in vitro* interaction experiments revealed several examples of non-cognate TA association, among different families. This

study challenges the “one toxin for one antitoxin” dogma and suggests that organisms, including *M. tuberculosis,* enlist a network of toxin-antitoxin systems to alter physiology in response to environmental clues (Zhu et al. 2010).

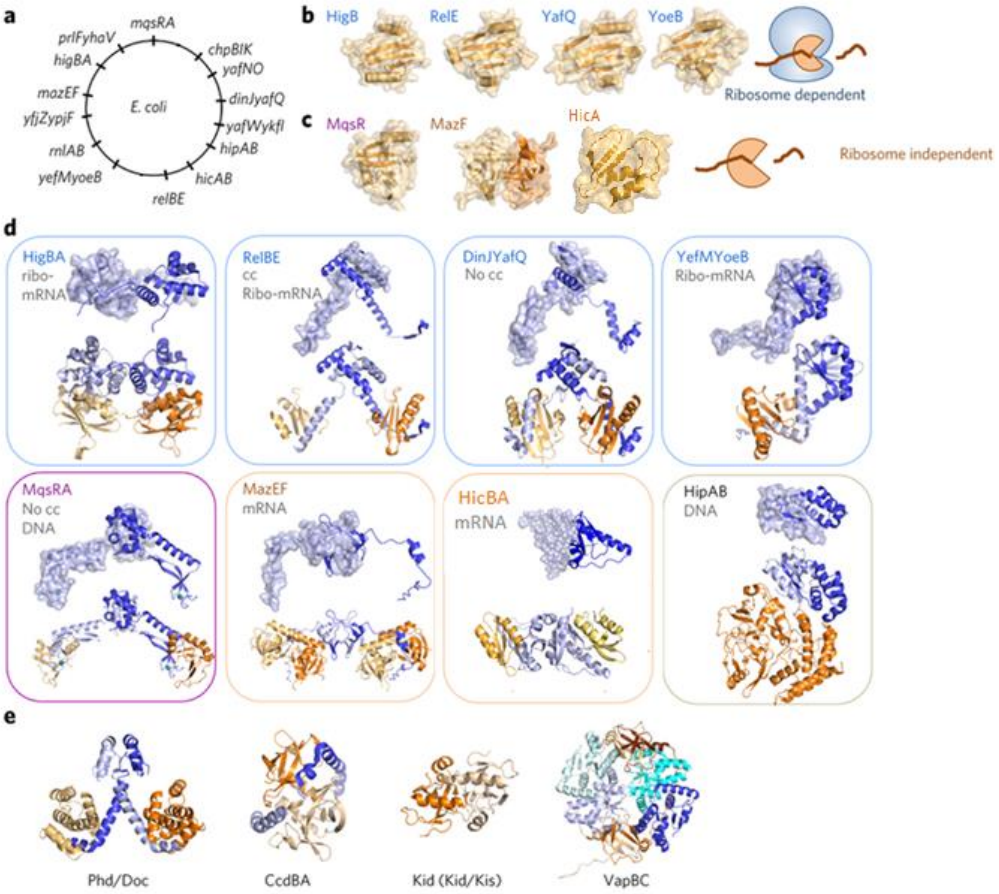

Figure 1.5 Summary of TA complex structures. (a) TA loci in the E. coli genome (b) Ribosome-dependent RNase toxins that adopt the microbial RNase fold. (c) Ribosome-independent RNase toxins; MqsR does not required the ribosome for activity despite the fact it adopts a microbial RNase fold, MazF is a dimer. (d) TA structures. Toxins are coloured orange and antitoxins coloured blue. TA systems with a ribosome-dependent toxin have a blue border (PDB IDs: HigBA, 4MCX47 RelBE, 4FXE51 ; DinJYafQ, 4Q2U90 ; YefMYoeB, 2A6Q95). MqsRA, which is an RNase with structural characteristics of ribosome-dependent toxins but functional characteristics of ribosome-independent toxins, is bordered in magenta (3HI239). The MazEF system and HicBA system from *Y. pestis* are bordered in orange (4MDX96). The HipAB system, in which the toxin is a kinase, is bordered in grey (4YG763, 4P78). cc signifies known regulation by conditional cooperativity and no cc, no regulation by conditional cooperativity. (e) Structures of other well-studied type II TA systems not present in E. coli: Phd/Doc (3K33), CcdBA (3G7Z75), Kid/Kis (1M1F99)), VapBC (3TND73) Antitoxins coloured blue and toxins orange. Figure adapted from Macmillan Publishers Ltd: Nature Chemical Biology, (Page & Peti 2016), Copyright 2016.

1.1.6 Interactions between type II toxins and TA systems

Transcriptional cross-activation between different type II TA systems of *E. coli* has been observed. The chromosomal *relBEF* operon was found to be activated by toxins MazF, MqsR, HicA and HipA. Furthermore, expression of the RelE toxin in turn induced transcription of several other TA operons. Previously, induction of TA operons was shown to depend on Lon protease which is activated by polyphosphate accumulation. However, transcriptional cross-activation was observed in *E. coli* strains deficient for Lon, ClpP, and HslV proteases and polyphosphate kinase (Kasari et al. 2013).

Additionally, toxins were found to cleave the TA mRNA *in vivo,* degrading the antitoxin-encoding fragments and allowing accumulation of toxin-encoding regions. These accumulating fragments can be translated to produce more toxin, possibly generating a positive feedback loop, which can fire other TA systems, forming a network of mutually activating regulators in bacteria (Kasari et al. 2013)

1.2 *Burkholderia pseudomallei*

Burkholderia pseudomallei is an opportunistic pathogen responsible for the disease melioidosis in humans.

1.2.1 Microbiology

B. pseudomallei is a Gram negative, non-spore forming, facultatively anaerobic rod. It exists in the environment as an opportunistic saprophyte, commonly found in tropical areas such as southeast Asia and northern Australia and has been isolated from mud, soil and water in endemic areas (Cheng & Currie 2005). The organism is able to survive in distilled water for 16 years and in desiccated soil for over 70 days (Pumpuang et al. 2011; Larsen et al. 2013; Cheng & Currie 2005). *B. pseudomallei* is also resistant to a large range of antibiotics (Schweizer 2012).

1.2.2 Genome

In the reference strain, *B. pseudomallei* K96243, the genome consists of two complex chromosomes, (chromosome 1 is 4.075Mbp and chromosome 2 is 3.173 Mbp) and is exceptionally large. The gene content between the two chromosomes also differs; core functions, such as those required for cell growth and central metabolism are encoded on chromosome 1, whilst accessory functions required for adaptation and survival are encoded on chromosome 2. The genome of *B. pseudomallei* K96243 is considered very diverse due to the high frequency of recombination associated with GIs. Studies have demonstrated that GI insertion is not random and 128 GIs were identified across all *B. pseudomallei* strains examined (Holden et al. 2004).

1.2.2.1 Toxin-antitoxin systems and persisters in *B. pseudomallei* K96243

To date, there is published data on four type II TA systems in *B. pseudomallei* K96243, *BPSS0390-BPSS0391*, *BPSL0174-BPSL0175*, *BPSS1060-BPSS1061* and *BPSS1583-BPSS1584*. Toxin BPSS0390 shared 78% sequence identity with HicA from *Acinetobacter baumannii* and BPLS0175 and BPSS0160 shared 54% sequence identity from RelE from *Klebsiella pneumonia*. Toxin BPSS1584 was found to be homologous to HipA from *E. coli*.

Ectopic expression of BPSL0175 (RelE1) or BPSS1060 (RelE2) caused growth to cease when expressed in *Escherichia coli*. In contrast, expression of BPSS0390 (HicA) or BPSS1584 (HipA) (in an *E. coli ΔhipBA* background) caused a reduction in the number of culturable bacteria. These toxin induced phenotypes were enhanced by an <3kDa extracellular factor that accumulated in the spent medium during growth. Expression of the cognate antitoxins restored growth and resuscitated cells. Interestingly, in *E. coli,* an increased number of persister cells were observed when *hicA* was expressed and cultures challenged with ciprofloxacin or ceftazidime, whilst removal of this system increased susceptibility to ciprofloxacin

Site directed mutagenesis identified two key residues within the HicA toxin that were essential for toxicity and persistence. This non-toxic variant allowed for over-expression and determination of the structure of *B. pseudomallei* HicA by NMR. NMR revealed that HicA forms a RNA binding domain like fold (Butt 2013; Butt et al. 2014; Butt et al. 2013).

1.3 Melioidosis

B. pseudomallei is the causative agent of melioidosis (Cheng & Currie 2005).

1.3.1 Overview

Melioidosis was recently described as “a disease so neglected, it’s missing from the WHO list of neglected tropical diseases” (Melioidosis: the most neglected tropical disease, 2017). Currently endemic to 45 countries (Figure 1.6), it was estimated that there were 165,000 cases with 89,000 fatalities in the year 2015 (Limmathurotsakul et al. 2016).

There are three routes of infection: inhalation, ingestion and inoculation (White 2003; Cheng & Currie 2005), with inoculation considered the major mode of acquisition, and paddy field workers especially at risk due to walking through mud or surface water with minor foot wounds (Cheng & Currie 2005). In humans, ingestion of *B. pseudomallei* occurs when domestic water supplies are not sufficiently chlorinated (Inglis et al. 2000), whilst inhalation of dust (Amadasi et al. 2014) or aspiration of contaminated water in near –drowning (Lee et al. 1985) can result in infection. Exposure to *B. pseudomallei* typically results in subclinical, symptomatic infections (Currie 2015), although host risk factors, including diabetes mellitus, excessive alcohol intake, chronic lung and kidney disease can significantly increase the likelihood of melioidosis developing after infection (Cheng & Currie 2005). Other risk factors that can impact disease presentation are the size of bacterial load, virulence of bacterial strain and route of infection (Currie 2015).

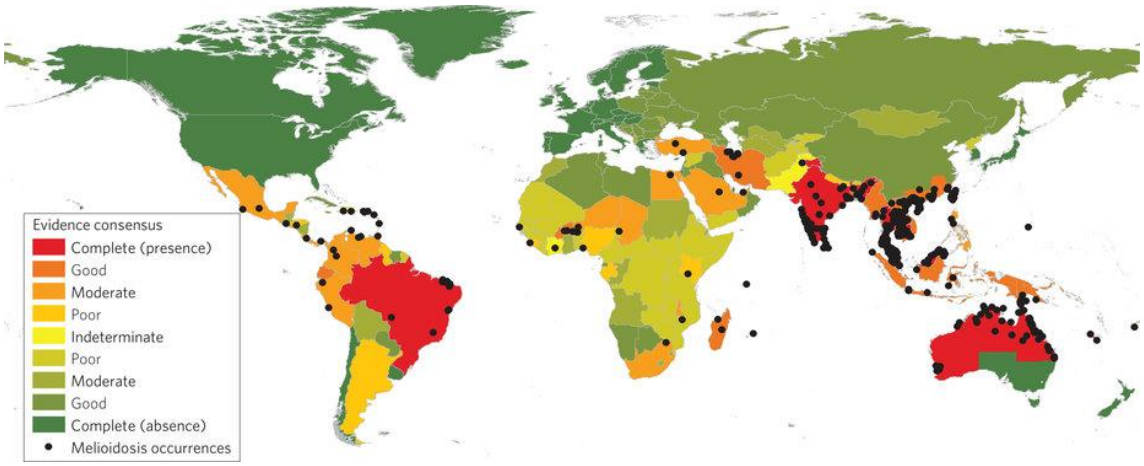

Figure 1.6: Geographic location of *B. pseudomallei* infection from 1910 to 2014. Green represents a complete consensus on absence of *B. pseudomallei*, whilst red signifies a complete consensus on the presence of *B. pseudomallei*. Macmillan Publishers Ltd: Nature Microbiology, (Limmathurotsakul et al. 2016), Copyright 2016.

1.3.2 Clinical presentation

Pneumonia is the most common presentation of melioidosis, with or without bacteraemia, and is involved in approximately half of all cases (Figure 1.7). Abscess formation is characteristic of the disease and may occur on a variety of organs (White 2003; Wiersinga et al. 2012) Encephalomyelitis, genitourinary infection, bone and joint infection or sepsis without an apparent focus may also be presented (Cheng & Currie 2005; Currie 2015).

Mortality rates vary from 14% in Northern Territory Australia (Currie et al. 2010) up to 43% in northeast Thailand (Limmathurotsakul et al. 2016) and are associated with disease presentation and severity; in Australia patients presenting with septic shock had a mortality rate of 50%, compared to a mortality rate of 4% for patients that presented with non-septic shock (Currie et al. 2010). Mortality is also increased in patients with one or more of the host risk factors (Currie et al. 2010).

Acute melioidosis has an incubation period of 1-21 days and symptoms of less than 2 month duration (Cheng & Currie 2005; Currie et al. 2010).

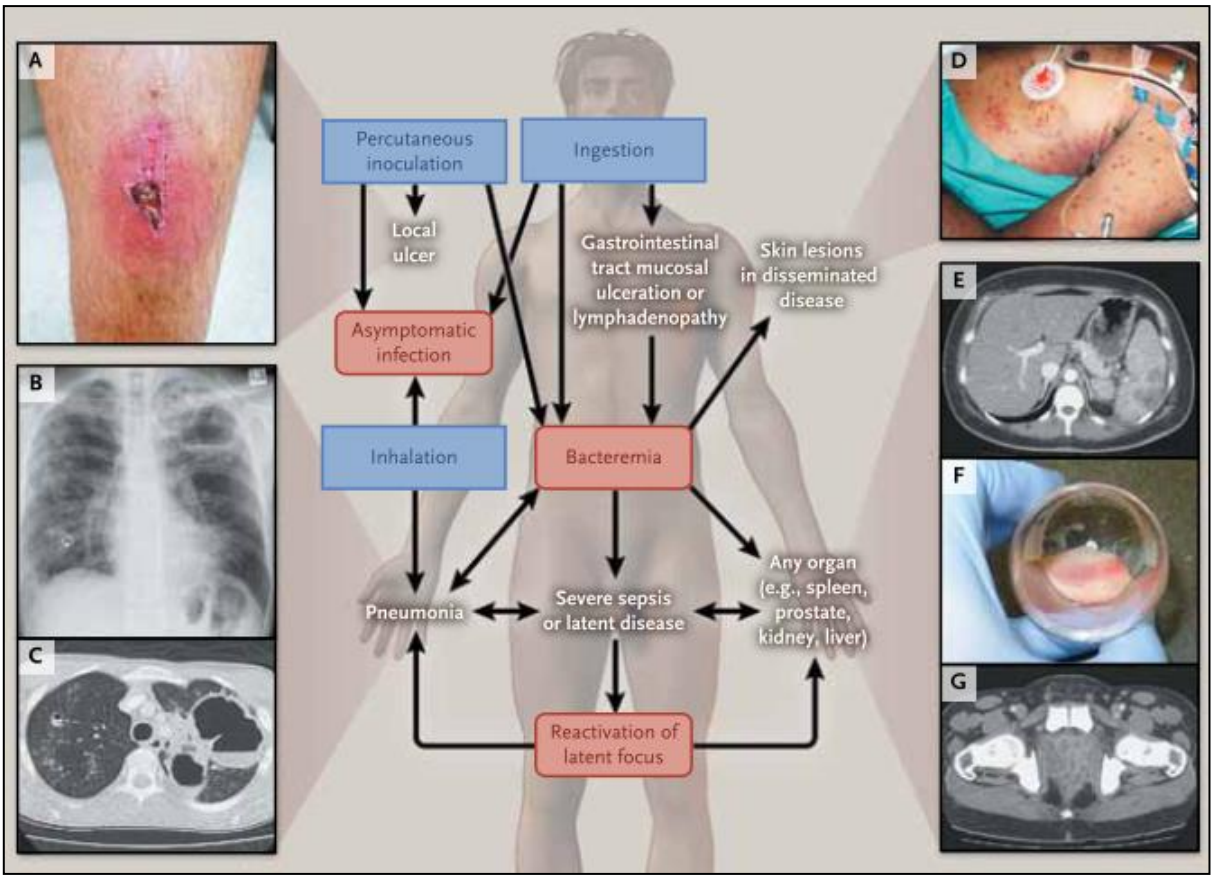

Figure 1.7: Various clinical manifestations of melioidosis. Three routes of infection are shown in blue boxes, which link to a natural history of infection (red boxes) and to clinical manifestations (white text). Panels show: A: cutaneous melioidosis in a healthy host; B: lung abscesses on the chest radiograph of a patient with acute melioidosis pneumonia and the corresponding computed tomographic (CT) scan (Panel C); D: skin manifestations in a fatal case of disseminated melioidosis; E: splenic abscesses on an abdominal CT scan; F: aspirated pus in a patient with prostatic and periprostatic abscesses, and G:bscesses on a CT scan from the patient.
Reproduced with permission from (Wiersinga et al. 2012), Copyright Massachusetts Medical Society.

1.3.3 Persistent melioidosis

Persistent melioidosis could be defined as disease where *B. pseudomallei* cells have existed in the human host for an extended period of time, whilst avoiding removal by antibiotics or by the host immune system. Chronic, latent and relapsed melioidosis can all be described as persistent melioidosis.

Chronic melioidosis, where symptoms have been present for more than two months, currently accounts for ~11-12% of all melioidosis presentations in clinical areas (Limmathurotsakul et al. 2006; Currie et al. 2010). Latent melioidosis indicates that there has been a period of months to years between initial infection with *B. pseudomallei* and presentation of melioidosis; the longest recorded latent period is 62 years (Ngauy et al. 2005). Relapsed melioidosis occurs when the same strain of *B. pseudomallei* is involved in recurrent infection (Limmathurotsakul et al. 2006).

B. pseudomallei has previously demonstrated the ability to form persister cells (Butt et al. 2014). Substantial evidence suggests that persisters contribute in other persistent diseases (Fauvart et al. 2011), and so it is likely that persisters contribute to persistent melioidosis. *B. pseudomallei* persisters *in vitro* have re-generated a population of cells after antibiotic mediated death of the majority of the population (Butt et al. 2014), suggesting that persisters *in vivo* could contribute to relapsed melioidosis despite antibiotic treatment. Persister cells are also apparent in travellers, who have visited endemic areas but live in non-endemic regions, and yet present with melioidosis many years later.

1.3.4 Diagnosis and treatment

A diagnosis for melioidosis should be considered in febrile patients with a predicted risk of occupational or recreational exposure, history of travel to endemic areas and patient risk factors, especially diabetes (Currie 2015). Positive diagnoses are confirmed by isolation of *B. pseudomallei* by culture from patients' bodily fluids, including but not limited to blood, urine, pus and swabs from a range of sites. Isolation of *B. pseudomallei* on selective media, such as Ashdown's media, remains the "gold standard" for a positive diagnosis and may be coupled with commercial biochemical testing or microscopy (Wuthiekanun et al. 1990; Currie 2015; Dance 2014).

Real time PCR to target the *B. pseudomallei* type three secretion system gene cluster (T3SS-1) (Kaestli et al. 2012) and latex agglutination assays, where a range of antibodies detect *B. pseudomallei* antigens (Amornchai et al. 2007), have also been used within a laboratory setting to identify *B. pseudomallei.* Outside the lab, a rapid antigen detection test using a dipstick lateral flow immunoassay, containing antibodies that target the capsular polysaccharide of *B. pseudomallei,* is being tested. If successful, this test would allow rapid diagnosis at point of care (Houghton et al. 2014; Currie 2015).

The treatment for melioidosis is currently at least 10 days of intravenous ceftazidime (or another 3rd generation cephalosporin, such as carbapenem and imipenem,) followed by a 20 week course of oral trimethoprim-sulfomethoazole, chloramphenicol and doxycycline (Dance 2014; Currie 2015). Even with this treatment regimen, there is still a 10% relapse rate. If the oral treatment is taken for less than 8 weeks then the relapse rate is 30% (Chaowagul et al. 1993).

1.4 Aims

- Evaluate toxin BPSS0390 as a potential novel antimicrobial compound,
- Identify residues or regions in BPSS0390 toxin involved in toxicity and BPSS0390-BPSS0391complex formation.
- Determine if type II TA antitoxins in *B. pseudomallei* form a co-operative network through non-cognate toxin-antitoxin interactions.

Chapter 2: Materials and Methods

2.1 Bacterial strains and plasmids

Bacterial strains used in this study are described in Table 2.0. Plasmids used in this study are described in Table 2.1.

2.2 Bacterial storage

2.2.1 Long term storage

Bacteria were kept at –80°C in an O ring sealed cryovial for months or years. A known volume of overnight culture was mixed with an equal volume of sterile 50% glycerol before freezing.

2.2.2 Fridge storage

For short term storage, *E. coli* and *B. thailandensis* strains on LB agar plates were kept for up to 2 weeks at 4°C. *Vibrio* species on LB agar plates were stored at room temperature for periods of up to 2 weeks.

2.3 Bacterial growth

2.3.1 Culture media

All bacterial strains were cultured on autoclaved Luria-Bertani (LB) medium (product 10638013, Fisher Scientific), aerobically with shaking at 37°C unless otherwise specified. Agar plates were LB agar, where 1.5% Bacto-agar number 2 (product MC006, Lab M) was added.

Conjugations into *B. thailandensis* were initially plated onto Brain Heart Infusion medium (Table 2.2) and Thiosulfate-citrate-bile salts-sucrose (TCBS) medium was used to select for *Vibrio* species after conjugation (Table 2.3).

Table 2.0: Bacterial strains used

Bacterial strain	Comments	Source
Escherichia coli K-12 MG1655	F^- λ^- ilvG- rfb-50 rph-1	Laboratory collection
E. coli DH5α λ*pir*	ΔlacU169(ΦlacZΔM15), recA1, endA1, hsdR17, thi-1, gyrA96, relA1, λpir phage lysogen	Laboratory collection
E. coli Δ*hipBA:*	*E. coli* MG1655 derivative Δ*hipBA: Cm*^{R}	(Butt 2013)
E. coli XL-10 Gold	endA1 glnV44 recA1 thi-1 gyrA96 relA1 lac Hte Δ(mcrA)183 Δ(mcrCB-hsdSMR-mrr)173 tet^R F'[proAB $lacI^qZ$ΔM15 Tn10(Tet^R Amy Cm^R)	Stratagene
Burkholderia thailandensis E264	Environmental isolate.	Laboratory collection
Yersinia pseudotuberculosis IP32953	Clinical isolate.	Laboratory collection
Salmonella enterica serovar Typhimurium SL1344	Animal isolate	Laboratory collection
Vibrio vulnificus E64MW	Environmental isolate	Laboratory collection
E. coli DH5a (pRK2013)	ΔlacU169(ΦlacZΔM15), recA1, endA1, hsdR17, thi-1, gyrA96, relA1, pRK2013 (KmR oriColE1 RK2-Mob^+ RK2-Tra^+	Laboratory collection

Table 2.1: Plasmids used or created in this study

Plasmids	Comments	Source
pBAD/his-*BPSS0390*	Ampicillin^{R} , *BPSS0390* cloned into *Nco*I and *Hind*III sites. N-terminus histidine tag.	(Butt et al. 2013)
pBAD/his-H24A	Ampicillin^{R} , mutated *BPSS0390* H24A cloned into *Nco*I and *Hind*III sites. N-terminus histidine tag.	(Butt et al. 2013)
pSCrhaB2	Trimethoprim^{R}, with a rhamnose inducible promoter	(Cardona & Valvano 2005) UK Defence Science and Technology Laboratory.
pSCrhaB2/his-*BPSS0390*	Trimethoprim^{R}, with a rhamnose inducible promoter and *BPSS0390* cloned into *Nco*I and *Hind*III.	This study
pSCrhaB2/his-H24A	Trimethoprim^{R}, rhamnose inducible promoter and mutated *BPSS0390* H24A cloned into *Nco*I and *Hind*III sites. N-terminus histidine tag.	This study

.

Table 2.2: BHI medium

Components	Per litre
Brain Heart Infusion	37 g
dH_2O	To 1 litre

To make BHI agar plates 1.5% bacto-agar was added before autoclaving.

Table 2.3: TCBS medium

Components	Per litre
Cholera medium TCBS	88 g
dH_2O	To 1 litre

Medium was boiled to dissolve completely. To make TCBS plates 1.5% bacto-agar was added before boiling.

2.3.2 Recovery from freezer storage

Freezer stocks were removed the freezer, a sterile loop used to remove a small amount of frozen culture and inoculated onto the surface of an LB agar plate. The inoculated plate was placed in a static 37°C incubator. The freezer stocks were returned to the freezer.

2.3.3 Growth of bacteria for assays

A single colony was removed from a streak plates and used to inoculate 5ml LB in 30ml universal. The culture was incubated at 37°C with 200rpm shaking overnight.

2.4 Growth curve analysis

Overnight cultures of *E. coli* harbouring pBAD/his-mutant alleles were diluted to an OD_{590nm} of 0.01 in fresh LB with 100 µg/ml ampicillin, before 100µl of the diluted culture was placed into individual wells in 96-well plate. Samples were loaded in triplicate, three wells were left empty and three were loaded with growth media only, as a control. The 96 well plate was incubated overnight at 37°C, without shaking, in a Softmax Pro-5 Microplate Reader (Versamax), programmed to take automated OD_{590nm} reading every 15 minutes.

2.5 Antibiotics used

All antibiotics used in this work are shown in table 2.4. Antibiotics supplied by Sigma-Aldrich. Antibiotics dissolved in distilled water were filter sterilised using a 0.2µm filter (Minisart Sigma-Aldrich) before use.

Table 2.4: Antibiotics used and their storage conditions

Antibiotic	Stock solution	Storage conditions	Final concentration in culture
Ampicillin	100 mg/ml in water	-20°C in solution	100 µg/ml
Gentamicin	100 mg/ml in water	-20°C in solution	100 µg/ml
Tetracycline	15 mg/ml in water	-20°C in solution	15 µg/ml
Trimethoprim	50 mg/ml in DMSO	Room temperature in solution	50 µg/ml(or 100 µg/ml for plasmid maintenance in *B. thailandensis* E264 or *V. vulnificus* E64MW)

2.6 Competent cells

2.6.1 Calcium competent cells

A calcium chloride method was used. 5ml of LB was inoculated with the appropriate *E. coli* strain and incubated with shaking overnight at 37°C. The overnight culture was diluted 1:100 into 100ml of fresh LB in a 500ml conical flask and grown with shaking until an OD_{590nm} between 0.5-0.7 was reached. The culture was poured into pre-chilled Falcon tubes and incubated on ice for 10 minutes. Cells were pelleted by centrifugation at 3,200 x g for 10 minutes in an eppendorf Centrifuge 5810 R chilled to 4°C and the subsequent pellet resuspended in 50ml ice cold, sterile 0.1M calcium chloride solution before incubation on ice for 30 minutes. Cells were pelleted again and the subsequent pellet resuspended in 600µl 0.1M calcium chloride and 300µl sterile 50% glycerol then aliquoted and stored at –80°C.

2.6.2 Electrocompetent cells

An overnight culture of the desired transformant strain was diluted 1:100 into 100ml of fresh LB in a 500ml conical flask and grown with shaking until an OD_{590nm} between 0.5-0.8 was reached. The culture was poured into pre-chilled Falcon tubes and incubated on ice for 10 minutes. Cells were pelleted by centrifugation at 3,200 x g for 10 minutes in an eppendorf Centrifuge 5810 R chilled to 4°C and the subsequent pellet resuspended in 50ml ice cold, sterile water. Cells were pelleted as described previously before resuspension in 25ml ice cold, sterile water before centrifugation again and resuspension in 5ml ice cold, 10% glycerol. Cells were pelleted a final time and aliquoted before storage at –80°C.

2.7 Transformation

2.7.1 Heat Shock

An aliquot of calcium chloride competent cells was thawed on ice and up to 2µl of purified plasmid (up to 500 ng of DNA) or an entire ligation reaction added. The sample was incubated on ice for 30 minutes before a heat shock at 42°C for exactly 90 seconds, then returned to ice for 2 minutes before 900µl of room temperature LB added. Cells were recovered at 37°C with shaking for 1 hour. After this, 100µl was plated on selective LB agar plates. The remainder of the sample was pelleted by centrifugation (eppendorf Centrifuge 5424, 17,000 x g) before resuspension in 100µl of fresh LB and plated onto selective media. When the plasmid transformed was pBAD/his-*BPSS0390* or pSCrhaB2/his-*BPSS0390* glucose (final concentration 2% (w/v)) was added to the recovery media and selective LB agar plates.

2.7.2 Electroporation

A 100µl aliquot of electrocompetent cells was thawed on ice and up to 500 ng of extracted plasmid added before the samples were transferred to pre-chilled electroporation cuvettes. A Bio-Rad MicroPulser was used to electroporate the cells with 2kV. Immediately after electroporation 1ml of LB broth was added the cuvette, then transferred to a 1.5ml Eppendorf and the cells allowed to recover aerobically with shaking for 1 hour. 100µl of cell suspension was spread onto selective LB agar plates. When the plasmid was pBAD/his-*BPSS0390* or pSCrhaB2/his-*BPSS0390* glucose (final concentration 2% (w/v)) was added to the recovery media and selective LB agar plates.

2.7.3. Conjugation into *V. vulnificus* E64MW

E. coli DH5α harbouring either pSCrhaB2/his-*BPSS0390* or pSCrhaB2/his-H24A was used as the donor strain. *E. coli* DH5α harbouring pRK2013 was used as a helper. The recipient was *V. vulnificus* E64MW. Cultures of the helper, donor and recipient strains were grown in LB media with the appropriate antibiotic selection at 37°C with shaking overnight. The next day, 1ml of each culture was transferred into 1.5ml Eppendorf tubes and cells isolated by centrifugation at 8,000 x g in an eppendorf Centrifuge 5424. The supernatant was removed, and the cells resuspended in 1ml of sterile PBS before centrifugation again as described. Supernatant was removed and the donor and helper strains resuspended in 200µl of LB without antibiotic. 100µl of donor and helper were then added to the cell pellet of the recipient strain and re-suspended to make a conjugation mix. 100µl of the mixed bacterial culture was then added to an LB plate and left as a pool for plasmid exchange. 100µl of donor, recipient and helper strain were also plated as controls. Plates were incubated at 37^{o}C in an upright position overnight in a static incubator. The next day the lawns of bacteria on the test and control plates were scraped off of the plate using a loop and resuspended in 1ml volumes of PBS in Eppendorf tubes. 100µl volumes were then plated onto TCBS plates containing 50 µg/ml trimethoprim. These plates were incubated for 2-3 days at 37^{o}C for colonies to grow. Colonies were then re-streaked onto LB trimethoprim to confirm that they were conjugants.

2.7.4 Conjugation into *B. thailandensis* E264

E. coli DH5α harbouring either pSCrhaB2/his-*BPSS0390* or pSCrhaB2/his-H24A was used as the donor strain. *E. coli* DH5α harbouring pRK2013 was used as a helper. The recipient was *B. thailandensis* E264. Cultures of the

helper, donor and recipient strains were grown in LB media with the appropriate antibiotic selection at 37°C with shaking overnight. The next day, 1ml of each culture was transferred into 1.5ml Eppendorf tubes and cells isolated by centrifugation at 8,000 x g in an eppendorf Centrifuge 5424. The supernatant was removed, and the cells resuspended in 1ml of sterile PBS before centrifugation again as described. Supernatant was removed and the donor and helper strains resuspended in 200µl of LB without antibiotic. 100µl of donor and helper were then added to the cell pellet of the recipient strain and re-suspended to make a conjugation mix. 100µl of the mixed bacterial culture was then added to a BHI agar plate and left as a pool for plasmid exchange. 100µl of donor, recipient and helper strain were also plated as controls. Plates were incubated at 37^{o}C in an upright position overnight in a static incubator. The next day the lawns of bacteria on the test and control plates were scraped off of the plate using a loop and resuspended in 1ml volumes of LB in Eppendorf tubes. 100µl volumes were then plated onto LB plates containing 100 µg/ml trimethoprim and 100 µg/ml gentamicin. These plates were incubated for 2-3 days at 37^{o}C for colonies to grow. Colonies were then re-streaked onto LB trimethoprim to confirm that they were conjugants.

2.8 Toxicity assays

2.8.1 Toxicity assays with *E. coli* harbouring pBAD/his cloned toxin genes or cloned mutant toxin genes

E. coli strains carrying pBAD/his cloned toxins or mutated toxins were inoculated into 5ml of LB containing 100 µg/ml ampicillin and a final concentration of 2% (w/v) glucose and grown overnight at 37^{o}C, 200rpm. Cultures were then diluted 1:100 into 50ml fresh LB in a 250ml conical flask and supplemented with fresh antibiotic. Cultures were grown at 37^{o}C in a shaking

incubator at 200rpm until reaching an OD_{590}nm of ~0.1 and 5ml volumes of culture were aliquoted into 30ml universal tubes. To induce gene expression from the P_{BAD} promoter arabinose was added to a final concentration of 0.2% (w/v). To repress expression glucose was added to a final concentration of 0.2% (w/v) glucose. Cultures were returned to the 37^{o}C incubator and grown for a further 3 hours taking samples every hour measuring the OD_{590}nm and determining CFU counts. Alternatively, the CFU was determined after 0 and 2 hours and the fold change in CFU counts was calculated. OD_{590}nm was measured using a spectrophotometer blanked with LB. CFU was determined by serial diluting cultures in LB in a 96 well plate and spot plating onto LB-ampicillin (100 µg/ml) glucose plates. Plates were incubated at 37^{o}C overnight in a static incubator.

2.8.2 Toxin expression in *B. thailandensis*, *V. vulnificus* and *Y. pseudotuberculosis*

Bacterial strains carrying pSCrhaB2/his-*BPSS0390* or pSCrhaB2/his-H24A were inoculated into 5ml of LB containing trimethoprim (100 µg/ml for *B. thailandensis* and *V. vulnificus* and 50 µg/ml for *Y. pseudotuberculosis*) and a final concentration of 2% (w/v) glucose and grown overnight at 37^{o}C, 200rpm. Cultures were then diluted 1:100 into 50ml fresh LB in a 250ml conical flask and supplemented with fresh antibiotic. Cultures were grown at 37^{o}C in a shaking incubator at 200rpm until reaching an OD_{590}nm of ~0.1 and 5ml volumes of culture were aliquoted into 30ml universal tubes. To induce gene expression rhamnose was added to a final concentration of 0.5% (w/v). To repress expression glucose was added to a final concentration of 0.5% (w/v). Cultures were returned to the 37^{o}C incubator and grown for a further 3 hours taking samples every hour measuring the OD_{590}nm and determining CFU counts.

OD_{590}nm was measured using a spectrophotometer blanked with LB. CFU was determined by serial diluting cultures in LB in a 96 well plate and spot plating onto LB-trimethoprim (100 µg/ml for *B. thailandensis* and *V. vulnificus* and 50 µg/ml for *Y. pseudotuberculosis*) and glucose (2%(w/v)) plates. Plates were incubated at 37^{o}C overnight in a static incubator.

2.8.3 Toxin expression in *E. coli* and *S.* Typhiumurium

Bacterial strains carrying pSCrhaB2/his-*BPSS0390* or pSCrhaB2/his-H24A were inoculated into 5ml of LB containing trimethoprim (50 µg/ml) and a final concentration of 2% (w/v) glucose and grown overnight at 37^{o}C, 200rpm. Cultures were then diluted 1:100 into 50ml fresh LB in a 250ml conical flask and supplemented with fresh antibiotic. Cultures were grown at 37^{o}C in a shaking incubator at 200rpm until reaching an OD_{590}nm of ~0.1 and 5ml volumes of culture were aliquoted into 30ml universal tubes. To induce gene expression rhamnose was added to a final concentration of 0.2% (w/v). To repress expression glucose was added to a final concentration of 0.2% (w/v). Cultures were returned to the 37^{o}C incubator and grown for a further 3 hours taking samples every hour measuring the OD_{590}nm and determining CFU counts. OD_{590}nm was measured using a spectrophotometer blanked with LB. CFU was determined by serial diluting cultures in LB in a 96 well plate and spot plating onto LB-trimethoprim (50 µg/ml) and glucose (2% (w/v)) plates. Plates were incubated at 37^{o}C overnight in a static incubator.

2.9 Co-expression assays

E. coli harbouring pBAD cloned toxin or mutant toxin and pME6032 cloned antitoxin were inoculated into 5ml LB supplemented with 15 µg/ml tetracycline,

100 µg/ml ampicillin and a final concentration of 2% (w/v) glucose and grown overnight at 37^{o}C, 200rpm. The following day the culture was diluted 1:100 in 50ml of fresh LB in a 250ml conical flask and supplemented with fresh ampicillin and tetracycline at the same concentration. Cultures were grown at 37^{o}C, 200rpm until reaching an OD_{590}nm of ~0.1. Cultures were then aliquoted into 3 x 5ml volumes in 30ml universal tubes supplemented with 0.2% (w/v) glucose or 0.2% (w/v) arabinose or 0.2% (w/v) arabinose and 1mM IPTG. Cultures were returned to the incubator and samples were taken after 2 hours, or hourly for three hours, for measurement of OD_{590}nm by spectrophotometry and CFU determination by serial dilutions in 96 well plates. Cells were spot plated onto LB ampicillin tetracycline glucose (2% (w/v)) plates and incubated overnight at 37^{o}C.

2.10 Preparation of samples for Scanning Electron Microscopy (SEM)

Samples were taken at T0 (before addition of inducer/repressor), T1 (one hour post induction/repression) and T3 (three hours post induction/repression) from cultures expressing BPSS0390 or BPSS0390 H24A The 1ml samples were centrifuged at 4°C for 5 minutes and the supernatant discarded. Samples were then washed three times in 1 x PBS before resuspension in 0.1M phosphate buffer or distilled, sterile water before pipetting onto grids, fixing for 1 hour using osmium tetroxide and dehydrated using ethanol. Grids were viewed using a Hitachi S3200N SEM-EDS.

2.11 DNA extraction

2.11.1 Extraction of digested DNA fragments and plasmids from agarose gel

Successfully digested fragments and/ or plasmids were excised from the agarose gel after electrophoresis using a scalpel and each piece of gel placed into an individual 1.5ml Eppendorf tube. Agarose gel pieces were weighed before a ThermoScientific Gel Extraction kit was used according to manufacturer's protocol to purify the DNA.

2.11.2 Plasmid extraction

Plasmid DNA was extracted from an overnight culture of bacteria (typical volume of 5ml) using a ThermoScientific GeneJET Plasmid Miniprep Kit according to manufacturer's instructions.

2.12 DNA amplification by Polymerase Chain Reaction (PCR)

A Biometra T Professional TRIO Thermocycler was used to amplify DNA by PCR following the variations on the programme listed in Table 2.4. All reactions used either Failsafe (Cambio) or Hot Star Taq (Qiagen) polymerase and had a final volume of either 20µl or 50µl with buffers and concentrations used according to the manufacturer's protocol.

2.12.1 Boilate preparation for colony PCR

To confirm the presence of a clone or to identify *V. vulnificus* or *B. thailandensis* after conjugation a colony boilate was used. A single colony was resuspended in 100 µl of distilled water and boiled for 5 minutes at 95°C using a Stuart Block heater. Alternatively, 1ml of overnight culture was pelleted by centrifugation (eppendorf Centrifuge 5424, 17,000 x g), washed in 1ml sterile 1xPBS and re-centrifuged to pellet the cells. The cells were then resuspended in 100µl of distilled water and boiled for 5 minutes at 95°C using a Stuart Block heater.

Boiling ruptured cells and released DNA. The boilate was centrifuged to pellet the boiled cells (eppendorf Centrifuge 5424, 17,000 x g) and the supernatant used in PCRs as a source of bacterial DNA.

2.13 PCR purification

GeneJET PCR Purification Kit was used according to manufacturer's instructions. DNA was eluted into EB or nuclease free water.

2.14 Agarose gel electrophoresis

Gel electrophoresis was used to separate DNA fragments generated by PCR or required for cloning. Samples were mixed with 6 x Loading dye (Thermo Scientific) and loaded into gels made from 1% (w/v) agarose dissolved in 1 x Tris-acetate-EDTA (TAE) with Midori Green Advanced DNA stain (Nippon Genetics Europe GmbH) added for band visualisation. Gels were also loaded with DNA molecular marker; 5µl 1 kb Plus DNA ladder (Thermo Scientific) was used. A Bio-Rad PowerPac power supply was used to electrophorese the gel for 45 minutes at 90V. Gels were visualised with UV light using a BioRad Gel Documentation Unit and QuantityOne software.

2.15 Determining DNA concentration

DNA concentration was determined by loading 2µl of sample onto a Thermo Scientific NanoDrop 1000 spectrophotometer with ND1000 software and following the procedure provided by the manufacturers. The machine was washed with water, before loading the sample.

2.16 Digestion of DNA using restriction enzymes

Plasmid DNA was digested using High Fidelity enzymes provided by NEB in a final reaction volume of 50µl (Table 2.5). Reactions also contained the

appropriate buffer as recommended by the manufacturer. Digests were incubated at 37°C overnight. The entire reaction was then electrophoresed the following day.

2.17 Ligations

All ligation reactions had a final volume of 15µl and contained 1µl of T4 DNA ligase (NEB) and 1.5µl of ligation buffer. Each reaction also contained 150 ng of digested vector DNA but the amount of digested insert varied; it was calculated using the formula described below:

Amount of insert (ng) =amount of vector (ng) x (Size of insert (kb)/ size of vector (kb)) x molar ratio (insert/vector)

A molar ratio of 4:1 was used and nuclease free water added to bring the final volume to 15µl. Reactions were incubated overnight at 15°C.

2.18 pGEM-T-Easy cloning

The gateway vector used was pGEM-T-Easy (Promega). Cloning was carried out as instructed by manufacturers. In summary, this involved incubating the PCR product with the gateway vector and T4 ligase at room temperature before transformation of the resulting ligated plasmid/PCR product into calcium competent cells. Blue/white screening was used to detect positive colonies by plating onto X-galactose and IPTG containing plates. White colonies were screened for presence of insert either by colony PCR.

Table 2.4: Table showing generic programme used for PCR

Number of cycles	Stage	Temperature (°C)	Time (seconds)
1	Initial denaturation	95	60
25-35	Denaturation	95	30
25-35	Annealing	55-72	60
25-35	Extension	72	60
1	Final extension	72	600
1	Final hold	4	∞

Table 2.5: Contents of 50 µl restriction digest

Component	**Volume or amount added**
Buffer	5µl
Enzyme	1µl
DNA	0.5 µg
Nuclease-free water	Up to final volume of 50µl

2.19 Sequencing of plasmid DNA

Source Bioscience was used to determine the sequence of plasmids. Samples were diluted to a concentration of 100 ng/µl and sent with appropriate specific primers. Resulting DNA sequences were downloaded and aligned with reference sequences using Clone Manager. When unknown nucleotides, 'N', or inconsistencies were present in the text output, the automated chromatogram was examined at the corresponding position. If there was a well formed, evenly spaced, tall, clean peak at that position, with little to no baseline noise then that was taken as the nucleotide for that position.

2.20 Site directed mutagenesis

Primers for site directed mutagenesis were designed on the Agilent website and synthesised by Eurofins MWG. Primers contained the base pair(s) substitution needed to encode the amino acid change. Site directed mutagenesis was carried out on the histidine tagged BPSS0390 toxin DNA as per manufacturer's instructions and using the Quick-change lightning kit. In summary, this involved the synthesis of forward and reverse mutant plasmid DNA strands using the designed primers, pBAD/his-BPSS0390 as a template and a pfu-based polymerase. *Dpn*I was subsequently used to digest the parental non-mutant methylated DNA before transformation of the mutant plasmid into XL10-gold ultracompetent cells, for nick repair and replication, by heat shock in the presence of β-mercaptoethanol. Transformants were plated onto LB ampicillin (100 µg/ml) glucose (2%(w/v)) plates and grown overnight at 37^{o}C. Colonies were then picked and plasmid DNA was re-isolated using the Qiagen miniprep kit as previously described and sent for sequencing to confirm that the appropriate nucleotides were mutated.

2.21 SDS-Polyacrylamide gel electrophoresis (PAGE)

For detection of protein, 1 ml sample was taken from a culture, centrifuged and either lysed using BugBuster, lysozyme and benzonase or resuspended in 20µl of 4 x SDS loading before boiling at 95^{o}C for 5 minutes in a heat block before loading. Novex NuPAGE 12% Bis-Tris gels (Life Technologies) were used. A total of 20µl of protein preparation were loaded into each well of the gel. 5µl of a protein ladder was loaded for size comparison. For the majority of gels the Protein perfect 10kDa-225kDa marker (Novagen) was used. Gels were run in 1 x MES or MOPS buffer at 180V for 35minutes or until the protein reached the bottom of the gel. After the gel was run it was washed in de-ionised water before staining with simply blue protein stain (Invitrogen). The protein gel was incubated with approximately 20ml of Simply Blue stain and microwaved in 30 second intervals until protein bands were visible. Following staining the gel was washed with de-ionised water 3 times and then incubated on a rocker in 100ml de-ionised water overnight to de-stain the gel.

2.22 Western blots

Protein samples were boiled, loaded and run on gels as previously described. After gel electrophoresis the gel was removed from its cast and washed twice in approximately 20ml of deionised water. The gel was then placed onto a nitrocellulose membrane using the iBlot dry blotting system (Invitrogen). The protein was blotted onto the appropriate membrane for 5-7 minutes using 20-23V. The membrane was then transferred to 30ml of a 3% (w/v) BSA solution dissolved in TBST (Tris buffer saline 1% Tween) which was used as a blocking

agent. The membrane was incubated in this solution overnight at 4^{o}C. The next day the solution was removed. The anti-Xpress epitope antibody (Invitrogen) was diluted 1:5000 in 15ml of 3% (w/v) BSA dissolved in TBST and added to the membrane, incubating for 1 hour at room temperature on a rocker. Following this incubation step, the BSA and antibody mix was discarded and then 20ml of TBST was added to wash and incubated on a rocker for 10 minutes before discarding. This washing process was repeated 3 times. A secondary IR Dye ® 800 CW Goat anti-mouse antibody was then diluted 1:10,000 in 10ml of fresh 3% (w/v) BSA dissolved in TBST and incubated with the membrane for a further hour. The wash steps in TBST were repeated as described above. Protein on the membrane was detected using Odyssey ® CLx Imaging system and Image Studio software.

2.23 Primer design

Primers (excluding those for site-directed mutagenesis) were designed by examining the regions upstream and downstream of the desired sequence in Artemis and suitable areas chosen that would allow the primer to have a GC clamp at the 3' end and no long repetitive sequences. Clone Manager was used to check that primers had similar Tm and no undesired homology to parent DNA.

2.23.1 Primers designed for site directed mutagenesis

Primers were designed using the Agilent QuickChange Primer design tool. For primer list please see Appendix.

2.24 Statistical analysis

When comparing two values, an unpaired, parametric t-test assuming equal variance was used. For three or more values a one-way ANOVA with Dunnett's post test (comparing experimental groups with a control) was used.

The null hypothesis was rejected and a significant difference concluded, if the significance probability was less than or equal to 0.05.

Chapter 3: Over-expression and host specificity of toxin gene BPSS0390

3.0 Introduction

The emerging antimicrobial resistance of many pathogenic bacteria threatens effective treatment of bacterial infections, a leading cause of human mortality worldwide (Chan et al. 2015; Lee & Lee 2016). The search for novel antimicrobial candidates has recently highlighted how TA systems could be exploited, including using toxin molecules as potential antimicrobials (Unterholzner et al. 2013; Lee & Lee 2016).

Expression of TA toxin HicA in *E. coli* has been shown to induce cell growth arrest through cleavage of mRNA at an unknown specificity residue (Jørgensen et al. 2009). Similarly, expression of BPSS0390 (*B. pseudomallei* HicA) in *E. coli* resulted in a rapid decrease in the number of culturable cells after induction (Butt et al. 2013). This suggests that BPSS0390 might have the potential to be active in a broad range of bacteria and could be exploited as a novel bacteriostatic and bactericidal compound.

Current studies and BSAC guidelines for testing of potential antimicrobial compounds state the minimum bactericidal concentration (MBC) of the novel compound as the lowest concentration of an agent that causes ≥ 3 log reduction in surviving cells within 24 hours of treatment (Schlievert et al. 2013; Peterson & Shanholtzer 1992). To investigate if BPSS0390 might meet these guidelines I decided to induce ectopic expression of the toxin from a broad host range plasmid in a range of Gram negative pathogenic bacteria and monitor patterns of growth inhibition. Using a range of pathogenic bacteria also allowed determination of the host specificity of BPSS0390.

Three of the bacterial species chosen had genomic homologues to *B. pseudomallei* HicB; it was hoped that induction of ectopic BPSS0390

expression in these species might results in a neutralisation phenotype and allow for identification of critical residues involved in toxin-antitoxin complex formation. The selection of bacterial species was limited as species chosen had to be readily available within the lab, possess the correct antibiotic sensitivity to facilitate use of the plasmid and grow relatively quickly.

3.1 Hypothesis

- Toxin BPSS0390 is toxic in a range of bacterial species.

3.1.1 Objectives

- To induce expression of *B. pseudomallei* toxin BPSS0390 in range of different bacterial species
- To evaluate toxin BPSS0390 as a potential antimicrobial compound.

3.2 Results

3.2.1 Generation of construct pBAD/his-BPSS0390 containing the native HicA sequence

Previously reported data (Butt et al. 2013) used construct pBAD/his-*BPSS*0390 where *BPSS0390* gene was cloned into pBAD under the control of the arabinose promoter, for HicA toxin expression. Unfortunately, when this construct re-isolated for use in this study is was found to contain mutations so it was necessary re-generate the construct pBAD/his-*BPSS*0390.

3.2.1.1 Cloning native BPSS0390 sequence directly into pBAD/his

PCR was used to amplify *BPSS0390* from genomic *B. pseudomallei* K96423 DNA. Both the PCR product insert and pBAD/his vector were treated with *Nco*I and *Hind*III before ligation. The ligation was recovered into *E. coli* DH5α. A screening PCR was used to identify clones containing the *BPSS0390* insert and seven constructs isolated and sent for nucleotide sequencing (Figure 3.1).

Sequencing analysis revealed that all of the constructs tested contained mutations within the *hicA* gene. Mutations included S3L, K42E, S23G, P41L, I47M and deletion of nucleotides that caused frame shift mutations in the gene.

3.2.1.2 Cloning native *BPSS0390* sequence into a holding vector.

PCR was used to amplify *BPSS0390* from genomic *B. pseudomallei* K96423 DNA and the resulting product was mixed with a TA cloning vector (pGEM T-easy). The ligation was recovered into *E. coli* DH5α. A screening PCR was used to identify clones where the pGEM T-easy contained the *BPSS0390* insert and three plasmids were extracted and nucleotide sequenced (Figure 3.2). Analysis of the sequencing data revealed that all of the constructs

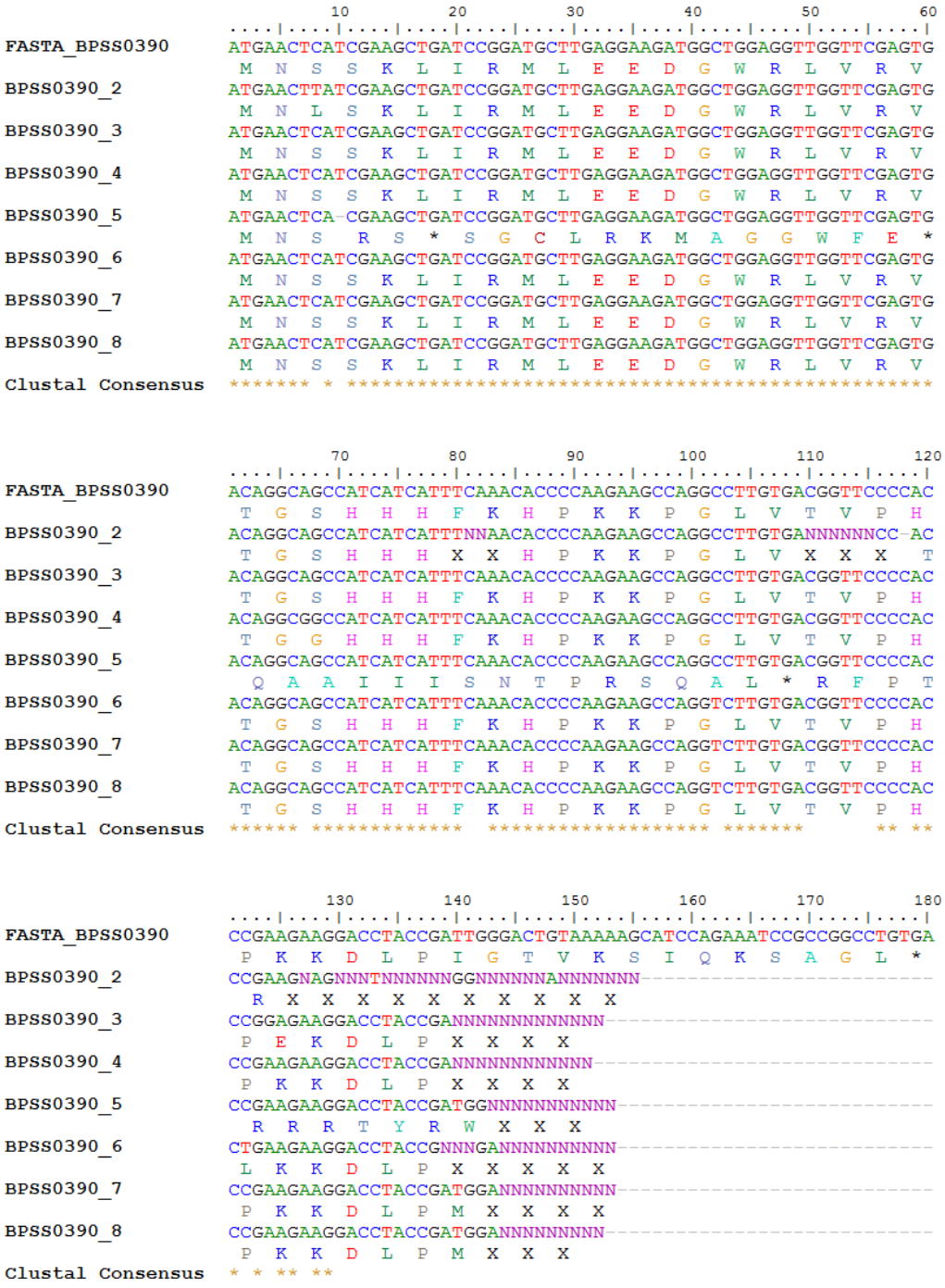

Figure 3.1: Sequencing data from cloning to attempt to generate pBAD/his-*BPSS0390*. The sequences of *BPSS0390* cloned into plasmid pBAD are shown as BPSS0390_2 to BPSS0390_8. FASTA sequence for gene *BPSS0390* is at the top as a reference sequence. Clustal consensus is the consensus sequence of all sequences shown in the figure. Sequences were aligned using ClustalW and image generated using BioEdit.

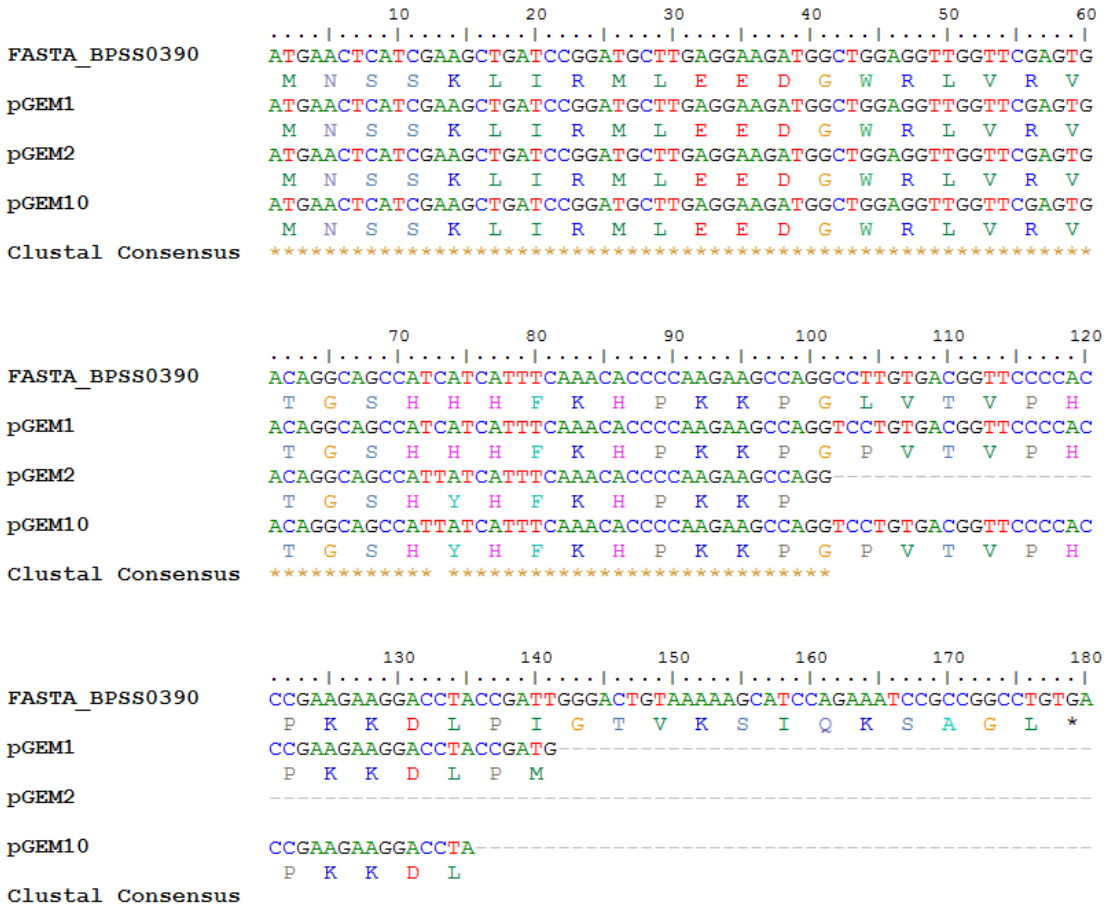

Figure 3.2: Sequencing data from cloning to attempt to generate pGEM-*BPSS0390*. The sequences of *BPSS0390* cloned into pGEM plasmid are shown as pGEM1, pGEM2 and pGEM10. FASTA sequence for *BPSS0390* is used as a reference. Clustal consensus is the consensus sequence of all sequences shown in the figure. Sequences were aligned using ClustalW and image generated using BioEdit.

contained mutations within the *hicA* gene sequence; two containing H25Y and one with L35P.

3.2.1.3 Site directed mutagenesis of pBAD/his-*BPSS0390* P41L

As it was not possible to generate pBAD/his-*BPSS0390* with an authentic *hicA* sequence, an Agilent QuikChange Lightning Site Directed Mutagenesis Kit was used to revert pBAD/his-*BPSS0390* P41L back to the *hicA* wild type sequence. Initial attempts using the recommended annealing temperature of 68°C failed. However, once the annealing and elongation temperatures were increased to 70°C, construct pBAD/his-*BPSS0390* was successfully generated and the sequence confirmed (Figure 3.3). The required increase in annealing and elongation temperatures for the PCR step may be due to the high GC content of the native sequence and mutagenic primers.

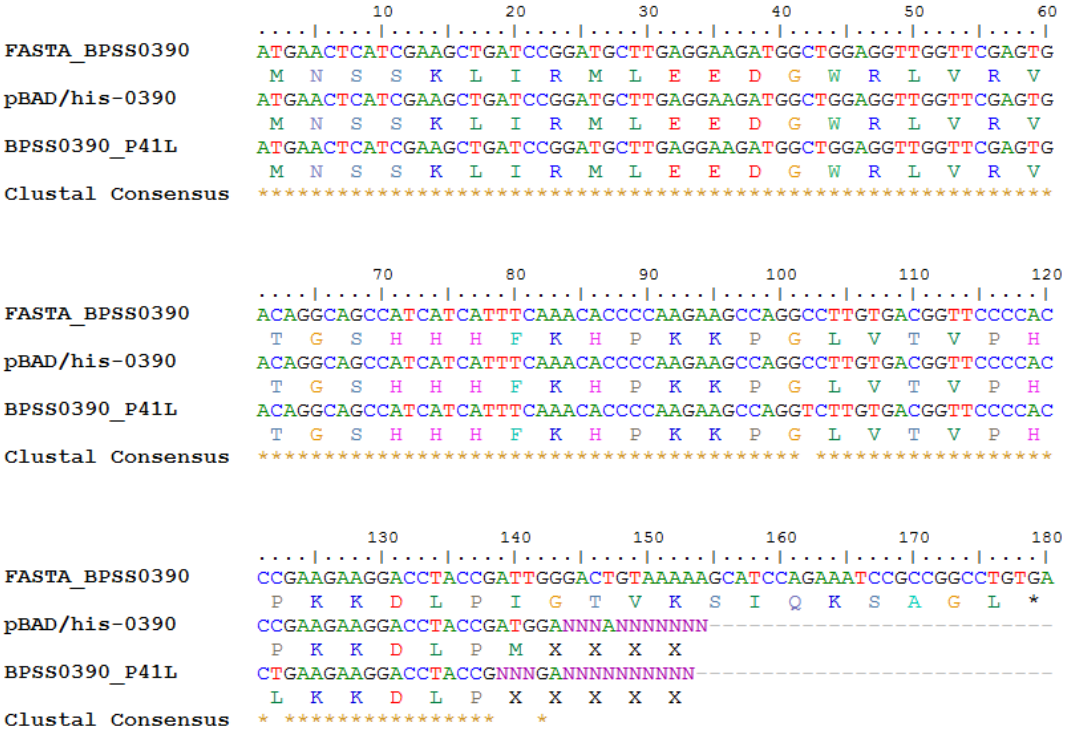

Figure 3.3: Sequencing data from site directed mutagenesis to revert pBAD/his-*BPSS0390* P41L to pBAD/his-*BPSS0390*. FASTA_BPSS0390 - wild type sequence; pBAD/his-0390 - the sequence of *BPSS0390* after reversion of P41L mutation; BPSS0390_P41L - sequence of *BPSS0390* cloned into pBAD containing the P41L mutation (template for site-directed mutagenesis); Clustal consensus- consensus of all sequences shown. Sequences aligned using CLUSTALW and figure generated with BioEdit.

3.2.2 Induction of Expression of *B. pseudomallei* toxin gene *BPSS0390* in wild type *E. coli*

Construct pBAD/his-*BPSS0390* was transformed into wild type *E. coli* MG1655. An overnight culture of *E. coli* pBAD/his-*BPSS0390* was then used to inoculate LB supplemented with ampicillin (100 µg/ml) and the culture incubated at 37°C with shaking until early log phase was reached (OD_{590} ~ 0.1) . The culture was split and either toxin expression induced (addition of arabinose to a final concentration of 0.2% (w/v) arabinose) or repressed (addition of glucose to a final concentration of 0.2% (w/v)). The optical density (OD) of the cultures was monitored every hour, for three hours (Figure 3.4a). The colony forming units (CFU) were also measured every hour by serially diluting samples in a 96- well plate in LB before plating onto LB ampicillin plates for CFU counts the following day (Figure 3.4b).

The addition of glucose to culture permitted *E. coli* cells to grow, as demonstrated by the increase in OD and increase in the number of culturable cells. However, when toxin expression was induced there was a decrease in the number of culturable cells after three hours. Despite this, the OD of the arabinose-supplemented culture continued to increase, although a reduced growth rate was observed when compared to the glucose control.

a)

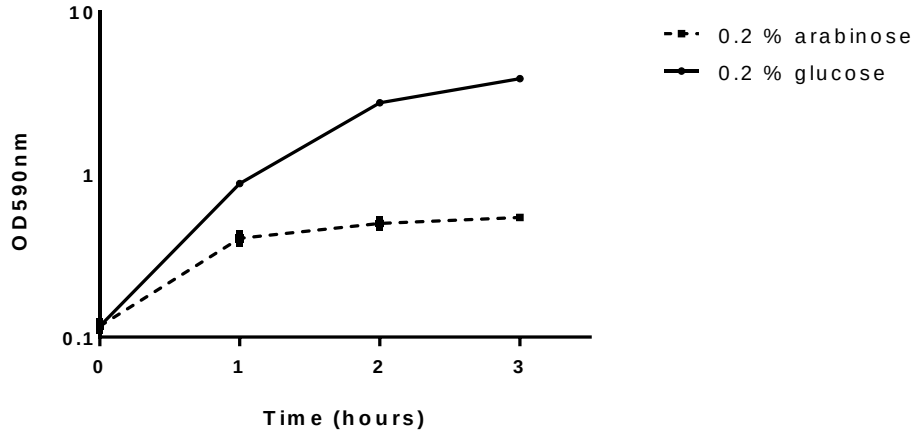

b)

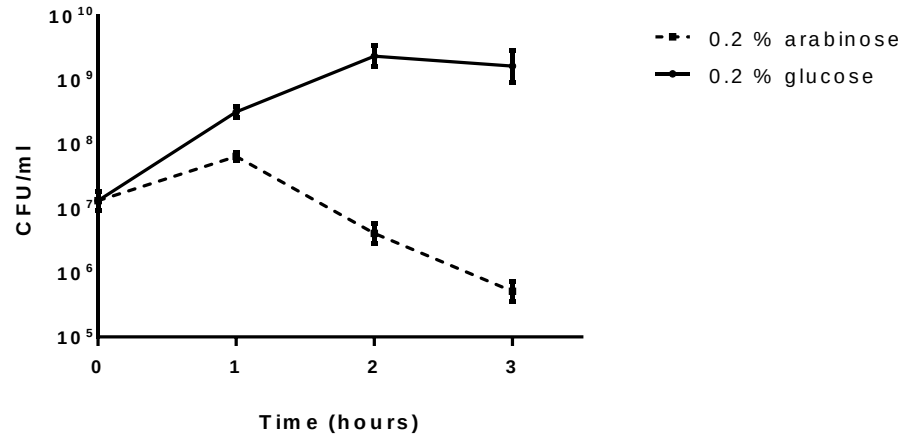

Figure 3.4: Effect of induction of BPSS0390 expression on *E. coli* MG1655:

a) OD_{590} over three hours following induction (addition of arabinose to a final concentration of 0.2% (w/v)) or repression (addition of glucose to a final concentration of 0.2% (w/v)) of toxin expression at T0. b) Number of culturable cells (CFU/ ml) after plating samples onto LB agar monitored every hour for three hours after toxin induction/repression at T0. Data is the average of three biological repeats and error bars represent SEM.

3.2.2.1 Induction of toxin expression using different concentrations of inducer.

An overnight culture of *E. coli* MG1655 pBAD/his-*BPSS0390* was used to inoculate LB supplemented with ampicillin (100 µg/ml) and the culture incubated at 37°C with shaking until early log phase (OD_{590} ~0.1). The culture was split and arabinose added (to a final concentration of 0.002% or 0.02% or 0.2% or 2% (w/v)) to induce toxin expression or glucose (final concentration of 0.2% (w/v)) added to repress toxin expression. Optical density and CFU were then measured hourly for 3 hours (Figure 3.5).

Addition of glucose permitted *E. coli* cells to continue growing; both the OD and number of culturable cells increased. Addition of final concentration of 0.002% (w/v) arabinose resulted in a reduced growth rate but the number of culturable cells increased. Increasing the final concentration of arabinose 10-fold to 0.02% (w/v) resulted in a reduced growth rate and the number of culturable cells becoming static. Increasing the final concentration of arabinose to 2% (w/v) resulted in immediate bacteriostasis followed by a decrease in culturable cells after 2 hours.

a)

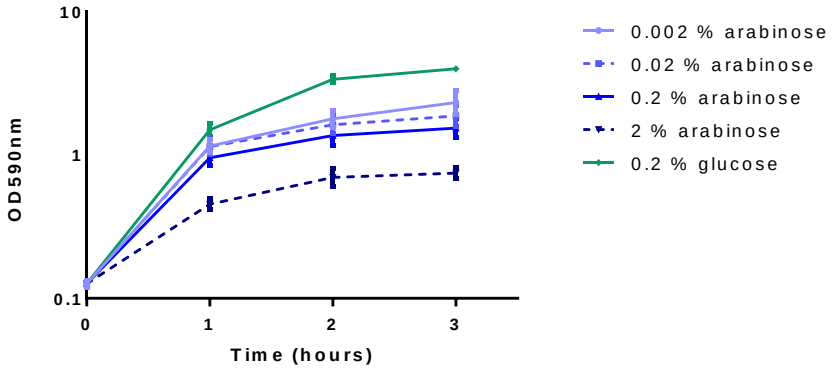

b)

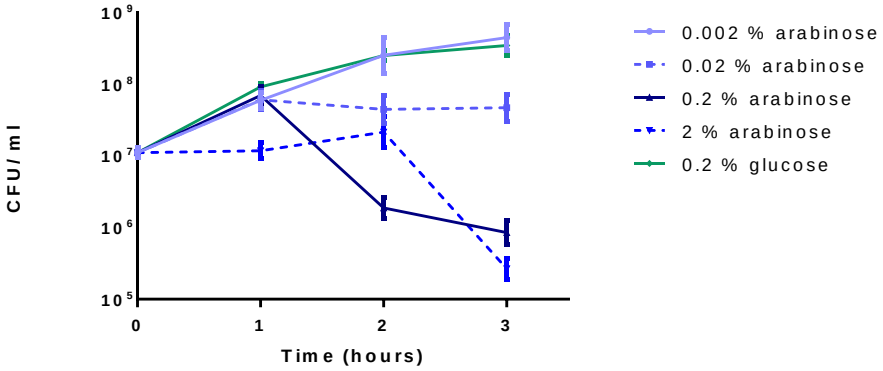

Figure 3.5: Effect of addition of different concentrations of inducer arabinose on a) optical density or b) number of culturable cells. Addition of arabinose to a higher final concentration reduced the growth rate. Adding arabinose to a final concentration higher than 0.2% (w/v) resulted in a decrease in the number of culturable cells, whilst adding only arabinose to a final concentration of 0.02% (w/v) led to bacteriostasis. Data shows mean of three biological repeats and error bars represent SEM.

3.2.2.2 Identification of mutated residues in gene *BPSS0390* within construct pBAD/his-*BPSS0390*

Induction of toxin expression in *E. coli* harbouring pBAD/his-*BPSS0390* in an early log phase culture did not reproducibly result in a decrease in culturable cells (Figure 3.5a). In some cultures, after induction of toxin expression at T0, the number of culturable cells continued to increase similar to the glucose-repressed control cultures.

When this different phenotype was observed, the pBAD/his-*BPSS0390* plasmids were isolated from cultures and nucleotide sequenced. Comparison against the wild type *BPSS0390* sequence revealed a mutation, resulting in a premature stop codon at position 31 in place of a lysine. (Figure 3.5b)

a)

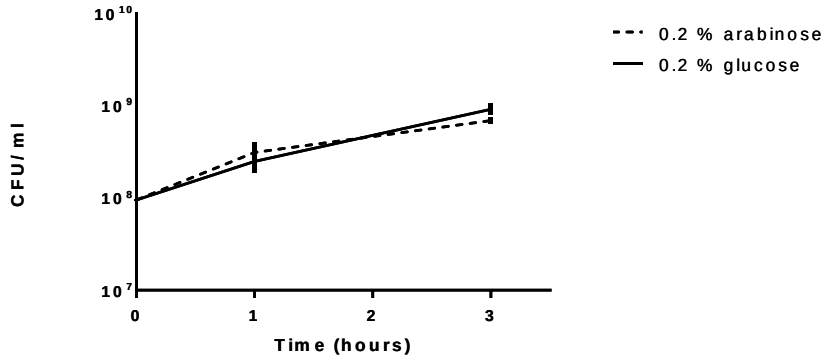

b)

```
                    10         20         30         40         50         60
                    |....|....|....|....|....|....|....|....|....|....|....|
FASTA_BPSS0390      ATGAACTCATCGAAGCTGATCCGGATGCTTGAGGAAGATGGCTGGAGGTTGGTTCGAGTG
                     M  N  S  S  K  L  I  R  M  L  E  E  D  G  W  R  L  V  R  V
BPSS0390 K31*       ATGAACTCATCGAAGCTGATCCGGATGCTTGAGGAAGATGGCTGGAGGTTGGTTCGAGTG
                     M  N  S  S  K  L  I  R  M  L  E  E  D  G  W  R  L  V  R  V
Clustal Consensus   ************************************************************

                    70         80         90         100        110        120
                    |....|....|....|....|....|....|....|....|....|....|....|....|
FASTA_BPSS0390      ACAGGCAGCCATCATCATTTCAAACACCCCAAGAAGCCAGGCCTTGTGACGGTTCCCCAC
                     T  G  S  H  H  H  F  K  H  P  K  K  P  G  L  V  T  V  P  H
BPSS0390 K31*       ACAGGCAGCCATCATCATTTCAAACACCCCTAGAAGCCAGGCCTTGTGACGGTTCCCCAC
                     T  G  S  H  H  H  F  K  H  P  *  K  P  G  L  V  T  V  P  H
Clustal Consensus   ****************************** ******************************

                    130        140        150        160        170        180
                    |....|....|....|....|....|....|....|....|....|....|....|....|
FASTA_BPSS0390      CCGAAGAAGGACCTACCGATTGGGACTGTAAAAAGCATCCAGAAATCCGCCGGCCTGTGA
                     P  K  K  D  L  P  I  G  T  V  K  S  I  Q  K  S  A  G  L  *
BPSS0390 K31*       CCGAAGAAGGACCTACCGATTGGGACTGTAAAAAGCATCCAGAAATCCGCCGGCCTGTGA
                     P  K  K  D  L  P  I  G  T  V  K  S  I  Q  K  S  A  G  L  *
Clustal Consensus   ************************************************************

                    190
                    |....|....|....|....
FASTA_BPSS0390      ------------------

BPSS0390 K31*       GAATTCGAAGCTTGGCTGT
                     E  F  E  A  W  L
Clustal Consensus
```

Figure 3.6: Abolished toxicity phenotype observed after induction of expression from toxin gene *BPSS0390* K31*.a) Example of a culture where the induction of toxin expression by addition of arabinose to a final concentration of 0.2% (w/v) did not result in the number of culturable cells decreasing. Data shows mean of two biological repeats and error bars represent SEM. b) Sequence alignment showing K31* mutation. FASTA_BPSS0390 - wild type sequence; BPSS0390 K31*- sequence of *BPSS0390* containing K31* mutation and isolated from cultures where the toxic phenotype was lost. Consensus sequence is consensus of sequences displayed. ClustalW used to align sequences and BioEdit used to generate image.

3.2.2.3 Monitoring stability of gene *BPSS0390* after prolonged induction of toxin expression

An overnight culture of *E. coli* MG1655 harbouring pBAD/his-*BPSS0390* was used to inoculate (1:100) LB media supplemented with ampicillin (100 µg/ml) , which was grown until early log phase (OD_{590nm} ~0.1). At this time either arabinose was added to a final concentration of 0.2% (w/v) to induce toxin expression or glucose to a final concentration of 0.2% (w/v) was added to repress toxin expression (Figure 3.7). Optical density and CFU were then measured hourly for 3 hours and cultures were then incubated at 37°C for a further 21 hours (a total of 24 hours). Samples for sequencing were taken after 3 hours and after 24 hours. These samples were plated onto LB ampicillin agar plates and incubated overnight. The following day, single colonies were picked at random from each plate and used to inoculate an overnight containing ampicillin (100 µg/ml) and glucose (2% (w/v)). The pBAD/his-*BPSS0390* construct was isolated from this overnight and sent for nucleotide sequencing.

Ten constructs were sent for sequencing from both three hours after and 24 hours after toxin expression or repression. None of the twenty constructs isolated after glucose repression of the toxin contained any mutations. Of the twenty constructs isolated after toxin induction, one had a mutation that changed the amino acid sequence; after three hours of expression there was a substitution of the histidine residue at position 29 with a proline.

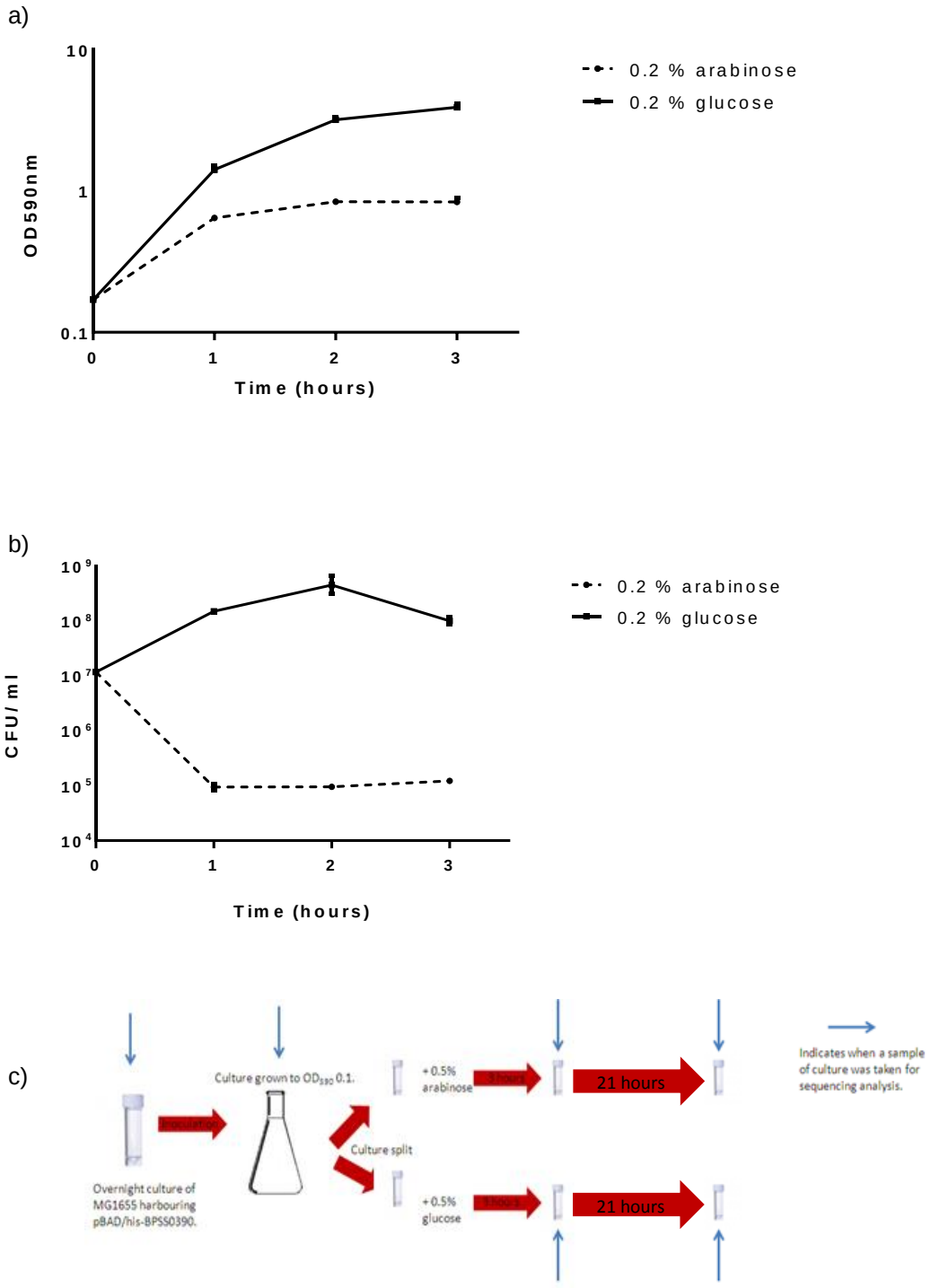

Figure 3.7: Monitoring stability of toxin gene *BPSS0390*: a) OD_{590} over three hours following induction (addition of arabinose to a final concentration of 0.2% (w/v) or repression (addition of glucose to a final concentration of 0.2% (w/v)) of toxin gene *BPSS0390* at T0; b) Culturability (CFU/ml) monitored every hour for three hours after toxin induction/repression at T0. Data represents one biological repeat and error bars represent SEM; c) schematic overview of sampling time points during the stability monitoring experiment. Blue lines indicate the time at which a sample was taken for analysis.

3.3. Induction of expression of toxin BPSS0390 in a range of bacterial species

3.3.1 Generation of suitable broad host range plasmids pSCrhaB2/his-*BPSS0390* and pSCrhaB2/H24A

To investigate whether the induction of ectopic expression of BPSS0390 caused growth arrest in a range of bacteria species it was first necessary to clone the *BPSS0390* gene into a broad host range construct capable of replication within many different Gram negative species. Plasmid pSCrhaB2 was chosen; it is a broad host range vector with a rhamnose inducible promoter, P_{rha} and a dihyrdofolate reductase gene encoding trimethoprim resistance (Cardona & Valvano 2005).

A DNA fragment encoding histidine tagged *BPSS0390* (*BPSS0390*/his) was released from pBAD/his-*BPSS0390* by restriction digestion with *Nco*I and *Hind*III. The digest was electrophoresed in an agarose gel and visualised under UV light. The appropriate band was cut out and the DNA extracted. The vector pSCrhaB2 was also restriction digested with *NcoI* and *Hind*III, electrophoresed and the linearised DNA extracted from the gel. The digested DNA fragment encoding BPSS0390/his was ligated into digested pSCrhaB2 and recovered into *E. coli* DH5α. A colony screening PCR was used to identify clones containing *BPSS0390/*his. 5ml overnight cultures of LB supplemented with trimethoprim (50 µg/ml) and glucose (final concentration 2% (w/v)) were inoculated with single colonies. Glycerol stocks were generated using 0.5ml of the overnight culture and the plasmid extracted from the remaining 4.5ml of culture. Nucleotide sequencing was used to confirm that the *BPSS0390* gene was intact and unmutated.

A control was required to ensure that any phenotypes observed were due to toxin expression only. A previously characterised mutation within *BPSS0390,* where a histidine residue at position 24 was deliberately mutated to an alanine, abolished toxicity completely (Butt et al. 2014). This mutated gene, *BPSS0390* H24A was released from pBAD/his-H24A by restriction digestion and ligated into pSCrhaB2 as described above to generate pSCrhaB2/his-H24A before recovery in *E. coli* DH5α. Nucleotide sequencing was used to confirm that the desired mutation was present.

3.3.2 Induction of expression of BPSS0390 from pSCrhaB2/his-*BPSS0390* in *E. coli* MG1655

Plasmids pSCrhaB2/his-*BPSS0390* and pSCrhaB2/his-H24A were transformed into *E. coli* MG1655 by electroporation. After electroporation, cells were recovered in LB supplemented with glucose (final concentration 2% (w/v)) and plated onto LB agar supplemented with glucose (final concentration 2% (w/v)) and trimethoprim (50 µg/ml). Overnight cultures in LB supplemented with trimethoprim (50 µg/ml) and glucose (final concentration 2% (w/v)) were inoculated using transformant single colonies. After culturing overnight, glycerol stocks were generated using 0.5ml of the overnight culture and the plasmid extracted from the remaining 4.5ml of culture. Nucleotide sequencing was used to confirm that the *BPSS0390* gene was intact and unmutated.

Overnight cultures in LB supplemented with glucose (final concentration 2% (w/v)) and trimethoprim (final concentration 50 µg/ml) of *E. coli* MG1655 harbouring either pSCrhaB2/his-*BPSS0390* or pSCrhaB2/his-H24A were used to inoculate (1:100) fresh LB media supplemented with trimethoprim and grown until early log phase (OD_{590} nm ~ 0.1). The cultures were split before addition of

either rhamnose (final concentration 0.2% (w/v) to induce toxin expression) or glucose (final concentration 0.2% (w/v) to repress toxin expression). The optical density and number of culturable cells was monitored hourly, for three hours for *E. coli* pSCrhaB2/his-*BPSS0390* (Figure 3.8a, b) and *E. coli* pSCrhaB2/his-H24A (Figure 3.8c, d).

Induction of expression from pSCrhaB2/his-*BPSS0390* resulted in a reduced growth rate and a rapid decrease in the number of culturable cells whilst the addition of glucose permitted cell growth. The growth of E. coli possessing pSCrhaB2/his-H24A was similar in cultures to which either rhamnose or glucose was added.

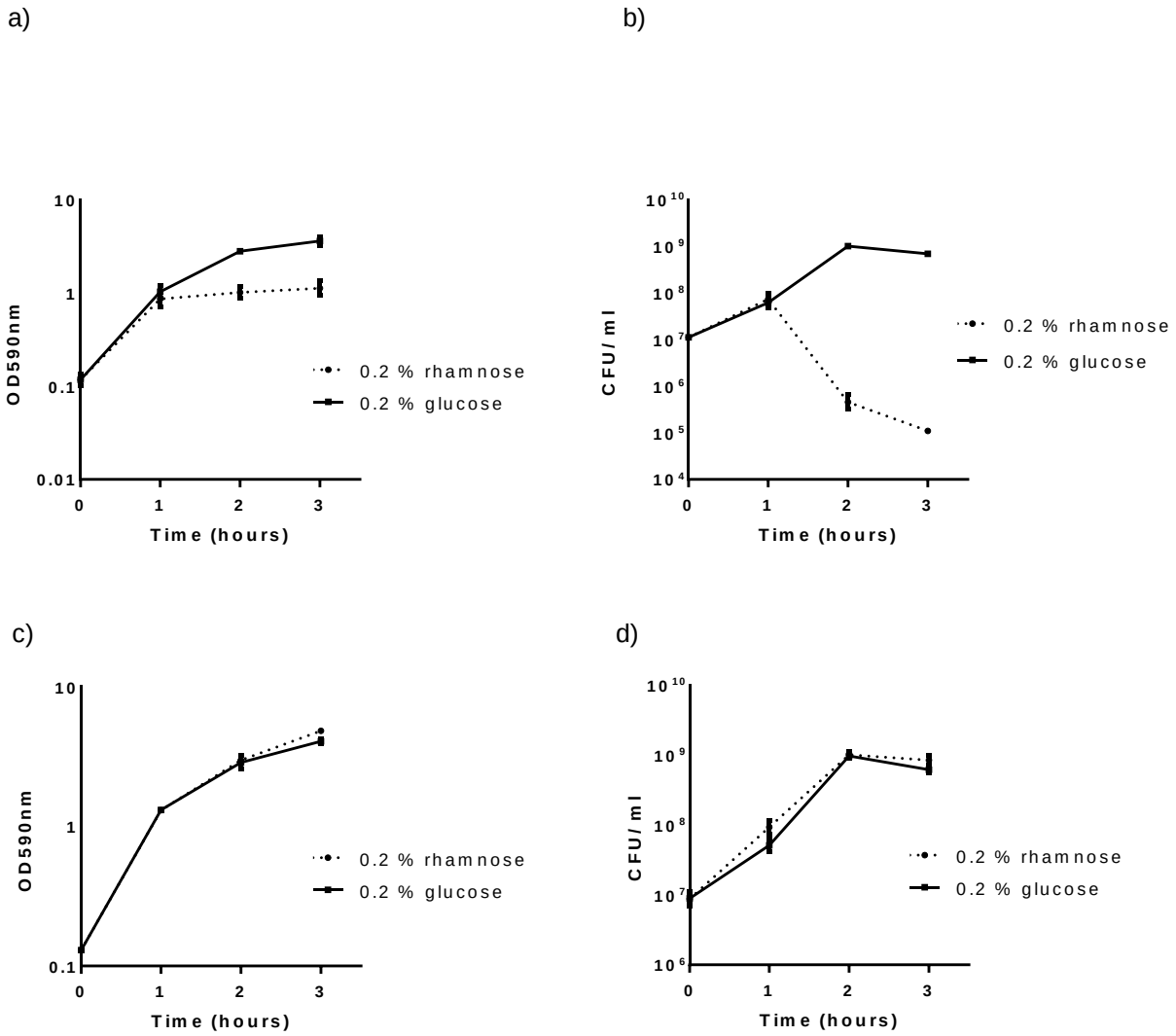

Figure 3.8: Effects of induction or repression of expression of BPSS0390 or BPSS0390 H24A from pSCrhaB2/his-*BPSS0390* and pSCrhaB2/his-H24A in E. coli MG1655: a) Growth over three hours following induction (0.2% (w/v) rhamnose) or repression (0.2% (w/v) glucose) of BPSS0390; b) Profile showing change in number of culturable cells after induction or repression of toxin expression at T0; c) Growth over three hours following induction (0.2% (w/v) rhamnose) or repression (0.2% (w/v) glucose) of expression of non-toxic mutant BPSS0390 H24A; d) Profile showing change in number of culturable cells after induction or repression of non-toxic control H24A at T0. Each graph shows mean of two biological replicates and error bars represent SEM.

3.3.2.1. Induction of toxin expression in *E. coli* using different concentrations of rhamnose.

Overnight cultures of *E. coli* MG1655 harbouring either pSCrhaB2/his-*BPSS0390* or pSCrhaB2/his-H24A that had been supplemented with glucose (final concentration 2% (w/v) and trimethoprim 50 µg/ml) were used to inoculate (1:100) fresh LB media supplemented with trimethoprim (50 µg/ml) and grown until early log phase (OD_{590} nm ~ 0.1) was reached. The culture was split and different concentrations of rhamnose (0.002%, 0.02%, 0.2% or 2% ((w/v) final concentrations)) were added to induce toxin expression or glucose (final concentration 2% (w/v)) was added to repress. Optical density and CFU were measured hourly for 3 hours (Figure 3.9).

When glucose was added the cells continued to grow, as demonstrated by the increase in OD and increase in number of culturable cells. The addition of rhamnose reduced the growth rate and decreased the number of culturable cells at three hours. However, 0.002% and 0.02% (w/v) rhamnose resulted in the number of culturable cells increasing initially at a similar rate to the glucose repressed control, before declining after one hour. Adding a final concentration of 2% rhamnose resulted in a decrease in the number of culturable cells, very similar to the profile observed when a final concentration of 0.2% (w/v) rhamnose was added (Figure 3.9a).

a)

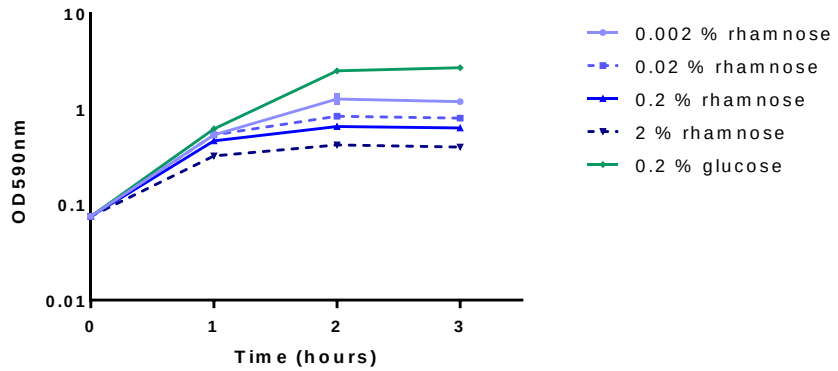

b)

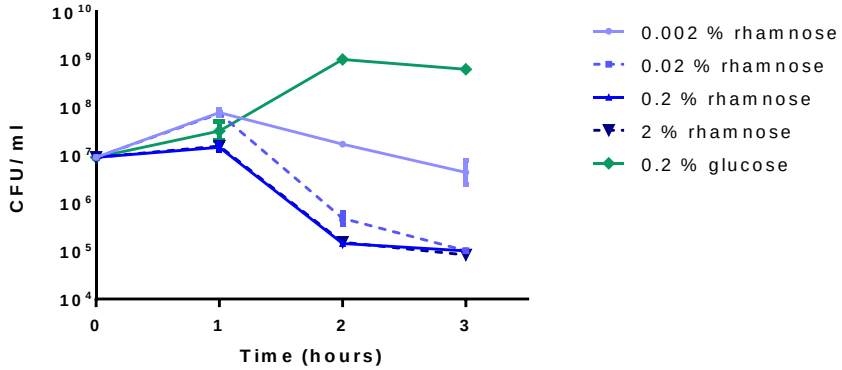

Figure 3.9: Effect of different concentrations of rhamnose or glucose on a) optical density and b) culturable cells. Cultures of *E. coli* MG1655 harbouring pSCrhaB2/his-*BPSS0390* were cultured in the presence of the final concentrations of rhamnose or glucose indicated. Any addition of rhamnose resulted in a decreased growth rate and a decrease in culturable cells over time. Data shows mean of two biological repeats and error bars represent SEM.

3.3.3 Expression of *BPSS0390* in *Salmonella enterica* serovar Typhimurium SL1344

Salmonella enterica subspecies are associated with a variety of intestinal diseases in a broad range of hosts. *S. enterica* serovar Typhimurium infection in humans results in salmonellosis, whilst infection in mice is frequently used as an animal model for systemic typhoid in humans (Northen et al. 2010).

A BLASTp alignment comparing the protein sequence of *B. pseudomallei* K96243 HicB against all available non-redundant protein sequences available for *S.* Typhimurium SL1344 was conducted and no significant similarity was found.

S. Typhimurium was screened for any trimethoprim resistance by streaking onto LB agar only, LB agar supplemented with trimethoprim (50 µg/ml) or LB agar supplemented with trimethoprim (100 µg/ml). Growth was only observed on the LB agar only plate indicating that *S.* Typhimurium SL1344 did not harbour any pre-existing trimethoprim resistance.

Constructs pSCrhaB2/his-*BPSS0390* or pSCrhaB2/his-H24A were transformed into *S.* Typhimurium by electroporation, cells were recovered in LB broth supplemented with glucose (final concentration 2% (w/v)) and plated onto LB agar with glucose (final concentration 2% (w/v)) and trimethoprim (50 µg/ml). Overnight cultures of LB containing trimethoprim (50 µg/ml) and glucose (final concentration 2% (w/v)) were inoculated using single colonies recovered after the electroporation. The following day, glycerol stocks were created using 0.5ml of the overnight cultures and plasmids extracted from the remaining 4.5ml of cultures. Nucleotide sequencing was used to confirm that the native *BPSS0390* gene in pSCrhaB2/his-*BPSS0390* did not contain any mutations and that the expected mutation was present in pSCrhaB2/H24A.

Overnight cultures of *S.*Typhimurium harbouring either pSCrhaB2/his-*BPSS0390* or pSCrhaB2/his-H24A, which had been supplemented with glucose (final concentration 2% (w/v) and trimethoprim at final concentration 50 µg/ml) overnight were used to inoculate (1:100) fresh LB media supplemented with trimethoprim (50 µg/ml) and grown until early log phase (OD_{590} nm ~ 0.1) was reached. The cultures were split before addition of either rhamnose to a final concentration of 0.2% (w/v) (to induce toxin expression) or glucose to a final concentration of 0.2% (w/v) (to repress toxin expression). The optical density and number of culturable cells was monitored for three hours (Figure 3.10).

The addition of glucose or rhamnose did not affect the growth of *S.*Typhimurium harbouring *BPSS0390* H24A. However, the induction of toxin BPSS0390 expression resulted in a rapid decrease of almost 10,000 culturable cells and a greatly reduced growth rate.

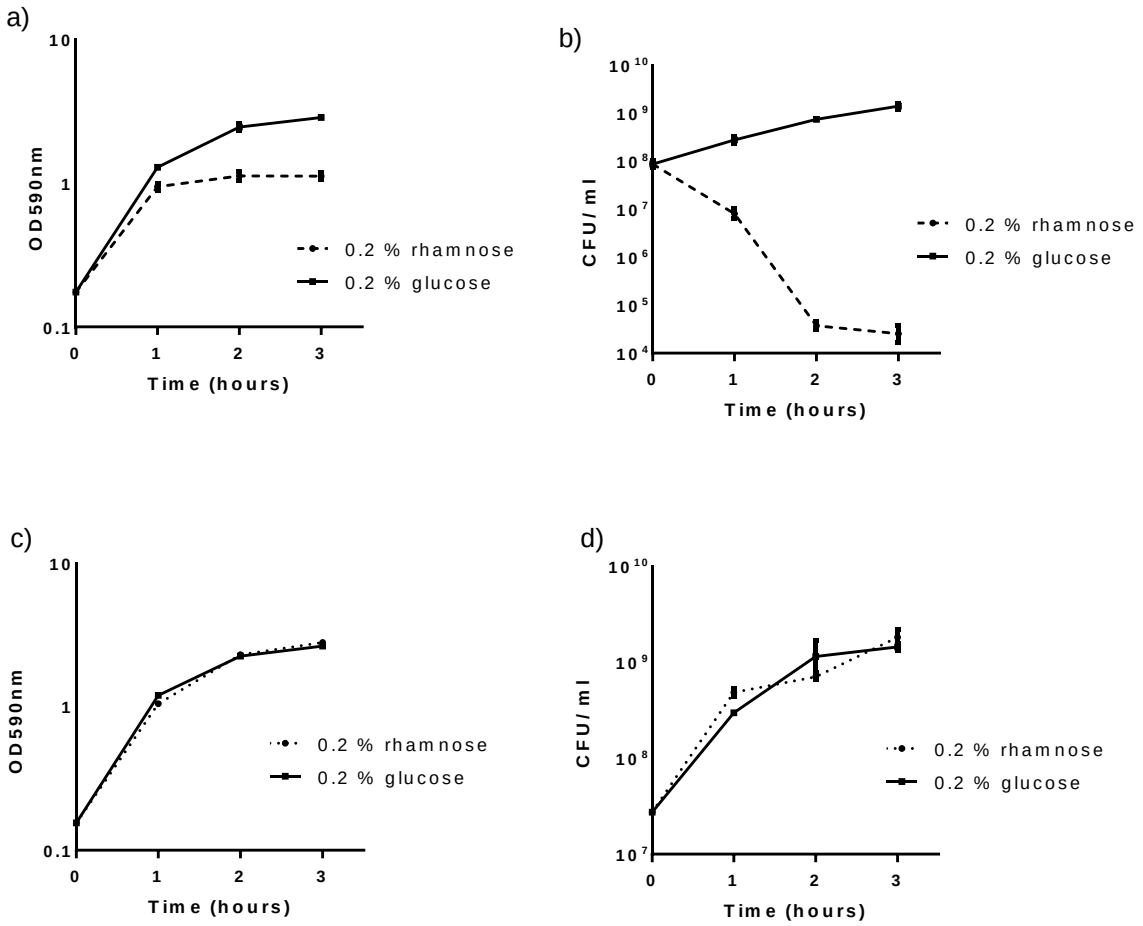

Figure 3.10: Induction of toxin expression in *S*. Typhimurium SL1344.

Growth over three hours following induction (0.2% (w/v) rhamnose) or repression (0.2% (w/v) glucose) of *BPSS0390*. a) OD_{590nm} b) culturable cells; or induction (0.2% (w/v) rhamnose) or repression (0.2% (w/v) glucose) of *BPSS0390* H24A c) OD_{590nm} d) culturable cells. Each graph shows mean of three biological replicates and error bars represent SEM.

3.3.4. Induction of expression of *BPSS0390* in species with partial HicB (*BPSS0391)* homologues

3.3.4.1 Selection of suitable bacterial species with partial HicB homologues

A BLASTp search of *B. pseudomallei* BPSS0391 against all non-redundant protein sequences was carried out and a distance tree of the results (Figure 3.11) used to identify bacteria from different classes that were readily available within the lab. Species were also chosen to have to have HicB homologues with less than 50% identity when compared to *B. pseudomallei* antitoxin; it was hoped that toxin expression in such a species might give rise to a partial neutralisation phenotype and identify critical residues in HicB involved in toxin-antitoxin complex formation.

Four species, *Yersinia pseudotuberculosis* IP32952, *Vibrio vulnificus* E64MW, *Pseudomonas aeruginosa* PA01 and *Pseudomonas syringae* were identified by this method and along with *B. thailandensis* were tested for trimethoprim resistance (Table 3.1).

Both *P. aeruginosa* and *P. syringae* were resistant to trimethoprim at 100 µg/ml and so were not investigated further. Induction of ectopic toxin expression was carried out in *Yersinia pseudotuberculosis, Vibrio vulnificus* and *B. thailandensis.*

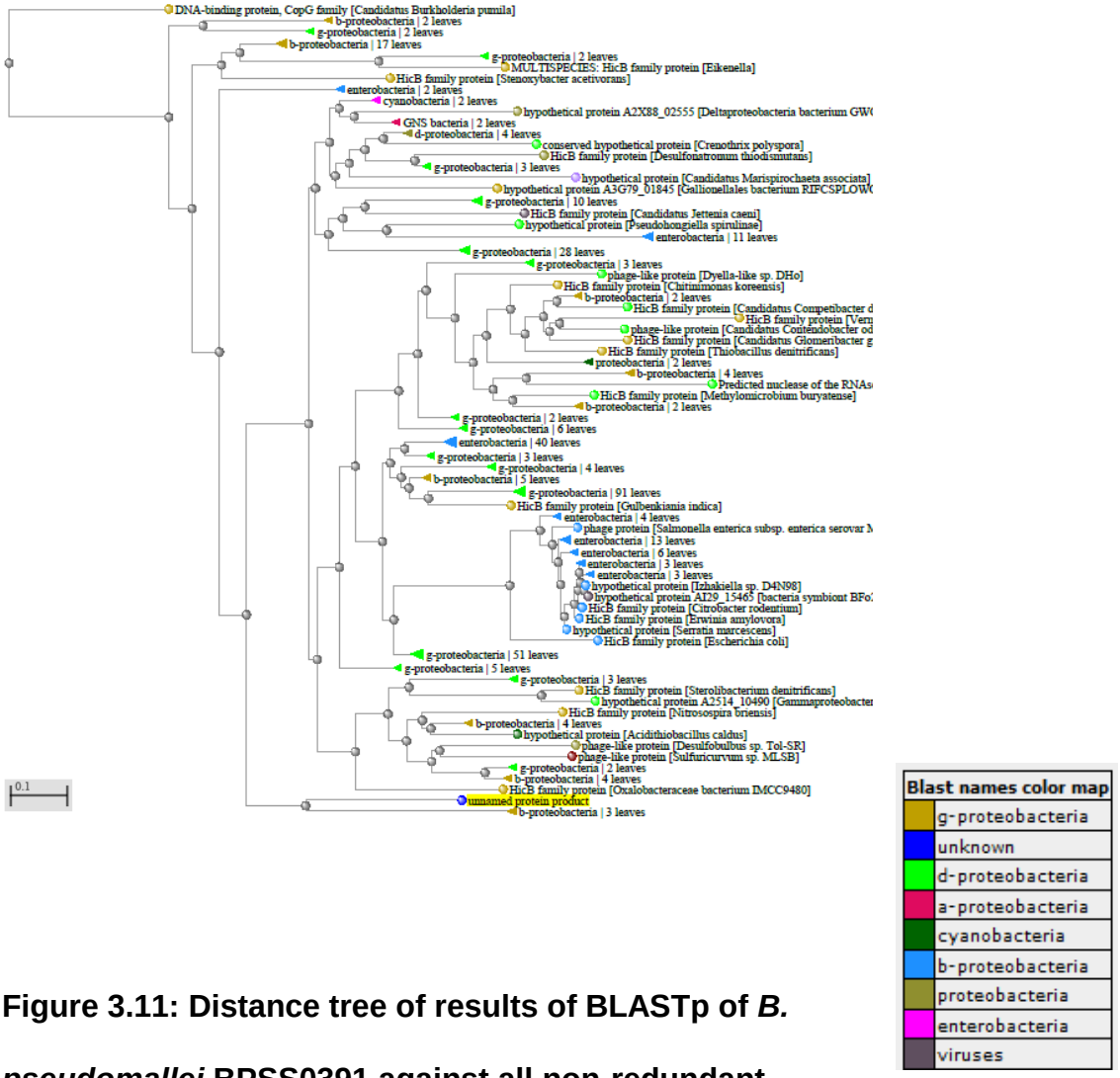

Figure 3.11: Distance tree of results of BLASTp of *B. pseudomallei* BPSS0391 against all non-redundant protein sequences. A BLASTp search of *B. pseudomallei* BPSS0391 against all non-redundant protein sequences was carried out, proteins with a less than 50% amino acid identity were selected. Distance tree generated using BLASTp with Fast Minimum Evolution tree method.

Table 3.1: Trimethoprim sensitivity of selected species. Species were streaked onto agar indicated, incubated at 37°C and growth recorded 24 hours later.

Species	**% amino acid identity of HicB homologue**	**Growth on LB agar only**	**Growth on LB agar with trimethoprim (50 µg/ml)**	**Growth on LB agar with trimethoprim (100 µg/ml)**
Yersinia pseudotuberculosis IP32953	28	✓	X	X
Vibrio vulnificus E64MW	40	✓	X	X
Pseudomonas aeruginosa PA01	41	✓	✓	✓
Pseudomonas syringae	44	✓	✓	✓
Burkholderia thailandensis E264	99	✓	X	X

3.3.4.2 Induction of expression of toxin BPSS0390 in *Y .pseudotuberculosis* IP32953

Y. pseudotuberculosis is a Gram negative bacterium known to cause fever, abdominal pain and diarrhoea in humans (Laukkanen et al. 2008; Jalava et al. 2006). Typically foodborne, *Y. pseudotuberculosis* infection is linked to the consumption of raw or undercooked pork or dairy products (Laukkanen et al. 2008) or contaminated food. For example, raw grated carrots were linked to an outbreak in May 2003 (Jalava et al. 2006). Zoonotic infection has also been reported; typically from livestock or family pets (Tertti et al. 1984).*Y. pseudotuberculosis* is closely related to *Y. pestis*, the causative agent of plague (Rasmussen et al. 2016).

A BLASTp search revealed that *Y. pseudotuberculosis* contained a protein with 28% amino acid sequence identity homology to HicB from *B. pseudomallei* (Figure 3.12a). Plasmids pSCrhaB2/his-*BPSS0390* or pSCrhaB2/his-H24A were transformed into *Y. pseudotuberculosis* IP32953 by electroporation. Cells were resuspended in LB broth with 2% (w/v) glucose then plated onto LB agar plates with glucose and trimethoprim (50 µg/ml). Successful transformants were used to inoculate overnight cultures of LB again supplemented with trimethoprim (50 µg/ml) and glucose (2% (w/v)). Sequencing confirmed that both genes inside the constructs were intact.

Overnight cultures containing either pSCrhaB2/his-*BPSS0390* or pSCrhaB2/his-H24A, which had been supplemented with glucose (final concentration 2% (w/v) and trimethoprim at final concentration 50 µg/ml) overnight, were used to inoculate (1:100) fresh LB broth supplemented with trimethoprim (50 µg/ml). Cultures were grown until early log phase was reached; split and either a final

concentration of 0.5% (w/v) rhamnose (to induce toxin expression) or a final concentration of 0.5% (w/v) glucose (to repress toxin expression) added. The optical density and number of culturable cells was monitored hourly, for three hours (Figure 3.12).

Induction of toxin expression resulted in a rapid decrease in the number of culturable cells after three hours and also a reduced growth rate assessed by change in OD_{590nm}. Glucose repression of the toxin gene and induction of expression/repression of the non-toxic control allowed cells to grow. Unfortunately, the viability data showing the change in the number of culturable cells after induction or repression of non-toxic BPSS0390 H24A protein expression was lost and so is absent from this study. However, the growth profile after induction or repression of BPSS0390 H24A expression demonstrates that both the OD_{590} continues to increase at a similar rate regardless of addition of inducer (0.5% (w/v) rhamnose) or repressor (0.5% (w/v) glucose).

a)

```
                    10        20        30        40        50        60
                    |....|....|....|....|....|....|....|....|....|....|...
B.pseudomallei      MEFPIAVHKDDGSVYGVTVPDIPGVHSWGETIDDAIKNTREAIVGHVETLIELGEDVEFTCST
Y.pseudotuberculosis MIYPIFIFKTVEGFDGY-FPDIDGCFFAGNTFADISKNAEEAFAVHIEALMNEGFPLPSPPKD
Clustal Consensus   * :** :.*   .. *  .*** * .  *:*: *  **: **:. *:*:*:: *  :  . .

                    80        90        100       110       120       130
                    |....|....|....|....|....|....|....|....|....|....|....|...
B.pseudomallei      PEY--AGAVWALVSVDLSQLDSKPERINVSIPRFVLHKIDAYVASR--HETRSGFLARAALEA
Y.pseudotuberculosis PRLKEEGGILGFVEIDPAKYESKAVKFNLTMSQNLLTAIDKFIATNRGYKNRSQFLAELAREK
Clustal Consensus   *     *.: .:*.:* :: :**. .:*:::.. :*  ** ::*:.  ::.** ***  * *

                    ..
B.pseudomallei      HA
Y.pseudotuberculosis --
Clustal Consensus
```

b)

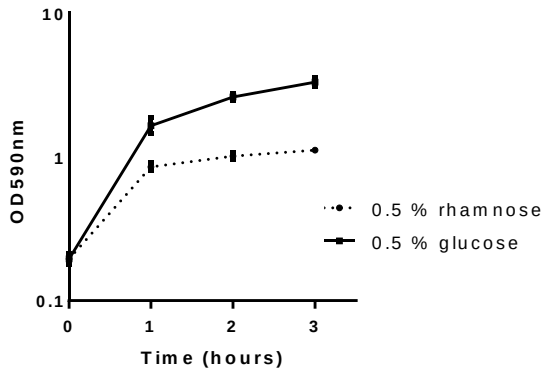

c)

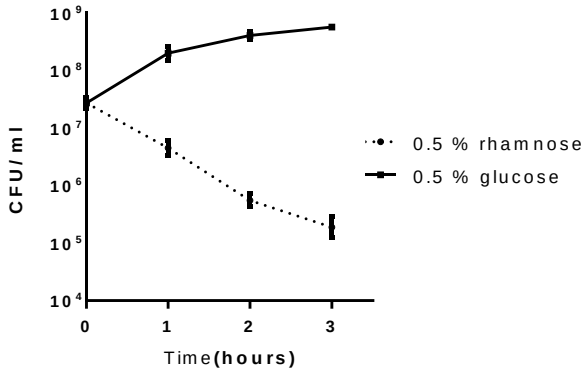

d)

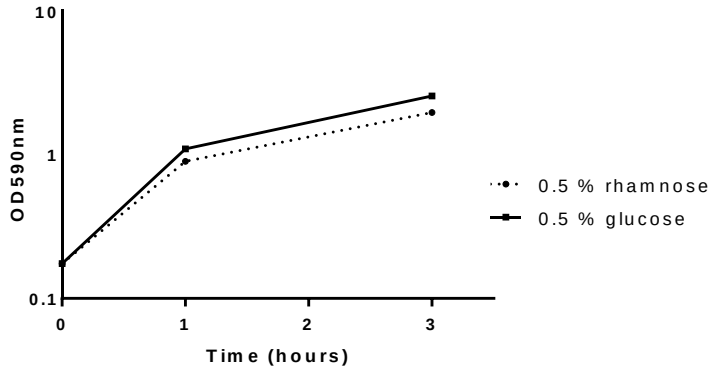

Figure 3.12: Toxin expression in *Y. pseudotuberculosis*: a) Alignment of *B. pseudomallei* HicB with the Y. pseudotuberculosis homologue. The consensus symbols: * denotes a single, fully conserved residue, : indicates conservation between groups of strongly similar properties and . marks conservation between groups of weakly similar properties. b) Growth profile after HicA expression (0.5% (w/v) rhamnose) or repression (0.5% (w/v) glucose) c) Change in culturable cells after expression (0.5% (w/v) rhamnose) or repression (0.5% (w/v) glucose) of BPSS0390 d) Growth profile of cells after expression (0.5% (w/v) rhamnose) or repression (0.5% (w/v) glucose) of the non-toxic mutant protein BPSS0390 H24A. CFU data is absent. Data shown is average of two biological replicates and error bars represent SEM.

3.3.4.3 Induction of expression of toxin BPSS0390 in *V. vulnificus* E64MW

V. vulnificus is frequently found in estuaries and shellfish; indeed it is the leading cause of all shellfish related deaths in the USA (Oliver & Bockian 1995) It is capable of causing two severe, though distinct syndromes dependent on the route of infection; either primary septicaemia or necrotizing wounds (Strom & Paranjpye 2000). Increasing temperatures due to climate change have been linked to new outbreaks and so this organism of increasing interest (Wu et al. 2015; Paz et al. 2007).

Conjugation was used to transform plasmids pSCrhaB2/his-*BPSS0390* or pSCrhaB2/his-H24A into *V. vulnificus*. Donor *E. coli* DH5α was mixed with recipient *V. vulnificus* and an *E. coli* helper strain harbouring plasmid pRK2013 and plated onto a non-selective LB agar plate. Following incubation overnight at 37°C, growth was scraped off and plated onto LB agar plates supplemented with 2% (w/v) glucose and 100 µg/ml trimethoprim for another overnight incubation. The next day growth was replated on TCBS plates containing 100 µg/µl trimethoprim and resultant green colonies were patched. A screening PCR was used to ensure the colonies were *V. vulnificus* and nucleotide sequencing confirmed that the transformed constructs contained no undesired mutations.

Overnight cultures containing either pSCrhaB2/his-*BPSS0390* or pSCrhaB2/his-H24A, which had been supplemented with glucose (2% (w/v) and trimethoprim at final concentration 50 µg/ml) overnight, were used to inoculate (1:100) fresh LB broth supplemented with trimethoprim 100 µg/ml. Cultures were grown until early log phase (OD_{590nm} ~ 0.1) was reached, before splitting and adding either a final concentration of 0.5% (w/v) rhamnose (to induce toxin expression) or a final concentration of 0.5% (w/v) glucose (to repress toxin expression). The

optical density and number of culturable cells was monitored for three hours (Figure 3.13)

Induction of toxin expression in *V. vulnificus* by addition of rhamnose resulted in a 3 log decrease in culturable cells after just 3 hours. This was accompanied by a decreased growth rate when compared to glucose controls. When glucose was added or expression of the non-toxic protein was induced, cells were able to continue growing.

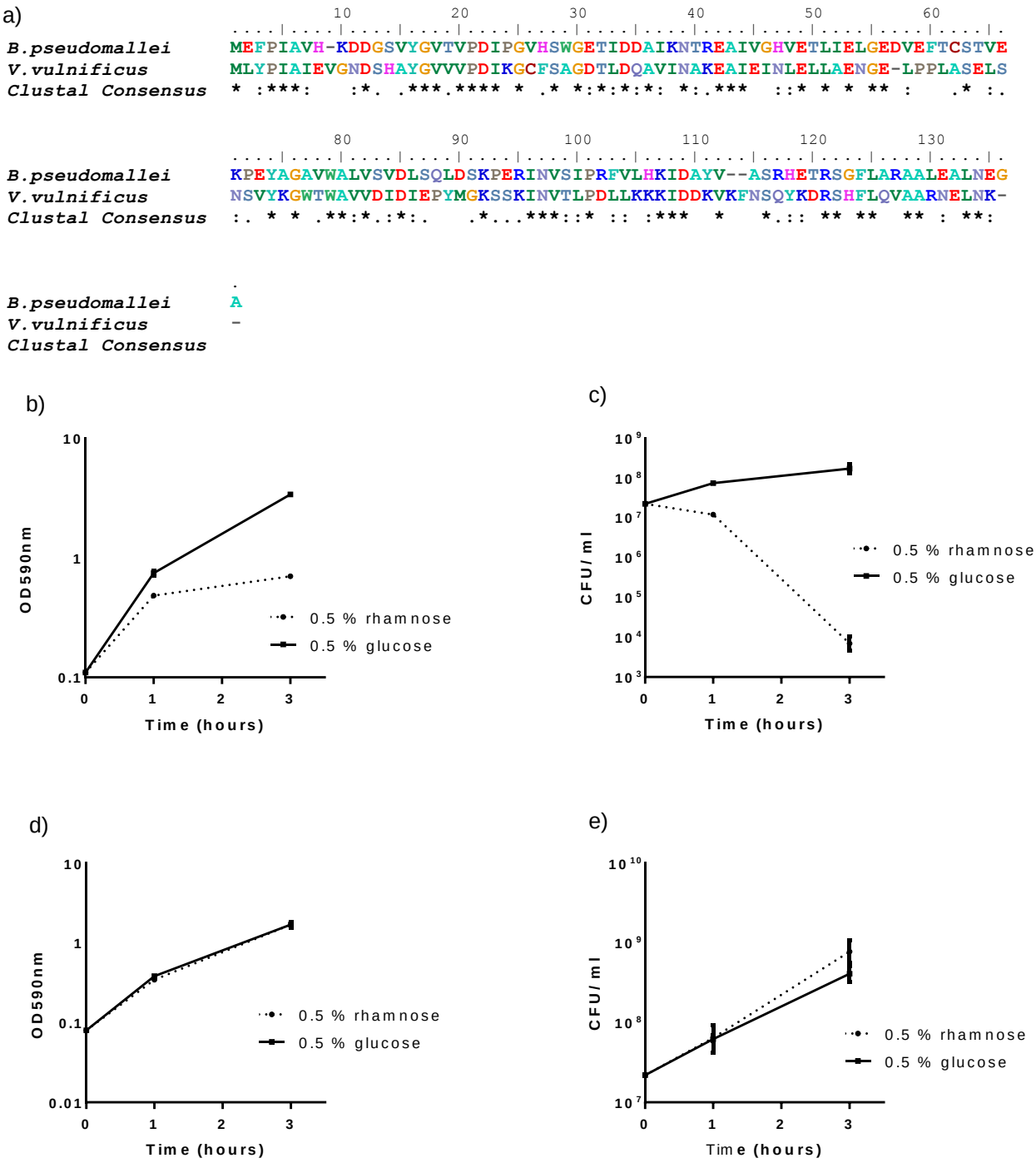

Figure 3.13: Induction of toxin expression in *V. vulnificus*: a) alignment of *B. pseudomallei* HicB with the homologue in *V. vulnificus*. The consensus symbols: * denotes a single, fully conserved residue, : indicates conservation between groups of strongly similar properties and . marks conservation between groups of weakly similar properties.; b) Profile showing change in OD after induction of expression (0.5% (w/v) rhamnose) or repression (0.5% (w/v) glucose) of the toxin and matching culturable cell counts; c). d) Profile showing change in OD after induction of expression (0.5% (w/v) rhamnose) or repression (0.5% (w/v) glucose) of the non-toxic control and matching culturable cell numbers e). Data shown is average of two biological repeats and error bars represent SEM.

3.3.4.4 Induction of expression of toxin BPSS0390 in *B. thailandensis* E264

B. thailandensis is closely related to *B. pseudomallei* and has a homologue of HicB with 99% amino acid identity. Only a single residue is different; at position 55 there is an aspartic acid rather than a glutamic acid (Figure 3.14a).

Plasmids pSCrhaB2/his-*BPSS0390* or pSCrhaB2/H24A were conjugated into *B. thailandensis*. Donor *E. coli* DH5α harbouring the appropriate pSCrhaB2 construct was mixed with recipient *B. thailandensis* and an *E. coli* helper strain harbouring plasmid pRK2013 before plating onto BHI agar and incubation overnight at 37°C. The following day the growth was replated onto selective LB agar plates containing trimethoprim (100 µg/ml) and gentamicin to kill any surviving *E. coli* strains. A colony PCR was used to confirm resultant colonies were *B. thailandensis* and plasmids were extracted for sequencing.

B. thailandensis overnight cultures that had been supplemented with glucose (2% (w/v)) overnight were used to inoculate fresh LB broth supplemented with trimethoprim (100 µg/ml). Cultures were grown until early log phase and then split. Either a final concentration of 0.5% (w/v) rhamnose (to induce toxin expression) or 0.5% (w/v) glucose (to repress toxin expression) was added. The optical density and number of culturable cells was monitored hourly, for three hours (Figure 3.14).

Induction of expression of toxin BPSS0390 (addition of rhamnose) in *B. thailandensis* resulted in a reduced growth rate when compared to a glucose control. Addition of rhamnose also results in a small decrease in culturable cells before bacteriostasis occurs. Both glucose repressed controls and non-toxic controls had no noticeable effect on growth rate or culturable cell numbers.

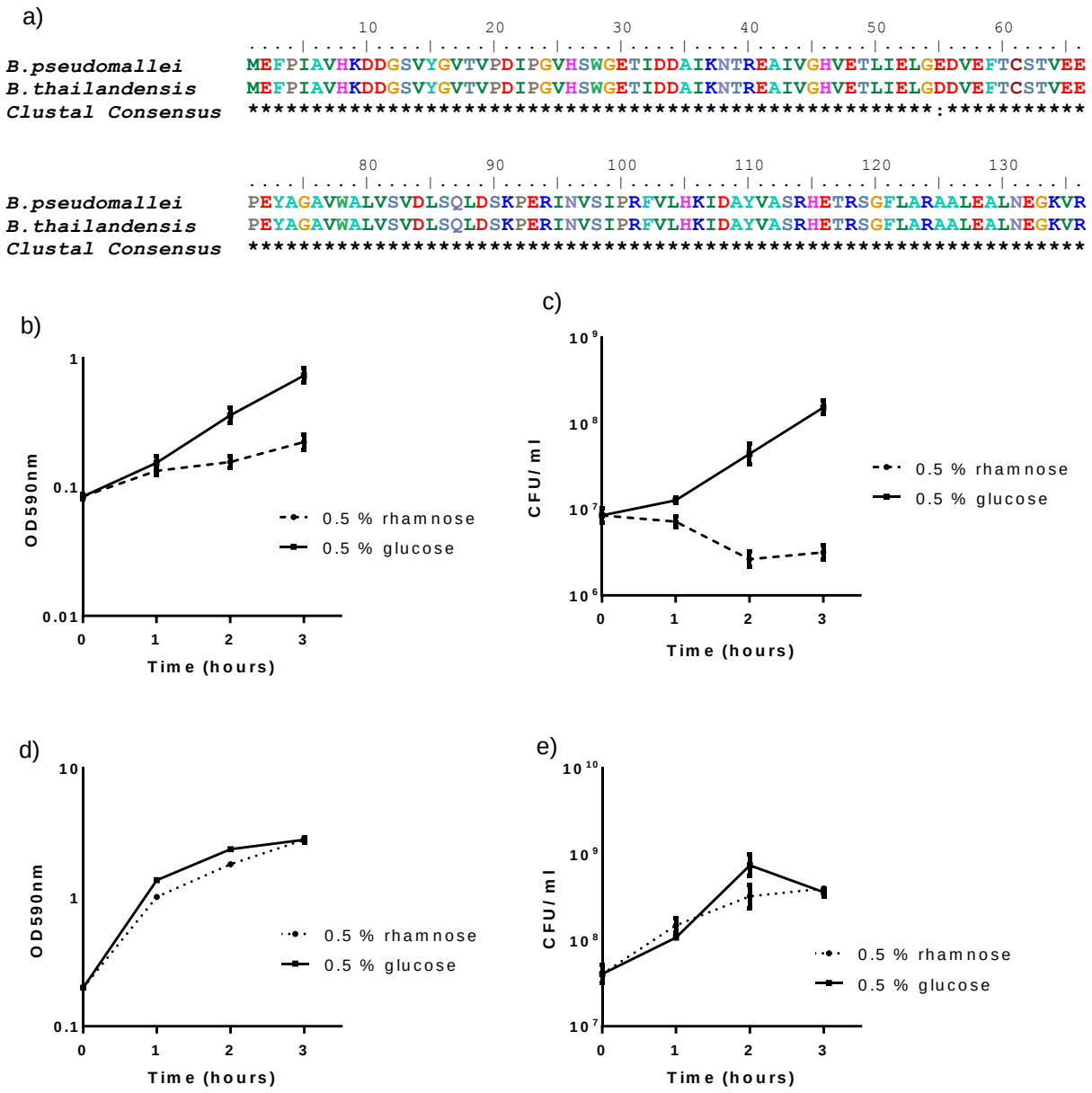

Figure 3.14: Induction of toxin expression in *B. thailandensis*: a) Alignment of HicB with its *B. thailandensis* homologue. The consensus symbols: * denotes a single, fully conserved residue, : indicates conservation between groups of strongly similar properties and . marks conservation between groups of weakly similar properties. b) Graph showing the changing optical density after induction of expression (0.5% (w/v) rhamnose) or repression (0.5% (w/v) glucose) of toxin BPSS0390. c) Change in culturable cells after induction of expression (0.5% (w/v) rhamnose) of toxin compared to a control where glucose was added. d) Changes in optical density after induction of expression (0.5% (w/v) rhamnose) or repression (0.5% (w/v) glucose) of non-toxic HicA control. e) Graph showing changes in culturable cell numbers after induction of expression (0.5% (w/v) rhamnose) or repression (0.5% (w/v) glucose) of non-toxic HicA control.

3.3.4.4.1 Induction of toxin BPSS0390 expression in *B. thailandensis* using different concentrations of rhamnose.

As described above *B. thailandensis* overnight cultures that had been supplemented with glucose and trimethoprim at final concentration 50 µg/ml overnight were used to inoculate fresh LB broth supplemented with trimethoprim (100 µg/ml). Cultures were grown until early log phase and then split and different concentrations of rhamnose added to induce toxin expression. There was a glucose control to repress toxin expression. Optical density and CFU were measured every hour (Figure 3.15a and b)

Addition of glucose allowed the cells to continue growing. Addition to a final concentration of 0.002% (w/v) rhamnose also allowed the cells to grow and so did likely not induce any/sufficient toxin expression. Once 0.02% and 0.2% (w/v) rhamnose (final concentration) was added the culturable cell counts became bacteriostatic, although the OD continued to increase. A concentration of 2% (w/v) rhamnose resulted in a small decrease in the number of cells and a noticeable decrease in growth rate.

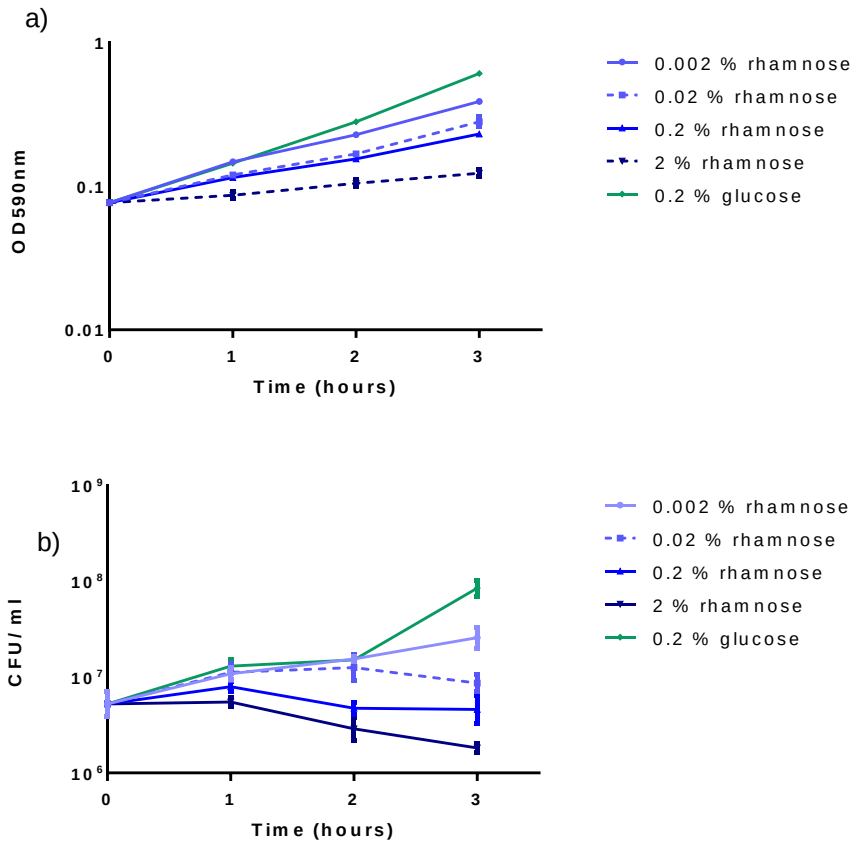

Figure 3.15: Effect of different concentrations of rhamnose (induction of toxin BPSS0390 expression) on a) optical density and b) culturable cells.

Different concentrations of rhamnose showed different effects. The highest concentration of rhamnose results in a decrease in culturable cells, whilst a final concentration of 0.02% and 0.2% rhamnose result in bacteriostatic culturable cell counts but an increase in growth profile observed by OD. Data shows mean of two biological repeats and error bars represent SEM.

3.3.4.4.2 Changes in cell size or shape after induction of BPSS0390 toxin expression in *B. thailandensis*.

To determine if the lack of correlation between OD and culturable cell counts, i.e., why the OD continues to increase after induction of toxin expression, despite a rapid decrease in culturable cells, may be due to changes in cell morphology or size, a preliminary electron microscopy experiment was carried out.

An overnight culture of *B. thailandensis* harbouring pSCrhaB2/his-*BPSS0390* that had been supplemented with glucose (2% (w/v)) and trimethoprim at final concentration 50 µg/ ml was used to inoculate fresh LB broth supplemented with trimethoprim (100 µg/ ml). Cultures were grown until early log phase and then split. Either 0.5% (w/v) rhamnose (to induce toxin expression) or 0.5% (w/v) glucose (to repress toxin expression) was added. Samples were taken at T0 (before addition of inducer/repressor), T1 (one hour post induction/repression) and T3 (three hours post induction/repression) from both cultures. The 1ml samples were centrifuged at 4°C for 5 minutes and the supernatant discarded. Samples were then washed three times in 1 x PBS before resuspension in 0.1M phosphate buffer or distilled, sterile water before fixing onto grids ready for imaging (Figures 3.16, 3.17).

There was no visible difference between cells before and after induction of toxin expression. Neither was there any difference between cells where toxin expression had been repressed or induced.

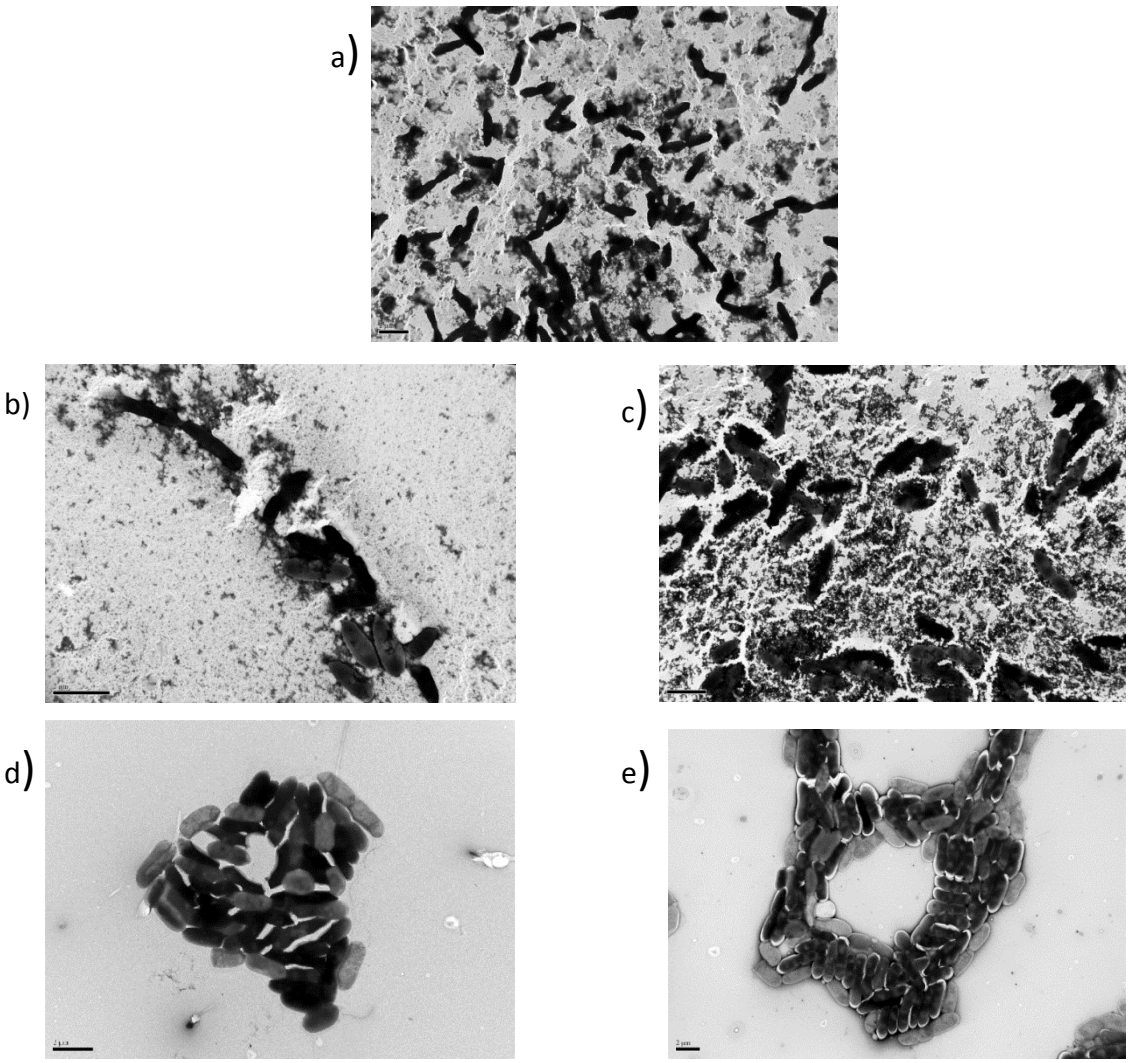

Figure 3.16: Monitoring changes in size or shape of *B. thailandensis* cells after induction of expression of BPSS0390. Scale bars are 2µm. Samples were fixed using glutaraldehyde and phosphate buffer before sputter coating. a) Image taken at T0, before induction or repression of expression; b) image taken 1 hour after rhamnose induction of expression; c) image taken 1 hour after glucose repression of expression; d) image taken 3 hours after rhamnose induction of expression; e) image taken 3 hours after glucose repression of expression.

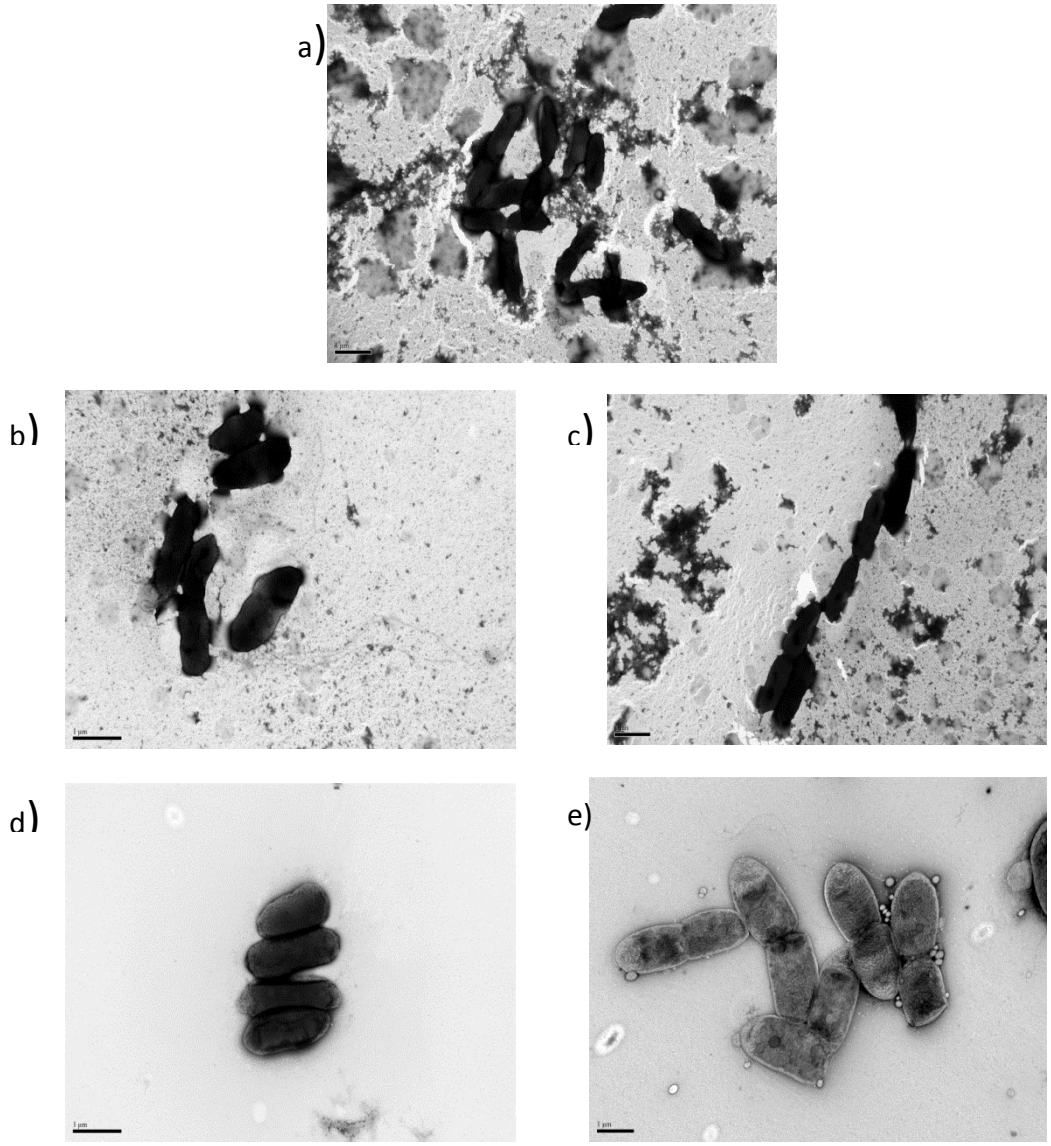

Figure 3.17: Monitoring changes in size or shape of *B. thailandensis* cells after induction of expression of BPSS0390. Scale bars are 1µm.Samples were fixed using glutaraldehyde and phosphate buffer before sputter coating. a) Image taken at T0, before induction or repression of expression; b) image taken 1 hour after rhamnose induction of expression; c) image taken 1 hour after glucose repression of expression; d) image taken 3 hours after rhamnose induction of expression; e) image taken 3 hours after glucose repression of expression.

3.4 Discussion.

It is necessary to confirm functionality of TA toxins experimentally, typically by over-expression of toxins in their native host or *E. coli* (Zheng et al. 2015; Iqbal, Guérout, et al. 2015). Frequently the putative toxin is cloned into pBAD expression plasmids as their expression is considered to be strictly controlled and reliable (Jurenaite et al. 2013; Hino et al. 2014; Qiu et al. 2008; Khlebnikov et al. 2001). However, expression of BPSS0390 from construct pBAD/his-*BPSS0390* did not always result in toxicity. When expression was not tightly regulated, by repression with glucose, mutations appeared in *BPSS0390* that abolished protein function. The predominant mutation was K31*, a premature stop codon at position 31 that abolished toxicity. Nucleotide sequencing of *hicA* revealed that a single point mutation, where a nucleotide substitution begat a codon change from AAG (lysine) to TAG (stop). Within the double-stranded RNA-binding domain like fold of HicA, residue 31 is located with the β2-β3 loop. Its function is unclear but it is not thought to be involved in the hydrophobic core, or catalysis or binding of substrate antitoxin (Butt et al. 2014). To prevent formation of escape mutants, all media used for growing overnights was subsequently supplemented with 2% (w/v) glucose, to tightly repress toxin expression.

Induction of expression of BPSS0390 in all of the bacterial species tested resulted in a decrease in the number of culturable cells. In some species this decrease was very dramatic; expression in *S.* Typhimurium, which lacks a HicB homologue, resulted in a 4 log decrease in the number of culturable cells over the three hour time course. Despite the presence of homologues with limited sequence homology to HicB in *Y. pseudotuberculosis* and *V. vulnificus*,

induction of expression of BPSS0390 resulted in a 2 log and 3 log decrease in culturable cells respectively. However, even with the recorded decrease in culturable cells, confirmation of expression of the toxin was never checked, despite the presence of a hexahistidine tag, which would have facilitated Western blotting. The hypothesis that toxin BPSS0390 is toxic in a range of bacterial species cannot be entirely supported as expression of the toxin in the species tested was not demonstrated; addition of rhamnose to cultures of *E. coli* or *Y. pseudotuberculosis* or *V. vulnificus* or *S.* Typhimurium or *B. thailandensis* harbouring pSCrhaB2/his-*BPSS0390* resulted in a decrease of culturable cells. The observation of the toxic phenotype suggests that toxin expression was induced in response to the addition of rhamnose, but does not prove it. In future work, expression studies must contain confirmation of expression of BPSS0390 after induction, either through Western blotting or by quantitative real time PCR, regardless of a toxic phenotype. .

It is difficult to extrapolate information on residues that are critical to HicBA complex formation from this data. Without quantitative data of expression levels of toxin BPSS0390 it was not possible to determine if different levels of expression of toxin BPSS0390 in different bacterial species could account for the log differences in decrease in culturable cells, rather than partial neutralisation by the native HicB homologue.

The HicB homologue identified in *B. thailandensis* E264 showed 99% amino acid identity with the *B. pseudomallei* K96423 BPSS0391, with a substitution of aspartic acid in place of a glutamic acid at residue 55. Despite having a homologue with almost identical amino acid identity, induction of BPSS0390 expression in *B. thailandensis* resulted in small decrease in culturable cells before the counts became static, suggesting that HicB

homologue was only able to partially neutralise BPSS0390. Plasmid pSCrhaB2 has a backbone originally derived from pMLBAD and so has a high copy number (Cardona & Valvano 2005) compared to the single chromosomal copy of the HicB homologue. This discrepancy in numbers would lead to a large excess of toxin molecules and could explain the bacteriostatic phenotype observed in *B. thailandensis.* Future work could confirm this by using real time PCR to confirm expression of the HicB homologue under the conditions of the expression study.

This work has demonstrated that when the concentration of the inducer was increased, a progressive decrease in growth was measured, indicating dose-dependency. Perhaps more interesting is the difference in the patterns of growth measured by changes in OD_{590} and the number of culturable cells. The highest concentration of inducer tested lead to a reduction in culturable cells, yet the OD_{590} continued to rise albeit at a reduced rate over the course of the experiment. This observation indicates that whilst an increasing proportion of the cells became non-culturable on agar, some retained the ability to grow and divide even 2 hours after induction of BPSS0390 expression. Optical density is affected by changes in cell size and shape as these alter light scattering (Najafpour 2007). Changes in morphology and clumping and clustering of cells are characteristics previously observed in viable but non-culturable cells of *Y. pestis* (Pawlowski et al. 2011). and expression of putative *V. parahaemolyticus* TA toxins in *E. coli* resulted in a filamentous cell shape (Hino et al. 2014). However, SEM of *B.thailandensis* cells expressing BPSS0390 revealed no obvious change in size or shape. Future work could include choosing a bacterial species where a greater decrease in culturable cells was observed after

induction of toxin expression and examining live cells, or using Gram staining to look for filamenting or clumping.

The potential “dose-dependency” of toxicity, coupled with the apparent lack of host specificity and toxic activity of *B. pseudomallei* HicA in all of the bacterial species tested, might suggest that *B. pseudomallei* HicA is a potential antimicrobial compound. However, ectopic expression of *B. pseudomallei* HicA toxin in *B. pseudomallei* has been demonstrated to increase the number of persister cells tolerant to ciprofloxacin and ceftazidime (Butt et al. 2014). Persister cells are believed to play a role in many chronic or persistent infectious diseases, including tuberculosis caused by *M. tuberculosis* and lung infections caused by *P. aeruginosa* (Getahun et al. 2015; Fauvart et al. 2011). Expression of toxin molecules has also been linked to biofilm formation and increased virulence within host bacteria (Van Acker et al. 2014; Sala et al. 2014; for more details please see sections 1.0.2.6-1.0.2.8) and when type II toxins are expressed in eukaryotic cells, cell death is induced through apoptosis apoptosis (Yamamoto et al. 2002; Shapira et al. 2012) .

Increasing the formation of persister cells, biofilms and increasing virulence, whilst potentially killing host eukaryotic cells are not desirable qualities in a novel antimicrobial and so whilst induction of expression of BPSS0390 was able to reduce the number culturable cells, it may also have had or may have undesirable side effects that would make the remaining bacteria more difficult to eradicate.

4. Identification of residues in HicA involved in toxicity and complex formation

4.0 Introduction

Protein toxin BPSS0390 (Figure 4.1) is able to cause growth cell arrest, a reduction in CFU and induce persister formation when expressed in *E. coli* and is neutralised when co-expressed with its antitoxin BPSS0391 (Butt et al. 2013). BPSS0390 shares sequence identity with *E. coli* HicA toxin, a translation independent mRNA interferase with an unknown mechanism of action and unidentified recognition motif (Jørgensen et al. 2009).

A previous site-directed mutagenesis study identified two residues, His24 and Gly22 as important for toxicity. The BPSS0390 H24A mutant was not toxic and so could be overexpressed, purified and its structure solved by NMR (Figure 4.1). BPSS0390 H24A consists of a double-stranded RNA-binding domain (dsRBD) fold, with a triple-stranded β-sheet and two α helices packed against one face (Butt et al. 2014). dsRBDs are small proteins able to bind to double-stranded RNA (dsRNA) (Masliah et al. 2013). Determining the structure of BPSS0390 allowed some insight into the structural and catalytic roles of amino acids conserved across HicA family proteins.

The first crystal structure of a TA complex from the HicAB family (HicA3-HicB3 TA system in *Yersinia pestis*) revealed a binding interface that completely occluded the catalytic site of HicA3 and packed the α2 helix of HicA3 against the β-sheet of HicB3, which was stabilised by both hydrophobic and polar interactions. No specific residues were mentioned (Bibi-Triki et al. 2014).

A systemic alanine scanning mutagenesis, where each individual amino acid in a protein is mutated, allows identification of residues involved in catalysis and binding and mutants can be screened for loss of function.

a)

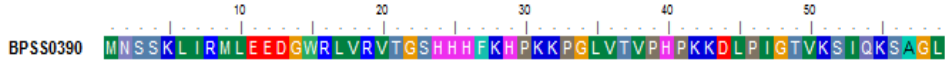

b)

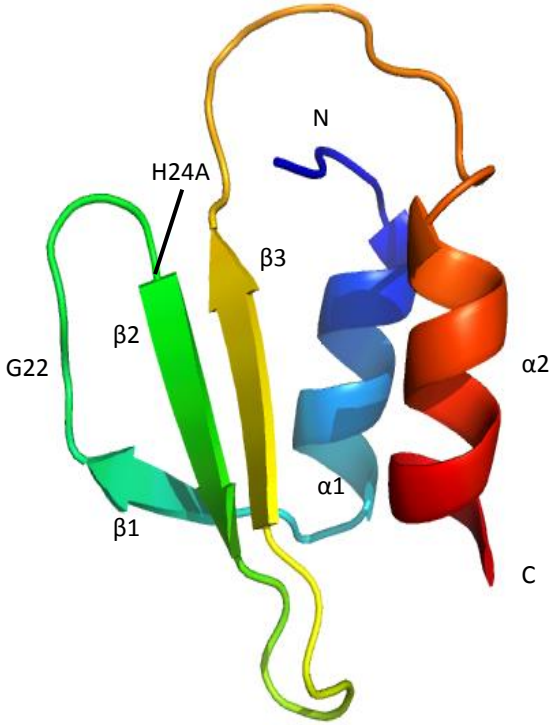

Figure 4.1: The amino acid sequence of BPSS0390 and the structure of BPSS0390 H24A as determined by NMR. a) Sequence of BPSS0390 showing all 59 amino acids. Image generated using BioEdit. b) Structure of BPSS0390 H24A, with the secondary structures, termini and residue Gly22 labelled. Image generating using PyMol, PDB 4C26.

4.1 Aim

Identify residues or regions in BPSS0390 toxin involved in toxicity and BPSS0390-BPSS0391complex formation.

.

4.2 Identification of conserved residues in BPSS0390

A sequence alignment of 25 diverse dsRNB domains revealed a consensus sequence of conserved residues, within the domain, which were critical for protein folding or double-stranded RNA binding and had been validated experimentally (Masliah et al. 2013). To identify residues or regions of BPSS0390 that might be critical for toxicity or antitoxin binding, a sequence alignment was performed. The protein sequence of BPSS0390 was BLASTp searched against NCBI. The top matching 100 sequences (E value less than < 0.001) were aligned using CLUSTALW with BPSS0390 as the reference sequence. BioEdit was then used to identify residues conserved in 75 or more of the 100 sequences (greater than 75%). (Table 4.1).

39 residues were conserved in 75 or more of the protein sequences. These residues were distributed throughout the molecule: 4 in α1 helix, 2 in the α1-β1 loop, 5 in β1-β2 loop, 3 in β2 sheet, 4 in β2-β3 loop, 4 in β3 sheet, 8 in β3- α2 loop, 7 in α2 helix, 2 at the N-terminus and none in β1 sheet. 6 residues were conserved in all 100 proteins, including three histidines (one is H24). The histidine at position 24 has previously been shown to be critical for toxicity (Butt et al. 2014).

As the conserved residues were scattered through the molecule I decided that the best way to investigate the contribution of each residue to toxicity was to perform alanine scanning mutagenesis. Alanine was chosen for the scanning mutagenesis as it has no side chain beyond its β-carbon; it can be incorporated

without altering the main chain conformation. This ensures that any changes observed are likely to be due to the loss of the side chain of the substituted amino acid.

Table 4.1: Table to show most conserved residues across 100 proteins with homology to BPSS0390. BPSS0390 sequence was BLASTp searched against NCBI and the first 100 sequences that gave a significant E-value of <0.001 chosen and aligned against BPSS0390 using BioEdit and CLUSTALW.

% Homologous proteins where residue conserved	Residue in BPSS0390	Location in BPSS0390 molecule
100	W15	α1-β1 loop
	G22	β1-β2 loop
	H24	β1-β2 loop
	H29	β2-β3 loop
	H40	β3- α2 loop
	A57	α2 helix
99	T37	β3 sheet
	P39	β3 sheet
	P41	β3- α2 loop
	T49	α2 helix
	I53	α2 helix
98	G34	β2-β3 loop
	V36	β3 sheet
	S3	N terminus
	S23	β1-β2 loop
97	G14	α1-β1 loop

96	H25	β2 sheet
	S52	α2 helix
	K55	α2 helix
95	K31	β2-β3 loop
	K43	β3- α2 loop
93	D44	β3- α2 loop
	L45	β3- α2 loop
	K42	β3- α2 loop
92	P46	β3- α2 loop
91	F27	β2 sheet
89	D13	α1 helix
86	M1	N terminus
	R19	β1-β2 loop
83	P30	β2-β3 loop
80	V18	β1-β2 loop
79	L35	β3 sheet
	V50	α2 helix
78	L59	α2 helix
77	H26	β2 sheet
76	L6	α1 helix
	L10	α1 helix
75	I7	α1 helix
	G48	β3- α2 loop

4.3 Results

4.3.1 Generation of mutated pBAD/his-*BPSS0390* constructs

An Agilent QuikChange Lightning Site Directed Mutagenesis Kit and mutagenic primers were used to individually mutate each of 58 residues to an alanine except for A57, which was mutated to a glycine.

The newly synthesised plasmid DNA was transformed into ultracompetent *E. coli* and transformants recovered onto LB agar with ampicillin (100 µg/ml) and glucose (2% (w/v)). Plasmid DNA was extracted from three colonies and sent for nucleotide sequencing to confirm that the desired mutation was present.

4.3.1.3 Repeated attempts at mutagenesis

Despite three repeated attempts it was not possible to generate mutant *BPSS0390* Q54A. A new primer pair was designed and residue Q54 was successfully mutated to a **glycine**, generating construct pBAD/his-*BPSS0390* Q54G.

4.3.2 Screening BPSS0390 mutants for changes in toxicity

4.3.2.1 Toxicity assays

The constructs were transformed into *E. coli* MG1655 Δ*hipBA* and transformants plated onto LB agar with ampicillin (100 µg/ml) and glucose (2% w/v). *E. coli* MG1655 Δ*hipBA* harbouring mutated *BPSS0390* constructs were grown to OD_{590} 0.1 and supplemented with a final concentration of 0.2% (w/v) arabinose to induce gene expression for two hours. It was not possible to test all 57 mutants in a single toxicity assay and so mutants were split into 6 groups of 8-12 different mutants. Two controls were used. One was the previously

described non-toxic mutant H24A, which was expressed in *E. coli* MG1655 Δ*hipBA* from pBAD plasmid (negative control). The second control was wild type BPSS0390, expressed from pBAD (positive control). Colony forming units (CFU) were measured before induction of expression with arabinose and two hours after induction of expression by serially diluting samples in a 96- well plate in LB and plating onto LB ampicillin (100 µg/ml) glucose (2% (w/v)) plates for CFU counts the following day. The fold change in CFU after two hours (T2/T0) was calculated (Figure 4.2).

In the first group (a) tested, *E. coli* MG1655 Δ*hipBA* harbouring pBAD/his-*BPSS0390* H24A demonstrated over a 10 fold increase in the number of culturable cells after two hours incubation, whilst cells harbouring pBAD/his-*BPSS0390* had over 10 fold decrease in the number of culturable cells after two hours incubation. *E. coli* MG1655 Δ*hipBA* expressing P46A or I53A showed a more than 100 fold decrease in culturable cells. Cells expressing H40A, G14A and T37A also demonstrated decreased culturable cells after two hours incubation. However, *E. coli* MG1655 Δ*hipBA* expressing either S3A or T49A increased more than 10 fold two hours after incubation, cells harbouring W15A, P41A or D44A also increased after two hours incubation, similar to the H24A non-toxic control.

In the second group (b), *E. coli* MG1655 Δ*hipBA* harbouring pBAD/his-*BPSS0390* demonstrated a 100 fold decrease in culturable cells after two hours incubation. However, *E. coli* MG1655 Δ*hipBA* harbouring pBAD/his-*BPSS0390* H24A demonstrated a 10 fold increase in the number of culturable cells after two hours incubation. Cells expressing K5A, L6A, R8A, M9A, E11A, E12A, D13, R16, I17A or V18A all showed decreases in the number of culturable cells after two hours incubation, similar to the BPSS0390 control. In contrast, *E. coli*

MG1655 Δ*hipBA* expressing I7A or L10A increased in culturable cells after incubation, similar to the H24A control.

In the third group (c), *E. coli* MG1655 Δ*hipBA* harbouring pBAD/his-*BPSS0390* demonstrated a 1000 fold decrease in culturable cells after two hours incubation, whilst cells expressing H24A showed a 10 fold increase in culturable cells after two hours incubation. *E. coli* MG1655 Δ*hipBA* expressing S23A, H26A, V36A, G54G or G58A had a decrease in culturable cells after two hours, similar to the BPSS0390 control. In contrast, cells harbouring pBAD/his, pBAD/his-*BPSS0390* T21A or pBAD/his-*BPSS0390* H29A showed increased numbers of culturable cells after two hours incubation, similar to the H24A control.

In the fourth group (d), *E. coli* expressing BPSS0390 showed a more than 10 fold decrease in culturable cells after two hours incubation, whereas expression of H24A resulted in a more than 10 fold increase in culturable cells. Similarly to cells expressing H24A, cells expressing K31A, K32A, G34A or V38A had an increased number of culturable cells after two hours incubation. Cells expressing K28A, P30A, P33A, L35A, P39A or K42 showed a decrease in the number of culturable cells, like the BPSS0390 control.

The toxin control in the fifth group (e), where *E. coli* MG1655 Δ*hipBA* expressed BPSS0390, showed a 100 fold decrease in culturable cells after two hours incubation. Cells expressing G48A, V50A, K51A, K55A or L59A, also showed a decrease in the number of culturable cells after two hours expression. However, cells expressing S52, S56A or A57G demonstrated an increase in the number of culturable cells, similar to the non-toxic H24A, where expression resulted in a 100 fold increase in the number of culturable cells after two hours incubation.

In the final group (f), *E. coli* MG1655 Δ*hipBA* expressing BPSS0390 demonstrated a 100 fold decrease in the number of culturable cells after two hours incubation, whereas cells expressing H24A demonstrated a 100 fold increase in the number of culturable cells after two hours. Increased fold change CFU were also observed after two hours incubation in cells expressing R19A, G22A, F27A and L45A. Cells expressing N2A, S4A, V20A, H25A, K43A or I47A showed a decrease in the fold change of culturable cells after two hours of incubation.

In total, expression of 20 of the mutants resulted in cell growth, suggesting that either toxicity was abolished or that there was no expression of the mutant allele. These mutants were S3A, I7A, L10A, W15A, R19A, T21A, G22A, F27A, H29A, K31A, K32A, G34A, V38A, P41A, D44A, L45A, T49A, S52A, S56A and A57G. Out of the remaining 57 mutants, expression of 22 of the mutants resulted in a similar or greater decrease in fold change CFU compared to the toxic BPSS0390 control, whilst expression from 15 mutants resulted in a reduced fold change in CFU compared to BPSS0390.

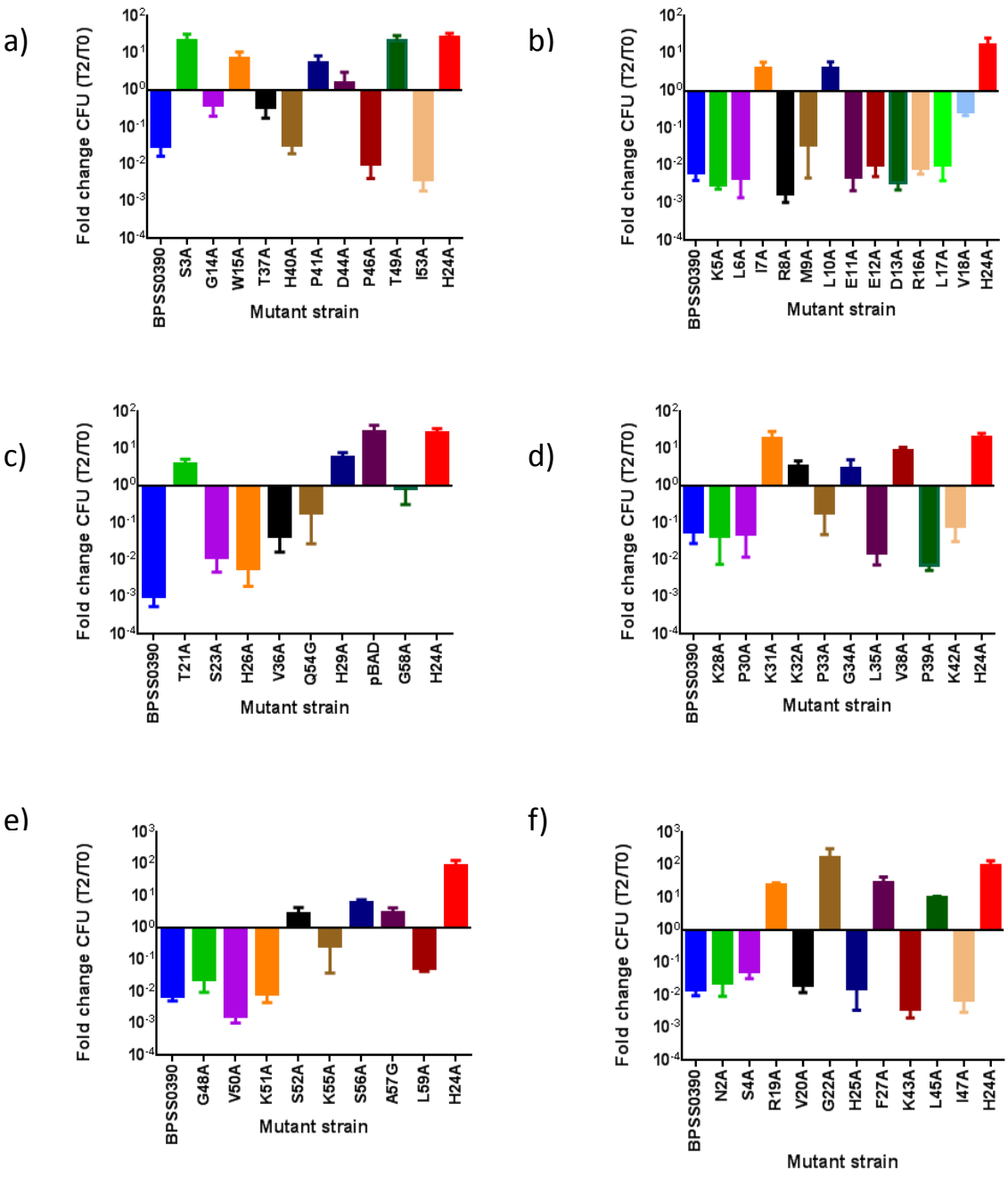

Figure 4.2: Fold change in CFU after expression of BPSS0390 mutants two hours. *E. coli* MG1655 Δ*hipBA* harbouring either pBAD/his-*BPSS0390,* or pBAD/his-*BPSS0390* H24A or *BPSS0390* mutant gene cloned into pBAD/his was grown to OD_{590} 0.1 before induction of expression (0.2% (w/v) arabinose). CFU counts were determined by plating cells onto LB ampicillin (100 µg/ml) glucose (2% (w/v)). Six groups labelled a-f. Data shown are an average of three biological repeats and error bars shown SEM.

4.3.2.2 Normalising toxicity data

To determine if increases or decreases in toxicity of mutants were significantly different compared to the wild type BPSS0390 control it was necessary to normalise fold change CFU (T2/T0) for each mutant against its BPSS0390 control.

For each group (a-f) the mean fold change in CFU after induction of expression of BPSS0390 for two hours was plotted as 100% toxicity whilst the mean fold change in CFU after induction of expression of BPSS0390 H24A mutant for two hours was plotted as 0% toxicity. A linear trend line was added (Figure 4.3). Each replicate of fold change in CFU was taken as x value and the equation of the linear trend line used to generate percentage toxicity. The mean of the percentage toxicity for each BPSS0390 mutant was plotted. The percentage for BPSS0390 and H24A mutant represents mean of all replicates across all six groups (Figure 4.4).

Inducing expression of 29 of the mutant alleles demonstrated no change or an apparent increase in toxicity compared to wild type BPSS0390, whilst 28 of the mutants expressed had a reduced toxicity compared to wild type BPSS0390. The H24A mutant had the lowest toxicity.

One-way ANOVA analysis revealed that the percentage toxicity of the H24A control, empty pBAD control and 14 BPSS0390 mutants were statistically significantly different from the percentage toxicity of BPSS0390 ($p<0.05$, 1 way ANOVA Dunnett post-test) (Figure 4.5).

All the mutants identified using one-way ANOVA were mutants that had been previously identified as their expression permitted cell growth. None of the mutants with increased toxicity were significantly different from BPSS0390.

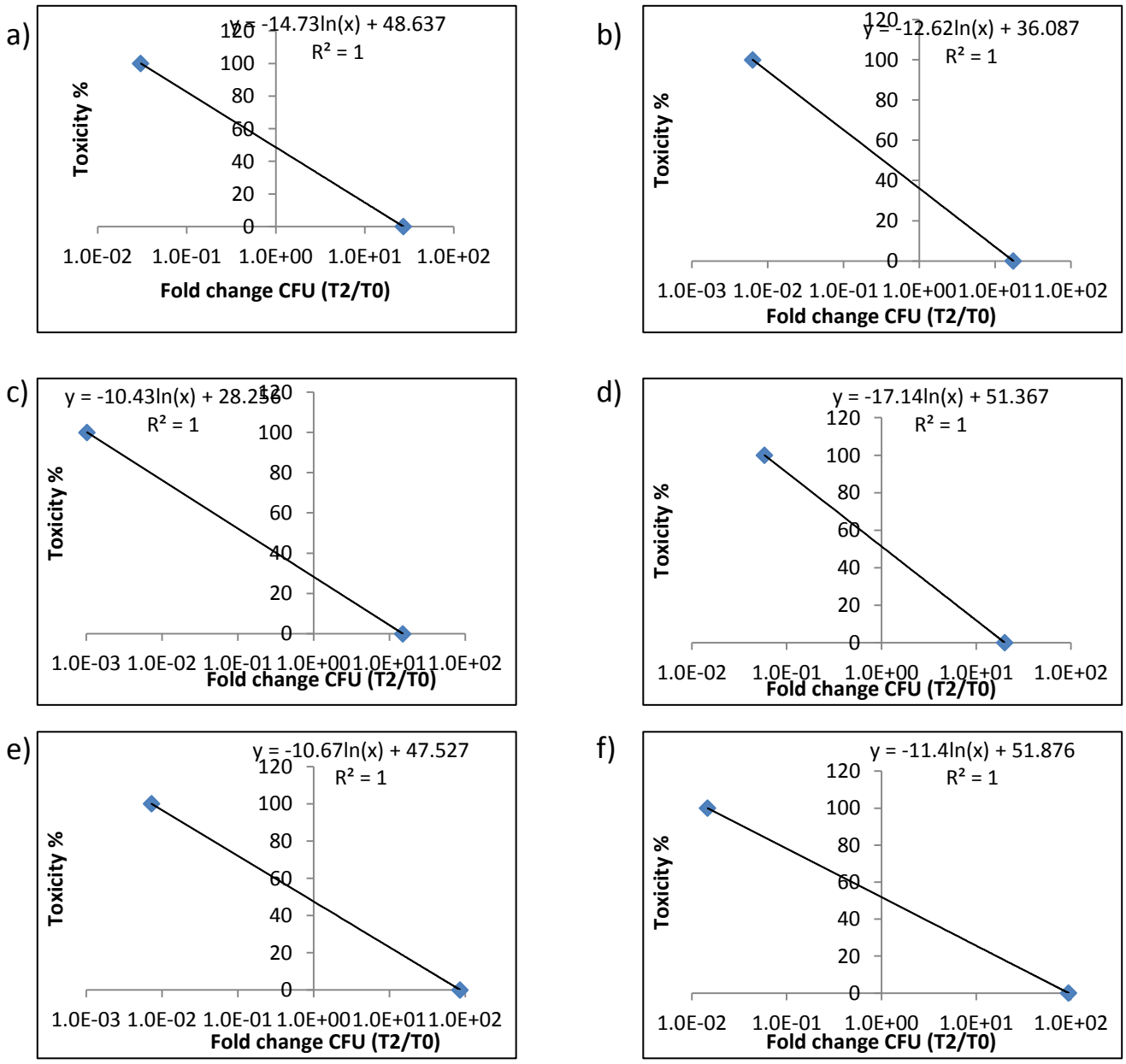

Figure 4.3: Mean fold change in CFU (T2/ T0) against toxicity. Each graph has the mean fold change in CFU after two hours of expression of BPSS0390 plotted with 100% toxicity and the mean fold change in CFU after two hours of expression of H24A plotted as 0% toxicity. A linear trend line was added and the equation generated used to convert fold change CFU for each replicate to % toxicity. Each graph corresponds to the graphs (a-f) in Figure 4.2.

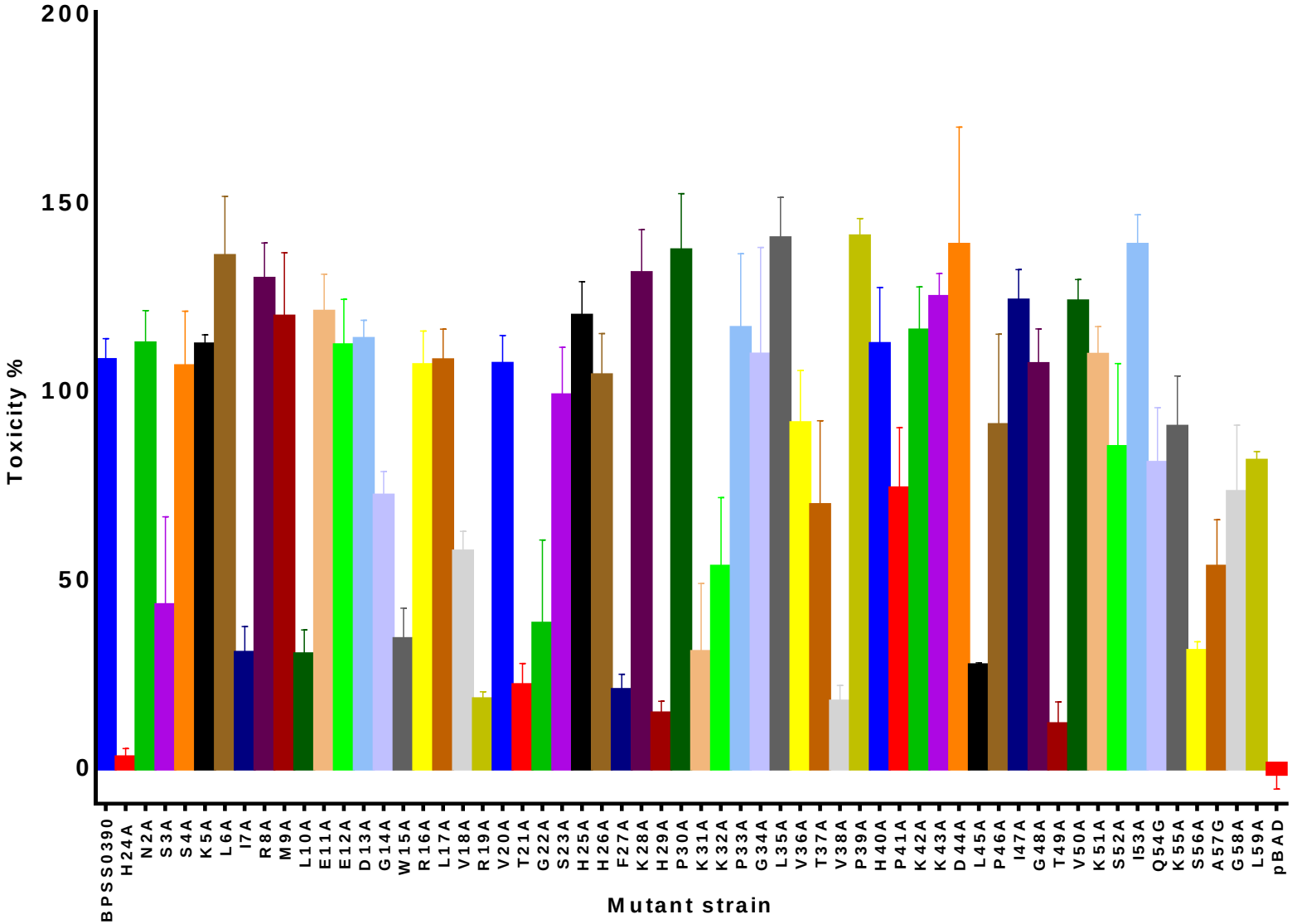

Figure 4.4: Percentage toxicity of each mutant expressed. Percentage toxicity was calculated using equation of the trend line on the graph of toxicity against fold change in CFU of each group. The fold change in CFU (T2/T0) was taken as x in the equation. Data shown are mean of three biological repeats and error bars represent SEM.

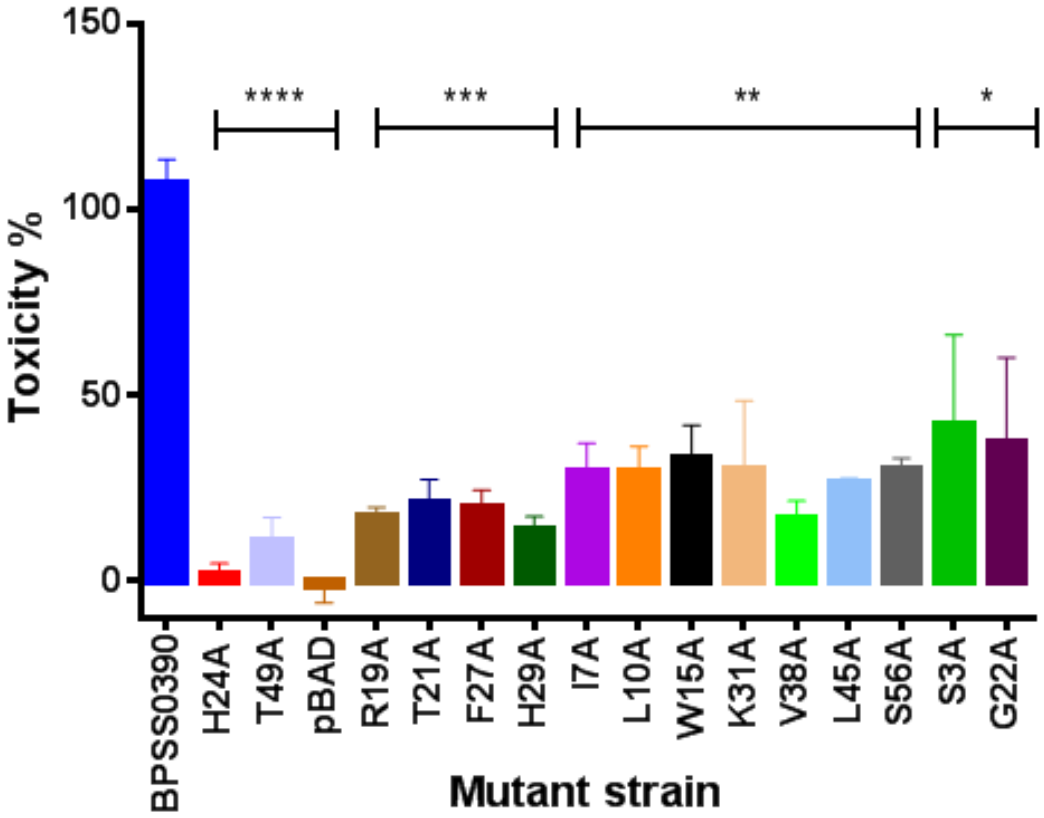

Figure 4.5: Mutants with significantly different toxicity to BPSS0390. The mean percentage toxicity for each mutant was analysed using one way ANOVA (Dunnett's post-test) with BPSS0390 as the reference strain. Data shown average of three biological replicates and error bars represent SEM. * = p≤ 0.05, ** = p≤ 0.01, *** = p≤0.001, **** = p ≤ 0.0001 after one way ANOVA (Dunnett's post-test)) against BPSS0390.

4.4 Further characterisation of BPSS0390 mutants

4.4.1 Effect of BPSS0390 mutations on growth

4.4.1.1 Growth curves of *E. coli* MG1655 Δ*hipBA* pBAD/his-*BPSS0390* and *E. coli* MG1655 Δ*hipBA* pBAD/his-*BPSS0390* H24A

Overnight cultures of *E. coli* MG1655 Δ*hipBA* harbouring pBAD/his-*BPSS0390* (encoding native toxin) or pBAD/his-*BPSS0390* H24A (encoding non-toxic mutant) were diluted to an OD_{590} of 0.01 and 100µl placed into individual wells in a 96-well plate. The plate and cultures were incubated at 37°C overnight and automated readings of the optical density of the culture in each well taken every 15 minutes (Figure 4.6).

E. coli MG1655 Δ*hipBA* harbouring pBAD/his-*BPSS0390* grew more slowly through exponential phase and reached a lower OD once in stationary phase than *E. coli* harbouring pBAD/his-*BPSS0390* H24A. An unpaired t-test comparing the growth of the two strains at 24 hours revealed that the growth of *E. coli BPSS0390* H24A was significantly different ($p \leq 0.001$) to the growth of the strain harbouring *BPSS0390* (Figure 4.6). This suggests that mutations in BPSS0390 do have an effect on bacterial growth.

To determine if other mutations in BPSS0390 affected growth, overnight cultures expressing the mutants were diluted to an OD_{590} of 0.01 and 100µl placed into individual wells in a 96-well plate. *E. coli* harbouring pBAD/his with either *BPSS0390* (native toxin) or H24A (non-toxic mutant) were grown and diluted in parallel as controls. The plate and cultures were incubated at 37°C overnight and readings of the optical density taken every 15 minutes. It was not possible to test all 57 mutants in a single 96-well plate and so mutants were split into 6 groups (a-f). The OD_{590} of each culture at 24 hours was plotted (Figure 4.7).

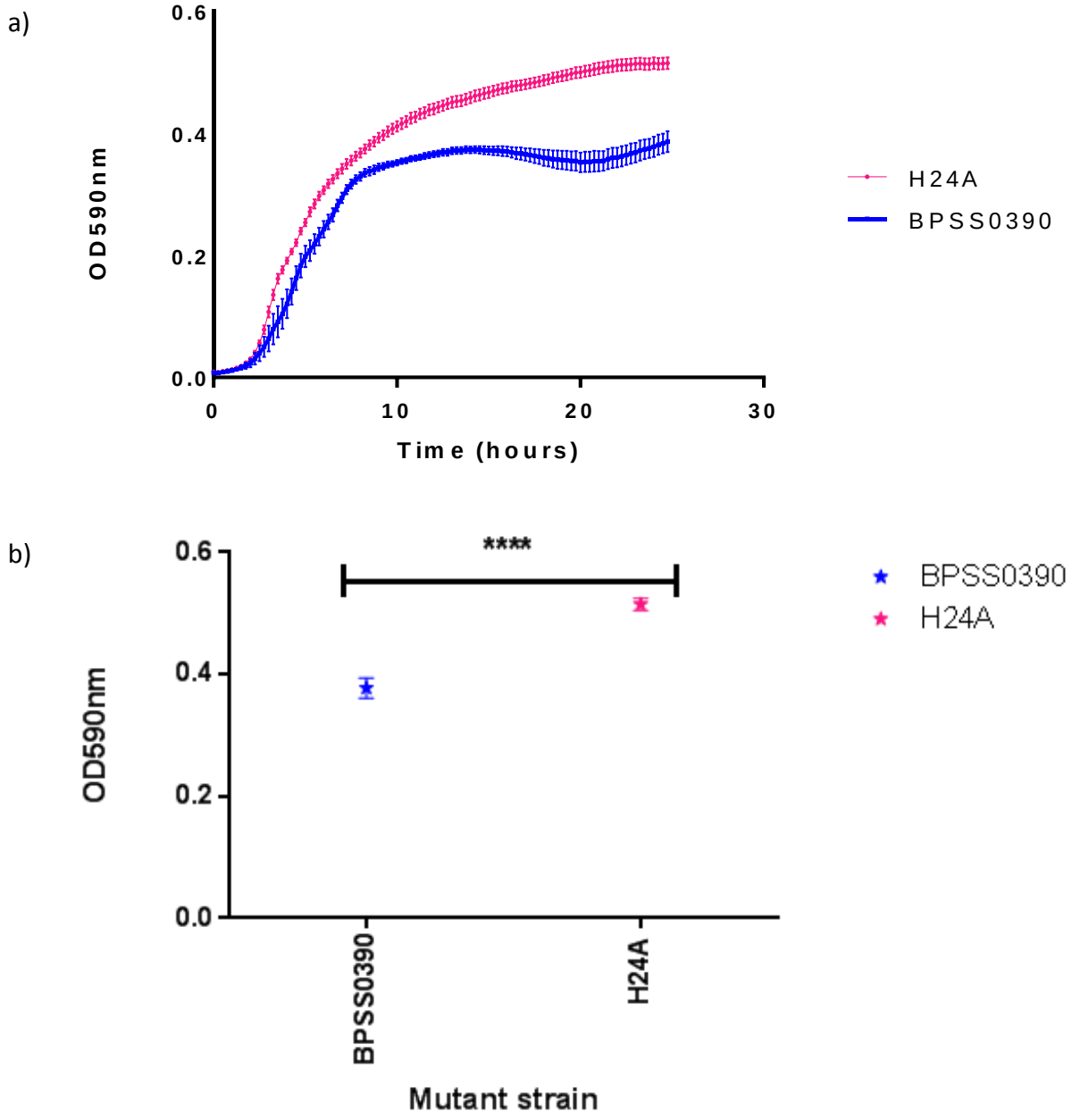

Figure 4.6: Analysis of growth of *E. coli* MG1655 *ΔhipBA* pBAD/his-*BPSS0390* and *E. coli* MG1655 *ΔhipBA* pBAD/his-*BPSS0390* H24A. a) OD_{590nm} reading taken every 15 minutes to generate growth curves. Data shown is average of three biological replicates and error bars represent SEM. b) Comparison of OD measurement for both strains at 24 hours. Unpaired t-test determined that *E. coli* MG1655 Δ*hipBA* pBAD/his-*BPSS0390* H24A is significantly different. **** = p≤ 0.0001. Data shown is average of three biological repeats and error bars represent SEM.

All cultures of *E. coli* MG1655 Δ*hipBA* harbouring a pBAD/his cloned BPSS0390 alanine substitution mutant grew to a higher OD at 24 hours that the cultures of *E. coli* MG1655 Δ*hipBA* pBAD/his-*BPSS0390*, except *E. coli* MG1655 Δ*hipBA* pBAD/his harbouring D13A, S4A and V50A, which have percentage toxicity similar or greater than BPSS0390.

A one way ANOVA (Dunnett's post-test) found that the growth of 40 of the *E. coli* pBAD/his mutant alleles at 24 hours was significantly different from the growth of *E. coli* expressing *BPSS0390* at 24 hours. All the *E. coli BPSS0390* H24A controls for each group and *E. coli* harbouring pBAD were also statistically significant from the control harbouring pBAD/his-*BPSS0390*.

Seventeen of the 40 cultures statistically significantly different from the *E.coli* harbouring pBAD/his-*BPSS0390,* harboured plasmids encoding alanine substitution mutants that also abolished BPSS0390 toxicity (S3A, W15A, I7A, L10A, K32A, G34A, V38A, R19A, G22A, F27A, L45A, S52A, S56A, A57G, T21A and H29A). Ten of the 40 cultures harboured plasmids encoding alanine substitution mutants with lower percentage toxicity that BPSS0390 (107.065%), (Table 4.2). Together, the 10 mutants with a lower percentage toxicity, plus the 17 mutants with abolished function suggest that mutants with reduced percentage toxicity permit more growth after 24 hours than wild type BPSS0390.

Interestingly, the remaining 13 cultures that were significantly different from *E. coli* harbouring pBAD/his-*BPSS0390* , harboured plasmids encoding mutants with a higher percentage toxicity than BPSS0390 (Table 4.3). This might suggest that the increased toxicity of these mutants does not directly affect growth of the host cells (when there is no expression induced). It could be that these mutants show

increased percentage toxicity as more protein is produced in response to induction of expression.

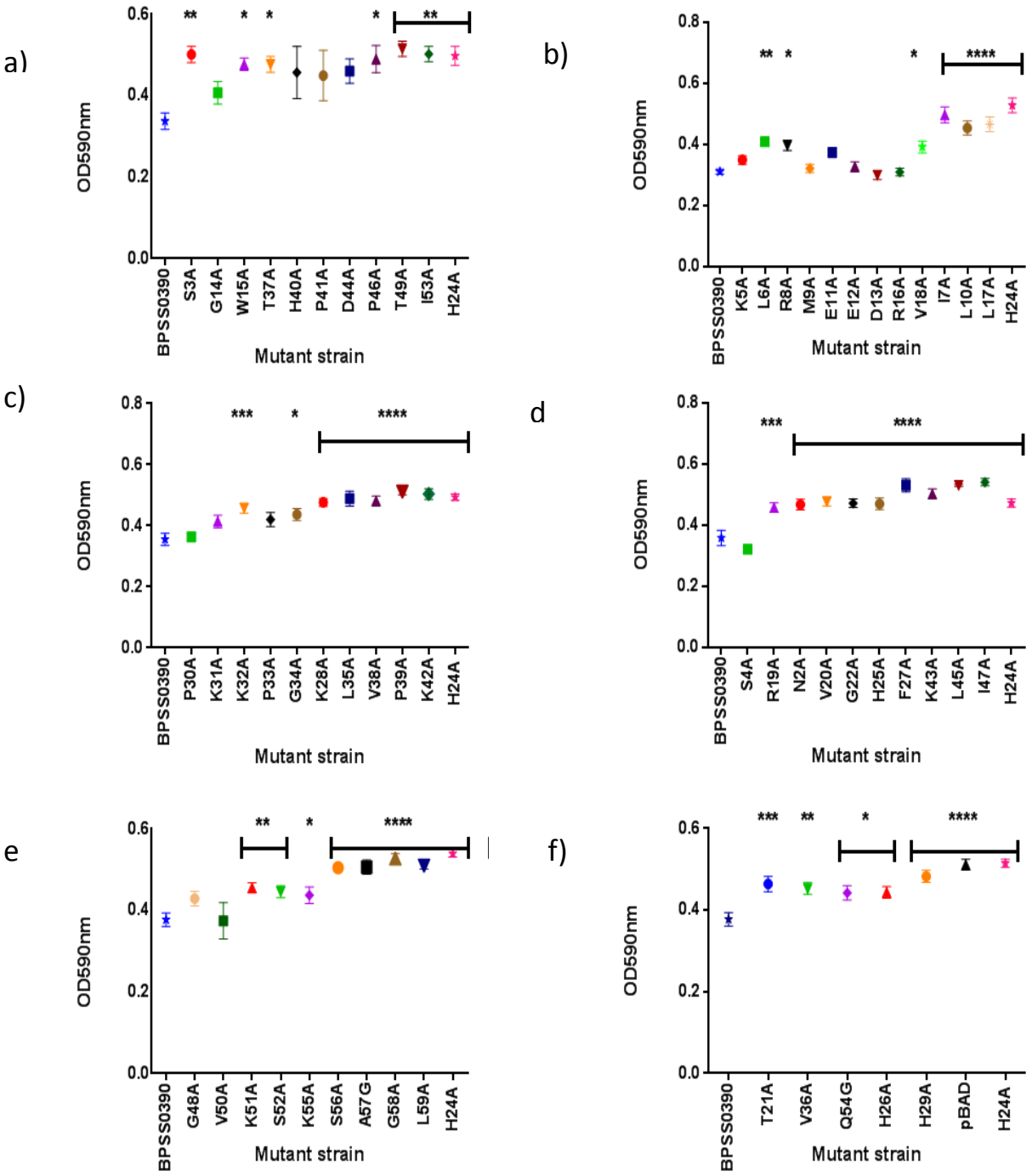

Figure 4.7: Analysis of growth of cultures of *E. coli* MG1655 *ΔhipBA* pBAD/his harbouring alanine substitution mutants. The final OD_{590} at 24 hours was analysed using one way ANOVA (Dunnett's post-test) with BPSS0390 as the reference strain. Data shown average of three biological replicates and error bars represent SEM. * = p≤ 0.05, ** = p≤ 0.01, *** = p≤0.001, **** = p ≤ 0.0001 after one way ANOVA (Dunnett's post-test)) against BPSS0390.

Table 4.2: Table to show the alanine substitution mutants with a lesser toxicity than BPSS0390, encoded by the plasmids harboured by cultures that reached a statistically significantly higher OD_{590} at 24 hours than cultures harbouring plasmids that encoded BPSS0390 only.

Mutant	Toxicity %
T37A	68.6167
P46A	89.8333
V18A	56.2667
V20A	106.033
K55A	89.3667
G58A	72.5
L59A	80.35
H26A	103.017
V36A	90.35
Q54G	79.8

Table 4.3: Table to show the alanine substitution mutants with a greater toxicity than BPSS0390, encoded by the plasmids harboured by cultures that reached a statistically significantly higher OD_{590} at 24 hours than cultures harbouring plasmids that encoded BPSS0390 only.

Mutant	Toxicity %
I53A	137.625
L6A	134.667
R8A	128.617
L17A	107
K28A	130.133
L35A	139.367
P39A	139.867
K42A	114.9
N2A	111.483
H25A	118.817
K43A	123.8
K51A	108.45
I47A	122.867

4.4.2 Monitoring expression of BPSS0390 mutant proteins

4.4.2.1 Quantifying protein expression through Western blotting

To determine if different BPSS0390 mutants produced different quantities of protein, it was necessary to calculate the relative concentration of protein detected for each mutant on Western blots. To do this a standard curve was generated using H24A mutant.

A culture of *E. coli* MG1655 Δ*hipBA* pBAD/his-*BPSS0390* H24A was grown to an OD_{590} 0.1 and a final concentration of 0.2% (w/v) arabinose added to induce expression. The culture was incubated for a further two hours before a 1 ml sample was taken, centrifuged and lysed using BugBuster, lysozyme and benzonase. The cell lysate was serially diluted, loaded onto an SDS-PAGE gel and electrophoresed before a Western blot was carried out. For the Western blot, an anti-Xpress 1° antibody, which was specific against the Xpress epitope in the N-terminus hexahistidine tag, was used. The secondary antibody used was IR Dye ® 800 CW Goat anti-Mouse IgG. The signal intensity of each band was measured using Odyssey software and plotted against theoretical concentration of the protein at each dilution (Figure 4.8). The graph was fitted with a linear trend line. The equation of this trend line was multiplied against the signal intensity (x) of each band detected on the Western blot, i.e. (=0.3268*signal intensity)-2.6406), for each mutant to generate the calculated relative concentration (Figure 4.8).

All of the mutants had a greater calculated relative concentration than BPSS0390 control. One way ANOVA (Dunnett's post-test) using the BPSS0390 strain as the reference, identified 27 mutants as having statistically significantly different concentrations. The non-toxic H24A control mutant was also statistically significantly different to the BPSS0390 control.

Five of the mutants identified as significantly different (bars coloured yellow) had an increased percentage toxicity and an increased OD_{590} at 24 hours when compared to BPSS0390 control (Table 4.2); the residues were L6A, R8A, L35A, I53 and N2A. This could suggest that the increase in percentage toxicity of these mutants is due to an increase in the relative concentration of protein in response to induction of expression. In contrast, four of the mutants identified as significantly different (bars coloured light blue) have a decreased percentage toxicity and an increased OD_{590} at 24 hours when compared to BPSS0390 control (Table 4.2); V36A, H26A, P46A and K55.

Eleven of the mutants identified as significantly different from expression of wild type BPSS0390, were mutants where expression of the mutant permitted cell growth (bars coloured purple). Mutation of S3 (N-terminus), I7, L10 (α1 helix), F27 (β2 strand) H29, K31, K32 and G34 (β2-β3 loop) or S52, S56 and A57 (α2 helix) resulted in significantly increased relative calculated concentration.

The remaining mutants identified by the one way ANOVA were K5A, M9A, E11A, D13A, P30A, P33A and G48A.

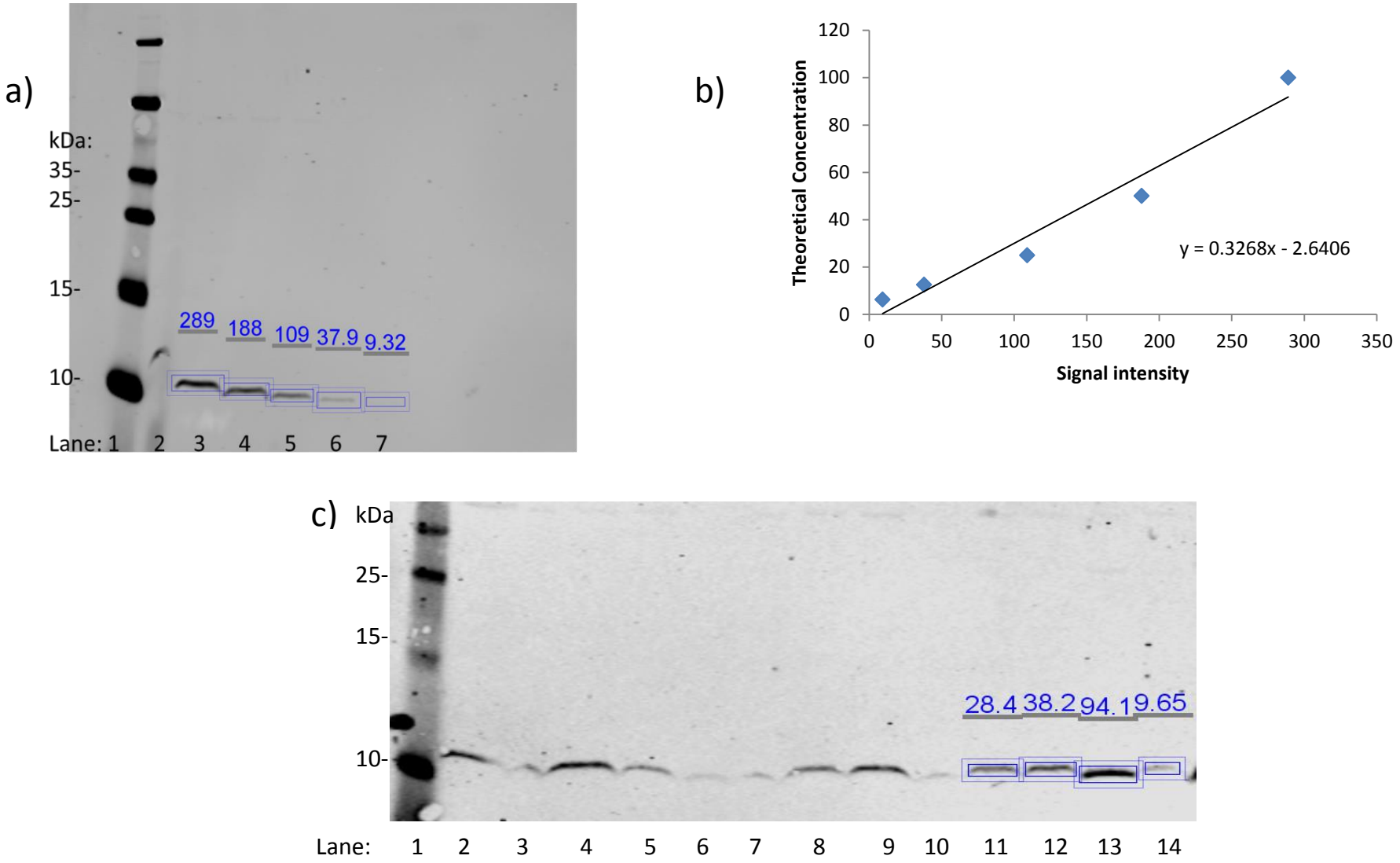

Figure 4.8: Quantifying protein expression through Western blotting. A prepared protein sample of BPSS0390 H24A was serially diluted before a) Western blotting. Diluted samples were loaded onto SDS-PAGE gel highest to lowest concentration, (lane 3-7), before electrophoresis. Protein on the gel was transferred to a nitrocellulose membrane, before blocking and treatment with primary and secondary antibody. The signal intensity was measured

for each band and b) plotted against the theoretical concentration of each dilution (so undiluted 100%, diluted once 50% etc.). A linear trend line was added the equation used to calculate the relative concentration of each BPSS0390 mutant protein; c) Example of a Western blot showing prepared protein samples of BPSSS0390 mutants: P46A (lane 2), I47A (lane 3), G48A (lane 4), T49A (lane 5), V50A (lane 6), K51A (lane 7), S52A (lane 8), I53A (lane 9), Q54G (lane 10), K55A (lane 11), S56A (lane 12), H24A (lane 13) and BPSS0390 (unmutated, lane 14). On this example image the signal intensity of K55A, S56A, H24A and BPSS0390 has been measured using Odyssey Image Studio software. This value was then used to determine the calculated relative concentration using the equation of the linear trend line from graph b).

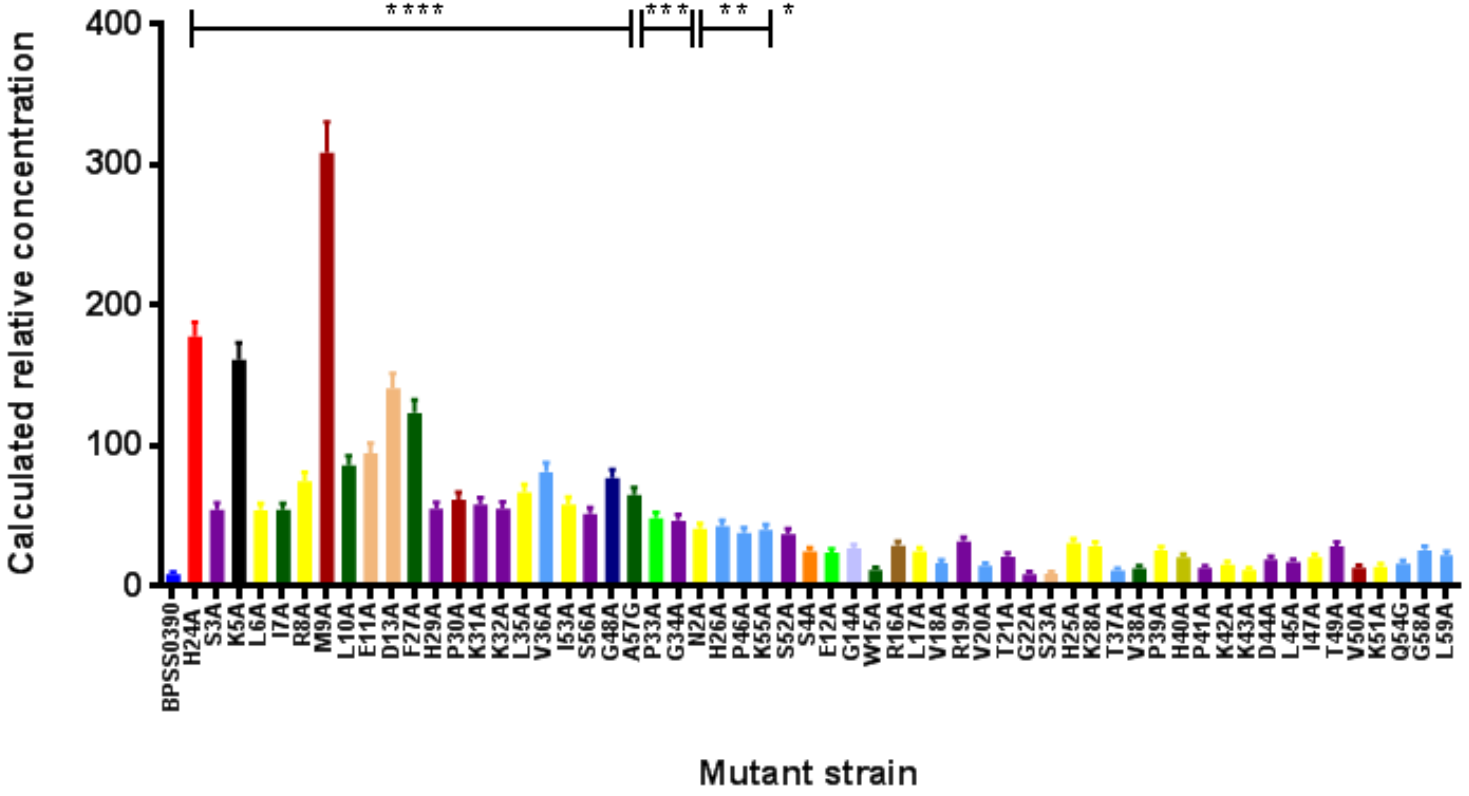

Figure 4.9: Calculated relative concentration of mutant protein after expression for two hours. Cultures of *E. coli* MG1655 Δ*hipBA* harbouring mutants were grown to OD_{590} of 0.1 and expression induced by 0.2% (w/v) arabinose. The cultures were incubated for a further two hours before samples were taken, and pelleted by centrifugation. Cells were resuspended in SDS-loading dye, boiled and electrophoresed through a SDS PAGE gel before transfer to a nitrocellulose membrane and blotting. The signal intensity of each band was multiplied by the equation generated by the standard curve to generate a calculated relative concentration. Bars coloured purple represent residues where alanine substitution abolishes toxicity. Bars coloured light blue represent residues where mutants with lower percentage toxicity (than BPSS0390) demonstrate significantly increased growth compared to BPSS0390. Bars coloured yellow represent mutants with increased percentage toxicity (compared to BPSS0390) and significantly increased growth at 24 hours. Data shown are the average of two biological repeats. Error bars show SEM. **** = p≤0.0001, *** = p ≤0.001, ** = p≤ 0.01, * = p≤ 0.05, following a one way ANOVA (Dunnett's post-test) using the BPSS0390 strain as a reference.

4.5 Description of BPSS0390 mutants where expression resulted in cell growth

Induction of expression of 20 of the mutants resulted in cell growth, suggesting that either there was no expression of the mutant allele or that the mutation prevented the toxicity of BPSS0390. Western blotting revealed that all of the mutants in the study had greater levels of expression, i.e. had a greater calculated relative concentration, than wild type BPSS0390. This implies that the mutations described below (organised by location) may have affected residues that are critical for either the structure or function of the protein. Toxin BPSS0390 forms a double stranded RNA binding (dsRNB) domain like fold, with two α helices packed against one face of a triple β sheet (Figure 4.10)

4.5.1 Residues at the N-terminus

4.5.1.1 Serine 3

This polar residue has not previously been identified as critical for function in either dsRBD-like domains or HicA. It was 98% conserved (Table 4.1). The N-terminus is mobile- NMR analysis revealed that it occupies different conformations in different states (Figure 4.10).

4.5.2 Residues located in α1 helix

4.5.2.1 Isoleucine 7

This large, Cβ branched, hydrophobic amino acid has not been previously attributed to the hydrophobic core (Butt et al. 2014) but analysis of relative solvent accessibility suggests that the residue is buried in structure and that its side chain points towards the core (Figure 4.11). This isoleucine was conserved in 75% of the BPSS0390 protein homologues (Table 4.1). This residue may be critical for protein structure.

4.5.2.2 Leucine 10

This large, hydrophobic, non-polar amino acid has previously been identified as part of the hydrophobic core (Butt et al. 2014). Its side chain points into the core and analysis of its relative solvent activity suggest it is buried (data not shown) (Figure 4.11). Leucine was 76% conserved across BPSS0390 protein homologues (Table 4.1). This residue may be critical for protein structure.

4.5.3 Residues located on the α1- β1 loop

4.5.3.1 Tryptophan 15

Conserved across all BPSS0390 homologues, this residue has its indole portion orientated towards the hydrophobic core (Figure 4.11). It has previously been assigned to the hydrophobic core (Butt et al. 2014). This residue may be critical for protein structure.

4.5.4 Residues located on the β1-β2 loop

This loop region was suggested to be involved in substrate catalysis. His24, a residue previously identified as critical to BPSS0390 toxicity is located here (Butt et al. 2014).

4.5.4.1 Arginine 19

This basic, positively charged amino acid was conserved in 86 of 100 proteins with homology to BPSS0390. The positive charge might be important for RNA binding (Figure 4.12).

4.5.4.2 Threonine 21

Threonine 21 was conserved in less than 75% of proteins homologous to BPSS0390. It is polar and Cβ branched; the bulky side chain limits conformations,

suggesting that this residue might be important for maintaining structure of the active site (Figure 4.12).

4.5.4.3 Glycine 22

Glycine 22 was conserved across all 100 homologues; its hydrogen atom side chain may offer the flexibility needed for the active site to change conformation (Yan & Sun Qing 1997) (Figure 4.12).

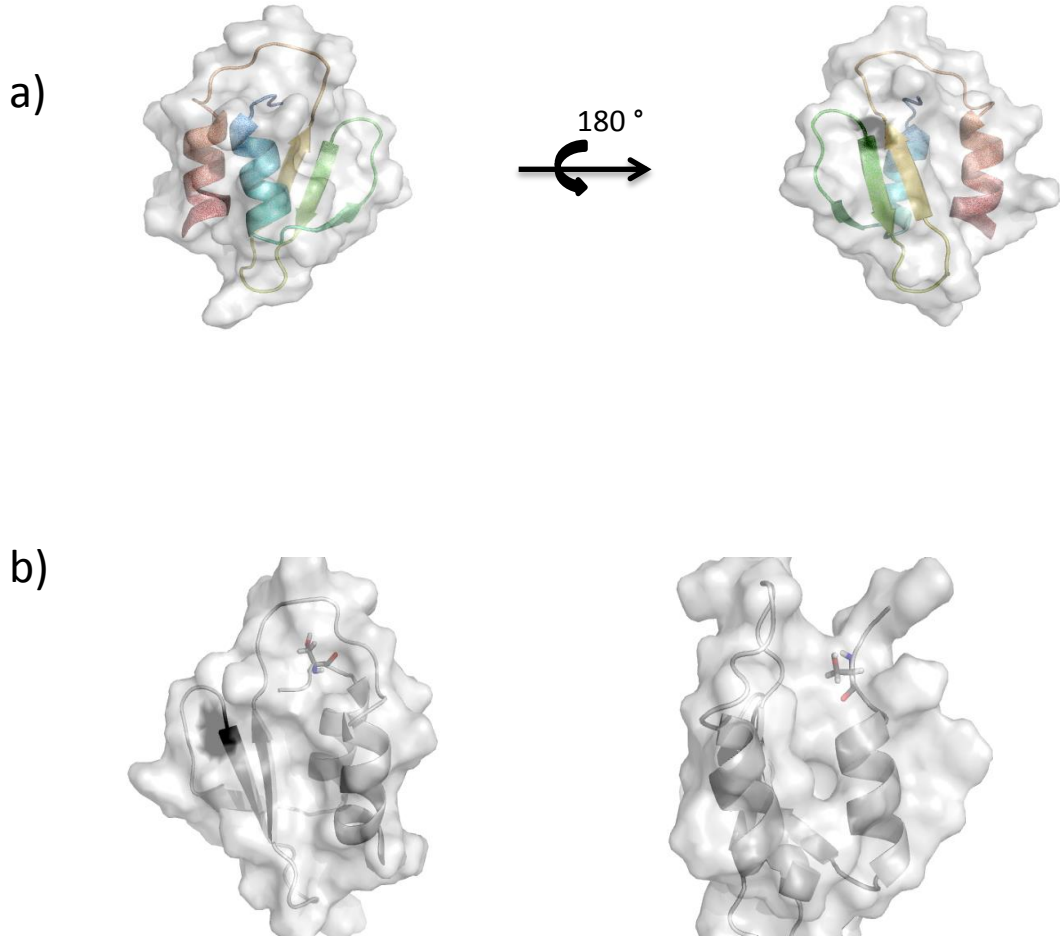

Figure 4.10: Structure of BPSS0390. a) Structure of the BPSS0390 (H24A) protein showing the dsRNB domain like fold with two α helices packed against one face of a triple β sheet. The secondary structure elements and surface are indicated. The N-terminus is coloured blue and the C-terminus coloured red. Residues -6 to 1 are omitted from all images as they are unstructured. b) Structure of the BPSS0390 (H24A) protein with serine 3 indicated in sticks, shown in two different states. Black is used to indicate the location of the H24A substitution. PyMol was used to generate the images (PDB code 4C26).

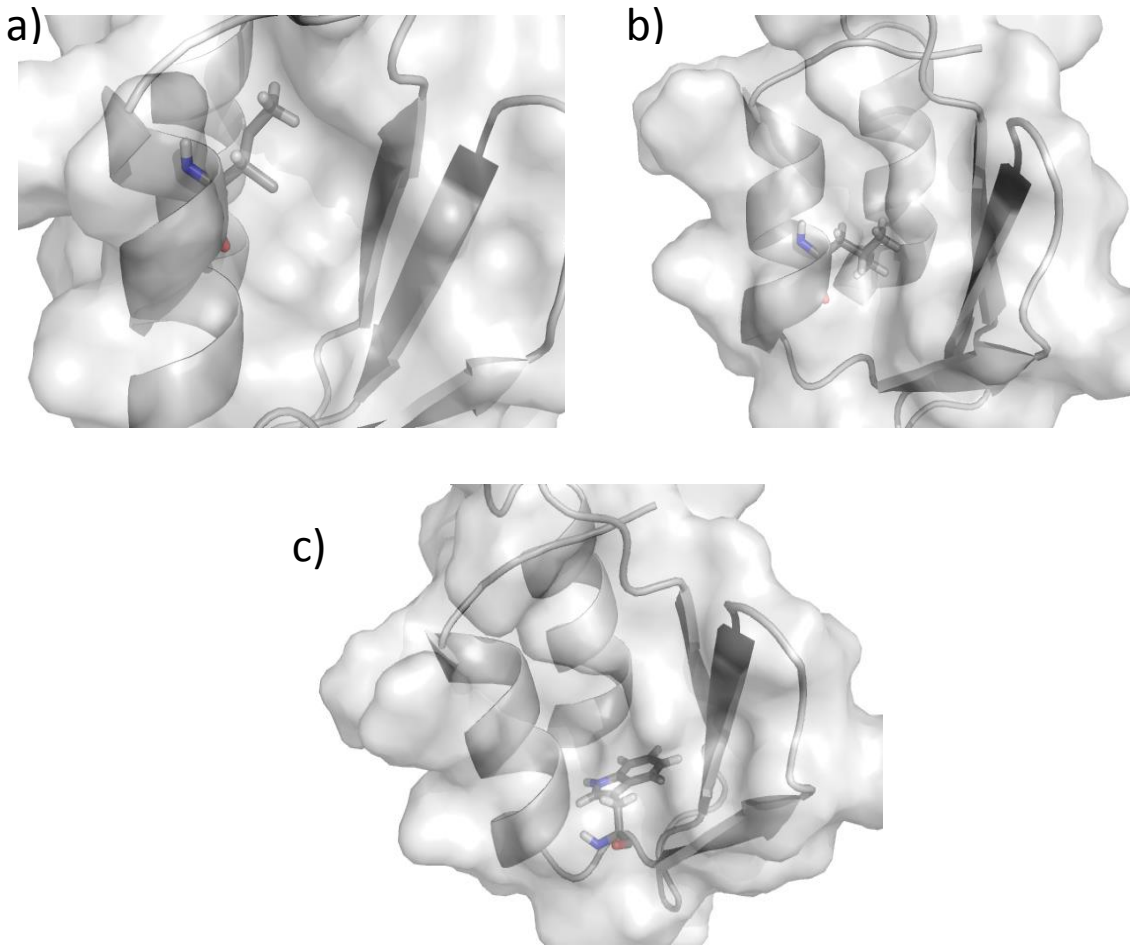

Figure 4.11: Location of residues in α1 helix and α1 - β1 loop of BPSS03390 where alanine substitution abolished toxicity. Sticks indicate the location of a) Ile7, b) Leu10, and c) Trp15. The side chains of the indicated residues point towards the core of the protein. Black at the N terminus of β2 sheet indicates the location of the H24A mutation. PyMol was used to generate the images (PDB code 4C26).

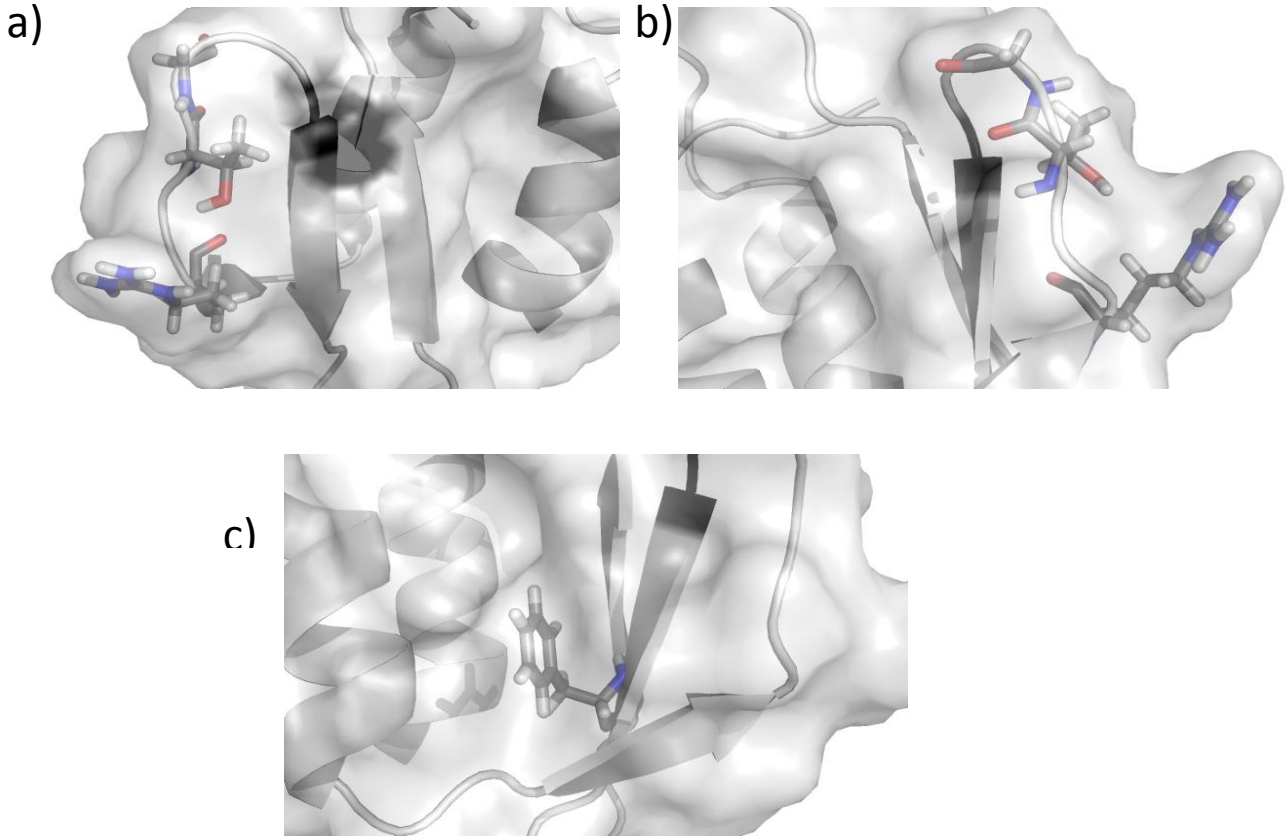

Figure 4.12: Location of residues in β1-β2 loop and β2 strand of BPSS03390 where alanine substitution abolished toxicity. a) Sticks indicate Arg19, Thr21 and Gly22, located on the β1-β2 loop immediately prior to the H24A substitution (marked in black). b) Sticks indicate Arg19, Thr21 and Gly22, located on the β1-β2 loop immediately prior to the H24A substitution (marked in black), image has been rotated. c) Sticks indicate location of Phe27 within the β2 sheet, showing side chain situated in the hydrophobic core. . PyMol was used to generate the images (PDB code 4C26).

4.5.5 Residues located in β2 strand

4.5.5.1 Phenylalanine 27

Phenylalanine 27 is an aromatic and hydrophobic residue previously identified in the hydrophobic core (Butt et al. 2014) , Phe27 may be also be indirectly involved as aromatic residues may help to main a positive charge on molecule. F27 was 91% conserved across BPSS0390 protein homologues (Figure 4.12).

4.5.6 Residues located in β2-β3 loop

This loop is located at the opposite end of the molecule from the proposed catalytic site.

4.5.6.1 Histidine 29

Found in all 100 proteins with homology to BPSS0390, the histidine imidazole functional group may play a role in catalysis as its pKa of 6 allows the amino acid to act as either a general acid or a base during catalysis depending on pH of active site. However, given its location, it may instead be important for folding and stabilising of the β sheet. A distance of 1.9 Å between the CO of His29 and the NH of Lys31 suggests that would be possible for a hydrogen bond to form, generating a γ turn (Figure 4.13).

4.5.6.2 Lysine 31

This amino acid (95% conservation) has a positively charged side chain, which can be used for binding to negatively charged molecules, such as RNA. Interestingly this and its adjacent Lys32 residue are the only lysines identified as critical for toxicity. May be part (i+2) of a γ turn (Figure 4.13).

4.5.6.3 Lysine 32

Lysine 32 was not conserved in 75 or more proteins homologous to BPSS0390. Along with Lys31 was identified as critical for toxicity and the positively charged side chain might interact with negatively charged RNA. The CO of Lys32 is 1.9 Å apart from NH of Gly34, suggesting that there might be hydrogen bonding stabilising the turn and the β sheet (Figure 4.13).

4.5.6.4 Glycine 34

Glycine 34 was conserved in 98 of the 100 proteins homologous to BPSS0390 and its NH group is only 1.9 Å from the CO of Lys32, suggesting that hydrogen bonding might be present (Figure 4.13).

4.5.7 Residue located in β3 strand

4.5.7.1 Valine 38

Valine 38 was not conserved in 75 or more of the 100 proteins homologous to BPSS0390. This Cβ –branched hydrophobic residue has previously been assigned to the hydrophobic core (Butt et al. 2014). Solvent accessibility analysis suggests that the residue is buried (data not shown) and structural analysis suggests that its side chain points into the hydrophobic core (Figure 4.14). This residue may be critical for protein structure.

4.5.8 Residues located in β3-α2 loop

NMR analysis suggests that this loop occupies multiple conformations in solution and may be involved in catalysis or binding of RNA substrate (Butt et al. 2014).

4.5.8.1 Proline 41

This imino acid was conserved in 99% of proteins homologous to BPSS0390. Proline is able to contribute to turns and kinks in the protein as its amino group is part of the cyclical ring of atoms and is conformationally rigid. (Figure 4.14)

4.5.8.2 Aspartic acid 44

This residue has an acidic side chain and was conserved in 93% proteins homologous to BPSS0390. Role is not clear as is negatively charged at physiological pH. (Figure 4.14).

4.5.8.3 Leucine 45

This hydrophobic residue was 93% conserved. Analysis of its relative solvent activity suggested it was buried (data not shown). It may be involved in protein structure and RNA substrate recognition (Figure 4.14).

4.5.8.4 Threonine 49

This polar, Cβ branched amino acid has limited conformations due to the bulky side chain and so might be important for maintenance of structure (Figure 4.15). Analysis of relative solvent accessibility suggests that the residue is buried within the structure (data not shown). T49 was 99% conserved across 100 proteins with homology to BPSS0390.

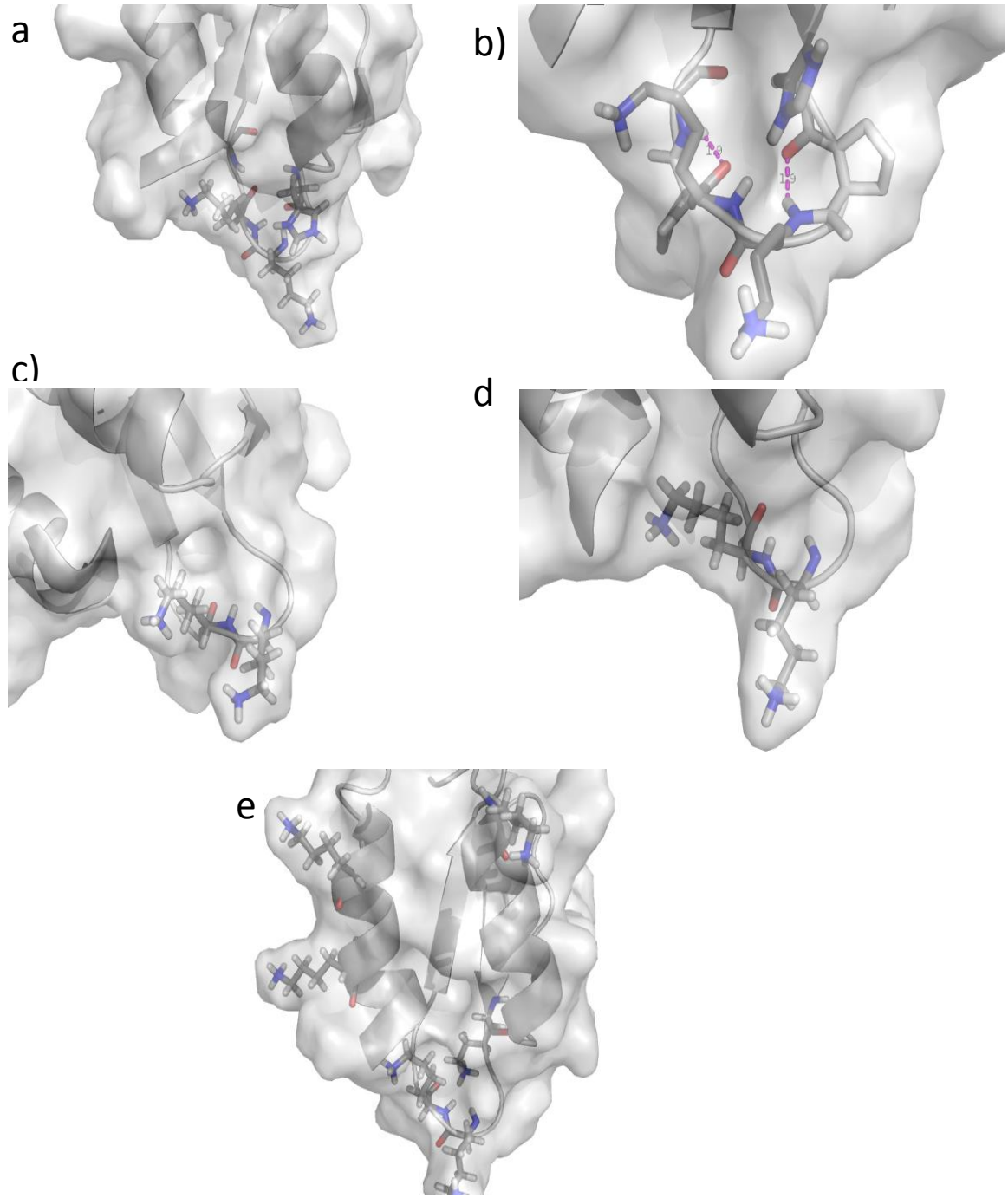

Figure 4.13: Location of residues in the β2-β3 loop of BPSS03390 where alanine substitution abolished toxicity. Structure of the β2-β3 loop of BPSS0390 (H24A). a) Sticks indicate His29, Lys 31, Lys 32 and Gly34. b) Dashes indicate distance between His29 (CO) and Lys31 (NH) and Lys 32 (NH) and Gly34 (CO) is calculated to be 1.9 Å, suggesting that hydrogen bonding is possible. c) and d) Lys 31 and Lys32 have different conformations in different states and are only two lysines critical for toxicity. e) Sticks represent all lysine residues present in BPSS0390. PyMol was used to generate the images (PDB code 4C26).

4.5.9 Residues located in α2 helix

4.5.9.1 Serine 52 and Serine 56

Serine 52 was 96% conserved across proteins homologous to BPSS0390, whilst Serine 56 was less than 75% conserved. These polar residues are located in the α2 helix, suggesting that the residues might be importance for structure. (Figure 4.15).

4.5.9.2 Alanine 57

Alanine 57 was previously identified as part of the hydrophobic core, which suggests it might have a structural role (Butt et al. 2014) This residue was conserved in all 100 homologues of BPSS0390 (Figure 4.15).

4.5.10 Summary of residues where alanine substitution abolished toxicity

Twenty residues were identified; four residues were not 75% conserved across protein homologues of BPSS0390: Thr21, Lys32, Val38 and Ser52. Six residues were identified as contributing to the hydrophobic core (Figure 4.16).

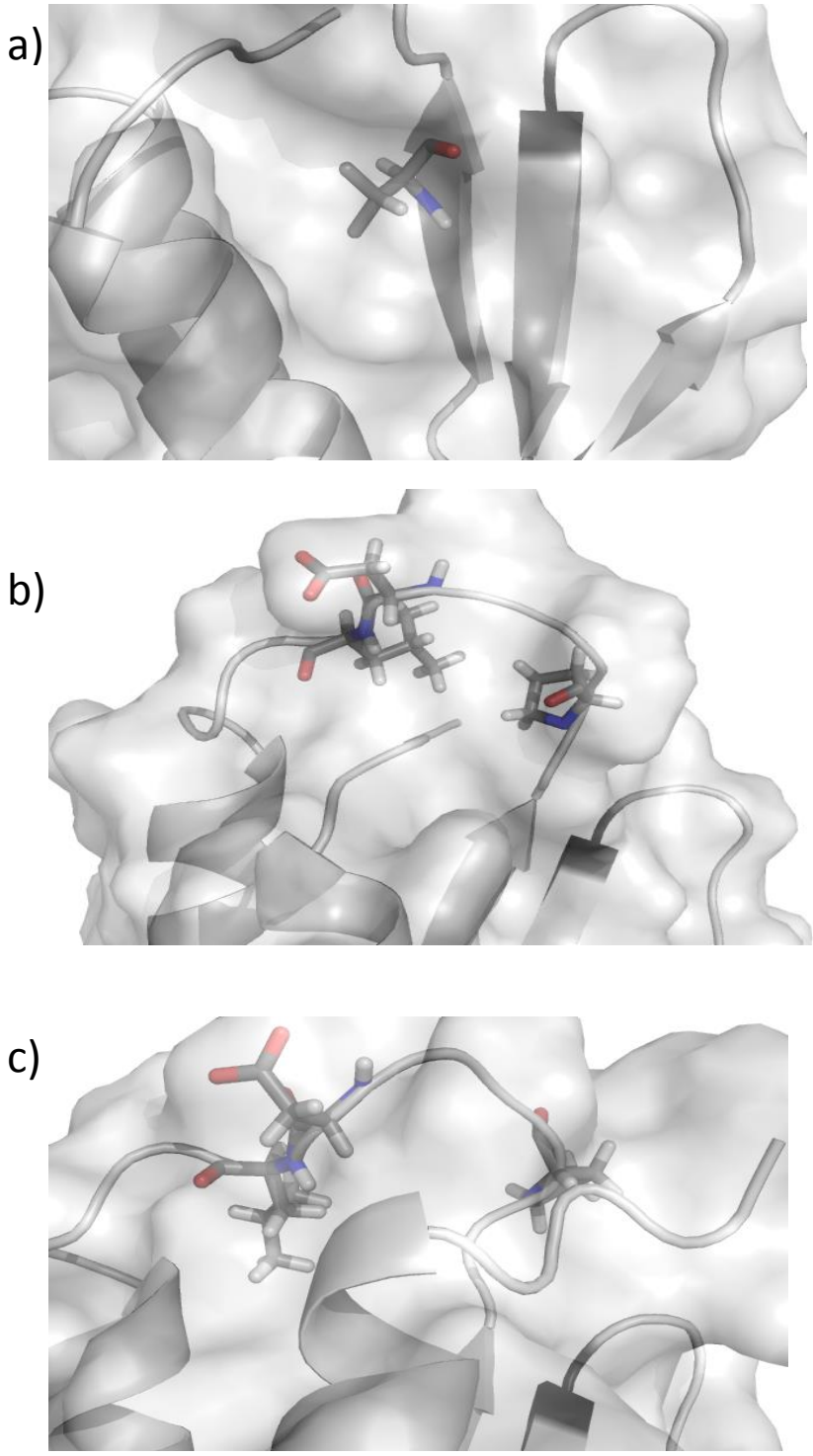

Figure 4.14: Location of residues in the β3 strand and β3-α2 loop of BPSS03390 where alanine substitution abolished toxicity. a) Sticks indicate position of Val38. b) Sticks indicate Pro41, Asp44 and Leu45. c) Sticks indicate Pro41, Asp44 and Leu45 in a different conformation indicating movement in different states. PyMol was used to generate the images (PDB code 4C26).

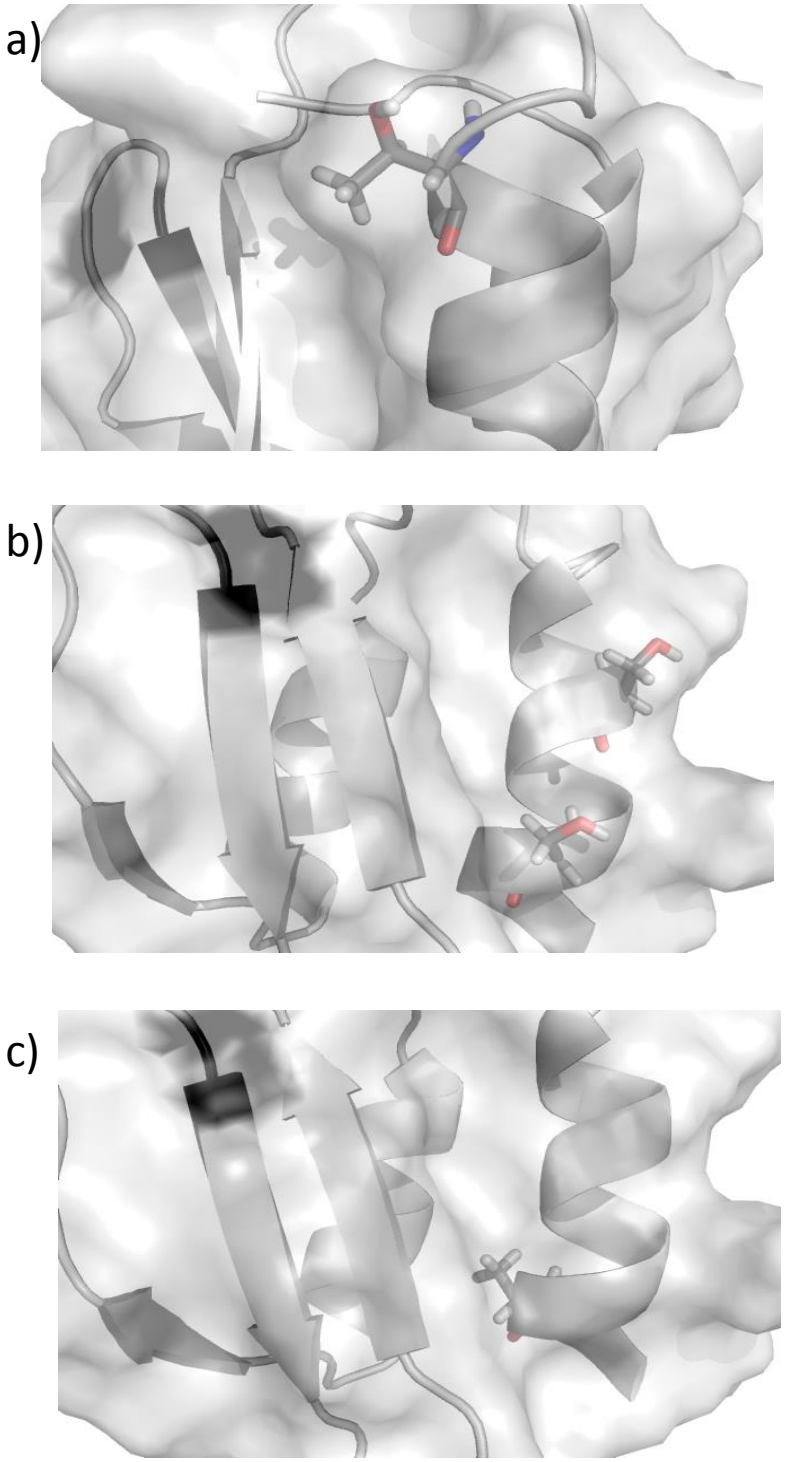

Figure 4.15: Location of residues in the β3-α2 loop and α2 helix of BPSS03390 where alanine substitution abolished toxicity. a) Sticks indicate Thr49. b) Sticks indicate Ser52 and Ser56 within helix. c) Sticks indicate Ala57, with the methyl side chains orientated towards the core of the protein. PyMol was used to generate the images (PDB code 4C26).

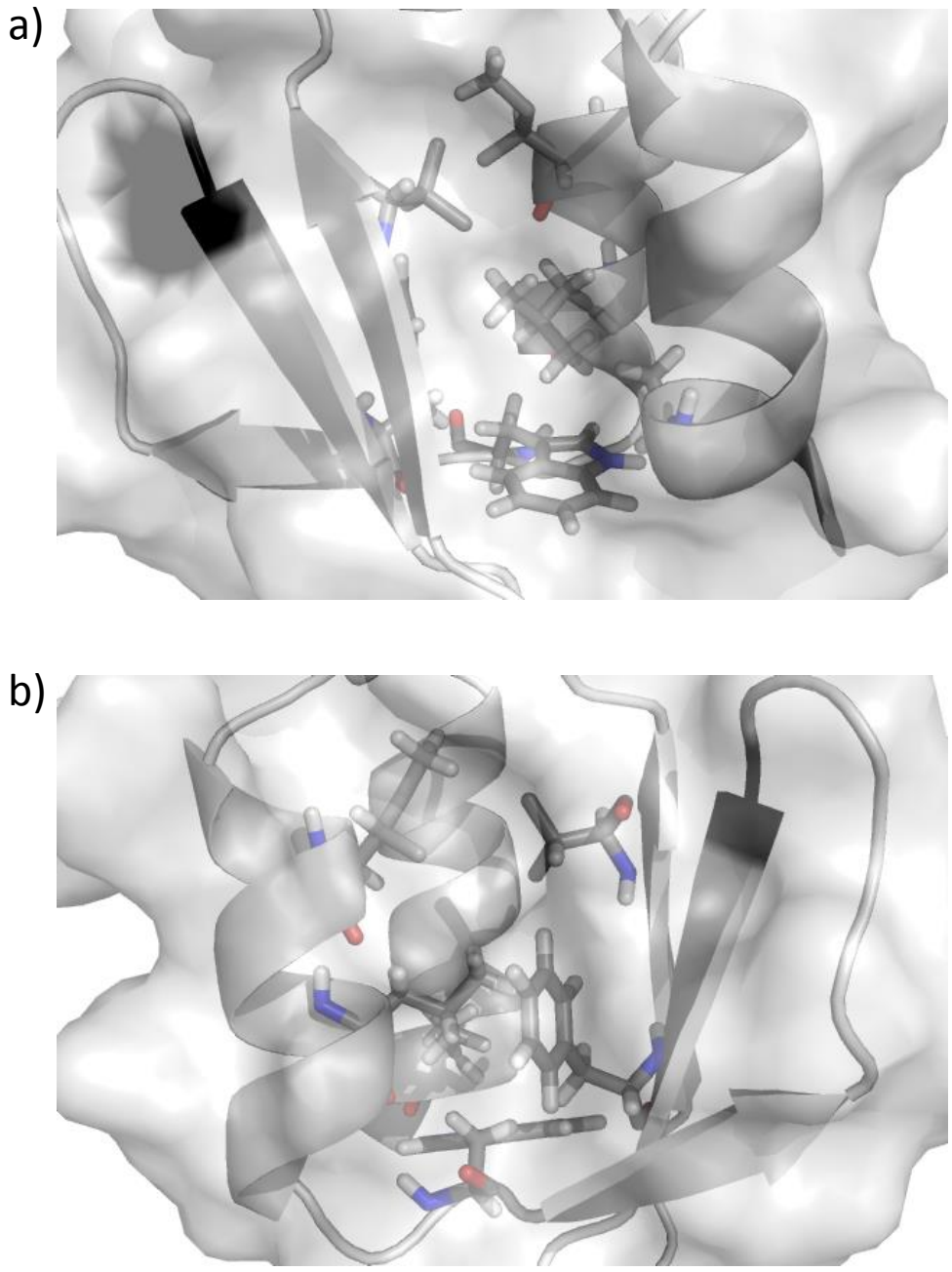

Figure 4.16: Location of residues believed to contribute to the hydrophobic core of BPSS0390 (H24A). a), b) Sticks indicate Ile7, Leu10, Trp15, Phe 27, Val38 and Ala57, with side chains orientated towards the core of the protein. PyMol was used to generate the images (PDB code 4C26).

4.6 Identification of BPSS0390 residues involved in binding antitoxin BPSS0391

Bibi-Triki *et al.* (2014) solved the structure HicA3-HicB3 complex, from a HicAB homologue in *Yersinia pestis*. Crystallisation was only possible after the C-terminus of HicB3 had been cleaved off, revealing that the HicA3-HicB3 complex formed a heterohexamer with α2 helix of HicA3 packed against the βsheet of HicB, and HicB3 α1 helix covering one face of the βsheet of HicA3 (Figure 4.17), burying the active site required for RNA degradation (Bibi-Triki et al. 2014).

4.6.1 Co-expression of BPSS0390 mutants with antitoxin BPSS0391

Mutants N2A, S4A, K5A, L6A, R8A, E11A, E12A, D13A, R16A, L17A, V18A, V20A, S23A, H25A, H26A, P30A,P33A, L35A, V36A, T37A, P39A, H40A, K42A, K43A, P46A, I47A, G48A, V50A, K51A, I 53A, G56A, A57G, G58A and L59A were all tested to determine if the mutated residues played a role in antitoxin binding. It was only possible to test BPSS0390 mutants that retained toxicity.

Competent *E. coli* MG1655 Δ*hipBA* harbouring pME6032-*BPSS0391* were transformed with pBAD/his containing a mutated *BPSS0390* allele and transformants recovered onto LB ampicillin (100 µg/ml) tetracycline (15 µg/ml) glucose (2%(w/v)) plates. An untransformed *E. coli* MG1655 Δ*hipBA* harbouring pME6032-*BPSS0391* control was also plated onto LB ampicillin (100 µg/ml) tetracycline (15 µg/ml) glucose (2% (w/v)) plates.

Plates inoculated with un-transformed *E. coli* MG1655 Δ*hipBA* harbouring pME6032-*BPSS0391* had no growth, whilst plates inoculated with transformed E*. coli* MG1655 Δ*hipBA* harbouring pME6032-*BPSS0391* and pBAD/his-*BPSS0390* mutant constructs had over 60 colonies.

Cultures of *E. coli* MG1655 Δ*hipBA* harbouring pME6032-*BPSS0391* and pBAD/his-*BPSS0390* mutant constructs were grown to OD_{590} 0.1 before induction of expression of mutant BPSS0390 toxin (0.2% (w/v) arabinose) and of antitoxin BPSS0391 (1mM IPTG) for 2 hours. The fold change in CFU after two hours (T2/T0) was calculated (Figure 4.18). A negative control, where *E. coli* MG1655 Δ*hipBA* harbouring pBAD/his-*BPSS0390* and empty pME6032, with no cloned antitoxin was used.

E. coli MG1655 Δ*hipBA* expressing both BPSS0390 and BPSS0391 had an almost 10 fold increase in CFU counts whilst strains expressing only BPSS0390 and no antitoxin showed a 1000 fold decrease in the number of culturable cells. Co-expression of BPSS0390 mutants S4A, L6A, R8A and P30A with BPSS0391 resulted in over a 10 fold increase in the number of culturable cells. Co-expression of BPSS0391 with mutants R16A, L17A, V18A, V20A, S23A and H25A also permitted cell growth. Cell growth was also observed when BPSS0391 was co-expressed with BPSS0390 mutants P33A, V36A, T37A, P39A, H40A, K42, K43, P46A, I47A, G48A, V50A, K51A, I53A, G58A and L59A. However, co-expression of mutants N2A, E11A, E12A and D13A with BPSS0391 resulted in a decrease in fold change CFU.

a)

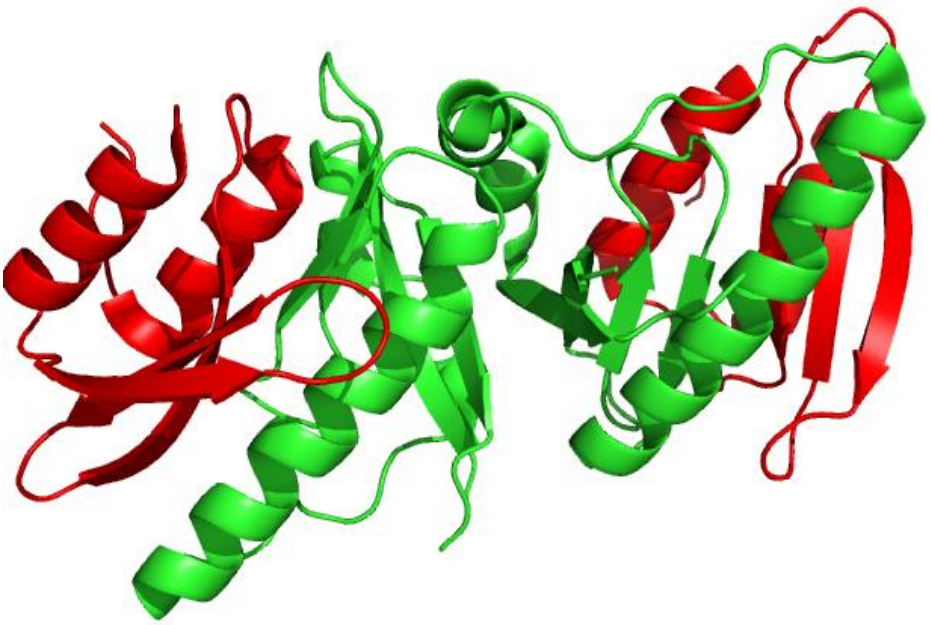

b)

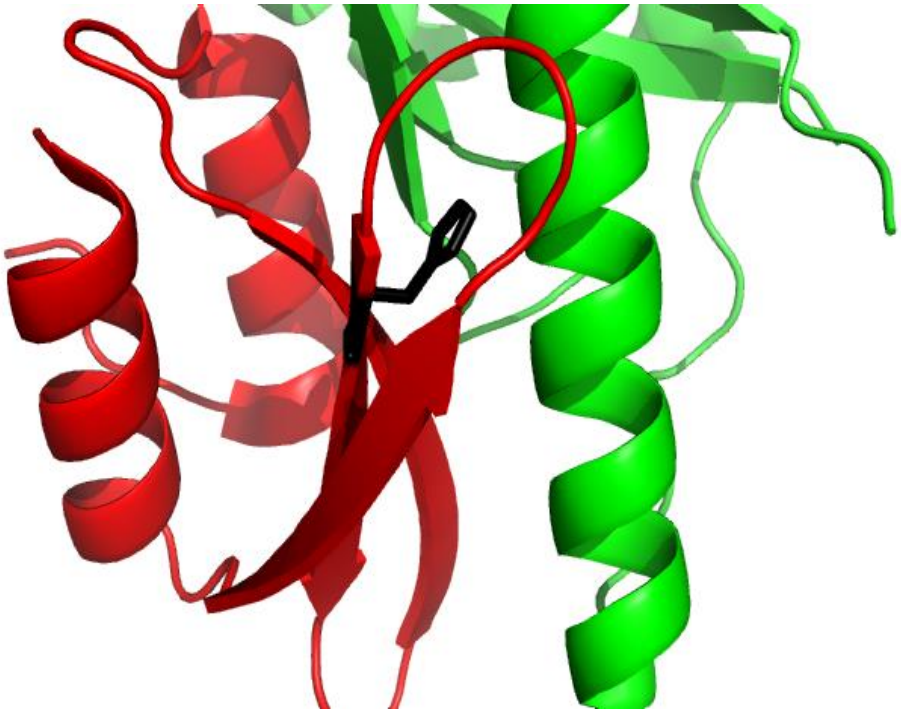

Figure 4.17: Structure of HicA3-HicB3 from Y. pestis. a) HicA3-HicB3-N terminus tetrameric complex. Red indicates the HicA3 toxin subunits, whilst HicB3 subunits are shown in green. b) HicA3 α2 helix packs against the βsheet of HicB. HicB3 α1 helix covers on face of the βsheet of HicA3, burying the histidine (indicated by black sticks) required for RNase activity.(Bibi-Triki et al. 2014). PyMol used to generate images. (PDB 4p78).

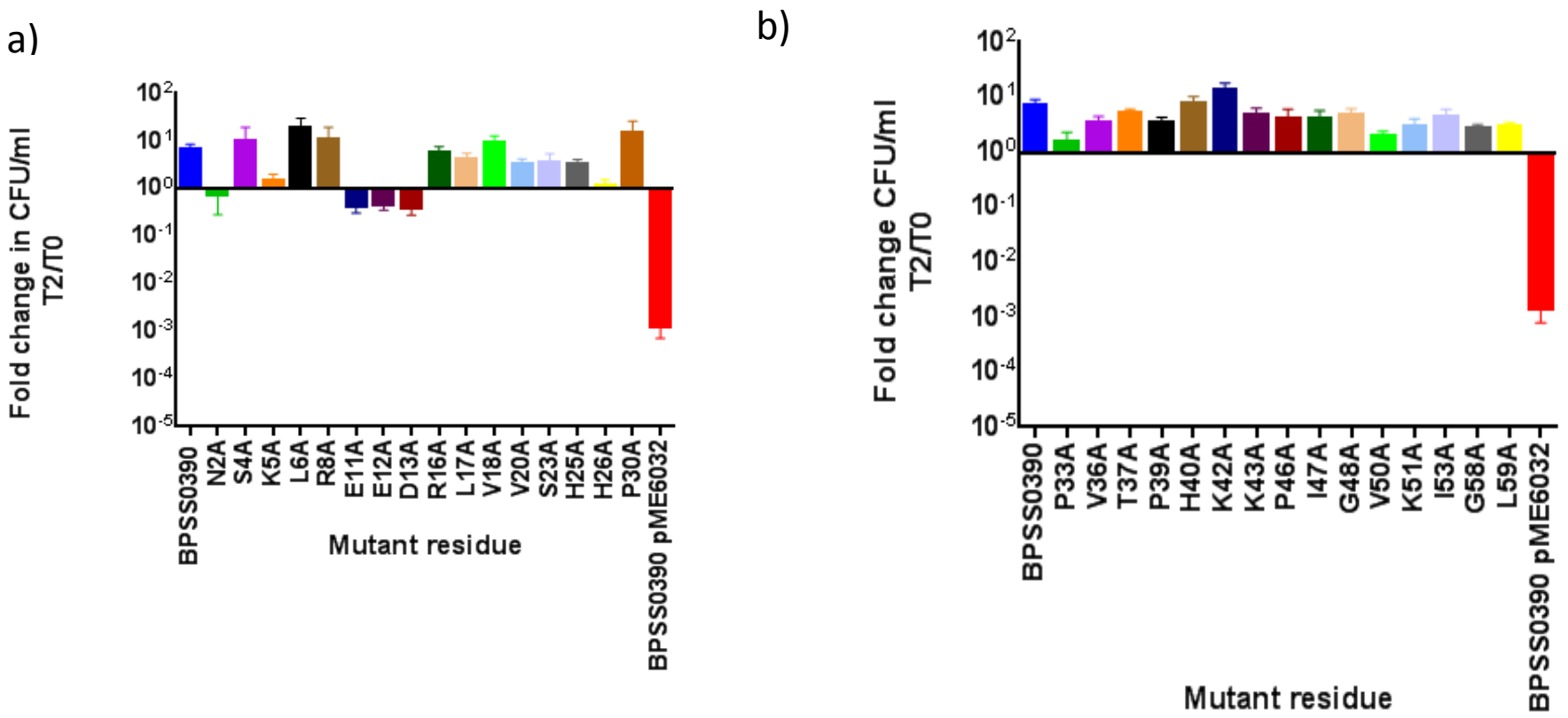

Figure 4.18: Fold change in CFU after co-expression of BPSS0390 mutants with antitoxin BPSS0391 for two hours. *E. coli* MG1655 Δ*hipBA* harbouring either pBAD/his-*BPSS0390* or *BPSS0390* mutant gene cloned into pBAD/his was grown to OD_{590} 0.1 before induction of toxin expression (0.2% (w/v) arabinose) and antitoxin expression (1mM IPTG). Data shown are an average of three biological repeats and error bars shown SEM.

4.6.2 Comparison of fold change in CFU after BPSS0390 mutant expression and after co-expression of BPSS0390 mutants and BPSS0391.

It was not possible to normalise the co-expression data as the toxicity of each BPSS0390 mutant differed. To determine if decrease in fold change in CFU observed after co-expression of N2A, E11A, E12A and D13A with BPSS0391 warranted further investigation, it was necessary to compare existing data; change in CFU after BPSS0390 mutant only expression (for 2 hours, blue bars) against the change in CFU after co-expression BPSS0390 mutants and BPSS0391 (for 2 hours, red bars) (Figure 4.19).

After expression of BPSS0390 for two hours, an almost 100 fold decrease in fold change in CFU was observed, whilst co-expression of BPSS0390 and BPSS0391 for two hours resulted in an increase fold change CFU. Co-expression of BPSS0391 and N2A, E11A, E12A or D13A for two hours resulted in a decrease in fold change CFU. However, expression of N2A or E12A for two hours resulted in a decrease in CFU of over 10 fold, whilst expression of E11A and D13A resulted in an over 100 fold decrease in the number of culturable cells (Figure 4.20). A ratio of fold change CFU after co-expression of N2A, E11A, E12A or D13A with BPSS0391 against fold change CFU after expression of N2A, E11A, E12A or D13A was positive (Figure 4.20), indicating that BPSS0391 was in fact able to neutralise BPSS0390 mutants N2A, E11A, E12A and D13A.

a)

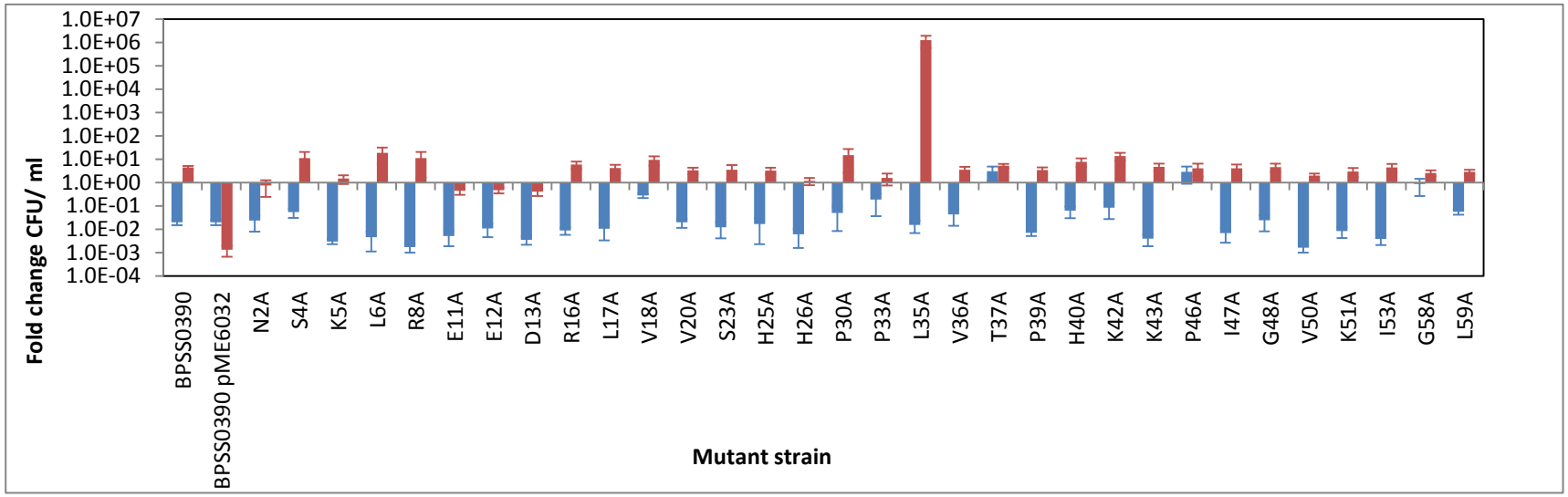

b)

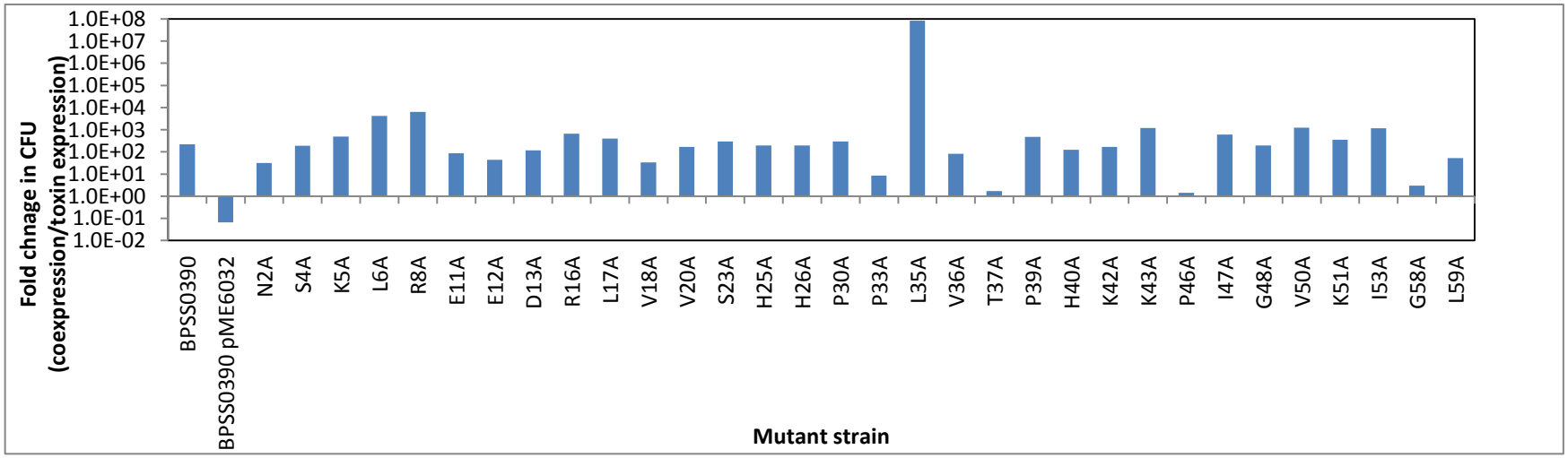

Figure 4.19: Comparison of change in CFU after BPSS0390 mutant expression for 2 hours and after co-expression of BPSS0390 mutants and BPSS0391 for 2 hours. a) Change in CFU after BPSS0390 mutant expression indicated in blue and change in CFU after co-expression of BPSS0390 mutant and antitoxin BPSS0391 in red. Data shown is average of three biological repeats and error bars represent SEM. b) Ratio of fold change CFU after co-expression: fold change CFU after BPSS0390 mutant expression.

4.7 Discussion

Most of the type II TA toxins characterised to date act as translation inhibitors by targeting the stability of RNA through an array of diverse mechanisms and structures (Unterholzner et al. 2013; Yamaguchi & Inouye 2009). Toxins in the RelE superfamily have a four β –strand core, surrounded by 4 α helices and cleavage of the mRNA occurs at the ribosomal A-site (Li et al. 2009; Christensen & Gerdes 2003). In contrast, VapC toxins contain a PIN domain, which consists of a 3-layer α/βα sandwich around a central 5- stranded β-sheet, which is able to bind Mg^{2+} or Mn^{2+} at the active sites and typically cleaves initiator $tRNA^{fMet}$ (although there is some evidence that VapC may target mRNA in a site specific manner) (Hamilton et al. 2014; Lee et al. 2015; Cook et al. 2013). Meanwhile, both Kid and MazF proteins cleave mRNA independently of the ribosome and have compact globular folds with a core β barrel, conserved β-strands on a large loop and a C-terminal α helix (Cook et al. 2013). Despite the similarities in structure, Kid toxin preferentially cleaves RNA at UA(A/C) triplets (Hargreaves et al. 2002; Muñoz-Gómez et al. 2005), whilst the recognition motif of MazF toxins varies in both length and sequence in different bacterial species (Cook et al. 2013; Unterholzner et al. 2013). Protein BPSS0390 has homology to HicA, a TA toxin that acts as an mRNA interferase, capable of cleaving free mRNA independently of the ribosome but with no obvious consensus recognition motif (Jørgensen et al. 2009). The structure of BPSS0390 H24A was determined by NMR to form a dsRBD-like domain fold, a structure not previously attributed to a TA toxin (Butt et al. 2014) and perhaps suggests that this toxin cleaves mRNA in the area of double-stranded (ds) regions (Bibi-Triki et al. 2014).

First identified as a conserved domain in 1992, dsRBD are small protein domains (65-70 amino acids) that adopt an αββββα fold, with two α-helices packed against a three stranded β- sheet (Johnston et al. 1992; Masliah et al. 2013; Drusin et al. 2016). Important for many cellular processes in both eukaryotes and prokaryotes, the dsRBD is one of the most abundant RNA binding domains and its interaction with dsRNA is well characterised (Maris et al. 2005; Drusin et al. 2016).

In solution dsRNA forms an A-form double helix, with two grooves. The minor groove is wide and shallow with the edge of bases easily accessible, while the major groove is deep and narrow, which hinders access to bases. The width of these grooves and the 2'OH functional groups on the ribose sugars in the minor groove, allow the dsRBD to discriminate between dsDNA and dsRNA (Saenger 1984; Dickerson et al. 1982).

High resolution structures of various dsRBDs in complex with dsRNA have revealed that three separate regions are required for recognition of dsRNA. (Ryter & Schultz 1998; Ramos et al. 2000; Gan et al. 2006; Gan et al. 2008; Gan et al. 2005; Blaszczyk et al. 2004; Z. Wang et al. 2011; Wu et al. 2004; Stefl et al. 2010; Huang et al. 2009; Yang et al. 2010; Masliah et al. 2013). Systemic mutational analysis of various dsRBDs also identified the same three regions and conserved residues that may be involved in dsRNA binding (Green & Mathews 1992; Green et al. 1995; Bycroft et al. 1995; Ramos et al. 2000; McMillan et al. 1995; Patel et al. 1996; Masliah et al. 2013). The three regions identified were: region 1 located at the N-terminus of the protein in helix α1, region 2 located in the β1-β2 loop and region 3 located at the N-terminal of α2 helix.

Expression of twenty mutants, S3A, I7A, L10A, W15A, R19A, T21A, G22A, F27A, H29A, K31A, K32A, G34A, V38A, P41A, D44A, L45A, T49A, S52A, S56A and A57G, permitted cell growth. Quantification of protein expression levels by Western blotting determined that expression levels for all substitution mutants were higher than the BPSS0390 control. These twenty mutants are interesting as they have no function despite being expressed. This suggests that the residues mutated are critical for function, either indirectly, through maintenance of structure and correct protein folding, or directly, because they are involved in binding or catalysing RNA.

Alanine substitution of three amino acids, Arg19, Thr21, Gly22 (excluding the previously identified His24) located on the β1-β2 loop of BPSS0390, abolished toxicity. The β1-β2 loop of canonical dsRBDs is thought to interact with the minor groove, one turn away from the minor groove interacting with region 1. Typically, this loop is six residues long and features the conserved amino acid motif GPxHxx, where both the histidine and glycine residues are absolutely required for function, whilst the proline residue is not essential (Masliah et al. 2013; Stefl et al. 2010). Structural resolution of many dsRBDs revealed that the carbonyl group of the peptide backbone of the histidine formed a hydrogen bond to the 2'OH group on one strand, while the imidazole portion stacked onto a ribose to make a hydrogen bond to the 2'OH group of the previous ribose on the other strand (Stefl et al. 2010; Z. Wang et al. 2011; Ryter & Schultz 1998). The residue immediately preceding the histidine has also been shown to bind dsRNA; the peptide backbone carbonyl group contacts the edge of a base, in the dsRBD1 of protein Hyponastic Leaves 1 (HYP1), the residue was a serine that formed a hydrogen bond with N3 of a guanine (Rasia et al. 2010). In some ways, this description describes the β1-β2 loop of BPSS0390. Both His24 and

Gly22 are critical to toxicity and NMR spectra indicate that this loop of six residues has increased local dynamics (Butt et al. 2014). However, the amino acid sequence does not contain the GPxHxx motif (amino acid sequence is RVTGSH). In fact, the sequence of the β1-β2 loop more closely resembles the Rx4-6H motif (where x is any amino acid and 4-6 indicates the number of amino acids between R and H), a novel RNase active site conserved in HEPN toxins (from HEPN-MNT TA system), although it lacks the polar residue immediately after the R (Yao et al. 2015).

The role of Arg19 and Thr21 in toxicity is less clear. In protein–dsRNA interactions, hydrogen bonds occur between the nitrogen atoms of arginine side chain and the hydroxyl or phosphate groups from RNA backbone. Arginine residues also form strong interactions with guanine bases (Lustig et al. 1997) It could be that Arg19 is required for attracting, orientating and binding to the RNA substrate (Drusin et al. 2016; Pathak et al. 2013) Thr21 is the third residue in the loop and evidence from high resolution structures (of dsRNA with dsRBDs) suggests that residues in this position form sequence specific contacts. The carbonyl group of the peptide backbone is able form a hydrogen bond with the exocyclic amino group of guanine, the only base that exhibits an amino group in the minor groove (Blaszczyk et al. 2004; Gan et al. 2008; Gan et al. 2006; Stefl et al. 2010; Ryter & Schultz 1998; Yang et al. 2010). It may be that Thr21 is involved in recognising the RNA substrate (threonine favours bonding with adenosine (Lustig et al. 1997)) of BPSS0390, which would also explain why it is not highly conserved in BPSS0390 homologues. Alternatively, it might be required for stabilising configuration of side chains within the active site (Hamilton et al. 2014), which would explain why the relative calculated

concentration of protein after two hours was not significantly different to the toxic control.

Unexpectedly, substitution of Ser23 with an alanine did not modify toxicity; this suggests that the hydroxymethyl side chain is not involved in substrate binding. However, it may be that the methyl side chain of the substituted alanine is also able to form hydrogen bonds with the substrate and future work could involve replacing Ser23 with a less reactive amino acid.

Region 3 of a canonical dsRBD is located at the N-terminus of the α2 helix and contains the well conserved amino acid sequence KKxAK. The orientation of the first and third lysines are pre-organised to allow their side chains to contact the phosphodiester of one strand, whilst the second lysine contacts the other strand of the major groove. Formation of this arch is stabilised by a series of Van der Waals forces between the lysine side chains and residues in the hydrophobic core, and also by the rigid peptide backbone embedded in the alpha helix. Variations of the KKxAK motif include replacement of one or more lysines with arginine, glutamate, a negatively charged residue or glycine. In all cases the presence of a lysine in α1 helix compensates for these variations (Johnston et al. 1992; Barraud et al. 2012; Ryter & Schultz 1998; Masliah et al. 2013). None of the residues identified as critical for function in the β3- α2 loop and α2 helix of BPSS0390 were lysines. This is unusual (Ramos et al. 2000; Nanduri et al. 1998; Patel et al. 1996; Bycroft et al. 1995).

One pair of lysines was located on the β3- α2 loop, one pair within the α2 helix and one located within the α1 helix ; mutation of K42 (β3- α2 loop) and K55 (α2 helix) did reduce toxicity but not significantly. NMR analysis of the β3- α2 loop of BPSS0390 was ill defined, suggesting that the loop was able to occupy multiple conformations (Butt et al. 2014). In Staufen protein, the individual lysine side

chains in the β3- α2 loop of the dsRBDs underwent a large amplitude of motion that lead to formation short- lived contacts to dsRNA (less than 10 picoseconds) before the side chains switched to new contacts within the dsRNA. This continuous flicking between polar interactions ensured constant association with dsRNA but allowed for a degree of freedom in the dsRBD-RNA complex (Castrignanò et al. 2002; McMillan et al. 1995; Hartman et al. 2013). It is possible that the β3- α2 loop and α2 helix of BPSS0390 also undergo this switching of polar interactions, and whilst all lysines do not contribute equally to binding (McMillan et al. 1995), abolishing individual lysines may not be sufficient to fully prevent interaction with phosphodiester backbone. For future work determine if these lysines are critical for dsRNA binding, it might be necessary to mutate all lysines to alanines within one protein and examine the mutant for changes in RNA binding and toxicity. RNA binding assays, where labelled RNA probe is mixed with mutant protein samples and then electrophoresed could also be used to look for changes in binding between controls and individual alanine mutants.

The residues critical for toxicity in the β3- α2 loop and α2 helix may be involved in forming further contacts between the phophodiester backbone and BPSS0390, or in helping orientate the residues that do. Indeed, both lysines in α2 helix are succeeded in the sequence by serines (Ser52 and Ser56), which likely do not contribute to binding dsRNA but may be packed against the β-sheet surface, stabilising the α2 helix and helping orientate the preceding lysines. Bulky side chains in this location would destabilise β-sheet surface by causing steric clashes (Wu et al. 2004; Ramos et al. 2000), although it is perhaps odd that substitution with alanine would cause this. Ala57 has been

assigned to the hydrophobic core, but substitution with a glycine may have also destroyed the tight packing of the α2 helix against the β-sheet.

It is not possible to definitively determine the roles of Pro41, Asp44, Leu45 and Thr49. The proximity of Asp44 to Lys 42 and Lys43 suggests it may be involved in contacting the phosphodiester backbone. However, proline residues are often located in turns and loops and may play an important role in chain compaction during early protein folding (Krieger et al. 2005; Qiu et al. 2008); suggesting that the role of Pro41 is structural rather than functional.

Unlike the β1-β2 and β3- α2 loop, the β2- β3 loop of dsRBDs is unremarkable; its flexibility is quenched despite having no direct contact with dsRNA. It may be that this rigid structure is required to ensure that regions 2 and 3 are spread the correct distance apart to discriminate between dsRNA and dsDNA (Castrignanò et al. 2002; Fu et al. 2009). Alanine substitution of four residues in the β2- β3 loop of BPSS0390 abolished toxicity (H29A, K31A, K32A and G34). It is possible that these four residues are required to make two γ turns in the loop and are responsible for stabilising the molecule. As neither these turns nor these residues are conserved in dsRBDs, it may also suggest that this positively charged region is important for antitoxin binding.

The final region involved in recognising dsRNA is located in the α1 helix and consists of 4-5 residues at specific locations, although only one residue is conserved (Ryter & Schultz 1998; Masliah et al. 2013) . There is some debate as to whether the interactions of these residues with the minor groove are shape, such as the UUGG tetraloop, or sequence specific, for example, contact of methyl group of methionine 4 in ADAR2 dsRBD with the edge of an adenine (Chang & Ramos 2005; Stefl et al. 2010; Masliah et al. 2013). In BPSS0390, alanine substitution revealed three residues where mutation abolished function;

S3, I7 and L10. Leucine 10 was assigned to the hydrophobic core. Interestingly, Ser3 of dsRBD in Staufen protein interacts with the 2'OH and phosphate oxygen of the RNA stem loop and so Ser3 of BPSS0390 may also interact with the dsRNA substrate (Chang & Ramos 2005). Ile7 was assigned to the hydrophobic core but also corresponds to the first of the four residues involved in recognition of minor groove in canonical dsRBDs. In *Xenopus leavis* RNA binding protein A (Xlrbpa) the side chain of the of the bulky and hydrophobic reside in this position was able to make Van der Waals contacts to the ribose moiety of dsRNA minor groove. It also interacted with alanines in α2 to assist in formation of the core (Krovat & Jantsch 1996; Masliah et al. 2013). The other three residues that might be involved in RNA binding are Arg8, Glu11 and Glu12. Arg8 in Dicer-like 1 (DCL1) protein, a ribonuclease III enzyme, was able to form hydrogen bonds with nitrogenous bases and preferentially bound to mismatched base pairs within the helix, acting as an anchor (Drusin et al. 2016). However, Arg8 is not conserved across proteins with homology to BPSS0390 and substitution with an alanine did not abolish toxicity.

The final two residues that might be involved are both glutamatic acids. In Xlrbpa and Staufen proteins, a glutamic acid carbonyl group makes a hydrogen bond with the 2'OH group of ribose sugar in minor groove. The second glutamic acid is conserved in both proteins and its mutation abolishes function (Ramos et al. 2000; Krovat & Jantsch 1996). However, in BPSS0390 neither residue was individually required for toxicity and both were conserved in less than 75% homologous proteins. It may both residues and the succeeding Asp13 are involved binding ribose moieties in the minor groove, in a sequence specific manner and so a reduction in toxicity would only be observed after alanine substitution of all three residues in the same mutant.

In the α1-β1 loop, Gly14 was 97% conserved across BPSS0390 homologues and yet substitution with an alanine reduced but did not abolish toxicity. Trp15 was assigned to the hydrophobic core. However, in dsRBD of *Saccharomyces cerevisiae* RNase III, the α1-β1 loop forms a hinge that facilitates the conformational changes required for both α1 helix and β1-β2 loop to find the minor groove (Hartman et al. 2013). Substitution of the flexible glycine with alanine in BPSS0390 may have partially impaired movement the movement of this hinge.

Masliah *et al.* (2013) determined that hydrophobic residues conserved in more than 40% of proteins in a multiple sequence alignment of various dsRBD were important for maintenance of a stable hydrophobic core, including but not limited to two leucines in the α1 helix, a proline on the α1- β1 loop, a phenylalanine in the β2 strand, valines in the β3 strand and alanine in the α2 helix (Masliah et al. 2013). These residues correspond well to I7 and L10 (α1 helix), W15 (aromatic, α1- β1 loop), F27 (β2 strand), V38 (β3 strand) and A57 (α2 helix) in BPSS0390, validating the assignment of these residues as part of the hydrophobic core. Western blot analysis indicated that cells expressed W15A and V38A mutant proteins at levels similar to wild type BPSS0390, whilst cells expressed I7A, L10A, F27A and A57G mutant proteins at a statistically significantly higher relative calculated concentration. Organisation of residues within the core is important both for structure and stability of a protein (Munson et al. 1996) so it might be that disruption of the W15 and V38 residues results in an unstable protein that degrades rapidly, whilst I7A, L10A, F27A and A57G proteins are more stable and non-toxic so larger quantities are produced as there is no cell growth arrest after expression.

It is hard to draw firm conclusions from expression data as Western blotting is a "semi-quantitative" method that relies on even transfer of protein onto membrane and even exposure to washing and antibodies, procedures where some variation is inevitable. Although use of quantitative fluorescent Western blotting with a fluorescent secondary antibody and a standard curve to generate a linear detection profile may have improved the sensitivity and accuracy compared to ECL labelling (Eaton et al. 2014). Only small quantities of BPSS0390 are produced in response to induction of expression as the toxic effects of the protein causes cell growth arrest and a decrease in the number of culturable cells, whereas large quantities of protein are produced when the mutant is non-toxic, for example, H24A. Small quantities of protein might be produced when the mutant is as or more toxic than native BPSS0390 or when the mutation has completely interrupted the structure of the protein and the protein cannot fold properly. It is therefore very difficult to interpret the expression data against the toxicity data and this is an area that will require more thought in future work.

The size of the BPSS0390 protein was also problematic for Western blotting; intact, histidine tagged BPSS0390 is 10kDa so any fragments produced due to instability are likely to be very small and lost from the SDS-PAGE gel. For future work, mutants showing increased calculated relative concentration could be further characterised using quantitative real-time PCR to quantify mutant gene expression and circular dichroism (CD) spectroscopy used to determine changes to secondary structure of the protein (Drusin et al. 2016; Butt 2013). Bibi-Triki *et al.* (2014) solved the structure of the HicA3-HicB3 complex to determine that the interface of the complex consisted of i) one face of the β-sheet of HicA3 covered by α1 helix of HicB-N-terminus, occluding the catalytic

site at β1-β2 loop and ii) the α2 helix of HicA3 packed against the β-sheet of HicB3-N-terminus. This interface was stabilised by ten hydrogen bonds and five salt bridges. However, it was only possible to determine this structure by removing the C-terminal third of the HicB protein (Bibi-Triki et al. 2014). This does not correlate with what has previously been observed with BPSS0390-BPSS0391 complex formation (Butt 2013) and so it would have been interesting to determine which residues were involved in the binding interface of BPSS0390-BPSS0391complex. However, it was not possible to identify residues involved in BPSS0390-BPSS0391 complex formation as all of the BPSS0390 alanine mutants tested were neutralised as growth was observed (or partially neutralised, negatively charged Glu11, Glu12 and Asp13) when expressed with antitoxin BPSS0391. The existing co-expression assay only allowed for BPSS0390 mutants that retained toxicity to be tested as mutants that were not neutralised in the assay, were identified as they retained their toxic phenotype (decrease in fold change in CFU compared to toxin expression only). Many of the residues necessary for maintaining the structure and function of the β1-β2 loop and α2 helix abolished toxicity and so could not be tested. In future, it would be good to test these mutants for interactions with BPSS0391 using a yeast two-hybrid system, although further work would be needed to demonstrate successful functional neutralisation in bacterial cells.

Chapter 5: Crosstalk between non-cognate toxin-antitoxin pairs identified in Burkholderia pseudomallei K96243.

5.0 Introduction

Butt *et al.* (2013) previously designed a novel co-expression assay where the candidate toxin and antitoxin genes in *B. pseudomallei* K96243 identified by RASTA, could be independently or simultaneously expressed in *E. coli*. Over-expression of toxin genes resulted in two toxic phenotypes; bacteriostasis or a rapid decrease in number of culturable cells, whilst co-expression of the toxin with its cognate antitoxin resulted in growth, as expected. Interestingly, when toxin BPSS0390 (homologous to HicA) was co-expressed with non-cognate antitoxin BPSL0174 (homologous to RelB) growth, an increase in OD and CFU, was also observed, suggesting that an antitoxin from one system could neutralise a toxin from a different system (Butt 2013).

Toxin-antitoxin systems are typically described as a gene pair where one gene encodes a protein toxin and the other gene encodes a cognate antitoxin capable of sequestering the toxin (Yamaguchi et al. 2011; Gerdes & Maisonneuve 2012). In type II systems this description suggests that only one antitoxin may neutralise one toxin.

The co-existence of multiple homologous and non-homologous TA systems within individual bacterial genomes may suggest that non-cognate interactions are possible (Goeders & Melderen 2014). In pathogenic *E. coli* O157:H7 two homologues of the *ccd* TA system have been identified, one plasmid-borne, $ccd_{F,}$ and one located on the chromosomal backbone, ccd_{O157}. Both systems co-exist and encode functional toxins, targeting DNA gyrase, and functional antitoxins, subject to degradation by Lon protease. Experiments to examine cross-interaction between the two systems revealed that the chromosomal toxin could be sequestered by the plasmid encoded antitoxin but that the toxin encoded by the plasmid could not be sequestered by the

chromosomal antitoxin (Wilbaux et al. 2007). Limited evidence suggests that non-cognate TA pairs in *Mycobacterium tuberculosis* can interact physically and functionally (Zhu et al. 2010). These functional interactions between non-cognate systems, within and without different families, suggest that TA systems may operate as networks that co-operate to enable adaptation to the host cell environment.

There is published data on four type II TA systems identified in *B. pseudomallei* K96243. Two systems, BPSS1060-1061 and BPSL0174-0175 are paralogous. Toxin BPSL0175 has 54% identity to RelE toxin from *Klebsiella pneumoniae* and antitoxin BPSS1060, 53% identity. One system, BPSS1583-1584, is homologous to *hipBA*, with toxin BPSS1584 sharing 100% identity with HipA in *B. mallei* and antitoxin BPSS1584 92%. Finally, system BPSS0390-0391, where toxin BPSS0390 has 78% identity with HicA toxin from *Acinetobacter baumannii* and antitoxin BPSS0391 43% identity with HicB *Neisseria subflava* (Butt 2013).

An existing co-expression assay was modified to allow for co-expression of non-cognate TA pairs. Six non-cognate pairs were co-expressed using this assay and the OD and number of culturable cells monitored over time (Figure 5.1).

		Toxin gene			
		BPSS0390	*BPSS1584*	*BPSS1060*	*BPSL0175*
Antitoxin gene	Homologous to:	*hicA*	*hipA*	*relE*	*relE*
BPSS0391	*hicB*	✓	✓	x	x
BPSS1583	*hipB*	✓	x	x	x
BPSS1061	*relB*	✓	x	x	✓
BPSL0174	*relB*	✓	x	✓	x

Figure 5.1: Matrix to show toxin-antitoxin pairs co-expressed in this study.
Antitoxin genes identified in *B. pseudomallei* are listed to the left and toxin genes identified are listed above. The cognate TA pair *BPSS0390-BPSS0391* was used to optimise the co-expression assay before other non-cognate pairs were co-expressed. Ticks indicate gene pairs that were co-expressed. Crosses indicate gene pairs that were not examined.

5.1 Aim

Determine if type II TA antitoxins in *B. pseudomallei* form a co-operative network through non-cognate toxin-antitoxin interactions.

5.2 Results

5.2.1 Existing method for co-expression of cognate toxin-antitoxin pairs

A co-expression assay designed to determine if antitoxin BPSS0391 could neutralise its cognate toxin BPSS0390 has previously been described (Butt et al. 2013; Butt 2013). This published expression system allowed for co-expression of both toxin and antitoxin genes as the toxin was cloned into the arabinose inducible pBAD/his vector and the antitoxin gene into the IPTG inducible pME6032 vector (both described previously). To co-express the toxin and the antitoxin both arabinose (final concentration of 0.2% (w/v)) and IPTG (final concentration of 25mM) were added to *E. coli* culture harbouring pBAD/his-*BPSS0390* and pME6032-*BPSS0391* and the optical density and number of culturable cells monitored hourly for two hours.

A culture of *E. coli* containing plasmid encoded toxin (pBAD/his-*BPSS0390)* and plasmid encoded antitoxin (pME6032-*BPSS0391*) was grown to early log phase (OD_{590} ~ 0.1) and split; supplemented with either arabinose (final concentration of 0.2% (w/v)) to induce toxin expression, or arabinose and IPTG (final concentration of 25mM) to induce both toxin and antitoxin expression, or IPTG only added to induce antitoxin expression, or glucose (final concentration 0.2% (w/v)) to repress toxin expression. The optical density and number of culturable cells were monitored hourly for three hours (Figure 5.2).

Glucose repression allowed the cells to continue growing, as did expression of only antitoxin BPSS0391 (25mM IPTG). Expression of BPSS0390 only (0.2% (w/v) arabinose), reduced both the growth rate and the number of culturable cells after three hours. However, addition of both arabinose and IPTG (0.2% (w/v) arabinose and 25mM IPTG) resulted in an increase in optical density and number of culturable cells after three hours.

a)

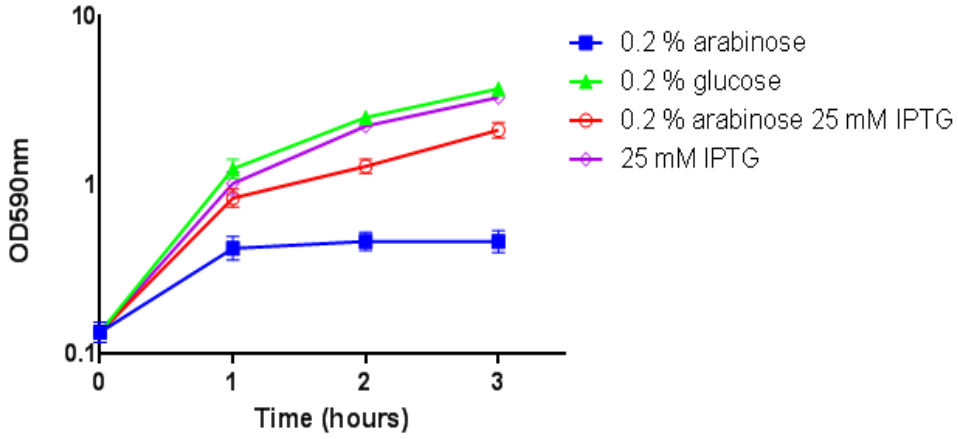

b)

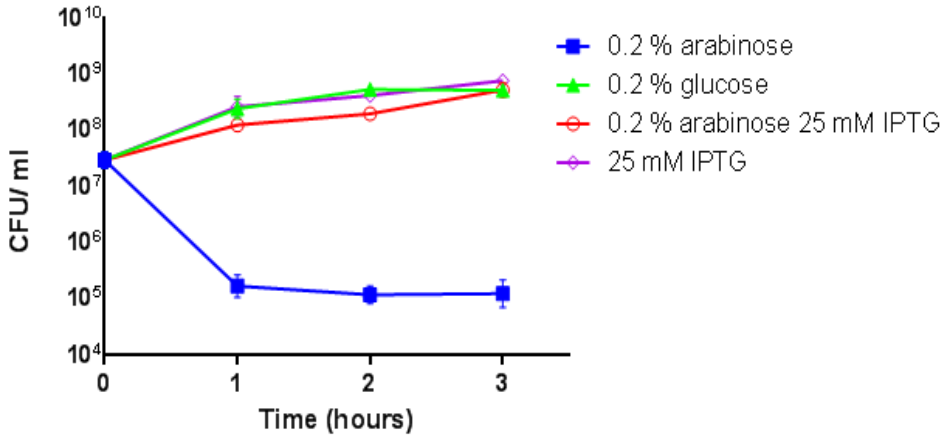

Figure 5.2: Co-expression of cognate toxin- antitoxin pair BPSS0390 and BPSS0391 in *E. coli* MG1655. a) Change in OD; b) number of culturable cells, after either: induction of toxin expression only (0.2% (w/v) arabinose), or repression of toxin expression (0.2% (w/v) glucose), or induction of toxin and antitoxin expression (0.2% (w/v) arabinose and 25mM IPTG) or induction of antitoxin only (25mM IPTG). Data shown represents two biological repeats and error bars represent SEM.

5.3 IPTG as an inhibitor of P_{BAD} expression system

Kim *et al.* (2007) have previously indicated that IPTG can inhibit expression from the P_{BAD} expression system. Therefore it was necessary to determine if the cell growth observed after co-expression of toxin gene *BPSS0390* with antitoxin *BPSS0391* (as described above) was a result of IPTG-induced repression of the P_{BAD} arabinose promoter or the neutralisation of toxic protein by the antitoxin.

An overnight culture of *E. coli* with plasmid encoded toxin HicA (pBAD/his-*BPSS0390*) was supplemented with ampicillin (100 µg/ml), and glucose (2% (w/v)) was used to inoculate fresh LB broth supplemented with ampicillin (100 µg/ml). The culture was grown until early log phase (OD_{590} ~0.1) before splitting; either glucose (final concentration 0.2% (w/v)) was added to repress toxin expression, or arabinose (final concentration 0.2% (w/v)) was added to induce toxin expression or the media was supplemented with IPTG (final concentration of 25mM) before induction of toxin expression by addition of arabinose (final concentration 0.2% (w/v)). The optical density and number of culturable cells were monitored for three hours (Figure 5.3)

The addition of glucose allowed the cells to continue growing as evidenced by the increase in optical density and number of culturable cells after three hours. When arabinose alone was added there was a rapid decrease in culturable cells after three hours and a reduced growth rate when compare to the glucose repressed control. However, when both IPTG and arabinose were added, the optical density and number of culturable cells increased, similar to the glucose control.

a)

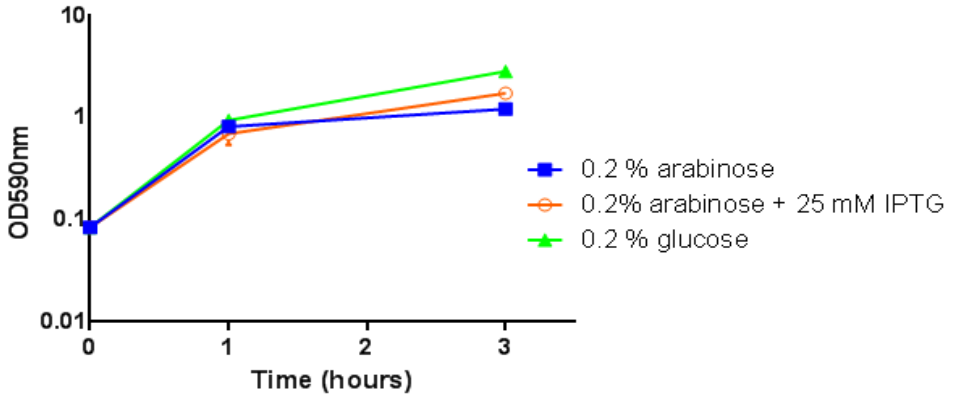

b)

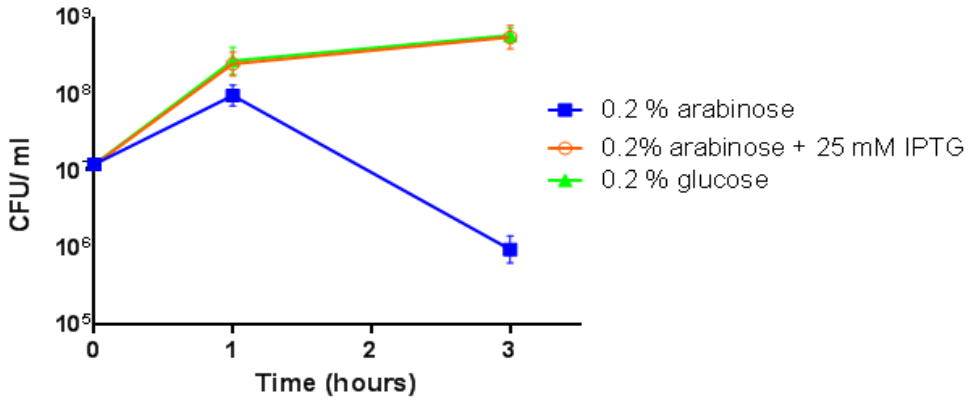

Figure 5.3: Addition of IPTG repressed expression from the PBAD promoter. Supplementing media with IPTG (25mM) before induction (0.2% (w/v) arabinose) of toxin expression, or toxin expression only (0.2% (w/v) arabinose) or repression (0.2% (w/v) glucose) of toxin expression. Graphs show changes in a) optical density and b) number of culturable cells. Data shown is average of three biological repeats and error bars represent SEM.

5.3.1 Determining the inhibitory concentration of IPTG

An overnight of culture of *E. coli* pBAD/his-*BPSS*0390 supplemented with ampicillin (100 µg/ml) and glucose (2% (w/v)) was used to inoculate fresh LB broth supplemented with ampicillin (100 µg/ml). The culture was grown until early log phase (OD_{590} ~0.1) before splitting. Cultures were supplemented with IPTG to a final concentration of either 1mM, 5mM, 10mM or 25mM IPTG before toxin expression was induced by addition of final concentration of 0.2% (w/v) arabinose. There were two controls where no IPTG was added; one where toxin expressed was induced by addition of final concentration of 0.2% (w/v) arabinose and the other where toxin expression was repressed by addition of a final concentration of 0.2% (w/v) glucose. The optical density and number of cultural cells were monitored for three hours (Figure 5.4)

The addition of glucose allowed the cells to continue growing. When arabinose alone was added, there was a decrease in the number of culturable cells after three hours and a reduced growth rate when compared to the glucose repressed control. However, when media was supplemented with either 10mM or 25mM IPTG the number of culturable cells increased after three hours, despite addition of arabinose to induce toxin expression. When media was supplemented with arabinose and 5mM IPTG the culturable grew for the first hour before becoming bacteriostatic. Only when media was supplemented with 1mM IPTG and toxin expression induced was a reduction in culturable cells observed.

a)

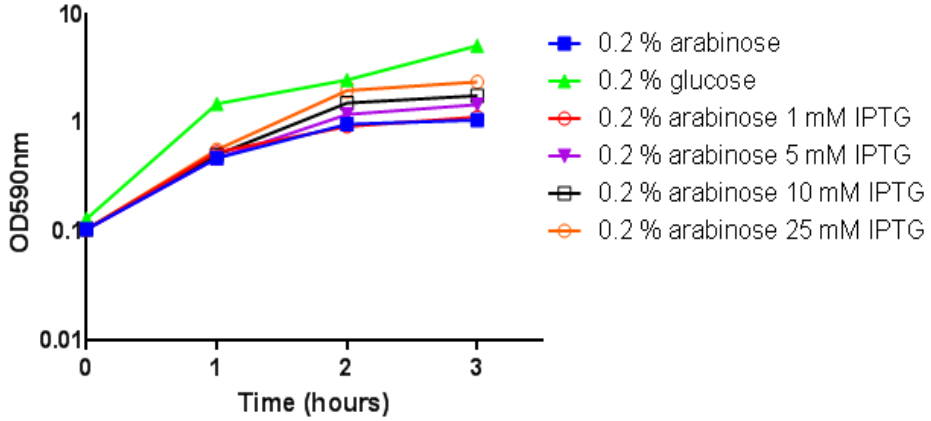

b)

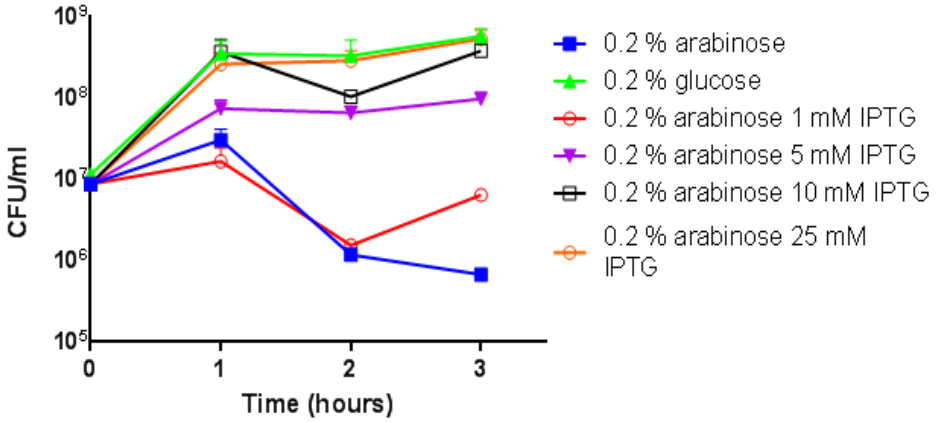

Figure 5.4: Determining the inhibitory concentrations of IPTG. Media was supplemented with different final concentrations of IPTG (1mM, 5mM, 10mM or 25mM) and toxin expression induced (0.2% (w/v) arabinose). Changes in a) optical density and b) number of culturable cells for three hours. Data shown represents two biological repeats and error bars represent SEM

5.3.2 IPTG toxicity

An overnight of culture of *E. coli* pBAD/his-*BPSS*0390 supplemented with ampicillin (100 µg/ ml) and glucose (2% (w/v)) was diluted to an OD_{590nm} of 0.01 in LB broth supplemented with ampicillin (100µg/ ml) and either no, 1mM, 5mM, 10mM or 25mM IPTG. 100µl aliquots of the cell suspension were pipetted into individual wells in a 96-well plate and incubated overnight at 37°C. A Softmax Pro-5 Microplate Reader (VersaMax) was used to take OD_{590} over 24 hour period (Figure 5.5).

Cultures that had been supplemented with 1, 2 or 5mM IPTG demonstrated similar growth profiles to the culture with no IPTG supplementation: normal growth. Cultures supplemented with either 10mM or 25mM IPTG showed a reduced growth rate.

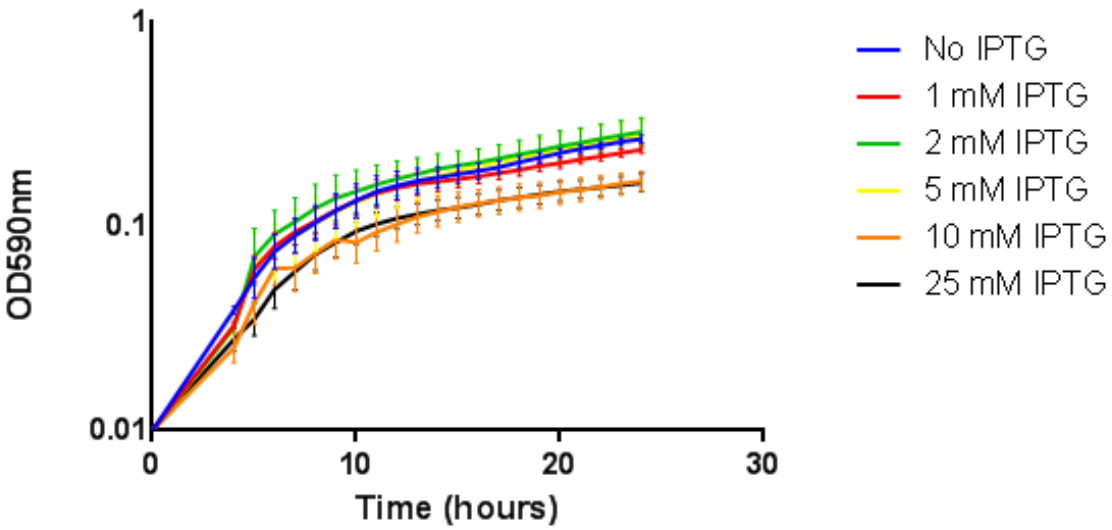

Figure 5.5: Growth of cultures supplemented with different final concentrations of IPTG. Diluted cells were supplemented with different concentrations of IPTG before transference to a 96-well plate. The optical density was monitored for 24 hours using a plate reader. Data shows mean of two biological replicates and error bars represent SEM.

5.3.3 Optimising the co-expression assay

The experiment shown at figure 5.4 indicated that concentrations of IPTG of 5mM and above were able to abolish the toxic phenotype observed when toxin expression was induced and so the co-expression assay was repeated as previously reported but using 1mM or 5mM IPTG to induce antitoxin expression and with *E. coli* MG1655 Δ*hipBA* as a host. This *E. coli* strain was chosen to ensure that there were no interactions between the native host TA systems and the *B. pseudomallei* TA components being ectopically expressed.

Heat shock was used to transform pME6032-*BPSS0391* into competent *E. coli* MG1655 Δ*hipBA* and transformants were recovered onto LB agar plates supplemented with tetracycline (15 µg/ml). Competent *E. coli* MG1655 Δ*hipBA* pME6032-*BPSS0391* cells were generated and transformed with pBAD/his-*BPSS0390* by heat shock and transformants selected by plating onto LB agar plates with ampicillin (100 µg/ml), tetracycline (15 µg/ml) and glucose (2% (w/v)).

An *E. coli* Δ*hipBA* pBAD/his-*BPSS0390* pME6032-*BPSS0391* culture was grown to an OD_{590} of approximately 0.1 (early log phase) and split into four cultures of equal size. Either: arabinose (final concentration of 0.2% (w/v)), or arabinose and IPTG (final concentration of either 1 or 5mM), or glucose (final concentration 0.2% (w/v)) were added to repress toxin expression. The optical density and number of culturable cells were monitored hourly for three hours (Figure 5.6).

As a control, a culture of *E. coli* Δ*hipBA* harbouring pBAD/his-*BPSS0390* pME6032 (lacking the antitoxin gene), was also grown and the culture split and treated as described above.

Addition of arabinose induced toxin expression for both strains; a decrease in the number of culturable cells and a reduced growth rate was observed. When toxin expression was repressed by addition of glucose, the number of culturable cells increased in both cultures. For cultures harbouring both pBAD/his-*BPSS0390* and pME6032-*BPSS0391*, induction of toxin and antitoxin expression (arabinose and either 1mM or 5mM IPTG) resulted in an increase in the number of culturable cells; a growth phenotype similar to glucose repression. For cultures harbouring pBAD/his-*BPSS0390* and empty pME6032, addition of final concentration 0.2% (w/v) arabinose and 1mM IPTG resulted in a decrease in culturable cells and OD similar to arabinose only toxin expression. However, when a final concentration of 0.2% (w/v) arabinose and 5mM IPTG were added to cultures harbouring pBAD/his-*BPSS0390* and empty pME6032, the number of culturable cells did not change.

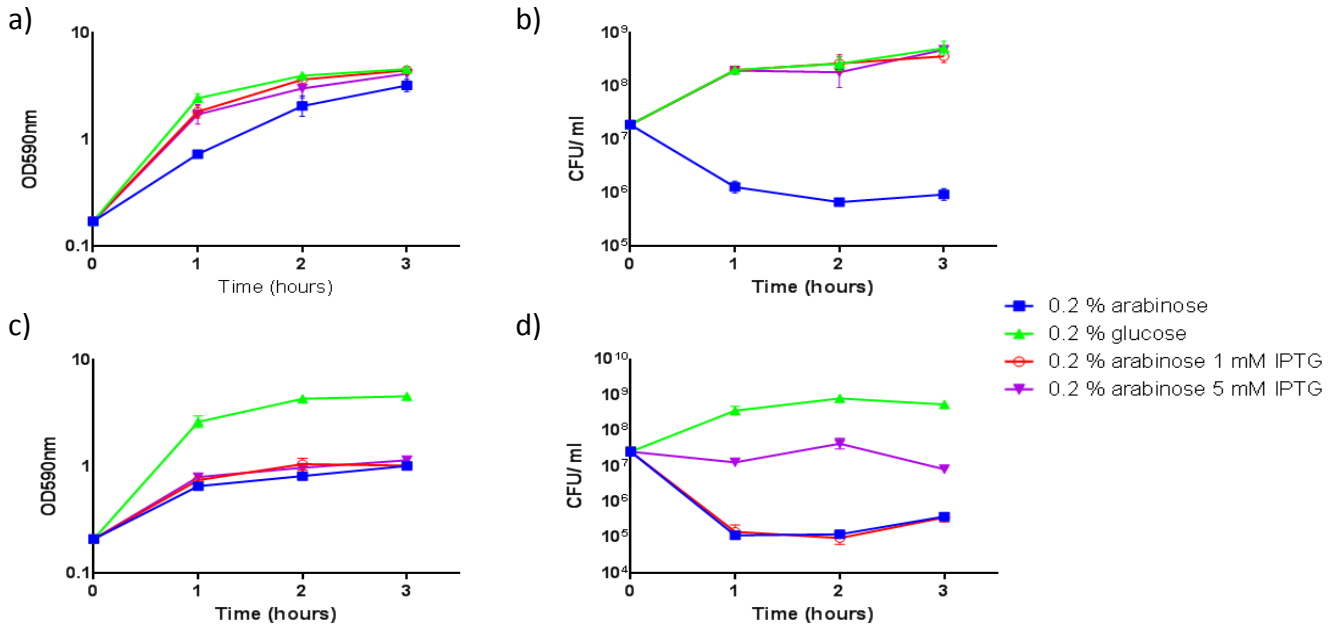

Figure 5.6: Optimising co-expression of cognate toxin-antitoxin pair *BPSS0390-BPSS0391* in *E. coli* MG1655 *ΔhipBA*. *E. coli* MG1655 Δ*hipBA* harbouring either pBAD/his-*BPSS0390* and pME6032-*BPSS0391* (a,b) or BAD/his-*BPSS0390* and empty pME6032 vector (control) (c,d) was grown to early log phase (OD_{590} 0.1) before cultures were split and either toxin expression induced (0.2% (w/v) arabinose), or repressed (0.2% (w/v) glucose) , or toxin and antitoxin expression induced (0.2% (w/v) arabinose and 1mM or 5mM IPTG) and the changes in optical density (a,c) and number of culturable cells (b,d) recorded hourly. Data shown represents two biological repeats and error bars represent SEM.

5.4 Co-expression of toxin gene *BPSS0390* with antitoxin genes from different families

5.4.1Co-expression of *BPSS0390* with *BPSL0174* (homologous to *relB*)

E. coli MG1655 Δ*hipBA* pME6032-*BPSL0174* competent cells were transformed with pBAD/his-*BPSS0390* by heat shock and transformants selected by plating onto LB agar plates with ampicillin (100 µg/ml), tetracycline (15 µg/ml) and glucose (2%(w/v)).

A culture of *E. coli* MG1655 Δ*hipBA* pBAD/his-*BPSS0390* pME6032-*BPSL0174* was grown until early log phase (OD_{590} ~ 0.1) and the culture split and supplemented with either arabinose (final concentration of 0.2% (w/v)) or arabinose and IPTG (final concentration 1mM) or IPTG only (final concentration 1mM) or glucose (final concentration of 0.2% (w/v)). The OD and number of culturable cells were monitored for three hours (Figure 5.7).

Induction of toxin expression (arabinose) resulted in a decreased growth rate and a 100-fold decrease in the number of culturable cells. Glucose-repression of toxin expression resulted in growth with both the OD and number of culturable cells increasing. When only IPTG was added, a growth phenotype was observed similar to glucose-repression. However, when both toxin BPSS0390 and antitoxin BPSL0174 were expressed a toxic phenotype, where both OD and number of culturable cells decreased, was observed. This suggests that in this assay, antitoxin BPSL0174 was not able to neutralise toxin BPSS0390.

a)

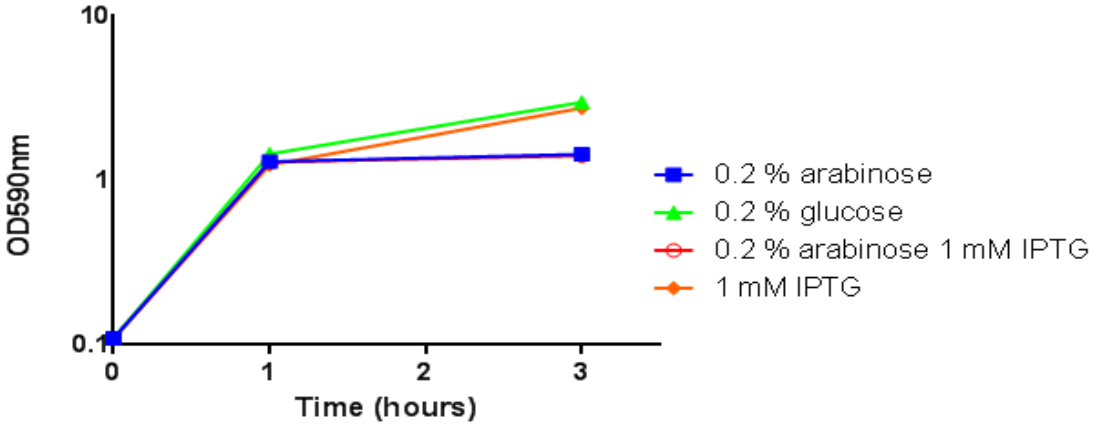

b)

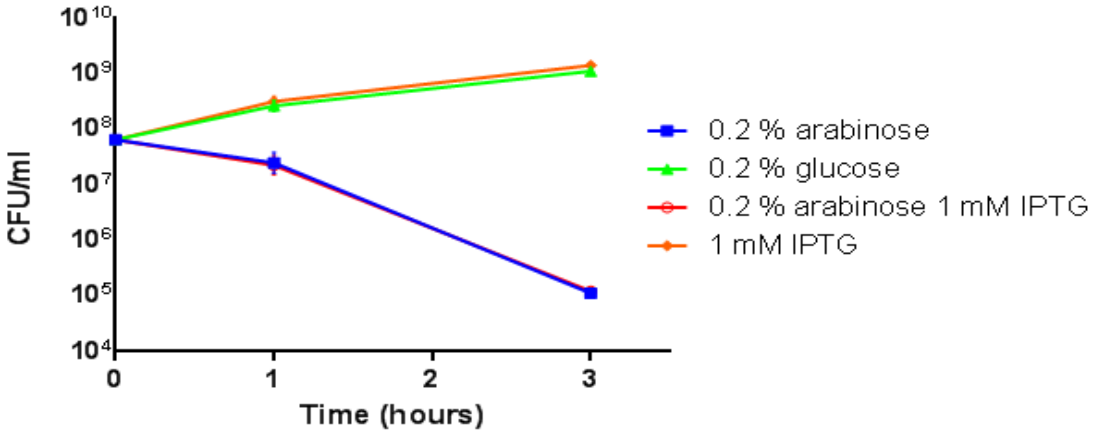

Figure 5.7: Co-expression of genes BPSS*0390* and BPSL*0174* in *E. coli* *ΔhipBA* pBAD/his-*BPSS0390* pME6032-*BPSL0174*. a) Change in OD ; b) change in number of culturable cells after induction of either toxin expression (arabinose), or toxin and antitoxin expression (arabinose and IPTG), or antitoxin expression (IPTG) or repression of toxin expression (glucose) in cultures of *E. coli* MG1655 Δ*hipBA* harbouring pBAD/his-*BPSS0390* and pME6032-*BPSL0174* . Data shown represents three biological repeats and error bars represent SEM.

5.4.2 Co-expression of *BPSS0390* with *BPSS1061* (homologous to *relB)*

E. coli MG1655 Δ*hipBA* pME6032-*BPSS1061* competent cells were transformed with pBAD/his-*BPSS0390* by heat shock and transformants selected by plating onto LB agar plates with ampicillin (100 µg/ml), tetracycline (15 µg/ml) and glucose (2% (w/v)).

A culture of *E. coli* MG1655 Δ*hipBA* pBAD/his-*BPSS0390* pME6032-*BPSS1061* was grown until early log phase (OD_{590} ~ 0.1) and the culture split and supplemented with either arabinose (final concentration of 0.2% (w/v)) or arabinose and IPTG (final concentration 1mM) or IPTG only (final concentration 1mM) or glucose (final concentration of 0.2% (w/v)). The OD and number of culturable cells were monitored for three hours (Figure 5.8).

When BPSS0390 toxin expression was induced, there was over a 100-fold decrease in culturable cells, whilst glucose-repression of BPSS0390 expression resulted in growth with the OD and number of culturable cells increasing after three hours. Addition of only IPTG resulted in a growth phenotype similar to glucose-repression, with the number of culturable cells increasing. When both BPSS0390 and BPSS1061 expression was induced there was a 100-fold decrease in the number of culturable cells, suggesting that in this assay antitoxin BPSS1061 was not able to neutralise BPSS0390.

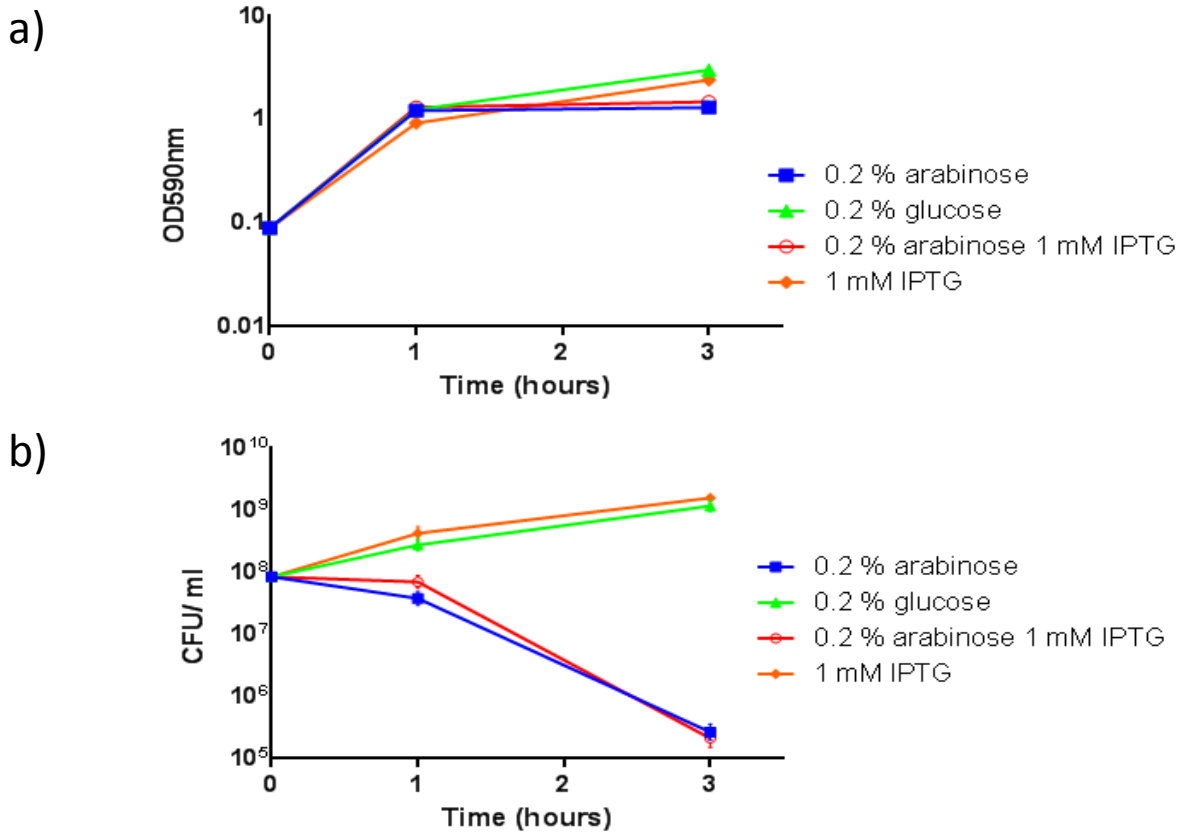

Figure 5.8: Co-expression of genes *BPSS0390* and *BPSS1061* in *E. coli ΔhipBA* pBAD/his-*BPSS0390* pME6032-*BPSS1061*. a) Change in OD; b) change in number of culturable cells after induction of either toxin expression (arabinose), or toxin and antitoxin expression (arabinose and IPTG), or antitoxin expression (IPTG) or repression of toxin expression (glucose) in cultures of *E. coli* MG1655 Δ*hipBA* harbouring pBAD/his-*BPSS0390* and pME6032-*BPSS1061* . Data shown represents three biological repeats and error bars represent SEM.

5.4.3 Co-expression of BPSS0390 with BPSS1583 (homologous to hipB)

E. coli MG1655 Δ*hipBA* pME6032-*BPSS1583* competent cells were transformed with pBAD/his-*BPSS0390* by heat shock and transformants selected by plating onto LB agar plates with ampicillin (100 µg/ml), tetracycline (15 µg/ml) and glucose (2% (w/v)).

E. coli MG1655 Δ*hipBA* pBAD/his-*BPSS0390* pME6032-*BPSS1583* culture was grown until early log phase (OD_{590} ~ 0.1) before being split and supplemented with either arabinose (final concentration of 0.2% (w/v)) or arabinose and IPTG (final concentration 1mM) or IPTG only (final concentration 1mM) or glucose (final concentration of 0.2% (w/v)). The OD and number of culturable cells were monitored for three hours (Figure 5.9)

Induction of toxin BPSS0390 expression resulted in a rapid decrease in the number of culturable cells, whereas both glucose repression and antitoxin only expression (IPTG) resulted in an increase in culturable cells and growth rate. However, co-expression of BPSS0390 and BPSS1583 (arabinose and IPTG) resulted in a rapid decrease in the number of culturable cells, similar to the toxin-only control. This suggests that in this assay, antitoxin BPSS1583 was not able to neutralise toxin BPSS0390.

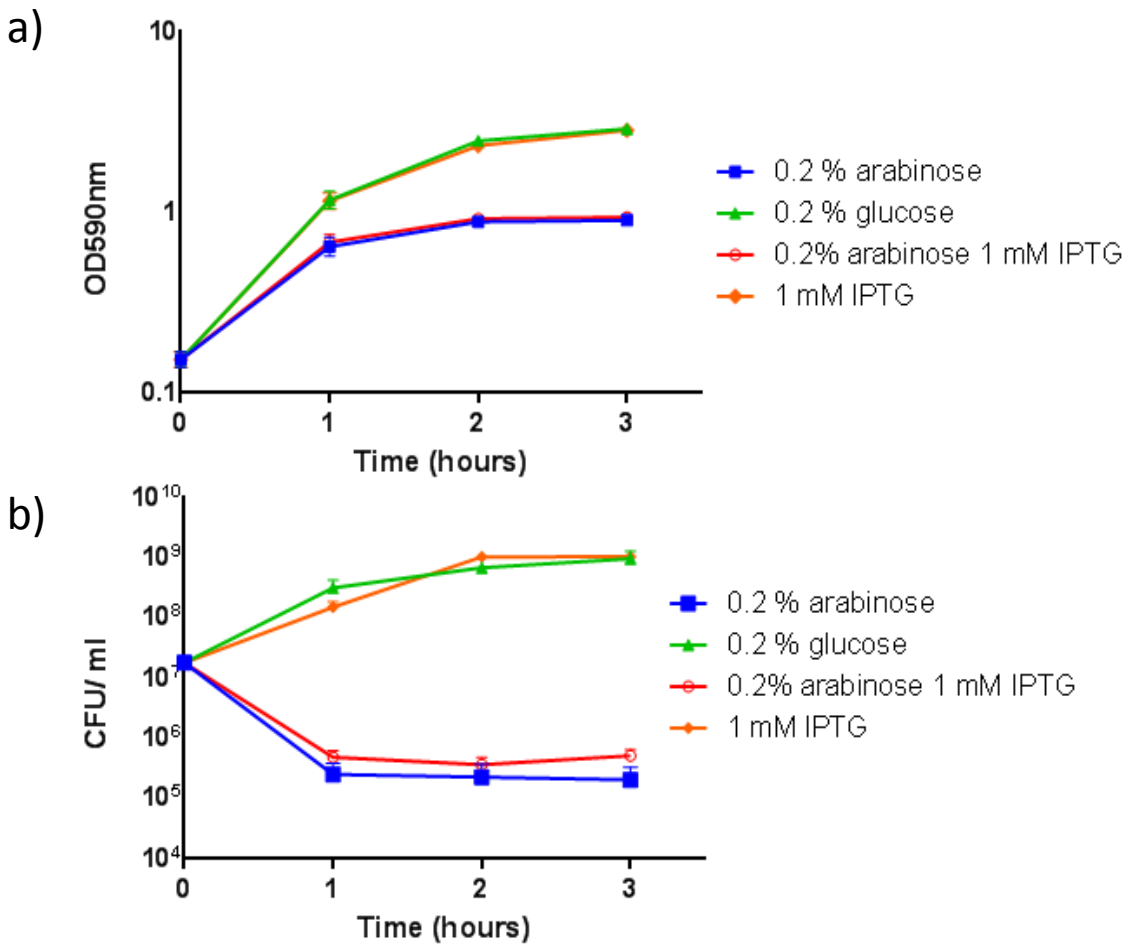

Figure 5.9: Co-expression of genes *BPSS0390* and *BPSS1583* in *E. coli ΔhipBA* pBAD/his-*BPSS0390* pME6032-*BPSS1583.* a) Change in OD ; b) change in number of culturable cells after induction of either toxin expression (arabinose), or toxin and antitoxin expression (arabinose and IPTG), or antitoxin expression (IPTG) or repression of toxin expression (glucose) in cultures of *E. coli* MG1655 Δ*hipBA* harbouring pBAD/his-*BPSS0390* and pME6032-*BPSS1583* . Data shown represents three biological repeats and error bars represent SEM.

5.5 Co-expression of antitoxin gene *BPSS0391* (homologous with *hicB*) with *BPSS1584* (homologous to *hipA*)

E. coli MG1655 Δ*hipBA* pME6032-*BPSS0391* competent cells were transformed with pBAD/his-*BPSS1584* by heat shock and transformants selected by plating onto LB agar plates with ampicillin (100 µg/ml), tetracycline (15 µg/ml) and glucose (2%(w/v)).

E. coli MG1655 Δ*hipBA* pBAD/his-*BPSS1584* pME6032-*BPSS0391* culture was grown until early log phase (OD_{590} ~ 0.1) before being split and supplemented with either arabinose (final concentration of 0.2% (w/v)) or arabinose and IPTG (final concentration 1mM) or IPTG only (final concentration 1mM) or glucose (final concentration of 0.2% (w/v)). The OD and number of culturable cells were monitored for three hours (Figure 5.10)

Repression of toxin BPSS1584 expression resulted in over a 10-fold increase in the number of culturable cells and the cells continued to grow. Induction of antitoxin BPSS0391 also allowed an over 10-fold increase in the number of culturable cells. However, induction of toxin BPSS1584 expression resulted in a 10-fold decrease in the number of culturable cells, as did induction of both toxin BPSS1583 and antitoxin BPSS0391 suggesting that antitoxin BPSS0391 was not able to neutralise BPSS1583 in this assay.

a)

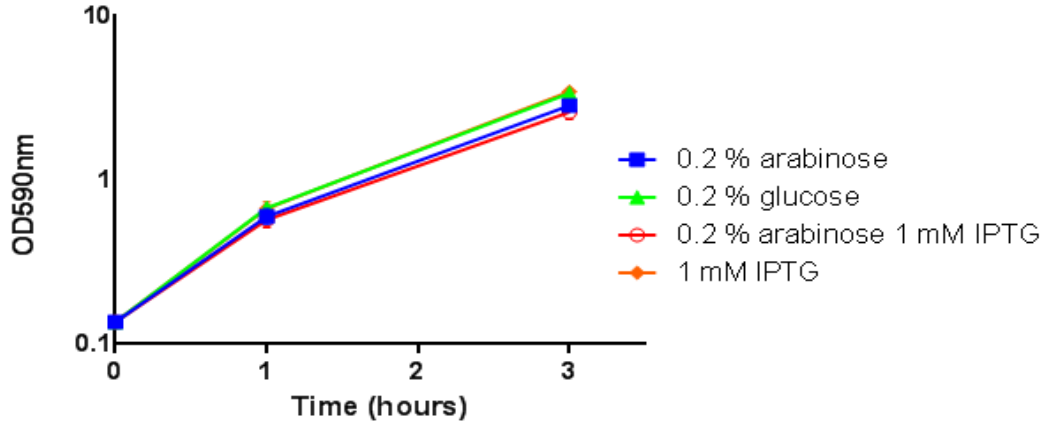

b)

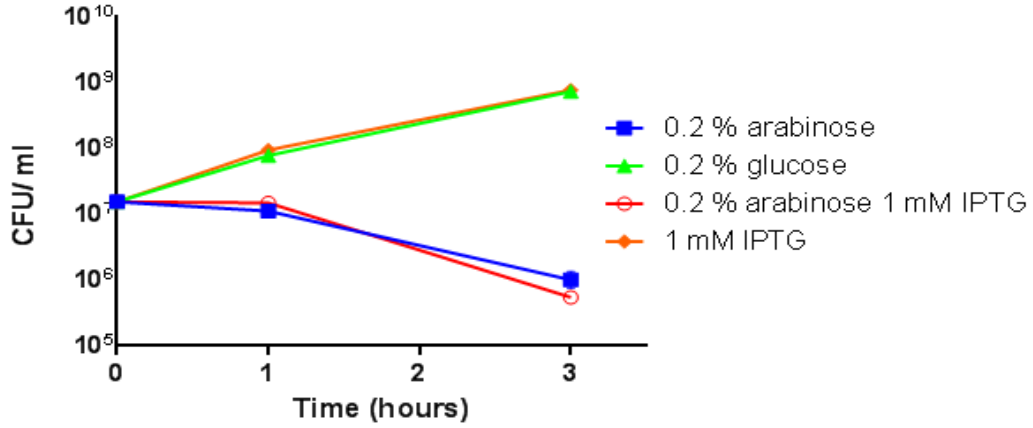

Figure 5.10: Co-expression of genes *BPSS1584* and *BPSS0391* in *E. coli ΔhipBA* pBAD/his-*BPSS1584* pME6032-*BPSS0391*. a) Change in OD; b) change in number of culturable cells after either: induction of toxin expression (arabinose), or toxin and antitoxin expression (arabinose and IPTG), or antitoxin expression (IPTG) or repression of toxin expression (glucose) in cultures of *E. coli* MG1655 Δ*hipBA* harbouring pBAD/his-*BPSS1584* and pME6032-*BPSS0391*. Data shown represents three biological repeats and error bars represent SEM.

5.6 Co-expression of toxin genes from one system with antitoxin genes from a different system but the same family

5.6.1. Co-expression of *BPSL0175* (homologous to *relE*) and *BPSS1061* (homologous to *relB*)

E. coli MG1655 Δ*hipBA* pME6032-*BPSS1061* competent cells were transformed with pBAD/his-*BPSL0175* by heat shock and transformants selected by plating onto LB agar plates with ampicillin (100 µg/ml), tetracycline (15 µg/ml) and glucose (2% (w/v)). A culture of *E. coli* MG1655 Δ*hipBA* pBAD/his-*BPSL0175 pME6032-BPSS1061* was grown until an early log phase (OD_{590} ~ 0.1) and the culture split. Cultures were supplemented with either: arabinose (final concentration of 0.2% (w/v)) to induce toxin expression, or glucose (final concentration of 0.2% (w/v)) to repress toxin expression or IPTG (final concentration 1mM) to induce antitoxin expression, or arabinose and IPTG to induce toxin and antitoxin expression. Changes in OD and culturable cells were monitored over three hours (Figure 5.11).

When BPSL0175 toxin expression was repressed, there was a 10-fold increase in both the OD and the number of culturable cells. Addition of only IPTG resulted in growth similar to glucose-repression. Induction of BPSL0175 expression resulted in a smaller increase in the number of culturable cells. When both BPSL0175 and BPSS1061 expression was induced there was a slight increase in the number of culturable cells, similar to the toxin only control.

a)

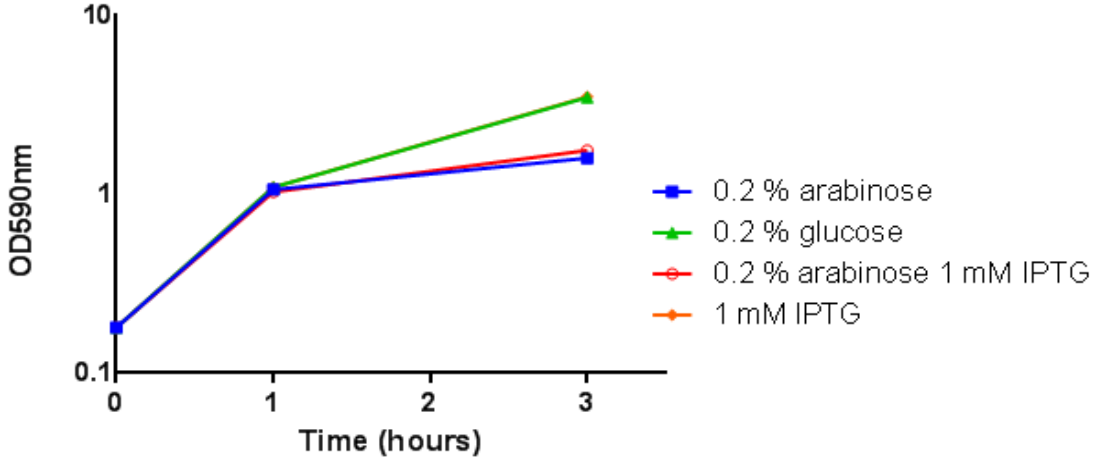

b)

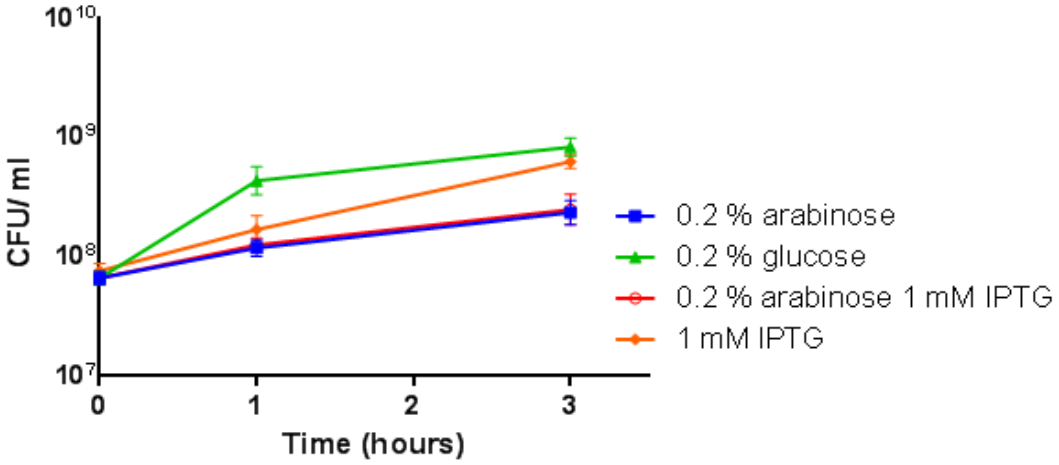

Figure 5.11: Co-expression of genes *BPSL0175* and *BPSS1061* in *E. coli ΔhipBA* pBAD/his-*BPSL0175* pME6032-*BPSS1061*. a) Change in OD; b) change in number of culturable cells after induction of either toxin expression (arabinose), or toxin and antitoxin expression (arabinose and IPTG), or antitoxin expression (IPTG) or repression of toxin expression (glucose) in cultures of *E. coli* MG1655 Δ*hipBA* harbouring pBAD/his-*BPSL0175* and pME6032-*BPSS1061*. Data shown represents three biological repeats and error bars represent SEM.

5.6.2 Co-expression of *BPSL0174* (homologous to *relB*) and *BPSS1060* (homologous to *relE*)

E. coli MG1655 Δ*hipBA* pME6032-*BPSL0174* competent cells were transformed with pBAD/his-*BPSS1060* by heat shock and transformants selected by plating onto LB agar plates with ampicillin (100 µg/ml), tetracycline (15 µg/ml) and glucose (2% (w/v)). A culture of *E. coli* MG1655 Δ*hipBA* pBAD/his-*BPSS1060 pME6032-BPSL0174* was grown until an early log phase (OD_{590} ~ 0.1) and the culture split and supplemented with either: arabinose (final concentration of 0.2% (w/v)) to induce toxin expression, or glucose (final concentration of 0.2% (w/v)) to repress toxin expression or IPTG (final concentration 1mM) to induce antitoxin expression, or arabinose and IPTG to induce toxin and antitoxin expression. Changes in OD and culturable cells were monitored over three hours (Figure 5.12).

Repression of BPSS1060 expression resulted in 10-fold increase in culturable cells and increased OD as the cells continued to grow. When IPTG was added to induce antitoxin BPSL0174 expression, growth was also observed. Only a small increase in the number of culturable cells was observed when toxin BPSS1060 expression was induced, regardless of antitoxin BPSL0174 expression.

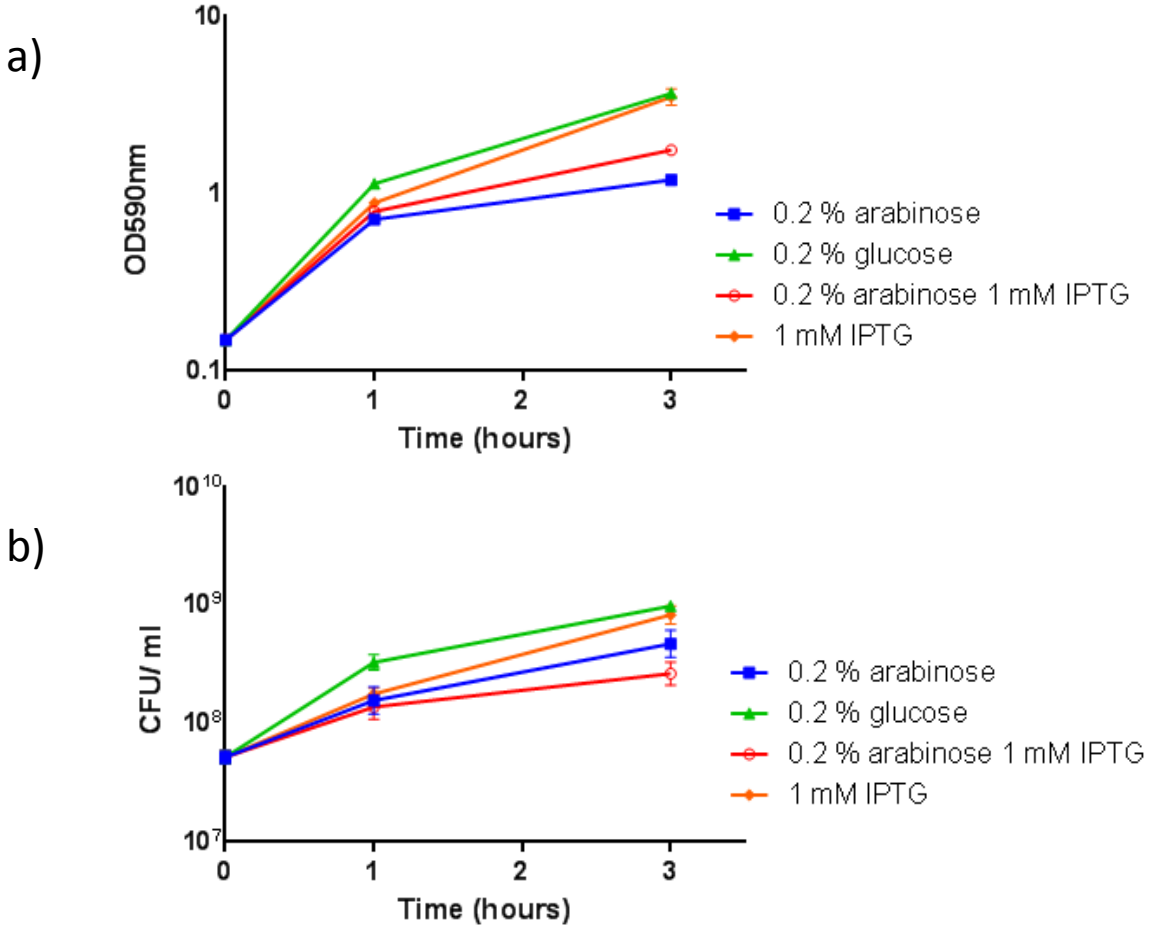

Figure 5.12: Co-expression of genes *BPSS1060* and *BPSL0174* in *E. coli ΔhipBA* pBAD/his-*BPSS1060* pME6032-*BPSL0174*. a) Change in OD; b) change in number of culturable cells after induction of either toxin expression (arabinose), or toxin and antitoxin expression (arabinose and IPTG), or antitoxin expression (IPTG) or repression of toxin expression (glucose) in cultures of *E. coli* MG1655 Δ*hipBA* harbouring pBAD/his-*BPSL0175* and pME6032-*BPSS1061* . Data shown represents three biological repeats and error bars represent SEM.

5.6 Discussion

In silico methods are frequently used to predict new TA systems, but confirmation of functionality is only possible by experimental validation (Guo et al. 2016; Bustamante et al. 2014; Zheng et al. 2015; Makarova et al. 2009). Typically, this involves over-expression of candidate toxin genes in either the native host species or in *E. coli*, and monitoring for changes in bacterial growth. Butt *et al.* (2013) designed an antibiotic- free expression system that allowed for both independent and co-expression of predicted TA genes. In this system, candidate toxin genes were cloned into the arabinose- inducible pBAD vector and candidate antitoxin genes into the IPTG inducible pME6032 vector. Toxin expression was induced by arabinose (0.2% (w/v)) and/or antitoxin expression induced by IPTG (25mM) and number of culturable cells monitored for 2 hours. When a growth phenotype was observed it was assumed that the candidate toxin had been sequestered by the candidate antitoxin. I demonstrated that the toxic phenotype associated with toxin overexpression in *E. coli* was completely abolished when media was supplemented with 25mM IPTG and so I suggest that the growth observed in the co-expression assay of Butt *et al.* (2013) was a result of IPTG inhibiting the P_{BAD} arabinose promoter and preventing toxin expression, not sequestration of the toxin by the antitoxin.

The interaction between IPTG and the P_{BAD} arabinose promoter is not well recognised and the mechanisms for this interaction are unclear. Activity from the P_{BAD} promoter is reduced in the presence of even low concentrations of IPTG, although the reduction is dependent on the relative concentrations of the two inducers within the cell (Lee et al. 2007). The P_{BAD} arabinose promoter system is regulated by dimeric AraC protein. In the absence of arabinose, AraC creates a DNA loop that prevents transcription by binding at two half sites on

the DNA. When arabinose is present, AraC is no longer able to bind to this site so releases the DNA loop, permitting transcription. The D-galactose moiety in IPTG has an identical ring structure to L-arabinose and so it is possible that IPTG could bind to AraC (Schleif 2010), although mutations in AraC that reduce IPTG inhibition are found both inside and outside the arabinose binding pocket suggesting that other parts of the IPTG molecule may also be involved (Lee et al. 2007).

To overcome this interaction it was necessary to reduce the concentration of IPTG used for induction of expression, although other groups have reported success using higher concentrations of arabinose (Coray 2014) or expression vectors that encoded IPTG- insensitive versions of AraC (Lee et al. 2007; Kasari et al. 2013).

For future work, it would be better to generate a different co-expression system to validate candidate genes. The optimised co-expression system did not allow for higher concentrations of IPTG inducer to be used to generate a greater amount of antitoxin, due to the interaction between IPTG and the P_{BAD} arabinose promoter. It was not possible to examine crosstalk between non-cognate pairs *in vivo*.

There are many limitations to generating a new system; suitable plasmids must occupy different incompatibility groups, harbour different antibiotic resistant cassettes and there can be no crosstalk between promoters and inducers. Despite this other co-expression systems could be produced: firstly the toxin and antitoxin separately and the entire TA encoding region could be cloned into separate copies of same vector (Guo et al. 2016; Yao et al. 2015). This would not allow for separate inducement of the two candidate genes but would allow

for consistent transcription in response to inducer. Secondly, both the toxin and antitoxin candidate genes could be cloned into different multiple cloning sites on a pETDuet-1 vector (Merfa et al. 2016) or into a newly generated vector containing two promoters on the same backbone (Zheng et al. 2015). Finally, existing constructs could be used to create a hybrid promoter, which would allow for more efficient transcription at lower concentrations of inducer (Comstock 1983). A reverse genetics approach, where in-frame deletions are created in each operon and candidate TA gene, could also be used to examine crosstalk between *in vivo*, although this method is limited if the antitoxins are essential to cell survival (Fiebig et al. 2010).

In this study, crosstalk was not observed between any of the non-cognate pairs of TA systems tested. It is not surprising that RelB1, RelB2 antitoxin and HipB antitoxins were not able to neutralise toxin HicA. Structurally neither RelB nor HipB are similar to HicB. RelB has a ribbon-helix-helix (RHH) at its N-terminus and associates with RelE to form an open v-shaped heterotetramer (Overgaard et al. 2009; Bøggild et al. 2012), whilst HipB also forms a heterotetramer with HipA, it binds HipA far from its active site and its interaction with DNA is via a helix -turn-helix (HTH) (Schumacher et al. 2009; Chan et al. 2016). A HicB homologue isolated from *Y. pestis* was determined to have a N-terminal domain that binds to the active site of HicA, forming a tetramer capable of binding two HicA toxin molecules, whilst the DNA binding domain was located at the C-terminus and folded as a RHH (Bibi-Triki et al. 2014). Previously there has been some reported evidence of across family interactions between VapB and MazF, and VapC and MazE, in *M. tuberculosis;* pull down experiments demonstrated physical interactions between toxins and non-cognate antitoxins. However, functional confirmation relied on a co-expression system using an arabinose-

inducible plasmid and an IPTG-inducible plasmid and so perhaps the interaction observed was between IPTG and P_{BAD} arabinose-inducible promoter rather than TA proteins (Zhu et al. 2010).

More surprising is the apparent lack of crosstalk in this study between the RelBE systems, BPSS1060-1061 and BPSL0174-0175, two systems considered paralogous with 98% identity (Butt 2013). With such high similarity, it would be expected that an antitoxin from one system would be able to neutralise the toxin from a second system. Indeed, non-cognate interactions within the same family have previously been observed in pathogenic *E. coli* O157:H7, which has two homologues of the *ccd* TA system, one plasmid-borne, ccd_F, and one located on the chromosome, ccd_{O157}. Experiments examining cross-interaction between the two systems revealed that both the chromosomally encoded toxin and the toxin encoded by the plasmid could be neutralised by the plasmid encoded antitoxin (although the chromosomal antitoxin could not sequester the plasmid encoded toxin) (Wilbaux et al. 2007). However, several studies have examined interactions between non-cognate pairs of VapB/VapC and found that neutralisation of the toxin was only possible using the cognate pair (Ramage et al. 2009; Ahidjo et al. 2011). One study examining interactions between non-cognate pairs of all 14 TA systems identified in *V. cholerae* concluded that there were no cross-interactions, even in non-cognate pairs within the same type II family. Almost all of these TA systems were located on a superintegron, and so the group theorised that the main role of the systems was stabilising the superintegron (Iqbal, Krin, et al. 2015). Within the *B. pseudomallei* genome, *BPSS0390-0391* is located on genomic island (GI) 15, *BPSL0174-0175* on GI2 and *BPSS1060-1061* on GI13

(Holden et al. 2004). One of the roles these TA systems may be to stabilise the *B. pseudomallei* genome.

Potential negative effects have also been linked to cross-interaction between different systems. Interaction between one antitoxin and multiple toxins from different systems would change the ratio of toxin: antitoxin leading to an excess of free toxin capable of inducing growth arrest (Park et al. 2013; Goeders & Melderen 2014). Cross-interactions have also been linked to TA system degradation (Goeders & Melderen 2014).

Alternatively, the lack of crosstalk observed between all the non-cognate pairs tested in this study might indicate that the non-cognate antitoxin was not expressed in the co-expression assay. The co-expression assay used for this study was optimised to the cognate TA system BPSS0390-BPSS0391 and concentrations of inducer could not exceed 1mM, without potentially inhibiting toxin expression. Whilst induction of toxin expression in response to the addition of arabinose was not definitively confirmed, a toxic phenotype was always observed. However, the toxic phenotype observed after co-expression of the non-cognate pair coupled with the lack of definitive confirmation of expression of the antitoxin (after addition of IPTG) undermines this study; it may be that there was no neutralisation because there was no antitoxin protein present in the assay. To validate these results, this co-expression assay should be tested using the cognate TA pairs BPSS1583-BPSS1584, BPSS1060-BPSS1061 and BPSL0174-BPSL0175. If a neutralisation phenotype (or absence of a toxic phenotype) is observed using the other cognate pairs, then it is likely that antitoxin is expressed in response to 1mM IPTG and these results are a true negative. Confirmation of expression of both the toxin and antitoxin proteins should also be sought, perhaps using quantitative real-time PCR to quantify

expression. A poly-histidine tag could also be incorporated into the antitoxin protein to allow for Western blotting but this would also require confirmation that the tag did not alter protein structures or interfere with binding affinities.

Although there is currently no evidence for protein cross-interactions between chromosomal non-cognate pairs in *B. pseudomallei* K96423, there is evidence to suggest that TA systems may form networks that facilitate adaption to the host environment. In *Enterococcus faecalis*, MazE and MazEF (type II system) function as autorepressors and activate RatA, the antitoxin in the type I TA system *txpS-ratA* (Wessner et al. 2015). Type II TA toxins can trans-activate other TA systems by relieving transcriptional regulation and degrading freshly generated antitoxin encoding mRNA (Wang et al. 2014; Kasari et al. 2013).

Chapter 6: Summary

This study had three broad aims: to evaluate *B. pseudomallei* toxin BPSS0390 as a potential antimicrobial compound, to identify residues in BPSS0390 involved in toxicity and BPSS0390-BPSS0391 complex formation and to determine if TA antitoxins in *B. pseudomallei* can neutralise non-cognate toxins from different type II systems to form a co-operative network.

Induction of expression of toxin BPSS0390 in all of the species tested resulted in a decrease in the number of culturable cells. Even in species with partial antitoxin homologues this decrease was remarkable (2 log and 3 log). In *B. thailandensis,* the activity of BPSS0390 was lowered, likely due to the presence of a homologue with 99% identity. Induction of expression of BPSS0390 in *E. coli* resulted in the formation of escape mutants, unless expression was actively repressed.

Site-directed mutagenesis of BPSS0390 identified 20 residues required for toxicity in *E. coli*. Most of these residues are undoubtedly critical for maintaining correct folding of the protein. The structure of the dsRBD like fold of BPSS0390 closely resembled the canonical dsRBD of many other proteins. It was interesting that none of the lysines in the BPSS0390 molecule were critical for function. It was disappointing that no residues involved in TA complex formation could be identified, but not unexpected. BPSS0390 is a small molecule and typically TA antitoxins bind toxins at the active site (M. a Schumacher et al. 2009) so any molecules required for toxicity may be required for antitoxin binding also.

Finally, there was no interaction between BPSS0390 and any non-cognate antitoxin. No interactions were observed between any of the non-cognate pairs tested. This is no surprising as TA systems rely on specificity for many of their

biological putative functions. However, this study did highlight the need for improved tools for examining interactions between TA components.

Bibliography

Aakre, C. et al., 2013. A Bacterial Toxin Inhibits DNA Replication Elongation Through a Direct Interaction with the β Sliding Clamp. *Mol Cell.*, 52(5), pp.617–628.

Van Acker, H. et al., 2014. Involvement of toxin-antitoxin modules in Burkholderia cenocepacia biofilm persistence. *Pathogens and Disease*, 71(3), pp.326–335.

Afif, H. et al., 2001. The ratio between CcdA and CcdB modulates the transcriptional repression of the ccd poison-antidote system. *Molecular Microbiology*, 41(1), pp.73–82.

Ahidjo, B.A. et al., 2011. VapC Toxins from Mycobacterium tuberculosis Are Ribonucleases that Differentially Inhibit Growth and Are Neutralized by Cognate VapB Antitoxins. , 6(6).

Allocati, N. et al., 2015. Die for the community: an overview of programmed cell death in bacteria. *Cell death & disease*, 6(1), p.e1609. Available at: http://www.scopus.com/inward/record.url?eid=2-s2.0-84927593954&partnerID=tZOtx3y1 [Accessed November 1, 2015].

Amadasi S, Dal Zoppo S, Bonomini A, et al., 2014. A Case of Melioidosis Probably Acquired by Inhalation of Dusts During a Helicopter Flight in a Healthy Traveler Returning From Singapore. *J Travel Med*.

Amornchai, P. et al., 2007. Accuracy of Burkholderia pseudomallei Identification Using the API 20NE System and a Latex Agglutination Test □. , 45(11), pp.3774–3776.

Anantharaman, V. & Aravind, L., 2003. New connections in the prokaryotic toxin-antitoxin network: relationship with the eukaryotic nonsense-mediated

RNA decay system. *Genome biology*, 4(12), p.R81. Available at: http://www.ncbi.nlm.nih.gov/pubmed/14659018%5Cnhttp://www.pubmedcentral.nih.gov/articlerender.fcgi?artid=PMC329420.

Audoly, G. et al., 2011. Effect of rickettsial toxin vapC on its eukaryotic host. *PLoS ONE*, 6(10).

Barbara, K. & Hayes, F., 2016. Emerging Roles of Toxin-Antitoxin Modules in Bacterial Pathogenesis.

Barraud, P. et al., 2012. Solution structure of the N-terminal dsRBD of Drosophila ADAR and interaction studies with RNA. *Biochimie*, 94(7), pp.1499–1509.

Belitsky, M. et al., 2011. The Escherichia coli Extracellular Death Factor EDF Induces the Endoribonucleolytic Activities of the Toxins MazF and ChpBK. *Molecular Cell*, 41(6), pp.625–635. Available at: http://dx.doi.org/10.1016/j.molcel.2011.02.023.

Bernard, P. et al., 1993. The F plasmid CcdB protein induces efficient ATP-dependent DNA cleavage by gyrase. *Journal of molecular biology*, 234(3), pp.534–541.

Bertram, R. & Schuster, C.F., 2014. Post-transcriptional regulation of gene expression in bacterial pathogens by toxin-antitoxin systems. *Frontiers in cellular and infection microbiology*, 4(January), p.6. Available at: http://www.pubmedcentral.nih.gov/articlerender.fcgi?artid=3905216&tool=pmcentrez&rendertype=abstract.

Bibi-Triki, S. et al., 2014. Functional and structural analysis of HicA3-HicB3, a novel toxin-antitoxin system of Yersinia pestis. *Journal of bacteriology*, 196(21), pp.3712–23. Available at: http://www.scopus.com/inward/record.url?eid=2-s2.0-

84907842145&partnerID=tZOtx3y1 [Accessed December 21, 2015].

Bigger, J.W., 1944. Treatment of staphylococcal infections with penicillin. *The Lancet*, 244(6320), pp.497–500.

Blaszczyk, J. et al., 2004. Noncatalytic assembly of ribonuclease III with double-stranded RNA. *Structure.*, 12((3)), p.457–466.

Bloom-Ackermann, Z. et al., 2016. Toxin-Antitoxin systems eliminate defective cells and preserve symmetry in Bacillus subtilis biofilms. *Environmental Microbiology*.

Blower, T.R. et al., 2011. A processed noncoding RNA regulates an altruistic bacterial antiviral system. *Nature Structural & Molecular Biology*, 18(2), pp.185–190. Available at: http://www.nature.com/doifinder/10.1038/nsmb.1981.

Blower, T.R., Short, F.L., et al., 2012. Identification and classification of bacterial Type III toxin-antitoxin systems encoded in chromosomal and plasmid genomes. *Nucleic Acids Research*, 40(13), pp.6158–6173.

Blower, T.R., Evans, T.J., et al., 2012. Viral Evasion of a Bacterial Suicide System by RNA-Based Molecular Mimicry Enables Infectious Altruism. *PLoS Genetics*, 8(10).

Blower, T.R. et al., 2014. Viral molecular mimicry circumvents abortive infection and suppresses bacterial suicide to make hosts permissive for replication. *Bacteriophage*, 2(4), p.e23830. Available at: http://www.pubmedcentral.nih.gov/articlerender.fcgi?artid=3594212&tool=pmcentrez&rendertype=abstract.

Blower, T.R., Salmond, G.P.C. & Luisi, B.F., 2011. Balancing at survival's edge: The structure and adaptive benefits of prokaryotic toxin-antitoxin partners. *Current Opinion in Structural Biology*, 21(1), pp.109–118. Available at:

http://dx.doi.org/10.1016/j.sbi.2010.10.009.

Boggild, A. et al., 2012. The crystal structure of the intact E. coli RelBE toxin-antitoxin complex provides the structural basis for conditional cooperativity. *Structure*, 20(10), pp.1641–1648.

Bøggild, A. et al., 2012. Short Article The Crystal Structure of the Intact E . coli RelBE Toxin-Antitoxin Complex Provides the Structural Basis for Conditional Cooperativity. *Structure/Folding and Design*, 20(10), pp.1641–1648. Available at: http://dx.doi.org/10.1016/j.str.2012.08.017.

Botelho-nevers, E. et al., 2012. Deleterious effect of ciprofloxacin on Rickettsia conorii-infected cells is linked to toxin-antitoxin module up-regulation. *Journal of Antimicrobial Chemotherapy*, 67(7), pp.1677–1682.

Brantl, S., 2012. Bacterial type I toxin-antitoxin systems. *RNA biology*, 9(12), pp.1488–90. Available at: http://www.mendeley.com/research-papers/search/?query=Bacterial+type+I+toxin-antitoxin+systems.

Brantl, S. & Jahn, N., 2015. SRNAs in bacterial type I and type III toxin-antitoxin systems. *FEMS Microbiology Reviews*, 39(3), pp.413–427.

Brombacher, E. et al., 2006. Gene expression regulation by the curli activator CsgD protein: Modulation of cellulose biosynthesis and control of negative determinants for microbial adhesion. *Journal of Bacteriology*, 188(6), pp.2027–2037.

Brown, J.S. et al., 2004. A Locus Contained within A Variable Region of Pneumococcal Pathogenicity Island 1 Contributes to Virulence in Mice. *Infection and Immunity*, 72(3), pp.1587–1593.

Bustamante, P., Tello, M. & Orellana, O., 2014. Toxin-Antitoxin Systems in the Mobile Genome of Acidithiobacillus ferrooxidans. , 9(11).

Butt, A. et al., 2013. Identification of type II toxin-antitoxin modules in

Burkholderia pseudomallei. *FEMS microbiology letters*, 338(1), pp.86–94. Available at: http://www.ncbi.nlm.nih.gov/pubmed/23082999.

Butt, A. et al., 2014. The HicA toxin from Burkholderia pseudomallei has a role in persister cell formation. *The Biochemical journal*, 459(2), pp.333–44. Available at: http://www.pubmedcentral.nih.gov/articlerender.fcgi?artid=3969222&tool=pmcentrez&rendertype=abstract.

Butt, A.T., 2013. *Identification and characterisation of toxin-antitoxin systems (TA) in Burkholderia pseudomallei Submitted by Aaron Trevor Butt to the University of Exeter*.

Bycroft, M. et al., 1995. NMR solution structure of a dsRNA binding domain from Drosophila staufen protein reveals homology to the N-terminal domain of ribosomal protein S5. *The EMBO journal*, 14(14), pp.3563–71. Available at: http://www.ncbi.nlm.nih.gov/pmc/articles/PMC394424/pdf/emboj00038-0285.pdf%5Cnhttp://www.ncbi.nlm.nih.gov/pubmed/7628456%5Cnhttp://www.pubmedcentral.nih.gov/articlerender.fcgi?artid=PMC394424.

Cardona, S.T. & Valvano, M.A., 2005. An expression vector containing a rhamnose-inducible promoter provides tightly regulated gene expression in Burkholderia cenocepacia. *Plasmid*, 54(3), pp.219–28. Available at: http://www.sciencedirect.com/science/article/pii/S0147619X05000302 [Accessed February 8, 2016].

Castrignanò, T. et al., 2002. Molecular dynamics simulation of the RNA complex of a double-stranded RNA-binding domain reveals dynamic features of the intermolecular interface and its hydration. *Biophys J*, 83(6), pp.3542–52. Available at: http://www.sciencedirect.com.gate1.inist.fr/science/article/pii/S0006349502

75354X.

Cataudella, I. et al., 2013. Conditional Cooperativity of Toxin - Antitoxin Regulation Can Mediate Bistability between Growth and Dormancy. *PLoS Computational Biology*, 9(8).

Chan, W.T., Balsa, D. & Espinosa, M., 2015. One cannot rule them all: Are bacterial toxins-antitoxins druggable? *FEMS microbiology reviews*, 39(4), pp.522–40. Available at: http://www.scopus.com/inward/record.url?eid=2-s2.0-84940007260&partnerID=tZOtx3y1 [Accessed December 16, 2015].

Chan, W.T., Espinosa, M. & Yeo, C.C., 2016. Keeping the Wolves at Bay : Antitoxins of Prokaryotic Type II Toxin-Antitoxin Systems. , 3(March), pp.1–20.

Chang, K.Y. & Ramos, A., 2005. The double-stranded RNA-binding motif, a versatile macromolecular docking platform. *FEBS Journal*, 272(9), pp.2109–2117.

Chaowagul, W, Suputtamongkol Y, Dance DA, Rajchanuvong A, Pattara-arechachai J, W.N., 1993. Relapse in melioidosis: incidence and risk factors. *J Infect Dis.*, 168((5):), p.1181–5.

Cheng, A.C. & Currie, B.J., 2005. Melioidosis: Epidemiology, pathophysiology, and management. *Clinical Microbiology Reviews*, 18(2), pp.383–416.

Chopra, N. et al., 2011. Modeling of the structure and interactions of the B. anthracis antitoxin, MoxX: Deletion mutant studies highlight its modular structure and repressor function. *Journal of Computer-Aided Molecular Design*, 25(3), pp.275–291.

Christensen-Dalsgaard, M. & Gerdes, K., 2006. Two higBA loci in the Vibrio cholerae superintegron encode mRNA cleaving enzymes and can stabilize plasmids. *Molecular Microbiology*, 62(2), pp.397–411.

Christensen, S.K. et al., 2004. Overproduction of the Lon protease triggers inhibition of translation in Escherichia coli: Involvement of the yefM-yoeB toxin-antitoxin system. *Molecular Microbiology*, 51(6), pp.1705–1717.

Christensen, S.K. et al., 2001. RelE, a global inhibitor of translation, is activated during nutritional stress. *Proceedings of the National Academy of Sciences of the United States of America*, 98(25), pp.14328–33.

Christensen, S.K. & Gerdes, K., 2003. RelE toxins from Bacteria and Archaea cleave mRNAs on translating ribosomes, which are rescued by tmRNA. *Molecular Microbiology*, 48(5), pp.1389–1400.

Chukwudi, C.U. & Good, L., 2015. The role of the hok/sok locus in bacterial response to stressfulgrowth conditions. *Microbial Pathogenesis*, 79, pp.70–79.

Comstock, J., 1983. The tac promoter: A functional hybrid derived from the. , 80(January), pp.21–25.

Cook, G.M. et al., 2013. Ribonucleases in bacterial toxin-antitoxin systems. *Biochimica et Biophysica Acta - Gene Regulatory Mechanisms*, 1829(6–7), pp.523–531. Available at: http://dx.doi.org/10.1016/j.bbagrm.2013.02.007.

Cooper, T.F. & Heinemann, J.A., 2000. Postsegregational killing does not increase plasmid stability but acts to mediate the exclusion of competing plasmids. *Proceedings of the National Academy of Sciences of the United States of America*, 97(23), pp.12643–8. Available at: http://www.pubmedcentral.nih.gov/articlerender.fcgi?artid=18817&tool=pmcentrez&rendertype=abstract.

Cooper, T.F., Paixão, T. & Heinemann, J. a, 2010. Within-host competition selects for plasmid-encoded toxin-antitoxin systems. *Proceedings. Biological sciences / The Royal Society*, 277(1697), pp.3149–55. Available

at:
http://www.pubmedcentral.nih.gov/articlerender.fcgi?artid=2982069&tool=pmcentrez&rendertype=abstract.

Coray, 2014. *The potential for toxin and antitoxin gene pairs to display a post-segregational killing phenotype, with regards to the ecology of mobile elements.*

Currie, B.J., 2015. Melioidosis: Evolving Concepts in Epidemiology, Pathogenesis, and Treatment. *Semin Respir Crit Care Med*, 36(1), pp.111–125.

Currie, B.J., Ward, L. & Cheng, A.C., 2010. The Epidemiology and Clinical Spectrum of Melioidosis : 540 Cases from the 20 Year Darwin Prospective Study. , 4(11).

Dance, D., 2014. Treatment and prophylaxis of melioidosis. *International Journal of Antimicrobial Agents*, 43(4), pp.310–318.

Darfeuille, F. et al., 2007. An Antisense RNA Inhibits Translation by Competing with Standby Ribosomes. *Molecular Cell*, 26(3), pp.381–392.

Diago-Navarro, E. et al., 2013. Cleavage of the antitoxin of the parD toxin-antitoxin system is determined by the ClpAP protease and is modulated by the relative ratio of the toxin and the antitoxin. *Plasmid*, 70(1), pp.78–85.

Diago-Navarro, E. et al., 2010. ParD toxin-antitoxin system of plasmid R1 - Basic contributions, biotechnological applications and relationships with closely-related toxin-antitoxin systems. *FEBS Journal*, 277(15), pp.3097–3117.

Dickerson, R.E. et al., 1982. The anatomy of A-, B-, and Z-DNA. *Science*, 216(4545), p.475 LP-485. Available at: http://science.sciencemag.org/content/216/4545/475.abstract.

Drusin, S.I. et al., 2016. dsRNA-protein interactions studied by molecular dynamics techniques. Unravelling dsRNA recognition by DCL1. *Archives of Biochemistry and Biophysics*, 596, pp.118–125. Available at: http://linkinghub.elsevier.com/retrieve/pii/S0003986116300650.

Durand, S. et al., 2012. Type I toxin-antitoxin systems in Bacillus subtilis. *RNA Biology*, 9(12), pp.1491–1497. Available at: http://www.tandfonline.com/doi/abs/10.4161/rna.22358.

Eaton, S.L. et al., 2014. A Guide to Modern Quantitative Fluorescent Western Blotting with Troubleshooting Strategies. *J. Vis. Exp.*, (93)(10.3791/52099 .), p.e52099.

Egan, E.S., Fogel, M.A. & Waldor, M.K., 2005. Divided genomes: Negotiating the cell cycle in prokaryotes with multiple chromosomes. *Molecular Microbiology*, 56(5), pp.1129–1138.

Famulla, K. et al., 2016. Acyldepsipeptide antibiotics kill mycobacteria by preventing the physiological functions of the ClpP1P2 protease. *Molecular Microbiology*, 101(2), pp.194–209.

Faridani, O.R. et al., 2006. Competitive inhibition of natural antisense Sok-RNA interactions activates Hok-mediated cell killing in Escherichia coli. *Nucleic Acids Research*, 34(20), pp.5915–5922.

Fasani, R.A. & Savageau, M.A., 2015. Unrelated toxin – antitoxin systems cooperate to induce persistence.

Fauvart, M., Groote, V.N. De & Michiels, J., 2011. Role of persister cells in chronic infections : clinical relevance and perspectives on anti-persister therapies. , (2011), pp.699–709.

Fiebig, A. et al., 2010. Interaction specificity, toxicity and regulation of a paralogous set of ParE/RelE-family toxin-antitoxin systems. *Molecular*

Microbiology, 77(1), pp.236–251.

Fineran, P.C. et al., 2009. The phage abortive infection system, ToxIN, functions as a protein-RNA toxin-antitoxin pair. *Proceedings of the National Academy of Sciences of the United States of America*, 106(3), pp.894–9. Available at: http://www.pnas.org/content/106/3/894.short.

Fozo, E.M. et al., 2010. Abundance of type I toxin-antitoxin systems in bacteria: Searches for new candidates and discovery of novel families. *Nucleic Acids Research*, 38(11), pp.3743–3759.

Fozo, E.M., 2012. New type I toxin-antitoxin families from “wild” and laboratory strains of E. coli: Ibs-Sib, ShoB-OhsC and Zor-Orz. *RNA biology*, 9(12), pp.1504–1512. Available at: http://www.landesbioscience.com/journals/rna/article/22568/%5Cnhttp://www.tandfonline.com/doi/abs/10.4161/rna.22568.

Frampton, R. et al., 2012. Toxin-antitoxin systems of Mycobacterium smegmatis are essential for cell survival. *Journal of Biological Chemistry*, 287(8), pp.5340–5356.

Fu, H. et al., 2009. Increasing protein stability by improving beta turns. *Proteins*., 77(3), pp.491–498.

Galvani, C., Terry, J. & Ishiguro, E.E., 2001. Purification of the RelB and RelE proteins of Escherichia coli: RelE binds to RelB and to ribosomes. *Journal of Bacteriology*, 183(8), pp.2700–2703.

Gan, J. et al., 2008. A stepwise model for double-stranded RNA processing by ribonuclease III. *Molecular Microbiology*, 67(1), pp.143–154.

Gan, J. et al., 2005. Intermediate states of ribonuclease III in complex with double-stranded RNA. *Structure*, 13(10), pp.1435–1442.

Gan, J. et al., 2006. Structural insight into the mechanism of double-stranded

RNA processing by ribonuclease III. *Cell*, 124(2), pp.355–366.

Gao, Y. et al., 2013. Inducible cell lysis systems in microbial production of bio-based chemicals. *Applied Microbiology and Biotechnology*, 97(16), pp.7121–7129.

Garcia-Pino, A. et al., 2010. Allostery and Intrinsic Disorder Mediate Transcription Regulation by Conditional Cooperativity. *Cell*, 142(1), pp.101–111.

Gelens, L. et al., 2013. A General Model for Toxin-Antitoxin Module Dynamics Can Explain Persister Cell Formation in E. coli. *PLoS Computational Biology*, 9(8).

Georgiades, K. & Raoult, D., 2011. Genomes of the most dangerous epidemic bacteria have a virulence repertoire characterized by fewer genes but more toxin-antitoxin modules. *PLoS ONE*, 6(3).

Gerdes, K., Christensen, S.K. & Lobner-Olesen, A., 2005. Prokaryotic toxin-antitoxin stress response loci. *Nat Rev Micro*, 3(5), pp.371–382. Available at: http://dx.doi.org/10.1038/nrmicro1147.

Gerdes, K., Christensen, S.K. & Løbner-Olesen, A., 2005. Prokaryotic toxin-antitoxin stress response loci. *Nature Reviews. Microbiology*, 3(5), pp.371–382.

Gerdes, K., Larsen, J.E.L. & Molin, S., 1985. Stable inheritance of plasmid R1 requires two different loci. *Journal of Bacteriology*, 161(1), pp.292–298.

Gerdes, K. & Maisonneuve, E., 2012. Bacterial Persistence and Toxin-Antitoxin Loci. *Annual Review of Microbiology*, 66(1), pp.103–123.

Gerdes, K., Rasmussen, P.B. & Molin, S., 1986. Unique type of plasmid maintenance function: postsegregational killing of plasmid-free cells. *Proceedings of the National Academy of Sciences of the United States of*

America, 83(10), pp.3116–3120.

Gerdes, K. & Wagner, E.G.H., 2007. RNA antitoxins. *Current Opinion in Microbiology*, 10(2), pp.117–124.

Germain, E. et al., 2013. Molecular Mechanism of Bacterial Persistence by HipA. *Molecular Cell*, 52(2), pp.248–254.

Germain, E. et al., 2015. Stochastic induction of persister cells by HipA through (p)ppGpp-mediated activation of mRNA endonucleases. *Proceedings of the National Academy of Sciences of the United States of America*, 112(16), pp.5171–6. Available at: http://www.pubmedcentral.nih.gov/articlerender.fcgi?artid=4413331&tool=pmcentrez&rendertype=abstract.

Getahun, H. et al., 2015. Latent Mycobacterium tuberculosis Infection. *New England Journal of Medicine*, 372(22), pp.2127–2135. Available at: http://dx.doi.org/10.1056/NEJMra1405427.

Ghafourian, S. et al., 2014. The mazEF toxin-antitoxin system as a novel antibacterial target in Acinetobacter baumannii. *Memorias do Instituto Oswaldo Cruz*, 109(4), pp.502–505.

Ghafourian, S. & Raftari, M., 2012. Toxin-antitoxin Systems : Classification , Biological Function and Application in Biotechnology. , (Figure 2), pp.9–14.

Goeders, N. & Melderen, L. Van, 2014. Toxin-Antitoxin Systems as Multilevel Interaction Systems. , pp.304–324.

González Barrios, A.F. et al., 2006. Autoinducer 2 controls biofilm formation in Escherichia coli through a novel motility quorum-sensing regulator (MqsR, B3022). *Journal of Bacteriology*, 188(1), pp.305–316.

Gotfredsen, M. & Gerdes, K., 1998. The Escherichia coli relBE genes belong to a new toxin-antitoxin gene family. *Molecular Microbiology*, 29(4), pp.1065–

1076.

Green, S.R., Manche, L. & Mathews, M.B., 1995. Two functionally distinct RNA-binding motifs in the regulatory domain of the protein kinase DAI. *Mol Cell Biol*, 15(1), pp.358–364. Available at: http://www.ncbi.nlm.nih.gov/entrez/query.fcgi?cmd=Retrieve&db=PubMed&dopt=Citation&list_uids=7799944.

Green, S.R. & Mathews, M.B., 1992. Two RNA-binding motifs in the double-stranded RNA-activated protein kinase, DAI. *Genes and Development*, 6(12 PART B), pp.2478–2490.

Guglielmini, J. & Van Melderen, L., 2011. Bacterial toxin-antitoxin systems. *Mobile Genetic Elements*, 1(4), pp.283–306. Available at: http://www.tandfonline.com/doi/abs/10.4161/mge.18477.

Guglielmini, J. & Van Melderen, L., 2011. Bacterial toxin-antitoxin systems: Translation inhibitors everywhere. *Mob. Genet. Elements*, 1, pp.283–290.

Guo, Y. et al., 2016. Characterization of the Deep-Sea Streptomyces sp. SCSIO 02999 Derived VapC/VapB Toxin-Antitoxin System in Escherichia coli.

Guo, Y. et al., 2014. RalR (a DNase) and RalA (a small RNA) form a type I toxin-antitoxin system in Escherichia coli. *Nucleic Acids Research*, 42(10), pp.6448–6462.

Gurnev, P.A. et al., 2012. Persister-promoting bacterial toxin TisB produces anion-selective pores in planar lipid bilayers. *FEBS Letters*, 586(16), pp.2529–2534.

Hall-Stoodley, L., Costerton, J. & Stoodley, P., 2004. Bacterial biofilms: from the natural environment to infectious diseases. *Nature Reviews. Microbiology*, 2(February), pp.95–108.

Hamilton, B. et al., 2014. Analysis of non-typeable haemophilous influenzae

vapc1 mutations reveals structural features required for toxicity and flexibility in the active site. *PLoS ONE*, 9(11).

Hargreaves, D. et al., 2002. Structural and functional analysis of the kid toxin protein from E. coli plasmid R1. *Structure*, 10(10), pp.1425–1433.

Harrison, J.J. et al., 2009. The chromosomal toxin gene yafQ is a determinant of multidrug tolerance for Escherichia coli growing in a biofilm. *Antimicrobial Agents and Chemotherapy*, 53(6), pp.2253–2258.

Hartman, E. et al., 2013. Intrinsic dynamics of an extended hydrophobic core in the S. cerevisiae RNase III dsRBD contributes to recognition of specific RNA binding sites. *Journal of Molecular Biology*, 425(3), pp.546–562. Available at: http://dx.doi.org/10.1016/j.jmb.2012.11.025.

Hazan, R. & Engelberg-Kulka, H., 2004. Escherichia coli mazEF-mediated cell death as a defense mechanism that inhibits the spread of phage P1. *Molecular Genetics and Genomics*, 272(2), pp.227–234.

Hazan, R., Sat, B. & Engelberg-Kulka, H., 2004. Escherichia coli mazEF-mediated cell death is triggered by various stressful conditions. *Journal of Bacteriology*, 186(11), pp.3663–3669.

Helaine, S. & Kugelberg, E., 2014. Bacterial persisters: Formation, eradication, and experimental systems. *Trends in Microbiology*, 22(7), pp.417–424.

Hernández-arriaga, A.N.A.M. et al., 2014a. Conditional Activation of Toxin-Antitoxin Systems : Postsegregational Killing and Beyond. , pp.1–17.

Hernández-arriaga, A.N.A.M. et al., 2014b. Conditional Activation of Toxin-Antitoxin Systems : Postsegregational Killing and Beyond. *Microbiology spectrum*, pp.1–17.

Hino, M. et al., 2014. Characterization of putative toxin/antitoxin systems in Vibrio parahaemolyticus. *Journal of Applied Microbiology*, 117(1), pp.185–

195.

Hobby, G.L., Meyer, K. & Chaffee, E., 1942. Observations on the Mechanism of Action of Penicillin. *Experimental Biology and Medicine*, 50(2), pp.281–285. Available at: http://ebm.sagepub.com/lookup/doi/10.3181/00379727-50-13773.

Holden, D.W. et al., 2004. Genomic plasticity of the causative agent of melioidosis , Burkholderia pseudomallei. , 101(39).

Houghton, R.L. et al., 2014. Development of a Prototype Lateral Flow Immunoassay (LFI) for the Rapid Diagnosis of Melioidosis. , 8(3).

Huang, Y. et al., 2009. Structural insights into mechanisms of the small RNA methyltransferase HEN1. *Nature*, 461(7265), pp.823–7. Available at: http://dx.doi.org/10.1038/nature08433%5Cnhttp://www.ncbi.nlm.nih.gov/pubmed/19812675.

Hurley, J.M. & Woychik, N.A., 2009. Bacterial toxin HigB associates with ribosomes and mediates translation-dependent mRNA cleavage at A-rich sites. *Journal of Biological Chemistry*, 284(28), pp.18605–18613.

Huys, I. et al., 2013. Paving a regulatory pathway for phage therapy. Europe should muster the resources to financially, technically and legally support the introduction of phage therapy. *EMBO reports*, 14(11), pp.951–4. Available at: http://www.scopus.com/inward/record.url?eid=2-s2.0-84887108922&partnerID=tZOtx3y1.

Inglis TJ et al., 2000. Burkholderia pseudomallei traced to water treatment plant in Australia. *Emerg Infect Dis*, 6((1)), pp.56–59.

Iqbal, N., Guérout, A.-M., et al., 2015. Comprehensive functional analysis of the eighteen\n Vibrio cholerae\n N16961 toxin-antitoxin systems substantiates their role in stabilizing the superintegron. *Journal of*

Bacteriology, 197(13), p.JB.00108-15. Available at: http://jb.asm.org/lookup/doi/10.1128/JB.00108-15.

Iqbal, N., Krin, E. & Mazel, D., 2015. Comprehensive Functional Analysis of the 18 Vibrio cholerae N16961 Toxin-Antitoxin Systems Substantiates Their Role in Stabilizing the. , 197(13), pp.2150–2159.

Jaffe, A., Ogura, T. & Hiraga, S., 1985. Effects of the ccd function of the F plasmid on bacterial growth. *Journal of Bacteriology*, 163(3), pp.841–849.

Jahn, N. & Brantl, S., 2013. One antitoxin-two functions: SR4 controls toxin mRNA decay and translation. *Nucleic Acids Research*, 41(21), pp.9870–9880.

Jalava, K. et al., 2006. An Outbreak of Gastrointestinal Illness and Erythema Nodosum from Grated Carrots Contaminated with Yersinia pseudotuberculosis. *Journal of Infectious Diseases* , 194(9), pp.1209–1216. Available at: http://jid.oxfordjournals.org/content/194/9/1209.abstract.

Johnson, E.P., Ström, A.R. & Helinski, D.R., 1996. Plasmid RK2 toxin protein ParE: Purification and interaction with the ParD antitoxin protein. *Journal of Bacteriology*, 178(5), pp.1420–1429.

Johnston, D.S.T. et al., 1992. A conserved double-stranded RNA-binding domain. , 89(November), pp.10979–10983.

Jørgensen, M.G. et al., 2009. HicA of Escherichia coli defines a novel family of translation-independent mRNA interferases in bacteria and archaea. *Journal of Bacteriology*, 191(4), pp.1191–1199.

Jurenaite, M., Markuckas, A. & Suziedeliene, E., 2013. Identification and characterization of type II toxin-antitoxin systems in the opportunistic pathogen Acinetobacter baumannii. *Journal of bacteriology*, 195(14), pp.3165–72. Available at:

http://www.pubmedcentral.nih.gov/articlerender.fcgi?artid=3697630&tool=pmcentrez&rendertype=abstract.

Kaestli, M. et al., 2012. Comparison of TaqMan PCR Assays for Detection of the Melioidosis Agent Burkholderia pseudomallei in Clinical Specimens. , 50(6), pp.2059–2062.

Kasari, V. et al., 2013. Transcriptional cross-activation between toxin-antitoxin systems of Escherichia coli.

Kaspy, I. et al., 2013. HipA-mediated antibiotic persistence via phosphorylation of the glutamyl-tRNA-synthetase. *Nature communications*, 4, p.3001. Available at: http://www.ncbi.nlm.nih.gov/pubmed/24343429.

Kawano, M., 2012. Divergently overlapping cis-encoded antisense RNA regulating toxin-antitoxin systems from E. coli: hok/sok, ldr/rdl, symE/symR. *RNA biology*, 9(12), pp.1520–7. Available at: http://www.tandfonline.com/doi/full/10.4161/rna.22757#.VP9jmkIRyJM.

Kawano, M., Aravind, L. & Storz, G., 2007. An antisense RNA controls synthesis of an SOS-induced toxin evolved from an antitoxin. *Molecular Microbiology*, 64(3), pp.738–754.

Keren, I. et al., 2004. Specialized Persister Cells and the Mechanism of Multidrug Tolerance in Escherichia coli Specialized Persister Cells and the Mechanism of Multidrug Tolerance in Escherichia coli. *Journal of bacteriology*, 186(24), pp.8172–8180.

Khlebnikov, A. et al., 2001. Homogeneous expression of the PBAD promoter in Escherichia coli by constitutive expression of the low-affinity high-capacity araE transporter. *Microbiology*, 147(12), pp.3241–3247.

Kim, Y. & Wood, T.K., 2010. Toxins Hha and CspD and small RNA regulator Hfq are involved in persister cell formation through MqsR in Escherichia

coli. *Biochemical and Biophysical Research Communications*, 391(1), pp.209–213.

Kolodkin-Gal, I. & Engelberg-Kulka, H., 2008. The extracellular death factor: physiological and genetic factors influencing its production and response in Escherichia coli. *Journal of bacteriology*, 190(9), pp.3169–75. Available at: http://www.pubmedcentral.nih.gov/articlerender.fcgi?artid=2347391&tool=pmcentrez&rendertype=abstract.

Komi, K.K. et al., 2015. ChpK and MazF of the toxin-antitoxin modules are involved in the virulence of Leptospira interrogans during infection. *Microbes and Infection*, 17(1), pp.34–47.

Korch, S.B. et al., 2015. The Mycobacterium tuberculosis relBE toxin:antitoxin genes are stress-responsive modules that regulate growth through translation inhibition. *Journal of Microbiology*, 53(11), pp.783–795.

Korch, S.B., Contreras, H. & Clark-Curtiss, J.E., 2009. Three Mycobacterium tuberculosis rel toxin-antitoxin modules inhibit mycobacterial growth and are expressed in infected human macrophages. *Journal of Bacteriology*, 191(5), pp.1618–1630.

Krieger, F., Möglich, A. & Kiefhaber, T., 2005. Effect of proline and glycine residues on dynamics and barriers of loop formation in polypeptide chains. *J Am Chem Soc.*, Mar 16;127((10):), pp.3346–52.

Kristoffersen, P. et al., 2000. Bacterial toxin-antitoxin gene system as containment control in yeast cells. *Applied and Environmental Microbiology*, 66(12), pp.5524–5526.

Krovat, B.C. & Jantsch, M.F., 1996. Comparative mutational analysis of the double-stranded RNA binding domains of Xenopus laevis RNA-binding protein A. *The Journal of biological chemistry*, 271(45), pp.28112–28119.

Kumar, S., Kolodkin-Gal, I. & Engelberg-Kulka, H., 2013. Novel quorum-sensing peptides mediating interspecies bacterial cell death. *mBio*, 4(3).

Larsen, E. et al., 2013. Survival, sublethal injury, and recovery of environmental Burkholderia pseudomallei in soil subjected to desiccation. *Applied and Environmental Microbiology*, 79(7), pp.2424–2427.

Laukkanen, R. et al., 2008. Transmission of yersinia pseudotuberculosis in the pork production chain from farm to slaughterhouse. *Applied and Environmental Microbiology*, 74(17), pp.5444–5450.

Lee, H.J. et al., 2015. Recovery of plasmid pEMB1, whose toxin-antitoxin system stabilizes an ampicillin resistance-conferring ??-lactamase gene in Escherichia coli, from natural environments. *Applied and Environmental Microbiology*, 81(1), pp.40–47.

Lee, I.-G. et al., 2015. Structural and functional studies of the Mycobacterium tuberculosis VapBC30 toxin-antitoxin system: implications for the design of novel antimicrobial peptides. *Nucleic acids research*, 43(15), pp.7624–37. Available at: http://www.pubmedcentral.nih.gov/articlerender.fcgi?artid=4551927&tool=pmcentrez&rendertype=abstract.

Lee, K.-Y. & Lee, B.-J., 2016. Structure, Biology, and Therapeutic Application of Toxin–Antitoxin Systems in Pathogenic Bacteria. *Toxins*, 8(10), p.305. Available at: http://www.mdpi.com/2072-6651/8/10/305.

Lee, N. et al., 1985. Pseudomonas pseudomallei infection from drowning: the first reported case in Taiwan. *J Clin Microbiol*, 22((3)), pp.352–354.

Lee, S.K. et al., 2007. Directed evolution of AraC for improved compatibility of arabinose- and lactose-inducible promoters. *Applied and Environmental Microbiology*, 73(18), pp.5711–5715.

Lehnherr, H. & Yarmolinsky, M.B., 1995. Addiction protein Phd of plasmid prophage P1 is a substrate of the ClpXP serine protease of Escherichia coli. *Proceedings of the National Academy of Sciences of the United States of America*, 92(8), pp.3274–7. Available at: http://www.pubmedcentral.nih.gov/articlerender.fcgi?artid=42148&tool=pmcentrez&rendertype=abstract.

Leplae, R. et al., 2011. Diversity of bacterial type II toxin-antitoxin systems: a comprehensive search and functional analysis of novel families. *Nucleic Acids Research*, 39(13), pp.5513–5525. Available at: http://nar.oxfordjournals.org/lookup/doi/10.1093/nar/gkr131.

Leplae, R. et al., 2011. Diversity of bacterial type II toxin-antitoxin systems: A comprehensive search and functional analysis of novel families. *Nucleic Acids Research*, 39(13), pp.5513–5525.

Leung, E. et al., 2011. Activators of Cylindrical Proteases as Antimicrobials: Identification and Development of Small Molecule Activators of ClpP Protease. *Chemistry and Biology*, 18(9), pp.1167–1178.

Lewis, K., 2010. Persister Cells. *Annu. Rev. Microbiol*, 64, pp.357–72.

Lewis, K., 2007. Persister cells, dormancy and infectious disease. *Nature reviews Microbiology*, 5(1), pp.48–56. Available at: http://www.ncbi.nlm.nih.gov/pubmed/17143318.

Li, G.Y. et al., 2009. Inhibitory mechanism of Escherichia coli RelE-RelB toxin-antitoxin module involves a helix displacement near an mRNA interferase active site. *Journal of Biological Chemistry*, 284(21), pp.14628–14636.

Limmathurotsakul, D. et al., 2016. Predicted global distribution of Burkholderia pseudomallei and burden of melioidosis. *Nature Microbiology*, 1(January), pp.1–5. Available at: http://www.nature.com/articles/nmicrobiol20158.

Limmathurotsakul, D. et al., 2006. Risk Factors for Recurrent Melioidosis in Northeast Thailand. , 43, pp.979–986.

Liu, M. et al., 2008. Bacterial addiction module toxin Doc inhibits translation elongation through its association with the 30S ribosomal subunit. *Proceedings of the National Academy of Sciences of the United States of America*, 105(15), pp.5885–5890. Available at: http://www.pnas.org/content/105/15/5885?ijkey=1fa6eabc4473ecc9985be9afc4cfc61a96b6f440&keytype2=tf_ipsecsha.

Lustig, B., Arora, S. & Jernigan, R.L., 1997. RNA base-amino acid interaction strengths derived from structures and sequences. *Nucleic Acids Research*, 25(13), pp.2562–2565.

Magnuson, R. & Yarmolinsky, M.B., 1998. Corepression of the P1 addiction operon by Phd and Doc. *Journal of Bacteriology*, 180(23), pp.6342–6351.

Maisonneuve, E. et al., 2011. Bacterial persistence by RNA endonucleases. *Proceedings of the National Academy of Sciences of the United States of America*, 108(32), pp.13206–13211.

Maisonneuve, E., Castro-Camargo, M. & Gerdes, K., 2013. (p)ppGpp controls bacterial persistence by stochastic induction of toxin-antitoxin activity. *Cell*, 154(5), pp.1140–1150.

Maisonneuve, E. & Gerdes, K., 2014. Molecular mechanisms underlying bacterial persisters. *Cell*, 157(3), pp.539–548.

Makarova, K.S. et al., 2011. Defense Islands in Bacterial and Archaeal Genomes and Prediction of Novel Defense Systems. *Journal of Bacteriology*, 193(21), pp.6039–6056.

Makarova, K.S., Grishin, N. V. & Koonin, E. V., 2006. The HicAB cassette, a putative novel, RNA-targeting toxin-antitoxin system in archaea and

bacteria. *Bioinformatics*, 22(21), pp.2581–2584.

Makarova, K.S., Wolf, Y.I. & Koonin, E. V, 2009. Comprehensive comparative-genomic analysis of type 2 toxin-antitoxin systems and related mobile stress response systems in prokaryotes. *Biology direct*, 4(1), p.19. Available at: http://www.biology-direct.com/content/4/1/19.

Maris, C., Dominguez, C. & Allain, F.H.T., 2005. The RNA recognition motif, a plastic RNA-binding platform to regulate post-transcriptional gene expression. *FEBS Journal*, 272(9), pp.2118–2131.

Markovski, M. & Wickner, S., 2013. Preventing bacterial suicide: A novel toxin-antitoxin strategy. *Molecular Cell*, 52(5), pp.611–612.

Martínez, L.C. & Vadyvaloo, V., 2014. Mechanisms of post-transcriptional gene regulation in bacterial biofilms. *Frontiers in cellular and infection microbiology*, 4(March), p.doi: 10.3389/fcimb.2014.00038. Available at: http://www.pubmedcentral.nih.gov/articlerender.fcgi?artid=3971182&tool=pmcentrez&rendertype=abstract.

Masliah, G., Barraud, P. & Allain, F.H.-T., 2013. RNA recognition by double-stranded RNA binding domains: a matter of shape and sequence. *Cellular and Molecular Life Sciences*, 70(11), pp.1875–1895. Available at: http://www.ncbi.nlm.nih.gov/pmc/articles/PMC3724394/.

Masuda, H. et al., 2012. A novel membrane-bound toxin for cell division, CptA (YgfX), inhibits polymerization of cytoskeleton proteins, FtsZ and MreB, in Escherichia coli. *FEMS Microbiology Letters*, 328(2), pp.174–181.

McKenzie, J.L. et al., 2012. A vapbc toxin-antitoxin module is a posttranscriptional regulator of metabolic flux in mycobacteria. *Journal of Bacteriology*, 194(9), pp.2189–2204.

McMillan, N. et al., 1995. Mutational analysis of the double-stranded RNA

(dsRNA) binding domain of the dsRNA-activated protein kinase, PKR. *J Biol Chem.*, 270((6)), p.2601–2606.

Meißner, C., Jahn, N. & Brantl, S., 2016. *In Vitro* Characterization of the Type I Toxin-Antitoxin System *bsrE* /SR5 from *Bacillus subtilis*. *Journal of Biological Chemistry*, 291(2), pp.560–571. Available at: http://www.jbc.org/lookup/doi/10.1074/jbc.M115.697524.

Van Melderen, L. et al., 1996. ATP-dependent degradation of CcdA by Lon protease. Effects of secondary structure and heterologous subunit interactions. *Journal of Biological Chemistry*, 271(44), pp.27730–27738.

Van Melderen, L., 2010. Toxin-antitoxin systems: Why so many, what for? *Current Opinion in Microbiology*, 13(6), pp.781–785.

Van Melderen, L. & De Bast, M.S., 2009. Bacterial toxin-Antitoxin systems: More than selfish entities? *PLoS Genetics*, 5(3).

Merfa, M. V et al., 2016. The MqsRA Toxin-Antitoxin System from Xylella fastidiosa Plays a Key Role in Bacterial Fitness , Pathogenicity , and Persister Cell Formation. , 7(June).

Miki, T. et al., 1992. Control of segregation of chromosomal DNA by sex factor F in Escherichia coli. Mutants of DNA gyrase subunit A suppress letD (ccdB) product growth inhibition. *Journal of Molecular Biology*, 225(1), pp.39–52.

Mitchell, H.L. et al., 2010. Treponema denticola biofilm-induced expression of a bacteriophage, toxin-antitoxin systems and transposases. *Microbiology*, 156(3), pp.774–788.

Monti, M.C. et al., 2007. Interactions of Kid-Kis toxin-antitoxin complexes with the parD operator-promoter region of plasmid R1 are piloted by the Kis antitoxin and tuned by the stoichiometry of Kid-Kis oligomers. *Nucleic Acids*

Research, 35(5), pp.1737–1749.

Moyed, H. & Bertrand, K., 1983. hipA, a newly recognized gene of Escherichia coli K-12 that affects frequency of persistence after inhibition of murein synthesis. 25. *J. Bacteriol.*, 155, p.768–775.

Muñoz-Gómez, A.J. et al., 2005. RNase/anti-RNase activities of the bacterial parD toxin-antitoxin system. *Journal of Bacteriology*, 187(9), pp.3151–3157.

Munson, M. et al., 1996. What makes a protein a protein? Hydrophobic core designs that specify stability and structural properties. *Protein science : a publication of the Protein Society*, 5(8), pp.1584–93. Available at: http://www.pubmedcentral.nih.gov/articlerender.fcgi?artid=2143493&tool=pmcentrez&rendertype=abstract.

Mutschler, H. et al., 2011. A novel mechanism of programmed cell death in bacteria by toxin-antitoxin systems corrupts peptidoglycan synthesis. *PLoS Biology*, 9(3).

Najafpour, G.D., 2007. *Biochemical Engineering and Biotechnology*, Elsevier. Available at: http://www.sciencedirect.com/science/article/pii/B9780444528452500148 [Accessed May 11, 2016].

Nanduri, S. et al., 1998. Structure of the double-stranded RNA-binding domain of the protein kinase PKR reveals the molecular basis of its dsRNA-mediated activation. *EMBO Journal*, 17(18), pp.5458–5465.

Ngauy, V. et al., 2005. CASE REPORTS Cutaneous Melioidosis in a Man Who Was Taken as a Prisoner of War by the Japanese during World War II. , 43(2), pp.970–972.

Northen, H. et al., 2010. Salmonella enterica serovar Typhimurium mutants

completely lacking the F0F1 ATPase are novel live attenuated vaccine strains. *Vaccine*, 28(4), pp.940–949.

Norton, J.P. & Mulvey, M.A., 2012. Toxin-Antitoxin Systems Are Important for Niche-Specific Colonization and Stress Resistance of Uropathogenic Escherichia coli. *PLoS Pathogens*, 8(10).

Ogura, T. & Hiraga, S., 1983. Mini-F plasmid genes that couple host cell division to plasmid proliferation. *Proceedings of the National Academy of Sciences of the United States of America*, 80(15), pp.4784–8. Available at: http://www.ncbi.nlm.nih.gov/pubmed/6308648%5Cnhttp://www.pubmedcentral.nih.gov/articlerender.fcgi?artid=PMC384129.

Oliver, J. & Bockian, R., 1995. In vivo resuscitation, and virulence towards mice, of viable but nonculturable cells of Vibrio vulnificus. *Appl. Envir. Microbiol.*, 61(7), pp.2620–2623. Available at: http://aem.asm.org/cgi/content/long/61/7/2620 [Accessed February 10, 2016].

Overgaard, M., Borch, J. & Gerdes, K., 2009. RelB and RelE of Escherichia coli Form a Tight Complex That Represses Transcription via the Ribbon – Helix – Helix Motif in RelB. *Journal of Molecular Biology*, 394(2), pp.183–196. Available at: http://dx.doi.org/10.1016/j.jmb.2009.09.006.

Page, R. & Peti, W., 2016. Toxin-antitoxin systems in bacterial growth arrest and persistence. *Nat Chem Biol*, 12(4), pp.208–214. Available at: http://dx.doi.org/10.1038/nchembio.2044.

Pandey, D.P. & Gerdes, K., 2005. Toxin-antitoxin loci are highly abundant in free-living but lost from host-associated prokaryotes. *Nucleic Acids Research*, 33(3), pp.966–976.

Park, J.-H. et al., 2013. ACA-specific RNA sequence recognition is acquired via

the loop 2 region of MazF mRNA interferase. *Proteins: Structure, Function, and Bioinformatics*, 81(5), pp.874–883. Available at: http://dx.doi.org/10.1002/prot.24246.

Park, S.J., Son, W.S. & Lee, B.J., 2013. Structural overview of toxin-antitoxin systems in infectious bacteria: A target for developing antimicrobial agents. *Biochimica et Biophysica Acta - Proteins and Proteomics*, 1834(6), pp.1155–1167.

Patel, R.C., Stanton, P. & Sen, G.C., 1996. Specific mutations near the amino terminus of double-stranded RNA- dependent protein kinase (PKR) differentially affect its double- stranded RNA binding and dimerization properties. *J Biol Chem*, 271(41), pp.25657–25663. Available at: http://www.ncbi.nlm.nih.gov/cgi-bin/Entrez/referer?http://www.jbc.org/cgi/content/full/271/41/25657.

Pathak, C. et al., 2013. Crystal structure of apo and copper bound HP0894 toxin from Helicobacter pylori 26695 and insight into mRNase activity. *Biochimica et Biophysica Acta - Proteins and Proteomics*, 1834(12), pp.2579–2590. Available at: http://dx.doi.org/10.1016/j.bbapap.2013.09.006.

Pawlowski, D.R. et al., 2011. Entry of Yersinia pestis into the viable but nonculturable state in a low-temperature tap water microcosm. *PLoS ONE*, 6(3).

Paz, S. et al., 2007. Climate change and the emergence of Vibrio vulnificus disease in Israel. *Environmental research*, 103(3), pp.390–6. Available at: http://www.sciencedirect.com/science/article/pii/S0013935106001526 [Accessed February 10, 2016].

Pecota, D.C. & Wood, T.K., 1996. Exclusion of T4 phage by the hok/sok killer

locus from plasmid R1. *Journal of Bacteriology*, 178(7), pp.2044–2050.

Peterson, L.R. & Shanholtzer, C.J., 1992. Tests for Bactericidal Effects of Antimicrobial Agents : Technical Performance and Clinical Relevance. , 5(4), pp.420–432.

Preston, M.A. et al., 2016. Repurposing a Prokaryotic Toxin-Antitoxin System for the Selective Killing of Oncogenically Stressed Human Cells. *ACS Synthetic Biology*, 5(7), pp.540–546.

Prigent-Combaret, C. et al., 2000. Developmental pathway for biofilm formation in curli-producing Escherichia coli strains: Role of flagella, curli and colanic acid. *Environmental Microbiology*, 2(4), pp.450–464.

Pumpuang, A. et al., 2011. Survival of Burkholderia pseudomallei in distilled water for 16 years. *Transactions of the Royal Society of Tropical Medicine and Hygiene*, 105(10), pp.598–600.

Qiu, D. et al., 2008. PBAD-based shuttle vectors for functional analysis of toxic and highly regulated genes in Pseudomonas and Burkholderia spp. and other bacteria. *Applied and Environmental Microbiology*, 74(23), pp.7422–7426.

Ramage, H.R., Connolly, L.E. & Cox, J.S., 2009. Comprehensive functional analysis of Mycobacterium tuberculosis toxin-antitoxin systems: Implications for pathogenesis, stress responses, and evolution. *PLoS Genetics*, 5(12).

Ramage, H.R., Connolly, L.E. & Cox, J.S., 2009. Comprehensive functional analysis of Mycobacterium tuberculosis toxin-antitoxin systems: implications for pathogenesis, stress responses, and evolution. *PLoS genetics*, 5(12), p.e1000767. Available at: http://www.pubmedcentral.nih.gov/articlerender.fcgi?artid=2781298&tool=p

mcentrez&rendertype=abstract.

Ramos, A. et al., 2000. RNA recognition by a Staufen double-stranded RNA-binding domain. *The EMBO Journal*, 19(5), pp.997–1009. Available at: http://www.pubmedcentral.nih.gov/articlerender.fcgi?artid=305639&tool=pmcentrez&rendertype=abstract.

Rasia, R. et al., 2010. Structure and RNA interactions of the plant MicroRNA processing-associated protein HYL1. *Biochemistry.*, 49((38)), p.8237–8239.

Rasmussen, S. et al., 2016. Early Divergent Strains of Yersinia pestis in Eurasia 5,000 Years Ago. *Cell*, 163(3), pp.571–582. Available at: http://dx.doi.org/10.1016/j.cell.2015.10.009.

Ren, D. et al., 2004. Gene expression in Escherichia coli biofilms. *Applied Microbiology and Biotechnology*, 64(4), pp.515–524.

Rowe-Magnus, D.A. et al., 2003. Comparative analysis of superintegrons: Engineering extensive genetic diversity in the vibrionaceae. *Genome Research*, 13(3), pp.428–442.

Rybtke, M.T. et al., 2011. The implication of Pseudomonas aeruginosa biofilms in infections. *Inflammation & allergy drug targets*, 10, pp.141–157.

Ryter, J.M. & Schultz, S.C., 1998. Molecular basis of double-stranded RNA-protein interactions: Structure of a dsRNA-binding domain complexed with dsRNA. *EMBO Journal*, 17(24), pp.7505–7513.

Saenger, W., 1984. *Principles of Nucelic Acid Structure*,

Sala, A., Bordes, P. & Genevaux, P., 2014. Multiple toxin-antitoxin systems in Mycobacterium tuberculosis. *Toxins*, 6(3), pp.1002–1020.

Samson, J.E. et al., 2013. Structure and activity of AbiQ, a lactococcal endoribonuclease belonging to the type III toxin-antitoxin system. *Molecular Microbiology*, 87(4), pp.756–768.

Sauer, K., Rickard, A.H. & Davies, D.G., 2007. Biofilms and Biocomplexity. *Microbe*, 2(7), pp.347–353.

Sayed, N. et al., 2012. Functional and structural insights of a staphylococcus aureus apoptotic-like membrane peptide from a toxin-antitoxin module. *Journal of Biological Chemistry*, 287(52), pp.43454–43463.

Sberro, H. et al., 2013. Discovery of Functional Toxin/Antitoxin Systems in Bacteria by Shotgun Cloning. *Molecular Cell*, 50(1), pp.136–148.

Schleif, R., 2010. Escherichia coli,.

Schlievert, P.M. et al., 2013. Menaquinone Analogs Inhibit Growth of Bacterial Pathogens. , 57(11), pp.5432–5437.

Schumacher, M.A. et al., 2009. NIH Public Access. , 323(5912), pp.396–401.

Schumacher, M. a et al., 2015. HipBA-promoter structures reveal the basis of heritable multidrug tolerance. *Nature*, 524(7563), pp.59–64. Available at: http://www.ncbi.nlm.nih.gov/pubmed/26222023.

Schumacher, M. a et al., 2009. Molecular mechanisms of HipA-mediated multidrug tolerance and its neutralization by HipB. *Science (New York, N.Y.)*, 323(5912), pp.396–401.

Schweizer, H.P., 2012. Mechanisms of antibiotic resistance in Burkholderia pseudomallei: implications for treatment of melioidosis. *Future microbiology*, 7(12), pp.1389–99. Available at: http://www.ncbi.nlm.nih.gov/pubmed/23231488%5Cnhttp://www.pubmedcentral.nih.gov/articlerender.fcgi?artid=PMC3568953.

Seok, K.K. et al., 2007. Molecular and structural characterization of the PezAT chromosomal toxin-antitoxin system of the human pathogen Streptococcus pneumoniae. *Journal of Biological Chemistry*, 282(27), pp.19606–19618.

Shah, D. et al., 2006. Persisters: a distinct physiological state of E. coli. *BMC*

microbiology, 6, p.53.

Shapira, A. et al., 2012. Removal of hepatitis C virus-infected cells by a zymogenized bacterial toxin. *PLoS ONE*, 7(2).

Shimazu, T. et al., 2014. Regression of solid tumors by induction of MazF, a bacterial mRNA endoribonuclease. *Journal of Molecular Microbiology and Biotechnology*, 24(4), pp.228–233.

Singh, R., Barry, C.E. & Boshoff, H.I.M., 2010. The three RelE homologs of Mycobacterium tuberculosis have individual, drug-specific effects on bacterial antibiotic tolerance. *Journal of Bacteriology*, 192(5), pp.1279–1291.

Smith, a S. & Rawlings, D.E., 1997. The poison-antidote stability system of the broad-host-range Thiobacillus ferrooxidans plasmid pTF-FC2. *Molecular microbiology*, 26(5), pp.961–970.

Socolovschi, C., Audoly, G. & Raoult, D., 2013. Connection of toxin-antitoxin modules to inoculation eschar and arthropod vertical transmission in Rickettsiales. *Comparative Immunology, Microbiology and Infectious Diseases*, 36(2), pp.199–209.

Solecki, O. et al., 2015. Converting a Staphylococcus aureus toxin into effective cyclic pseudopeptide antibiotics. *Chemistry and Biology*, 22(3), pp.329–335.

Soo, V.W.C. & Wood, T.K., 2013. Antitoxin MqsA represses curli formation through the master biofilm regulator CsgD. *Scientific reports*, 3, p.3186. Available at: http://www.ncbi.nlm.nih.gov/pubmed/24212724.

Srivastava, P. & Chattoraj, D.K., 2007. Selective chromosome amplification in Vibrio cholerae. *Molecular Microbiology*, 66(4), pp.1016–1028.

Stefl, R. et al., 2010. The Solution Structure of the ADAR2 dsRBM-RNA

Complex Reveals a Sequence-Specific Readout of the Minor Groove. *Cell*, 143(2), pp.225–237.

Stewart, P.S. & Franklin, M.J., 2008. Physiological heterogeneity in biofilms. *Nature Reviews Microbiology*, 6(3), pp.199–210. Available at: http://www.nature.com/doifinder/10.1038/nrmicro1838.

Strom, M.S. & Paranjpye, R.N., 2000. Epidemiology and pathogenesis of Vibrio vulnificus. *Microbes and Infection*, 2(2), pp.177–188. Available at: http://www.sciencedirect.com/science/article/pii/S1286457900002707 [Accessed February 10, 2016].

Szekeres, S. et al., 2007. Chromosomal toxin-antitoxin loci can diminish large-scale genome reductions in the absence of selection. *Molecular Microbiology*, 63(6), pp.1588–1605.

Tertti, R. et al., 1984. An Outbreak of Yersinia pseudotuberculosis Infection. *Journal of Infectious Diseases* , 149(2), pp.245–250. Available at: http://jid.oxfordjournals.org/content/149/2/245.abstract.

Tian, Q.B. et al., 2001. Specific Protein–DNA and Protein–Protein Interaction in the hig Gene System, a Plasmid-Borne Proteic Killer Gene System of Plasmid Rts1. *Plasmid*, 45(2), pp.63–74.

Tsilibaris, V. et al., 2007. What is the benefit to Escherichia coli of having multiple toxin-antitoxin systems in its genome? *Journal of Bacteriology*, 189(17), pp.6101–6108.

Unterholzner, S.J., Poppenberger, B. & Rozhon, W., 2013. Toxin-antitoxin systems: Biology, identification, and application. *Mobile genetic elements*, 3(5), p.e26219. Available at: http://www.pubmedcentral.nih.gov/articlerender.fcgi?artid=3827094&tool=pmcentrez&rendertype=abstract.

Verstraeten, N. et al., 2015. Obg and Membrane Depolarization Are Part of a Microbial Bet-Hedging Strategy that Leads to Antibiotic Tolerance. *Molecular Cell*, 59(1), pp.9–21.

Vesper, O. et al., 2011. Selective translation of leaderless mRNAs by specialized ribosomes generated by MazF in Escherichia coli. *Cell*, 147(1), pp.147–157.

Walhout, a J. et al., 2000. GATEWAY recombinational cloning: application to the cloning of large numbers of open reading frames or ORFeomes. *Methods in enzymology*, 328(1998), pp.575–592.

Wang, X. et al., 2012. A new type V toxin-antitoxin system where mRNA for toxin GhoT is cleaved by antitoxin GhoS. *Nature chemical biology*, 8(10), pp.855–61. Available at: http://dx.doi.org/10.1038/nchembio.1062.

Wang, X. et al., 2011. Antitoxin MqsA helps mediate the bacterial general stress response. *Nature Chemical Biology*, 7(6), pp.359–366. Available at: http://dx.doi.org/10.1038/nchembio.560%5Cnhttp://www.nature.com/doifinder/10.1038/nchembio.560.

Wang, X. et al., 2014. Type II Toxin/Antitoxin MqsR/MqsA Controls Type V Toxin/ Antitoxin GhoT/GhoS. *Environ Microbiol*, 15(6), pp.1734–1744.

Wang, X. et al., 2013. Type II toxin/antitoxin MqsR/MqsA controls type V toxin/antitoxin GhoT/GhoS. *Environmental Microbiology*, 15(6), pp.1734–1744.

Wang, Z. et al., 2011. Structure of a yeast RNase III dsRBD complex with a noncanonical RNA substrate provides new insights into binding specificity of dsRBDs. *Structure.*, 19(7), p.999–1010.

Weaver, K.E., 2015. The Type I toxin-antitoxin par locus from Enterococcus faecalis plasmid pAD1: RNA regulation by both cis- and trans-acting

elements. *Plasmid*, 78, pp.65–70. Available at: http://dx.doi.org/10.1016/j.plasmid.2014.10.001.

Wen, Y., Behiels, E. & Devreese, B., 2014. Toxin-Antitoxin systems: Their role in persistence, biofilm formation, and pathogenicity. *Pathogens and Disease*, 70(3), pp.240–249.

Wessner, F. et al., 2015. Regulatory crosstalk between type I and type II toxin-antitoxin systems in the human pathogen *Enterococcus faecalis*. *RNA Biology*, 12(10), pp.1099–1108. Available at: http://www.tandfonline.com/doi/full/10.1080/15476286.2015.1084465.

White, N., 2003. Melioidosis. *The Lancet*, 361(9370), pp.1715–1722. Available at: http://www.sciencedirect.com/science/article/pii/S0140673603133740.

Wiersinga, W.J., Currie, B.J. & Peacock, S.J., 2012. review article. *New England Journal of Medicine*, pp.1035–1044.

Wilbaux, M. et al., 2007. Functional interactions between coexisting toxin-antitoxin systems of the ccd family in Escherichia coli O157:H7. *Journal of Bacteriology*, 189(7), pp.2712–2719.

Williams, J.J. & Hergenrother, P.J., 2008. Exposing plasmids as the Achilles' heel of drug-resistant bacteria. *Current Opinion in Chemical Biology*, 12(4), pp.389–399.

Winther, K.S. & Gerdes, K., 2011. Enteric virulence associated protein VapC inhibits translation by cleavage of initiator tRNA. *Proceedings of the National Academy of Sciences of the United States of America*, 108(18), pp.7403–7407.

Wood, T.K., 2009. Insights on Escherichia coli biofilm formation and inhibition from whole-transcriptome profiling. *Environmental Microbiology*, 11(1), pp.1–15.

Wozniak, R.A.F. & Waldor, M.K., 2009. A toxin-antitoxin system promotes the maintenance of an integrative conjugative element. *PLoS Genetics*, 5(3).

Wright, O. et al., 2015. GeneGuard: A modular plasmid system designed for biosafety. *ACS Synthetic Biology*, 4(3), pp.307–316.

Wu, H. et al., 2004. Structural basis for recognition of the AGNN tetraloop RNA fold by the double-stranded RNA-binding domain of Rnt1p RNase III. *Proceedings of the National Academy of Sciences of the United States of America*, 101(22), pp.8307–12. Available at: http://www.pubmedcentral.nih.gov/articlerender.fcgi?artid=420390&tool=pmcentrez&rendertype=abstract.

Wu, X. et al., 2015. Impact of climate change on human infectious diseases: Empirical evidence and human adaptation. *Environment international*, 86, pp.14–23. Available at: http://www.sciencedirect.com/science/article/pii/S0160412015300489 [Accessed October 20, 2015].

Wuthiekanun, V. et al., 1990. Blood culture techniques for the diagnosis of melioidosis. *Eur J Clin Microbiol Infect Dis.*, Sep;9((9):), p.654–8.

Yamaguchi, Y. & Inouye, M., 2009. mRNAinterferases, sequence-specific endoribonucleases from the toxin- antitoxin systems. *Prog.Mol. Biol. Transl. Sci.*, (85), pp.467–500.

Yamaguchi, Y. & Park, J., 2011. Toxin-Antitoxin Systems in Bacteria and Archaea.

Yamaguchi, Y., Park, J.-H. & Inouye, M., 2011. Toxin-Antitoxin Systems in Bacteria and Archaea. *Annual Review of Genetics*, 45(1), pp.61–79.

Yamamoto, T.A., Gerdes, K. & Tunnacliffe, A., 2002. Bacterial toxin RelE induces apoptosis in human cells. *FEBS Letters*, 519(1–3), pp.191–194.

Yan, B.X. & Sun Qing, Y., 1997. Glycine residues provide flexibility for enzyme active sites. *Journal of Biological Chemistry*, 272(6), pp.3190–3194.

Yang, S. et al., 2016. Construction of a novel, stable, food-grade expression system by engineering the endogenous toxin-antitoxin system in Bacillus subtilis. *Journal of Biotechnology*, 219, pp.40–47.

Yang, S.W. et al., 2010. Structure of arabidopsis Hyponastic Leaves1 and its molecular implications for miRNA Processing. *Structure*, 18(5), pp.594–605. Available at: http://dx.doi.org/10.1016/j.str.2010.02.006.

Yao, J. et al., 2015. Identification and characterization of a HEPN-MNT family type II toxin – antitoxin in Shewanella oneidensis.

Yuan, J., Yamaichi, Y. & Waldor, M.K., 2011. The three Vibrio cholerae chromosome II-encoded ParE toxins degrade chromosome I following loss of chromosome II. *Journal of Bacteriology*, 193(3), pp.611–619.

Zalucki, Y.M., Power, P.M. & Jennings, M.P., 2007. Selection for efficient translation initiation biases codon usage at second amino acid position in secretory proteins. *Nucleic Acids Research*, 35(17), pp.5748–5754.

Zhang, X.-S., García-Contreras, R. & Wood, T.K., 2008. Escherichia coli transcription factor YncC (McbR) regulates colanic acid and biofilm formation by repressing expression of periplasmic protein YbiM (McbA). *The ISME journal*, 2(6), pp.615–31. Available at: http://www.ncbi.nlm.nih.gov/pubmed/18309357.

Zhang, Y. et al., 2003. MazF cleaves cellular mRNAs specifically at ACA to block protein synthesis in Escherichia coli. *Molecular Cell*, 12(4), pp.913–923.

Zhao, J. et al., 2013. Escherichia coli toxin gene hipA affects biofilm formation and DNA release. *Microbiology (United Kingdom)*, 159(PART3), pp.633–

640.

Zheng, C. et al., 2015. Identification and characterization of the chromosomal yefM-yoeB toxin-antitoxin system of Streptococcus suis. *Scientific reports*, 5(August), p.13125. Available at: http://www.pubmedcentral.nih.gov/articlerender.fcgi?artid=4536659&tool=pmcentrez&rendertype=abstract.

Zhu, L. et al., 2010. Noncognate Mycobacterium tuberculosis toxin-antitoxins can physically and functionally interact. *Journal of Biological Chemistry*, 285(51), pp.39732–39738.

Zielenkiewicz, U. & Cegłowski, P., 2005. The toxin-antitoxin system of the streptococcal plasmid pSM19035. *Journal of Bacteriology*, 187(17), pp.6094–6105.

Appendix

Table to show sequences of primers used for site-directed mutagenesis of HicA:

Primer name	**Sequence**
H29A_FOR	ggcttcttgggggctttgaaatgatgatggctgcctg
H29A_REV	caggcagccatcatcatttcaaagccccccaagaagcc
H40A_FOR	aggtccttcttcggggcgggaaccgtcacaag
H40A_REV	cttgtgacggttcccgccccgaagaaggacct
W15A_FOR	cactcgaaccaacctcgcgccatcttcctcaagc
W15A_REV	gcttgaggaagatggcgcgaggttggttcgagtg
P46A_FOR	cagtcccaatcgctaggtccttcttcggg
P46A_REV	cccgaagaaggacctagcgattgggactg
S3A_FOR	cggatcagcttcgatgcgttcatgagctcggatcc
S3A_REV	ggatccgagctcatgaacgcatcgaagctgatccg
H25A_FOR	ggggtgtttgaaatgagcatggctgcctgtcactcgaac
H25A_REV	gttcgagtgacaggcagccatgctcatttcaaacacccc
S23A_FOR	gttggttcgagtgacaggcgcccatcatcatttcaaacac
S23A_REV	gtgtttgaaatgatgatgggcgcctgtcactcgaaccaac
G34A_FOR	gaaccgtcacaagggctggcttcttgggg
G34A_REV	ccccaagaagccagcccttgtgacggttc
V36A_FOR	gtggggaaccgtcgcaaggcctggctt
V36A_REV	aagccaggccttgcgacggttccccac
D44_FOR	gtcccaatcggtagggccttcttcgggtgg
D44_REV	ccacccgaagaaggccctaccgattgggac
T49A_FOR	ctggatgctttttacagccccaatcggtaggtcc
T49A_REV	ggacctaccgattggggctgtaaaaagcatccag
I53A_FOR	ggccggcggatttctgggcgctttttacagtcccaatc
I53A_REV	gattgggactgtaaaaagcgcccagaaatccgccggcc
T37A_FOR	ggtggggaaccgccacaaggcctgg
T37A_REV	ccaggccttgtggcggttccccacc
P46A_FOR	cagtcccaatcgctaggtccttcttcggg
P46A_REV	cccgaagaaggacctagcgattgggactg
G22A_FOR	gaaatgatgatggctggctgtcactcgaaccaac
G22A_REV	gttggttcgagtgacagccagccatcatcatttc
P41A_FOR	gtaggtccttcttcgcgtggggaaccgtc
P41A_REV	gacggttccccacgcgaagaaggacctac
G14A_FOR	cgaaccaacctccaggcatcttcctcaagcatc
G14A_REV	gatgcttgaggaagatgcctggaggttggttcg
H24A_FOR	gggtgtttgaaatgatgagcgctgcctgtcactcgaac

H24A_REV	gttcgagtgacaggcagcgctcatcatttcaaacaccc
A57G_FOR	cgaattctcacaggccgccggatttctggatgc
A57G_REV	gcatccagaaatccggcggcctgtgagaattcg
G58A_FOR	cgaattctcacagggcggcggatttctgg
G58A_REV	ccagaaatccgccgccctgtgagaattcg
N2A_FOR	ggatcagcttcgatgaggccatgagctcggatcccc
N2A_REV	ggggatccgagctcatggcctcatcgaagctgatcc
S4A_FOR	gatcagcttcgctgagttcatgagctcggatcc
S4A_REV	ggatccgagctcatgaactcagcgaagctgatc
K5A_FOR	caagcatccggatcagcgccgatgagttcatgagctc
K5A_REV	gagctcatgaactcatcggcgctgatccggatgcttg
L6A_FOR	cctcaagcatccggatcgccttcgatgagttcatgag
L6A_REV	ctcatgaactcatcgaaggcgatccggatgcttgagg
I7A_FOR	cttcctcaagcatccgggccagcttcgatgagttcatg
I7A_REV	catgaactcatcgaagctggcccggatgcttgaggaag
R8A_FOR	ccatcttcctcaagcatcgcgatcagcttcgatgag
R8A_REV	ctcatcgaagctgatcgcgatgcttgaggaagatgg
M9A_FOR	gccatcttcctcaagcgcccggatcagcttcgatg
M9A_REV	catcgaagctgatccgggcgcttgaggaagatggc
L10A_FOR	ccagccatcttcctcagccatccggatcagcttc-
L10A_REV	gaagctgatccggatggctgaggaagatggctgg
E11A_FOR	ctccagccatcttccgcaagcatccggatc
E11A_REV	gatccggatgcttgcggaagatggctggag
E12A_FOR	cctccagccatctgcctcaagcatccgg
E12A_REV	ccggatgcttgaggcagatggctggagg
D13A_FOR	ggatgcttgaggaagctggctggaggttgg
D13A_REV	ccaacctccagccagcttcctcaagcatcc
R16A_FOR	ctgtcactcgaaccaacgcccagccatcttcctc
R16A_REV	gaggaagatggctgggcgttggttcgagtgacag
L17_FOR	gcctgtcactcgaaccgccctccagccatcttcc
L17_REV	ggaagatggctggagggcggttcgagtgacaggc
V18A_FOR	gcctgtcactcgagccaacctccagcc
V18A_REV	ggctggaggttggctcgagtgacaggc
R19_FOR	ctgcctgtcactgcaaccaacctccagccatc
R19_REV	gatggctggaggttggttgcagtgacaggcag
V20A_FOR	gatggctgcctgtcgctcgaaccaacctc
V20A_REV	gaggttggttcgagcgacaggcagccatc
T21A_FOR	gatgatggctgcctgccactcgaaccaacc
T21A_REV	ggttggttcgagtggcaggcagccatcatc
H26A_FOR	cttcttggggtgtttgaaagcatgatggctgcctgtcac
H26A_REV	gtgacaggcagccatcatgctttcaaacaccccaagaag
F27A_FOR	ggcttcttggggtgtttggcatgatgatggctgcctg
F27A_REV	caggcagccatcatcatgccaaacaccccaagaagcc
K28A_FOR	ggcttcttggggtgtgcgaaatgatgatggctgcctg
K28A_REV	caggcagccatcatcatttcgcacaccccaagaagcc
P30A_FOR	caaggcctggcttcttggcgtgtttgaaatgatgatgg

P30A_REV	ccatcatcatttcaaacacgccaagaagccaggccttg
K31A_FOR	catcatttcaaacaccccgcgaagccaggccttgtgac
K31A_REV	gtcacaaggcctggcttcgcggggtgtttgaaatgatg
K32A_FOR	ccgtcacaaggcctggcgccttggggtgtttgaaatg
K32A_REV	catttcaaacaccccaaggcgccaggccttgtgacgg
P33A_FOR	cgtcacaaggcctgccttcttggggtg
P33A_REV	caccccaagaaggcaggccttgtgacg
L35A_FOR	ggggaaccgtcacagcgcctggcttcttgg
L35A_REV	ccaagaagccaggcgctgtgacggttcccc
V38A_FOR	cttcgggtggggagccgtcacaaggcc
V38A_REV	ggccttgtgacggctccccacccgaag
P39A_FOR	cttcgggtgggcaaccgtcacaaggcc
P39A_REV	ggccttgtgacggttgcccacccgaag
K42A_FOR	cggtaggtccttcgccgggtggggaaccg
K42A_REV	cggttccccacccggcgaaggacctaccg
K43A_FOR	ccaatcggtaggtccgccttcgggtggggaac
K43A_REV	gttccccacccgaaggcggacctaccgattgg
L45A_FOR	cagtcccaatcggtgcgtccttcttcgggtgg
L45A_REV	ccacccgaagaaggacgcaccgattgggactg
I47A_FOR	gatgctttttacagtcccagccggtaggtccttcttcggg
I47A_REV	cccgaagaaggacctaccggctgggactgtaaaaagcatc
G48A_FOR	ggatgctttttacagtcgcaatcggtaggtccttc
G48A_REV	gaaggacctaccgattgcgactgtaaaaagcatcc
V50A_FOR	gatttctggatgctttttgcagtcccaatcggtagg
V50A_REV	cctaccgattgggactgcaaaaagcatccagaaatc
K51A_FOR	ggatttctggatgcttgctacagtcccaatcggtaggtccttc
K51A_REV	gaaggacctaccgattgggactgtagcaagcatccagaaatcc
S52A_FOR	cggatttctggatggcttttacagtcccaatcggtaggtcc
S52A_REV	ggacctaccgattgggactgtaaaagccatccagaaatccg
Q54A_FOR	ggccggcggatttcgcgatgctttttacagtccc
Q54A_REV	gggactgtaaaaagcatcgcgaaatccgccggcc
K55A_FOR	ctcacaggccggcggatgcctggatgctttttacag
K55A_REV	ctgtaaaaagcatccaggcatccgccggcctgtgag
S56A_FOR	caggccggcggctttctggatgctttttacag
S56A_REV	ctgtaaaaagcatccagaaagccgccggcctg
L59A_FOR	ccagaaatccgccggcgcgtgagaattcgaagc
L59A_REV	gcttcgaattctcacgcgccggcggatttctgg
Q54G_FOR	ggccggcggatttcccgatgctttttacagtccc
Q54G_REV	gggactgtaaaaagcatcgggaaatccgccggcc